INTERNATIONAL JOURNAL OF MEDICAL BIOCHEMISTRY



ORIGINALS

The impact of endothelin-1 on the efficacy of anti-VEGF therapy: A rationale for dual antagonism Mohamed MSA

Urokinase-type plasminogen activator and related microRNAs in hepatocellular carcinoma; a bioinformatic based study Seydel GS, et al.

Tau protein expression and phosphorylation in a glucose-repressed yeast model: Insights into the cancer-alzheimer's disease link Yilmazer M, et al.

Adaptive mitochondrial modules: Going with the flow of cancer-specific metabolic rewiring $Yildiz\ MT$

Can cinnamon reduce endoplasmic reticulum stress in diabetic nephropathy?: An experimental rat model Oztas B. et al.

Platelet-normalized biomarkers as diagnostic and prognostic indicators in crimean-congo hemorrhagic fever Bolat S, et al.

Determination of analytical performances of NT-proBNP and aPTT tests with three methods $Ye ilde{g} in D$

Adult references intervals for thyroid hormones using beckman coulter from Türkiye Sahin I, et al.

Evaluation of the analytical performance of the access vitamin B12 II assay with the new calibrator *Madenci OC*, et al.





EDITOR-IN-CHIEF Prof. DILDAR KONUKOGLU, MD.

Istanbul University-Cerrahpasa, Cerrahpasa Faculty of Medicine, Istanbul, Turkiye

ASSOCIATE EDITOR Prof. NECIP ILHAN, MD.

Fırat University, Faculty of Medicine, Elazıg, Turkiye

EDITORIAL ASSISTANT E. CUNEYT CANBULAT, MD.

General Manager of KBUDEK External Quality Control Programme, Istanbul, Turkiye

PUBLISHING MANAGER Prof. DILDAR KONUKOGLU, MD.

Istanbul University-Cerrahpasa, Cerrahpasa Faculty of Medicine, Istanbul, Turkiye

PUBLISHING MANAGER ASSISTANT FIKRET ERSAN TALU, MD.

Secretary of Association of Clinical Biochemistry Specialists, Turkiye

LINGUISTIC EDITOR Prof. UZAY GORMUS DÉGRIGO, MD., PhD.

Karolinska Institutet, Solna, Sweden

EXTERNAL EDITORS ERDINC SEZGIN, PhD.

Karolinska Institutet, Department of Women's and Children's Health, Scilifelab, Sweden

Prof. EVIN ADEMOGLU, MD.

Istanbul University, Faculty of Medicine, Department of Medical Biochemistry, Istanbul, Turkiye

ADVISORY BOARD

Prof. KHOSROW ADELI, MD., PhD.

Toronto University, The Hospital for Sick Children and Departments of Laboratory Medicine and Pathobiology, Biochemistry, and Physiology, Ontario, Canada

Prof. ANGELO AZZI, MD., PhD.

Tufts University, Jean Mayer USDA Human Nutrition Research Ctr. on Aging (HNRCA), Boston, Massachusetts

Prof. BANU ISBILEN BASOK, MD.

University of Health Sciences, Izmir Faculty of Medicine, Dr. Behcet Uz Child Disease and Pediatric Surgery Training and Research Hospital, Izmir, Turkiye

Prof. ETIENNE CAVALIER, MD.

Centre Hospitalier Universitaire de Liège, Specialist in Laboratory Medicine, EuSpLM, University of Liège, Liège, Belgium

Prof. AMITAVA DASGUPTA, PhD.

University of Texas Health Sciences Center, Department of Pathology and Laboratory Medicine, Houston, USA

Prof. KAYA EMERK, PhD.

Istanbul Kent University, Faculty of Dental Medicine, Department of Biochemistry, Istanbul, Turkiye

Prof. AMMAD AHMAD FAROOQI, MD.

Institute of Biomedical and Genetic Engineering (IBGE), Islamabad. Pakistan

Prof. KYM FRANCIS FAULL, PhD.

University of California Los Angeles, Pasarow Mass Spectrometry Laboratory, Los Angeles, USA

Prof. ASUMAN GEDIKBASI, MD., PhD.

Istanbul University, Institute of Child Health, Pediatric Basic Sciences, Medical Genetics, Istanbul, Turkiye

Prof. UZAY GORMUS DÉGRIGO, MD., PhD.

Karolinska Institutet, Department of Medical Biochemistry and Biophysics, Solna, Sweden

Prof. ASLIHAN GURBUZ BOLKAN, MD.

Ankara University, Faculty of Medicine, Department of Biochemistry, Ankara, Turkiye

Prof. NEVIN ILHAN, MD., PhD.

Firat University, Faculty of Medicine, Department of Medical Biochemistry, Elazig, Turkiye

Prof. FERRUH K. ISMAN, MD.

Istanbul Medeniyet University, Goztepe Training and Research Hospital, Department of Clinical Chemistry, Istanbul, Turkiye

Prof. CIGDEM KARAKUKCU, MD.

Erciyes University, Faculty of Medicine, Department of Biochemistry, Kayseri, Turkiye

Prof. HUSEYIN KAYADIBI, MD.

Eskisehir Osmangazi University, Faculty of Medicine, Department of Biochemistry, Eskisehir, Turkiye

Prof. GABOR L. KOVACS, MD., PhD, DSc.

University of Pécs, Faculty of Medicine, Department of Laboratory Medicine, Pécs, Hungary

Prof. MINE KUCUR, MD.

Istanbul University Cerrahpasa, Cerrahpasa Faculty of Medicine, Department of Biochemistry, Istanbul, Turkiye

Prof. ASIM OREM, MD.

Karadeniz Technical University, Faculty of Medicine, Trabzon, Turkive

Assoc. Prof. ISHAK OZEL TEKIN, MD. PhD.

Bulent Ecevit University, Faculty of Medicine, Department of Immunology, Zonguldak, Turkiye

Prof. MAURO PANTEGHINI, MD.

Milan University, Faculty of Medicine, Department of Clinical Biochemistry and Clinical Molecular Biology, Milano, Italy

Prof. JORGE L. SEPULVEDA, MD, PhD.

Columbia University, Department of Patology and Cell Biology, New York. USA

Prof. MUHITTIN ABDULKADIR SERDAR, MD.

Acibadem Mehmet Ali Aydinlar University, Faculty of Medicine, Department of Medical Biochemistry, Istanbul, Türkiye

Prof. ANA-MARIA SIMUNDIC, PhD.

Sveti Duh University, Department of Medical Laboratory Diagnostics, University Hospital "Sveti Duh", Zagreb, Croatia

Prof. STEVEN SOLDIN, MD.

Deputy Director of Chemistry, Senior Scientist and Director Post-Doctoral Training Program, Department of Laboratory Medicine, NIH Clinical Center Bethesda, USA and Adjunct Professor, Division of Endocrinology and Metabolism Georgetown University, Department of Medicine, USA

Prof. FATMA TANELI, MD.

Celal Bayar University, Faculty of Medicine, Department of Biochemistry, Manisa, Turkiye

DOUGLAS THOMPSON, PhD.

Leeds University, Leeds Teaching Hospitals, Department of Blood Science, Leeds, UK

${\sf Prof.\ TOMRIS\ OZBEN\ TOMASI,\ MD.,\ PhD.}$

Akdeniz University, Faculty of Medicine, Department of Biochemistry, Antalya, Turkiye

Prof. TURAN TURHAN, MD.

Ankara Bilkent City Hospital Health Application and Research Center, Department of Medical Biochemistry, Ankara, Turkiye

ALEXANDER ZOUGMAN, MD, PhD.

St. James's University Hospital, Clinical and Biomedical Proteomics Group, Cancer Research UK Centre, Leeds, UK

VOLUME VIII ISSUE 4 YEAR 2025

The Owner and Publishing Manager on behalf of the Association of PROF. DILDAR KONUKOGLU Clinical Biochemistry Specialists (Klinik Biyokimya Uzmanları Derneği)

Address: Maslak Mah. AOS 55. Sok. No: 2, 42 Maslak A

Blok Daire: 23 I Sarıyer, İstanbul-Türkiye

Phone: +90 2|2 24| 26 53 Fax: +90 2|2 24| 26 54 e-mail: www.kbud.org.tr web: info@kbud.org.tr KARE

Publisher: KARE MEDIA

Address: Göztepe Mah. Fahrettin Kerim Gökay Cad.

No: 200 D: 2, Göztepe, Kadıköy, İstanbul

Phone: +90 216 550 61 11 Fax: +90 216 550 61 12 e-mail: info@karepb.com web: www.kareyayincilik.com

> Yayın Turu: Uluslararası Sureli Basım Tarihi: Ekim 2025 Basım: Filmevi Grafik Renk Ayrımı Sistemleri San. Tic. LTD. ŞTİ. İstanbul-Türkiye

International Journal of Medical Biochemistry is a peer-reviewed journal published triannually.

Materials published in the Journal is covered by copyright 2025. All rights reserved.

This publication is printed on paper that meets the international standard ISO 9706:1994.

National Library of Medicine (USA) recommends the use of permanent, acid-free paper in the production of biomedical literature.



AIM AND SCOPE

International Journal of Medical Biochemistry (IJMB) publishes articles relating to clinical and experimental chemistry, molecular biology, genetics, therapeutic drug monitoring, toxicology, immunology, hematology and laboratory medicine with the focus on analytical and clinical investigation of laboratory tests used for diagnosis, prognosis, and monitoring of diseases.

BASIC PUBLICATION RULES

Authors are responsible for the accuracy of data. The journal is in compliance with the uniform requirements for manuscripts submitted to biomedical journals published by the ICMJ. The editorial and publication processes of the journal are conducted in accordance with the guidelines of the World Association of Medical Editors (WAME), International Committee of Medical Journal Editors (ICMJE), the Council of Science Editors (CSE), the European Association of Science Editors (EASE), and the Committee on Publication Ethics (COPE) as well.

DISCLAIMER

Statements or opinions expressed in the manuscripts published in International Journal of Medical Biochemistry reflect the views of the author(s) and not the opinions of the editors, the editorial board and the publisher; the editors, the editorial board and the publisher disclaim any responsibility or liability for such materials.

ABSTRACTING AND INDEXING

International Journal of Medical Biochemistry is indexed in TUBITAK TR Index (2019), CNKI (2019), TurkMedline (2019), Open Ukrainian Citation Index (2019), ProQuest (2019), CABI (2021), CEEAS (2021), EBSCO (2022), CAS (American Chemical Society) (2022), Directory of Open Access Journals - DOAJ (2022), Scopus (2023), Gale Cengage (2023), Sherpa Romeo (2024) and Asian Science Citation Index (ASCI) (2024).

ABBREVIATION

Int | Med Biochem

PUBLICATION FEE

International Journal of Medical Biochemistry is an open access journal. Manuscripts are available on the journal web page at no cost.

As of March 1, 2025, in order to further improve the quality and accessibility of the journal, a fee will be charged as a contribution to the cost of production. This fee will be charged during the process of application of submitted articles and will be charged regardless of eventual acceptance/rejection of the manuscript.

Foreign authors can complete the article submission process after depositing to the USD account below. No publication fee is charged for articles submitted by authors from Türkiye.

ACCESS TO JOURNAL CONTENT

The abstracts and full texts of published articles can be accessed free of charge at www.internationalbiochemistry.com.

JOURNAL FREQUENCY

The International Journal of Medical Biochemistry published three issues per year from its establishment until 2024. The journal has started publishing four issues per year since 2025. The publication months are January, April, July, and October.



INSTRUCTIONS FOR AUTHORS

OPEN ACCESS AND COMMONS USER LICENSES

Open Access: The International Journal of Medical Biochemistry is an open access journal which means that all content is freely available without charge to the user or his/her institution. Users are allowed to read, download, copy, distribute, print, search, or link to the full texts of the articles, or use them for any other lawful purpose, without asking prior permission from the publisher or the author. This is in accordance with the BOAI definition of open access.

Commons User Licenses: Creative Commons Attribution-NonCommercial (CC BY-NC) For non-commercial purposes, lets others distribute and copy the article, and to include in a collective work, as long as they credit the author(s) and provided they do not alter or modify the article.

AIMS & SCOPE

International Journal of Medical Biochemistry publishes articles relating to clinical chemistry, molecular biology and genetics, therapeutic drug monitoring and toxicology, hematology, immunology and laboratory medicine with the focus on analytical and clinical investigation of laboratory tests used for diagnosis, prognosis, treatment and therapy, and monitoring of disease. The official language of the Journal is English.

Abstracting and Indexing: International Journal of Medical Biochemistry is indexed in TUBITAK TR Index (2019), CNKI (2019), TurkMedline (2019), Open Ukrainian Citation Index (2019), ProQuest (2019), CABI (2021), CEEAS (2021), EBSCO (2022), CAS (American Chemical Society) (2022), Directory of Open Access Journals - DOAJ (2022), Scopus (2023), Gale Cengage (2023), Sherpa Romeo (2024) and Asian Science Citation Index (ASCI) (2024).

Main Topics

- Clinical Biochemistry
- Molecular Biology
- Clinical Haematology
- Clinical Immunology
- Drug Monitoring and Analysis
- Diagnostic Biomarkers
- Disease-Oriented Topics (Cardiovascular Disease, Cancers, Diabetes, Obesity, Genetic Disorders, Neurodegenerative Disease etc.)
- Pediatric Biochemistry
- Inherited Metabolic Disorders
- Newborn Screening: Congenital and Genetic Disorders
- New Reagents, Instrumentation, Technologies and Methodologies
- · Laboratory Medicine; Quality, Safety, Translational laboratory
- Bioinformatics
- Artificial intelligence applications in clinical biochemistry
- Metrology

INSTRUCTIONS FOR AUTHORS

International Journal of Medical Biochemistry is published in accordance with the principles of independent, unbiased, and double-blinded peer review Research-articles, review-articles, short communications, case-reports, opinion papers, letter to editor, technical notes, editorials and article-commentaries that have not been published elsewhere, are published in the journal.

The journal evaluates only the manuscripts submitted through its online submission system on the web site http://www.internationalbiochemistry.com Manuscripts sent by other means will not be accepted.

The primary conditions for the acceptance of manuscripts for publication are originality, scientific value and citation potential.

PUBLISHING FEE

International Journal of Medical Biochemistry is an open access journal. Manuscripts are available on the journal web page at no cost.

As of March I, 2025, in order to further improve the quality and accessibility of the journal, a fee will be charged as a contribution to the cost of production. This fee will be charged during the process of application of submitted articles and will be charged regardless of eventual acceptance/rejection of the manuscript.

Foreign authors can complete the article submission process after depositing to the USD account below. No publication fee is charged for articles submitted by authors from Türkiye.

Research Article - USD 1000.- (VAT included)

Systematic reviews and meta-analyses/Review - 1000.- (VAT included)

Case Report/Technical Note/Letter/Opinion - USD 700.- (VAT included)

Account Holder: KARE MEDYA LIMITED SIRKETI

Account Number: 26297654

IBAN: TR71 0006 7010 0000 0026 2976 54

SWIFT CODE: YAPITRISXXX

Address: Sahrayicedit, Ataturk Cad. No: 43A, Kadikoy, Istanbul, Turkiye

STATEMENTS AND GUIDELINES

Statements: All statements and opinions expressed in the manuscripts published in International Journal of Medical Biochemistry reflect the views of the author(s). All liability for the advertisements rests with the appropriate organization(s). Association of Clinical Biochemistry Specialists, the Editor-in-Chief and Kare Media do not accept any responsibility for articles and advertisements.

The manuscripts submitted to the journal, except abstracts, presentations, reviews and parts of theses, should not have been accepted and published previously elsewhere in electronic or printed format. Manuscripts evaluated and rejected by other journals must mention any previous submissions and supply reviewer's reports. This will help to accelerate the evaluation process. If the submitted manuscript has been previously presented at a meeting, the name, date, city and country must be specified.

The authors transfer all copyrights of the manuscript in the framework of national and international regulations to the Association of Clinical Biochemistry Specialists as of evaluation process. A Copyright Transfer Form signed by corresponding author in order must be submitted to the journal with manuscript. After acceptance of manuscript, all of authors must fill and sign Copyright Transfer form. A separate form for each manuscript should be submitted. Manuscripts submitted without a Copyright Transfer Form will not be accepted. In the case of rejection, all copyrights transfer to the authors again. Authors must confirm that they will not submit the work to another journal, publish it in the original or another language and or allow a third party to use the manuscript without the written permission of the Association of Clinical Biochemistry Specialists.

All contents are the authors' responsibility. All financial liability and legal responsibility associated with the copyright of submitted tables, figures and other visual materials protected by national and international laws rest with the authors. The authors take responsibility for any legal proceedings issued against the journal.



Rejected manuscripts will not be returned except for artwork.

To clarify scientific contributions and responsibilities and any conflict of interest issues relevant to the manuscript, all parts of the 'Authors' Contribution' form must be completed by the corresponding author and the 'ICMJE Uniform Disclosure Form for Potential Conflicts of Interest' must be completed online by all authors. Both forms should be included in the manuscript at the time of original submission.

Guidelines: The format of the manuscripts must be in accordance with the ICMJE Recommendations for the Conduct, Reporting, Editing and Publication of Scholarly Work in Medical Journals (updated in December 2014:http://www.icmje.org/icmje-recommendations.pdf).

The presentation of the manuscripts must be in accordance with international guidelines. CONSORT should be used for randomized trials, STROBE for observational studies, STARD for diagnostic studies, PRISMA for systematic reviews and meta-analyses, ARRIVE for animal studies, and TREND for non-randomized behavior and public health studies.

Ethics: All manuscripts will be vetted by the Editor-in-Chief's Office for possible plagiarism and duplication. Sanctions will be imposed in accordance with the guidelines of the Committee on Publication Ethics (COPE) when non-ethical issues arise. The authors must obtain the permission of the copyright holder for non-original tables, figures, graphs, images and other visuals.

The authors should acknowledge and provide detailed information on any contributions in kind and financial support given by any foundations, institutions and firms.

An ethics committee report prepared in conformity with the WMA Declaration of Helsinki - Ethical Principles for Medical Research Involving Human Subjects and the Guide for the Care and Use of Laboratory Animals is required to be submitted with experimental and clinical studies, drug trial studies and some case reports. Authors may be asked by the Editor-in-Chief's Office for an ethics committee report or similar in other circumstances also. Manuscripts reporting the results of experimental studies must explain in detail all procedures which volunteer subjects and patients have undergone and a statement indicating that consent for the study has been obtained from all subjects should be included in the text. Animal studies should clearly specify how pain or discomfort has been relieved.

PREPARATION AND SUBMISSION OF MANUSCRIPTS

Manuscript files should be prepared with Microsoft Office Word. The online submission system will direct authors during all stages of submission and provide necessary support for accelerating the submission process. A list of the files that should be supplied through the online submission system is provided below.

- I. Title Page
- 2. Main Text
- 3. Tables, Graphs and Figures
- 4. Copyright Transfer Form
- 5. Author Contribution Form

ICMJE Uniform Disclosure Form for Potential Conflicts of Interest.

MANUSCRIPT TYPES

Contributions may be in the form of clinical and basic Original Research articles, Reviews, Short communications, Case reports, Letters to the Editor, Opinion papers, Technical notes and Editorial Comment. The Journal also publishes brief reports on original studies or evaluations, book reviews, and proceedings of scientific meetings.

Original Research: Consists of Title, Authors, their addresses, Abstract, Key Words, Introduction, Materials and Methods, Results, Discussion, Ethical Considerations (if necessary), Acknowledgements, Conflict of Interest, References, Figure Legends, Figures, and Tables. It should not exceed 5000 words excluding the references. The manuscript should have no more than 50 references and a total of 6 tables and/or figures.

Review: Reviews prepared by authors with extensive knowledge on a particular field, which has been reflected in international literature by a high number of publications and citations, are evaluated. The authors may be invited by the Editor-in-Chief. A review should be prepared in the format describing, discussing and evaluating the current level of knowledge or topic that is to be used in the clinical practice and it should guide further studies. A review article consists of Title, Authors, their addresses, Abstract, Key Words, Introduction, Main Sections under headings written in bold and sentence case, Subsections (if any) under headings written in italic and numbered consecutively with Arabic numerals, Conclusion, Acknowledgements, Conflict of Interest, References, Figure Legends, Figures, and Tables. The manuscript should have no more than 75 references and a total of 6 tables and/or figures. Supplemental data are permitted for Review articles. Abstract should not include subheadings and should be limited to 300 words. Keywords section should contain a minimum of three and a maximum of six items in accordance with Medical Subject Headings (MeSH) terms prepared by the National Library of Medicine (NLM) and should be provided just below the abstract. Main Text should include Introduction, other subheadings and Conclusion sections and should be limited to 5000 words excluding the references. Tables, Figures and Images should be provided after the reference list according to their order of appearance in the text.

NOTE: The originality of the visuals included in the reviews should be assured by submission of an accompanying letter by the authors. Appropriate citation should be done for the visuals adapted from previously published sources, in accordance with the original versions of the printed or electronic copies. The written permission obtained from the copyright holder (publisher, journal or authors) should be sent to the Editor-in-Chief's Office.

Short communications: These manuscripts are intended to concise and quick publishing of a new finding. Publishing of research articles under this concept is decided by the Editorial Board, providing that the authors adhere to the publishing format. The general format of this type of manuscript is similar to that of research articles except the word and reference limitations. For the short communications, main text should not exceed 1,500 words and number of references should not exceed 15.

Case Report: Since a limited number of case reports is published, only reports which are related to rare cases and conditions that constitute challenges in diagnosis and treatment, offer new methods or suggest knowledge not included in books, and are interesting and educational are accepted for publication. A case presentation consists of Title, Authors, their addresses, Abstract, Key Words, Introduction, Patients and Methods, Results, Discussion, Conclusion, Ethical Considerations, Acknowledgements, Conflict of Interest, References, Figure Legends, Figures, and Tables. Main Text should not exceed 1500 words excluding the references. The reference list should follow the main text and the number of references should be limited to 15. Tables, Figures and Images should be provided after the reference list according to their order of appearance in the text and should be limited to two.

Letter to the Editor: Letters to the Editor aim to discuss the importance of a manuscript previously published in the journal. This type of manuscripts should also include a comment on the published manuscript. Moreover, articles on topics of interest to readers within the scope of the journal, especially on educational issues, can be published in the format of a Letter to the Editor. It consists of title, main text and references sections. Abstract, Keywords, Tables, Figures and Images, and other visuals are



not included. Main Text should not include subheadings and it should be limited to 500 words. The reference list should follow the main text and the number of references should be limited to five. The volume, year, issue, page numbers, authors' names and title of the manuscript should be clearly stated, included in the list of references and cited within the text.

Opinion papers: Opinions on the topics within the scope of the journal that are prepared by the experts are published in this section. An opinion consists of Title, Authors, their addresses, Abstract, Key Words, Introduction, Discussion, Conclusion, Ethical Considerations (if necessary), Acknowledgements, Conflict Of Interest, References, Figure Legends, Figures, and Tables. Editorial Board decides the eligibility of an opinion with respect to its concept and language. For the opinions, main text should not exceed 1,500 words and number of references should not exceed 15.

Technical reports: Manuscripts on development and application of new methodologies are published in this category. A technical report consists of Title, Authors, their addresses, Abstract, Key Words, Introduction including the main aspects of the method involved, Materials and Methods, Results, Discussion, Ethical Considerations (if necessary), Acknowledgements, Conflict of Interest, References, Figure Legends, Figures, and Tables. Data analysis should be presented in Materials and Methods. Clinical technical reports should include and discuss the clinical significance of values and their deviations. For the technical reports, main text should not exceed 1,500 words and number of references should not exceed 10.

Editorial Comment: Authors are selected and invited by the Editorin-Chief. This type of manuscript aims at providing a brief commentary on an article published in the journal by a researcher who is an authority in the relevant field or by the reviewer of the article. It should consist of title, main text and references sections. Main Text should not include subheadings and should be limited to 500 words. The reference list should follow the main text and the number of references should be limited by 15. Abstract, Keywords, Tables, Figures, Images and other visuals are not included in editorial comments.

PREPARATION OF MANUSCRIPTS

Manuscripts should be prepared according to the above mentioned word and reference limitations and other related information. Language: Manuscripts should be written in clear and concise English. Please have your text proofread by a native English speaker before you submit for consideration.

The manuscripts submitted to our journal are classified and evaluated according to the manuscript types stated below. During preliminary evaluation, the editors assess whether a manuscript's format and subheadings are prepared in accordance with the journal's guidelines. Therefore, it is important that authors check the accuracy of the main text in terms of the following.

Title Page: Title should be concise and informative and reflect the content of the manuscript and should not exceed 15 words. Avoid abbreviations and formulae where possible. It should be written in sentence case; that is, first letter of the initial word should be written in capital letter and rest of the title should be typed with lower case letters except proper nouns and abbreviations.

Information about the authors and their institutions should not be included in the main text, tables and figures. Since submitted manuscripts are evaluated by the reviewers through the online system, personal identification is excluded in the interests of unbiased interpretation. Thus, only information about the manuscript as specified below should be included on the title page. For each type of manuscript, it is mandatory to upload a title page as a separate Microsoft Word document through the online submission system. The title page should include the names of the authors with their latest academic degrees, and the name of the department and institution, city and country where the study was conducted. If the study was conducted in several institutions, the affiliation of each author must be specified with

symbols. The first letters of authors' names and surnames should begin with capital letter and the rest should be written in lower case letters. If there is more than one author, corresponding author should be indicated.

The correspondence address should contain the full name of the corresponding author, postal and e-mail addresses, phone and fax numbers. If the content of the manuscript has been presented before, the name, date and place of the meeting must be noted. Disclosure of conflict of interest, institutional and financial support, author contributions and acknowledgments should be included on the title page.

Structured Abstract: It should be structured with Objective, Methods, Results and Conclusion subheadings and should be limited to 300 words. The abstract should state briefly the purpose of the research, the principal results and major conclusions. An abstract is often presented separately from the article, so it must be able to stand alone. For this reason, References should be avoided. Also, non-standard or uncommon abbreviations should be avoided, but if essential they must be defined at their first mention in the abstract itself. Level of evidence has to be stated at the end of the abstract as a separate paragraph.

Keywords: This section should contain a minimum of three and a maximum of six items in accordance with Medical Subject Headings (MeSH) terms prepared by the National Library of Medicine (NLM) and should be placed just below the abstract.

Main Text: Text should be prepared with MS Word document. All text should be written with Arial font type at 12 font size and double spaced on A4 sized paper with 1 cm right margin and 3 cm other margins. Header and/or footer should not be inserted in the text except that the pages should be numbered with Arabic numerals. Main text should consist of title, introduction, materials and methods, results and discussion

Introduction: State the objectives of the work and provide an adequate background, avoiding a detailed literature survey or a summary of the results. The unnecessary details and excessive references should be avoided. Hypothesis and the aim of the study should be stated in the introduction.

Material and methods: Provide sufficient detail to allow the work to be reproduced. Methods already published should be indicated by a reference: only relevant modifications should be described. Design and place of the study, subjects/patients, if applicable, information on the treatment procedures, statistical methods and information on the adherence to the ethical rules should be indicated.

Statistical analysis should be conducted in accordance with the guidelines on reporting statistical data in medical journals. The software used for statistical analysis must be described. The outcomes of statistical analyses and interpretation of the results must be in evidence-based scientific language. Statistics- statistical methods should be explained in detail in the Materials and Methods so that if original data is given, the results can be verified. If possible, quantitative results should be given and appropriate indicators should be used to indicate measurement error or uncertainty.

Results: Results should be clear and concise. Results must be concise and include figures and tables. Descriptive statistics should be compatible with the nature of data and statistical analyses used. The graphs should be prepared to reflect the important features of data. Please avoid excessive figures and tables.

Tables, Graphs and Figures

- Tables, Graphs, Figures and other visuals should be numbered in the order of their citation within the text and names of patients, doctors and institutions should not be disclosed.
- Tables should be prepared in a Microsoft Office Word document using the command 'Insert Table' and inserted at the end of the references in the main text.



- Tables should not be submitted in JPEG, TIFF or other visual formats.
 For microscopic images, the magnification ratio and staining technique used should be specified in addition to figure legends.
- Roman numbers should be avoided in tables and figures within the text and their titles. Each table should be clearly labeled and numbered consecutively with Arabic numerals (Table 1, Table 2, etc.). The abbreviations used must be defined. As with the text, reporting of concentration units consists of analyte concentrations expressed in the text in the traditional mass unit (mg/dL, ng/ml, and so forth) followed by the SI unit in parentheses
- The thickness of the lines in graphs should be sufficient to minimize loss of quality if size reduction is needed during the printing process.
 The width of the graphs should be 9 cm or 18 cm. Drawings should be performed by professionals. No grey colours should be used.
- Abbreviations should be explained in alphabetical order at the bottom of the tables, graphs and figures.
- Explanations should be at the bottom of the table as footnotes.
- Tables should not be divided into parts. Separate parts (Table IA, Table IB, etc.) will be considered separate tables and will count toward your overall table/figure count.
- Table captions should be limited to 60 words.
- Tables should be easily understandable and should not repeat the data in the main text.
- In addition to the pictures included in case reports and original images, video and movie images are published on the journal's website. These images should be prepared in MPEG format with a maximum size of 2 MB. They should be submitted to the journal with the manuscript documents. The names of patients, doctors, institutions and places should be omitted from all documents.
- All figures must be uploaded separately as image files in Tagged Image
 File Format (.TIFF) or Encapsulated Postscript (.EPS). Microsoft
 Power Point (.PPT) is also acceptable; however, the graphics must
 contain embedded fonts with one image per slide, one slide per file.
 Each image should have a resolution of 600 dots-per-inch (dpi).
- Indicate each footnote in a table with a superscript lowercase letter.

Discussion: This should explore the significance of the results of the work, not repeat them. A combined Results and Discussion section is often appropriate. Avoid extensive citations and discussion of published literature.

Conclusions: The main conclusions of the study may be presented in a short Conclusions section, which may stand alone or form a subsection of a Discussion or Results and Discussion section.

Appendices: If there is more than one appendix, they should be identified as A, B, etc. Formulae and equations in appendices should be given separate numbering: Eq. (A.1), Eq. (A.2), etc.; in a subsequent appendix, Eq. (B.1) and so on. Similarly for tables and figures: Table A.1; Fig. A.1, etc.

Abbreviations: Define abbreviations that are not standard in this field in a footnote to be placed on the first page of the article. Such abbreviations that are unavoidable in the abstract must be defined at their first mention there, as well as in the footnote. Ensure consistency of abbreviations throughout the article.

Acknowledgements: Collate acknowledgements in a separate section at the end of the article before the references and do not, therefore, include them on the title page, as a footnote to the title or otherwise. Financial and/or technical (running of tests, evaluation of results, providing language help, writing assistance or proof reading the article, etc.) supports of the study should be mentioned following Ethical Considerations including the

project number. If the study originates from a thesis or has been previously presented in a meeting, this should also be indicated in this section. Contribution of each author should be declared in this section.

Nomenclature and units: Follow internationally accepted rules and conventions: use the international system of units (SI). If other quantities are mentioned, give their equivalent in SI. Authors wishing to present a table of nomenclature should do so on the second page of their manuscript. You are urged to consult IUB: Biochemical Nomenclature and Related Documents for further information.

Footnotes: It should be used sparingly. Number them consecutively throughout the article, using superscript Arabic numbers. Many word processors build footnotes into the text, and this feature may be used. Should this not be the case, indicate the position of footnotes in the text and present the footnotes themselves separately at the end of the article. Do not include footnotes in the Reference list.

Math formulae: Please submit math equations as editable text and not as images. Present simple formulae in line with normal text where possible and use the solidus (/) instead of a horizontal line for small fractional terms, e.g., X/Y. In principle, variables are to be presented in italics. Powers of e are often more conveniently denoted by exp. Number consecutively any equations that have to be displayed separately from the text (if referred to explicitly in the text).

Special Terms and Conditions: For double-blinded peer-review process, the names of the corresponding author and other authors, their affiliations and any information on the study centres should not be included in any part of the submitted manuscripts and images, except the Title Page. This information should be added to the relevant section of the online submission system and included in the Title Page.

Pharmaceutical products should be written with their generic names and brand and company names, city and country should be specified for medical equipment and devices.

For centrifugation, angular velocity (xg) should be given. Period should be used to show decimals.

Enzymes: Full name of an enzyme and its International Union of Biochemistry and Molecular Biology (IUBMB) Enzyme Commission number (EC number) should be given when that enzyme was first mentioned in the text. Its abbreviation can be used after that. For detailed information, authors can refer to the Enzyme Nomenclature of IUBMB (www.chem. qmul.ac.uk/iubmb/enzyme). Enzyme activity should be given in terms of U/L in serum or plasma and U/mg protein in tissues. Unit (U) should be given as reaction rate triggered under defined conditions. SI unit for enzyme activity is defined as katal which is the moles of substrate converted to product per second. However, it can also be defined as μmol/sec or μmol/min as long as clear and precise definitions are given.

References

- References should start on a separate page. Published manuscripts
 and manuscripts that have been accepted and are pending publication
 should be cited in the reference list. Acceptance letter of the
 manuscripts that are pending publication should be submitted with
 the manuscript. Unpublished results should be written in text
 in parenthesis as "(unpublished result)". If such a work is cited,
 permission from the responsible researcher should be obtained and
 submitted with the manuscript.
- At least two-thirds of the references should be articles published in the last 5 years. The reference list containing all authors mentioned in the text, should be arranged in the order of appearance and numbered accordingly by Arabic numerals in in square brackets in line with the text. When more than one reference is cited consecutively, not all of the reference numbers should be written separated by comas; instead the numbers of first and the last reference cited for that section

INTERNATIONAL JOURNAL OF MEDICAL BIOCHEMISTRY

should be written with a dash in the middle (i.e.: writing as "10, 11, 12, 13" is wrong, but "10-13" is correct). Citation of a reference as 'in press' implies that the item has been accepted for publication.

- References that are inaccessible and not indexed in any database should not be cited.
- The actual authors can be referred to, but the reference number(s) must always be given. Example: '.... as demonstrated [7,8]. Dildar and Murat [9] obtained a different result'
- Authors' names are inverted (last name, first/second initial). Do not add periods or commas within an individual author name; however, separate author names with a comma and end the author list with a period (Konukoglu D, Ilhan N, Orem A)
- The Journal names should be abbreviated as indicated at PubMed.
- For references with six and fewer authors, all authors should be listed. For references with more than six authors, the first six authors should be listed, followed by 'et al'.
- Do not add a period after the journal abbreviation, but continue with a space followed by the year.
- The year should be followed by a semicolon and then the volume number, which is followed by a colon and then the page numbers.
 Delete redundant numbers, for example 2017;12:101-15.
- Do not include the months in parentheses; this information is not needed.
- Use inclusive page numbers for articles and book chapters.

Data References: This journal encourages you to cite underlying or relevant datasets in your manuscript by citing them in your text and including a data reference in your Reference List. Data references should include the following elements: author name(s), dataset title, data repository, version (where available), year, and global persistent identifier. Add [dataset] immediately before the reference so we can properly identify it as a data reference. The [dataset] identifier will not appear in your published article.

Web References: As a minimum, the full URL should be given and the date when the reference was last accessed. Any further information, if known (DOI, author names, dates, reference to a source publication, etc.), should also be given. Web references can be listed separately (e.g., after the reference list) under a different heading if desired, or can be included in the reference list.

References in a Special Issue: Please ensure that the words 'this issue' are added to any references in the list (and any citations in the text) to other articles in the same Special Issue. The style and punctuation of the references should be formatted as in the following examples.

Technical Reports: Surname(s) and initial(s) of the author(s), title of the technical report, name and place of the publisher, report number, if applicable, publication year. The style and punctuation of the references should be formatted as in the following examples. Journal Article

- Journal article with six or fewer authors: Bozluolcay M, Andican G, Firtina S, Erkol G, Konukoglu D. Inflammatory hypothesis as a link between Alzheimer's disease and diabetes mellitus. Geriatr Gerontol Int 2016 16(10):1161-66
- Journal article with more than six authors: Koca SS, Kara M, Özgen M, Dayanan R, Demir CF, Aksoy K, et al. Low prevalence of obesity in Behçet's disease is associated with high obestatin level. Eur J Rheumatol 2017; 4 (2):113-17.
- Abstract: Hortin GL, King C, Kopp J. Quantification of rhesus monkey albumin with assays for human microalbumin [Abstract]. Clin Chem 2000;46:A140-
- Editorial: Demers LM. New biochemical marker for bone disease: is it a breakthrough? [Editorial]. Clin Chem 1992;38:2169–70.
- Letter to the Editor: Davey L, Naidoo L. Urinary screen for acetaminophen (paracetamol) in the presence of N-acetylcysteine [Letter]. Clin Chem 1993;39:2348–9.

- Book Chapter: Rifai N, Warnick GR. Lipids, lipoproteins, apolipoproteins, and other cardiovascular risk factors. In: Burtis CA, Ashwood ER, Bruns DE, editors. Tietz textbook of clinical chemistry and molecular diagnostics. 4th Ed. St. Louis (MO): Elsevier Saunders; 2006. p. 903-81.
- Book: Personal Author Harrell FE Jr. Regression modeling strategies. New York (NY): Springer; 2001. Bailar JC III, Mosteller F, editors. Medical uses of statistics. 2nd Ed. Boston (MA): NEIM Books; 1992:449 p.
- Book with Single Author Cohn PF. Silent myocardial ischemia and infarction. 3rd ed. New York: Marcel Dekker; 1993.
- Editor(s) as author: Norman IJ, Redfern SJ, editors. Mental health care for elderly people. New York: Churchill Livingstone; 1996
- Technical Reports Tschantz BA, Moran B. Modeling of the hydrologic transport of mercury in the Upper East Fork Poplar Creek (UEFPC) watershed. Technical Report for Lockheed Martin Energy Systems: Bethesda, MD, September 2004.
- Supplement Castelli WP. Lipids, risk factors and ischaemic heart disease. Atherosclerosis 1996;124 Suppl:S1-9.
- Epub ahead of print Milbury CA, Li J, Makrigiorgos GM. PCR-based methods for the enrichment of minority alleles and mutations. [Epub ahead of print] Clin Chem February 6, 2009 as doi:10.1373/ clinchem.2008.113035.
- Internet Source: American Association for Clinical Chemistry. AACC continuing education. http://www.aacc.org/education-and-career/ continuing-education(Accessed June 2016).

Reviewer Suggest: Authors may suggest at least two reviewer in the Comments to Editorial Office pane in the submission process.

EVALUATION AND PUBLICATION

The main text submitted to the journal must be in English. Manuscripts written in other languages are not accepted. Citation potential is higher for manuscripts in English.

The Editor-in-Chief's Office checks the conformity of the manuscript with the journal's general guidelines before sending it to associate editors and reviewers. Any manuscripts not prepared in accordance with the journal's guidelines will be returned for revision. The evaluation period is limited to 30 days. If revision is requested, authors should submit their revised manuscripts within 45 days. Manuscripts and revisions should be submitted through the online manuscript submission system at the website http://www.internationalbiochemistry.com. Manuscripts sent by e-mail will not be accepted.

Manuscripts are evaluated in accordance with the principles of doubleblinded peer review. Of the submitted manuscripts, those considered to be suitable are subjected to evaluation in terms of style, format and in terms of their content by the Editor-in-Chief. Manuscripts considered to be scientifically adequate are assigned to three reviewers. These reviewers are independent experts and members of the editorial board who have published internationally on the topic of the manuscript. Research articles, systematic reviews and meta-analyses are also evaluated by the Editor-in-Chief's statistician counsellors in addition to peer review. When needed, the manuscripts are scanned by the Editor-in-Chief's Office using the iThenticate program for determination of plagiarism and non-ethical situations. Also, all manuscripts are reviewed and edited for compliance with the rules of English grammar. All contributing authors of a manuscript accepted for publication are deemed to have accepted the right of editors to make corrections provided that no fundamental change is made to the basic meaning of the original text. Manuscripts not accorded priority for publication by the Editorin-Chief, Editor, Associate Editors and Referees are rejected.

The retraction requests of the manuscripts close to the final decision in evaluation process, without any reasonable explanation (not contrary to

INTERNATIONAL JOURNAL OF MEDICAL BIOCHEMISTRY

the Publication Ethics) is considered in the scope of rejection decision. Manuscripts that are not revised and resubmitted within the specified time and fail to notify the journal accordingly will be rejected.

Once a manuscript is accepted for publication, addition to the author list, removal from the author list and order change cannot be effected.

Manuscripts accepted for publication are prepared as 'Epub ahead of print articles' and published with an assigned DOI on the journal website http://www.internationalbiochemistry.com.

Information on the latest status of manuscripts submitted for evaluation and other information about the journal are available on the website http://www.internationalbiochemistry.com. Contact details for the Editor-in-Chief's Office and the publisher are given below.

Online proof correction: Corresponding authors will receive an e-mail with a link to our online proofing system, allowing annotation and correction of proofs online. The environment is similar to MS Word: in addition to editing text, you can also comment on figures/tables and answer questions from the Copy Editor. Web-based proofing provides a faster and less error-prone process by allowing you to directly type your corrections, eliminating the potential introduction of errors.

If preferred, you can still choose to annotate and upload your edits on the PDF version. All instructions for proofing will be given in the e-mail we send to authors, including alternative methods to the online version and PDF.

We will do everything possible to get your article published quickly and accurately. Please use this proof only for checking the typesetting, editing, completeness and correctness of the text, tables and figures. Significant changes to the article as accepted for publication will only be considered at this stage with permission from the Editor. It is important to ensure that all corrections are sent back to us in one communication. Please check

carefully before replying, as inclusion of any subsequent corrections cannot be guaranteed. Proofreading is solely your responsibility.

Submission checklist: You can use this list to carry out a final check of your submission before you send it to the journal for review. Please check the relevant section in this Guide for Authors for more details.

Ensure that the following items are present: One author has been designated as the corresponding author with contact details:

- · ORCID ID for all authors
- E-mail address
- Full postal address
- All necessary files have been uploaded: Manuscript: Include keywords
- All figures (include relevant captions)
- All tables (including titles, description, footnotes)
- Ensure all figure and table citations in the text match the files provided
 Indicate clearly if color should be used for any figures in print Graphical Abstracts / Highlights files (where applicable) Supplemental files (where applicable) Further considerations
- Manuscript has been 'spell checked' and 'grammar checked'
- All references mentioned in the Reference List are cited in the text, and vice versa
- Permission has been obtained for use of copyrighted material from other sources (including the Internet)
- A competing interests statement is provided, even if the authors have no competing interests to declare
- Journal policies detailed in this guide have been reviewed
- Referee suggestions and contact details provided, based on journal requirements

ETHICS AND POLICIES

Advertisement Policy

The International Journal of Medical Biochemistry does not accept advertisements; the journal is sponsored by the Association of Clinical Biochemistry Specialists Turkey. The Journal has no direct marketing policy.

Archiving Policy

The content published by the International Journal of Medical Biochemistry is electronically preserved by using internet archive. https://internationalbiochemistry.com/jvi.aspx?pdir=ijmb&plng=eng&list=pub

Authorship Policy

All statements and opinions expressed in the manuscripts published in the International Journal of Medical Biochemistry reflect the views of the author(s).

Each individual listed as an author should fulfill the authorship criteria recommended by the International Committee of Medical Journal Editors (ICMJE). The ICMJE recommends that authorship should be based on the following 4 criteria:

Substantial contributions to the conception or design of the work, or the acquisition, analysis, or interpretation of data for the work; AND

Drafting the work or revising it critically for important intellectual content; $\ensuremath{\mathsf{AND}}$

Final approval of the version to be published; AND

Agreement to be accountable for all aspects of the work in ensuring that questions related to the accuracy or integrity of any part of the work are appropriately investigated and resolved.

In addition to being accountable for their own work, authors should have confidence in the integrity of the contributions of their co-authors and each author should be able to identify which co-authors are responsible for other parts of the work.

All of those designated as authors should meet all four criteria for authorship, and all who meet the four criteria should be identified as authors. Those who provided a contribution but do not meet all four criteria should be recognized separately on the title page and in the Acknowledgements section at the conclusion of the manuscript.

The International Journal of Medical Biochemistry requires that corresponding authors submit a signed and scanned version of the authorship contribution form (available for download through) during the initial submission process in order to appropriately indicate and observe authorship rights and to prevent ghost or honorary authorship. Please note that the list of authors on the final manuscript will be presented in the order provided on this form. If the editorial board suspects a case of "gift authorship," the submission will be rejected without further review. As part of the submission of the manuscript, the corresponding author should also send a short statement declaring that they accept all responsibility for authorship during the submission and review stages of the manuscript.

Complaint and Appeal Policy

Appeal and complaint cases are handled within the scope of COPE guidelines by the Editorial Board of the journal. Appeals should be based on the scientific content of the manuscript. The final decision on the appeal and complaint is made by Editor in Chief. An Ombudsperson or the Ethical Editor is assigned to resolve cases that cannot be resolved internally. Authors should get in contact with the Editor in Chief regarding their appeals and complaints via e-mail at kare@karepb.com



Corrections Policy

If the editors or publisher learn from a third party that a published work contains a material error or inaccuracy, the authors must promptly correct or retract the article or provide the journal editors with evidence of the accuracy of the article.

Ethics Policy

The Editorial Board of the International Journal of Medical Biochemistry and the Publisher adheres to the principles of the International Council of Medical Journal Editors (ICMJE), the World Association of Medical

Editors (WAME), the Council of Science Editors (CSE), the Committee on Publication Ethics (COPE), the US National Library of Medicine (NLM), the World Medical Association (WMA) and the European Association of Science Editors (EASE).

The manuscripts should be prepared in accordance with ICMJE-Recommendations for the Conduct, Reporting, Editing, and Publication of Scholarly Work in Medical Journals (updated in May 2022 - https://www.icmje.org/recommendations/).

Authors are required to prepare manuscripts in accordance with the international guidelines* below.

Case Report	CARE (CAse REport)
Methodological Studies (Developing Tests)	COSMIN (COnsensus based Standarts fort the selection of Health Measurement Instruments- Study Design for Patient-reported outcome measurement instruments)
Adapting Tests)	COOMIN (CO
Methodological Studies (Translating and	ITC (International Test Commission) Guidelines for Translating and Adapting Tests
	-COREQ (COnsolidated criteria for REporting Qualitative research: interviews and focus groups
Qualitative Research	-SRQR (the Standards for Reporting Qualitative Research)
Systematic Reviews and Meta-Analyses Protocol	PRISMA-P (the Preferred Reporting Items for Systematic Reviews and Meta-Analyses - Protocol)
Systematic Reviews and Meta-Analyses	PRISMA (the Preferred Reporting Items for Systematic Reviews and Meta-Analyses)
Observational Epidemiologic Studies (cohort, case-control, cross-sectional)	STROBE (the STrengthening the Reporting of OBservational studies in Epidemiology)
Trial Protocol	SPIRIT (Standard Protocol Items Recommendations for Interventional Trials)
Non-Randomized Trial **	TREND (Transparent Reporting of Evaluations with Non-randomised Designs)
Randomized Controlled Trial **	CONSORT (Consolidated Standards of Reporting Trials)

 $^{^{*}}$ Enhancing the QUAlity and Transparency of Health Research (equator network).

In accordance with the journal's policy, an approval of research protocols by an ethics committee in accordance with international agreements "WMA Declaration of Helsinki - Ethical Principles for Medical Research Involving Human Subjects (last updated: October 2013, Fortaleza, Brazil)", "Guide for the care and use of laboratory animals (8th edition, 2011)" and/or "International Guiding Principles for Biomedical Research Involving Animals (2012)" is required for all research studies. If the submitted manuscript does not include ethics committee approval, it will be reviewed according to COPE's guideline (Guidance for Editors: Research, Audit and Service Evaluations). If the study should have ethical approval, authors will be asked to provide ethical approval in order to proceed the review process. If they cannot provide ethical approval, their manuscript will be rejected and also their institutions and when needed, the related bodies in their country will be informed that such studies must have ethics committee approval. If they provide approval, review of the manuscript will continue.

If the study does not need ethics committee approval after the editorial board's review, the authors will be asked to provide an ethics committee approval or a document given by a related independent committee that indicates the study does not need ethics committee approval according to the research integrity rules in their country. If the authors provide either an approval or a document showing that ethics approval is not needed, the review process can be continued. If the authors cannot provide either documents, the manuscript may be rejected.

For articles concerning experimental research on humans, a statement should be included that shows informed consent of patients and volunteers was obtained following a detailed explanation of the procedures that they may undergo. The journal may request a copy of the Ethics Committee Approval received from the relevant authority. Informed consent must also be obtained for case reports and clinical images.

Studies using human or animal subjects should be approved by the appropriate institutional and local Ministry of Health ethics committees. Ethics approval of research protocols in accordance with international agreements is required for experimental, clinical, and drug studies, as well as for some case reports. Ethics committee reports or an equivalent official document may be requested from the authors. For manuscripts involving experimental research on humans, a statement should be included that shows that written, informed consent of patients and volunteers was obtained. For studies carried out on animals, the measures taken to prevent pain and suffering of the animals should be stated clearly. A statement regarding patient consent, and the name of the ethics committee, the ethics committee approval date, and number should be stated in the Materials and Methods section of the manuscript. It is the authors' responsibility to carefully protect patients' anonymity.

Research Ethics for Vulnerable Populations

At the International Journal of Medical Biochemistry, we are committed to upholding the highest ethical standards in all research involving human participants, especially vulnerable populations such as children. In line with our dedication to responsible and respectful research practices, we have established the following guidelines to ensure the protection and ethical treatment of these groups:

Consent Requirements for Children

Parental/Guardian Consent: For all research involving children under the age of 18, written informed consent must be obtained from a parent or legal guardian. This consent must be informed, voluntary, and documented.

Assent from Children: In addition to parental consent, researchers are required to obtain assent from children who are capable of forming an

^{**} The International Journal of Medical Biochemistry encourages the registration of all clinical trials (randomized and non-randomized) via ClinicalTrials.gov or one of the registries of the WHO's International Clinical Trials Registry Platform (ICTRP). The name of the trial registry and the registration number together should be provided at the end of the abstract.

opinion and making a decision regarding their participation in the study. This process must be age-appropriate and must respect the child's level of understanding and autonomy.

Privacy and Confidentiality: Extra precautions will be taken to protect the privacy and confidentiality of child participants. This includes using pseudonyms, removing identifiable details from published data, and securely storing data.

Ethical Review: All studies involving children must undergo a rigorous ethical review process to ensure that the research is justified, and the potential benefits outweigh any risks. The ethical review will also ensure that the study adheres to the principles of beneficence, non-maleficence, and justice.

Oversight and Monitoring

To ensure adherence to these ethical guidelines, the International Journal of Medical Biochemistry requires that all studies involving vulnerable populations be reviewed and monitored by an Institutional Review Board (IRB) or an equivalent ethical oversight committee. This committee will oversee the study from its inception to its completion, ensuring continuous protection of the participants' rights and well-being.

For more details on our research ethics policies and procedures, or to report any concerns regarding the ethical conduct of a study published in our journal, please contact our ethics committee at kare@karepb.com.

Fee Waiver Policy

There is no fee waiver.

Funding Sources Policy

All authors are required to declare what support they received to carry out their research. Declaring funding sources acknowledges funders' contributions, fulfills funding requirements, and promotes greater transparency in the research process.

Each author must individually declare all sources of funding received for the research submitted to the journal. This information includes the name of granting agencies, grant numbers, and a description of each funder's role. If the funder has played no role in the research, this must be stated as well.

Authors are not required to provide the complete list of every single grant that supports them if the grant is not related to the research published.

Licenses and Copyright Policy

Authors publishing with the journal retain the copyright to their work licensed under the Creative Commons Attribution-NonCommercial 4.0 International license (CC BY-NC 4.0) and grant the Publisher non-exclusive commercial right to publish the work. CC BY-NC 4.0 license permits unrestricted, non-commercial use, distribution, and reproduction in any medium, provided the original work is properly cited.

Open Access Policy

The International Journal of Medical Biochemistry supports the Budapest Open Access Initiative statement of principles that promotes free access to research literature. The declaration defines open access to academic literature as free availability on the internet, permitting users to read, record, copy, print, search, or link to the full text, examine them for indexing, use them as data for software or other lawful purposes without financial, legal, or technical barriers. Information sharing represents a public good, and is essential to the advancement of science. Therefore, articles published in this journal are available for use by researchers and other readers without permission from the author or the publisher provided that the author and the original source are cited. The articles in the International Journal of Medical Biochemistry are accessible through search engines, websites, blogs, and other digital platforms. Additional details on the Budapest Open Access Initiative and their guidelines are available at https://www.budapestopenaccessinitiative.org.

Open Access Policy is based on rules of Budapest Open Access Initiative the International Journal of Medical Biochemistry applies the Creative Commons Attribution-NonCommercial 4.0 International (CC BY-NC 4.0) license articles we publish. If you submit your paper for publication, you agree to have the CC BY-NC 4.0 license applied to your work. Under this Open Access license, you as the author agree that anyone can copy, distribute or reuse the content of your article for non-commercial purposes for free as long as the author and original source are properly cited. The corresponding author must sign the Creative Commons License Agreement after their articles are accepted.

Open Access Statement

The journal is an open access journal and all content is freely available without charge to the user or his/her institution. Except for commercial purposes, users are allowed to read, download, copy, print, search, or link to the full texts of the articles in this journal without asking prior permission from the publisher or the author. This is in accordance with the BOAI definition of open access. The open access articles in the journal are licensed under the terms of The open access articles in the journal are licensed under the terms of the Creative Commons Attribution-NonCommercial 4.0 International (CC BY-NC 4.0) license.



Peer Review Policy

Only those manuscripts approved by its every individual author and that were not published before in or sent to another journal, are accepted for evaluation.

Submitted manuscripts that pass preliminary control are scanned for plagiarism using iThenticate software. After plagiarism check, the eligible ones are evaluated by Editor-in-Chief for their originality, methodology, the importance of the subject covered and compliance with the journal scope. Editor-in-Chief evaluates manuscripts for their scientific content without regard to ethnic origin, gender, sexual orientation, citizenship, religious belief or political philosophy of the authors and ensures a fair double-blind peer review of the selected manuscripts.

The selected manuscripts are sent to at least two national/international referees for evaluation and publication decision is given by Editor-in-Chief upon modification by the authors in accordance with the referees' claims.

Editor-in-Chief does not allow any conflicts of interest between the authors, editors and reviewers and is responsible for final decision for publication of the manuscripts in the Journal.

Reviewers' judgments must be objective. Reviewers' comments on the following aspects are expected while conducting the review.

- Does the manuscript contain new and significant information?
- Does the abstract clearly and accurately describe the content of the manuscript?
- Is the problem significant and concisely stated?
- Are the methods described comprehensively?
- Are the interpretations and consclusions justified by the results?
- Are adequate references made to other Works in the field?
- Is the language acceptable?

Reviewers must ensure that all the information related to submitted manuscripts is kept as confidential and must report to the editor if they are aware of copyright infringement and plagiarism on the author's side.

A reviewer who feels unqualified to review the topic of a manuscript or knows that its prompt review will be impossible should notify the editor and excuse himself from the review process.



The editor informs the reviewers that the manuscripts are confidential information and that this is a privileged interaction. The reviewers and editorial board cannot discuss the manuscripts with other persons. The anonymity of the referees is important.

Plagiarism Policy

All submissions are screened using similarity detection software at least two times: on submission and after completing revisions. In the event of alleged or suspected research misconduct, e.g., plagiarism, citation manipulation, or data falsification/fabrication, the editorial board will follow and act in accordance with COPE guidelines. Plagiarism, including self-plagiarism, that is identified at any stage will result in rejection of the manuscript.

Publication Charges Policy

As of March I, 2025, in order to further improve the quality and accessibility of the journal, a fee will be charged as a contribution to the cost of production. This fee will be charged during the process of application of submitted articles and will be charged regardless of eventual acceptance/ rejection of the manuscript.

Foreign authors can complete the article submission process after depositing to the USD account below. No publication fee is charged for articles submitted by authors from Türkiye.

Research Article - USD 1000.- (VAT included)

Systematic reviews and meta-analyses/Review - 1000.- (VAT included)

Case Report/Technical Note/Letter/Opinion - USD 700.- (VAT included)

Account Holder: KARE MEDYA LIMITED SIRKETI

Account Number: 26297654

IBAN: TR7I 0006 7010 0000 0026 2976 54

SWIFT CODE: YAPITRISXXX

Address: Sahrayicedit, Ataturk Cad. No: 43A, Kadikoy, Istanbul, Turkiye

Retraction Policy

The publisher will take all appropriate measures to modify the article in question, in close cooperation with the editors, in cases of alleged or proven scientific misconduct, fraudulent publication, or plagiarism. This includes the prompt publication of an erratum, disclosure, or retraction of the affected work in the most severe case. Together with the editors, the publisher will take reasonable steps to detect and prevent the publication of articles in which research misconduct occurs and will under no circumstances promote or knowingly allow such abuse to occur.

Withdrawal Policy

The International Journal of Medical Biochemistry is committed to providing high quality articles and uphold the publication ethics to advance the intellectual agenda of science. We expect our authors to comply with, best practice in publication ethics as well as in quality of their articles.

Withdrawal of a manuscript will be permitted only for the most compelling and unavoidable reasons. For withdrawal of a manuscript authors need to submit an "Article withdrawal Form", signed by all authors mentioning the reason for withdrawal to the Editorial Office. The form is available from the web page of the journal. Authors must not assume that their manuscript has been withdrawn until they have received appropriate notification to this effect from the editorial office.

In a case where a manuscript has taken more than five months' time for review process, that allows the author to withdraw manuscript.

Manuscript withdrawal penalty: After receiving the Article withdrawal Form, the International Journal of Medical Biochemistry Editorial Board will investigate the reason of withdrawal.

If the reason finds to be acceptable, the author is allowed to withdraw the manuscript without paying any withdrawal penalty. If not the International Journal of Medical Biochemistry will not accept any manuscripts from the same author for one year.

Important notes: Manuscripts may be withdrawn at any stage of review and publication process by submitting a request to the editorial office. Manuscript withdrawal will be permitted after submission only for the most compelling and unavoidable reasons.



CONTENTS VOLUME VIII ISSUE 4 YEAR 2025

EDITORIAL

From analytical precision to molecular insight: Integrating biomarker science across the clinical continuum Konukoglu D	XII
ORIGINAL ARTICLES	
The impact of endothelin-I on the efficacy of anti-VEGF therapy: A rationale for dual antagonism Mohamed MSA	25 ا
Urokinase-type plasminogen activator and related microRNAs in hepatocellular carcinoma; a bioinformatic based study Seydel GS, Ayan D	241
Tau protein expression and phosphorylation in a glucose-repressed yeast model: Insights into the cancer-alzheimer's disease link Yilmazer M, Uzuner SK	
Adaptive mitochondrial modules: Going with the flow of cancer-specific metabolic rewiring Yildiz MT	282
Can cinnamon reduce endoplasmic reticulum stress in diabetic nephropathy?: An experimental rat model Oztas B, Eraldemir FC, Akbal S, Acar E, Hunc F, Yardimoglu Yilmaz M	292
Platelet-normalized biomarkers as diagnostic and prognostic indicators in crimean-congo hemorrhagic fever Bolat S, Buyuktuna SA	300
Determination of analytical performances of NT-proBNP and aPTT tests with three methods Yeğin D	306
Adult references intervals for thyroid hormones using beckman coulter from Türkiye Sahin I, Eraldemir FC, Oztas B, Yildirim Şik B, Kir HM	312
Evaluation of the analytical performance of the access vitamin B12 II assay with the new calibrator	318



EDITORIAL

From analytical precision to molecular insight: Integrating biomarker science across the clinical continuum

The current issue of the International Journal of Medical Biochemistry exemplifies the journal's mission to connect analytical rigor with molecular understanding in laboratory medicine. The studies in this collection range from the discovery of biomarkers and the exploration of mechanisms to the validation of analyses and the establishment of reference intervals. Together, they show the diverse and connected nature of today's clinical biochemistry.

Mohamed MSA provides a thought-provoking perspective on endothelin-I and anti-VEGF therapy, presenting a rationale for dual antagonism to overcome therapeutic resistance in angiogenesis-driven diseases. In the field of infectious disease diagnostics, Bolat and Buyuktuna demonstrate that platelet-normalized biomarkers can serve as sensitive diagnostic and prognostic indicators in Crimean-Congo hemorrhagic fever, a valuable contribution to hematology-based prognostication.

At the interface of cancer biology and bioinformatics, Seydel and Ayan investigate the urokinase-type plasminogen activator system and related microRNAs microRNAs in hepatocellular carcinoma at the interface of cancer biology and bioinformatics, identifying potential regulatory nodes for molecular intervention.

A series of analytical and reference interval studies reinforce the journal's foundation in clinical laboratory standardization and metrology. The analytical performance of NT-proBNP and aPTT is assessed by Yeğin across three methods. In another study, Sahin et al. establish adult reference intervals for thyroid hormones using Beckman Coulter analyzers in the Turkish population. Madenci and Kutukcu further evaluate the Access Vitamin B12 II assay with a new calibrator, emphasizing harmonization and quality assurance across analytical systems.

In the field of fundamental molecular and metabolic research, Yilmazer and Uzuner examine tau protein expression and phosphorylation in a glucose-repressed yeast model. Yildiz discusses how cancer cells adapt through dynamic metabolic rewiring via mitochondrial modules. Finally, Oztas and colleagues report that cinnamon supplementation attenuates endoplasmic reticulum stress in an experimental diabetic nephropathy model, offering insight into natural compound interventions targeting cellular stress pathways.

Together, these contributions capture the interdisciplinary essence of clinical biochemistry, where analytical performance, molecular biology, and translational relevance converge. By integrating laboratory precision with mechanistic depth, this issue reflects the journal's continuing commitment to advancing biomarker-driven diagnostics, monitoring, and therapy for various human diseases.

Prof. Dildar Konukoglu, MD.

Editor-in-Chief

INTERNATIONAL JOURNAL OF

MEDICAL BIOCHEMISTRY

DOI: 10.14744/ijmb.2025.35682 Int J Med Biochem 2025;8(4):251–260

Research Article



The impact of endothelin-1 on the efficacy of anti-VEGF therapy: A rationale for dual antagonism

Mohamed S. A. Mohamed

MSAM Clinic and Medical School Brandenburg, Brandenburg, Germany

Abstract

Objectives: Angiogenesis-associated disease conditions are often treated with anti-angiogenic therapy. Many of the anti-angiogenic agents approved as adjuvant cancer therapy target the vascular endothelial growth factor (VEGF) axis, as VEGF signaling is regarded as the primary angiogenesis promoter. These drugs are expected to enhance immunity, antagonizing the immunosuppressive functions of VEGF, and to control angiogenesis. Despite a mechanistic rationale that strongly supports their benefits, anti-VEGF agents have shown limited success rates in most cases, along with an association with hypertensive side effects. This article briefly reviews the approved anti-VEGF agents and offers a possible explanation for their limitations.

Methods: PubMed and Scopus databases were searched with the corresponding keywords (such as anti-VEGF), and the relevant knowledge was collected. The included studies were limited to these, which report indications, responses, and side effects. In addition to the review, HuH7 and HEK293T cells were subjected to chemical induction of hypoxia by means of treatment with cobalt chloride (CoCl₂). This treatment induced hypoxia inducible factor 1 alpha (HIF-1) under normoxic conditions. Target protein levels were then assessed with immunoblotting to confirm the review results.

Results: The results support the fact that both VEGF and endothelin-1 (ET-1) levels are elevated in response to hypoxia. Consequently, the modulation of the proangiogenic and vasodilatory effects of the VEGF axis by anti-VEGF agents is anticipated to have an incomplete impact on angiogenesis, while resulting in hypertensive complications due to the ongoing proangiogenic activity and unopposed vasoconstrictive effects of endothelin-1.

Conclusion: Given the uncertainty regarding the capacity of anti-VEGF therapy to concurrently inhibit ET-1, the dual antagonism of VEGF and ET-1 appears to be the preferred approach for effective management of angiogenesis-related pathologies. Additional studies are necessary to validate this conclusion.

Keywords: Adjuvant therapy, angiogenesis, anti-VEGF therapy, endothelin-1, vascular endothelial growth factor

How to cite this article: Mohamed MSA. The Impact of Endothelin-1 on the Efficacy of Anti-VEGF Therapy: A Rationale for Dual Antagonism. Int J Med Biochem 2025;8(4):251–260.

Angiogenesis refers to the formation of new blood vessels through the migration, growth, and differentiation of endothelial cells. This process is regulated by various chemical signals within the human body, with some, such as vascular endothelial growth factor (VEGF) signaling, acting as promoters, while others function as inhibitors [1]. Under normal physiological conditions, there is a balance between angiogenesis-stimulating and inhibiting signals, ensuring the formation of new blood vessels only when and where

necessary, such as during growth or tissue repair. However, disruptions in this balance can lead to pathological conditions or diseases, such as angiogenesis in cancer and metastasis or in age-related wet macular degeneration [2].

Vascular endothelial growth factor A (VEGF-A) is one of the most important and extensively studied stimulators of angiogenesis [3]. It has become a target for numerous angiogenesis inhibitors, many of which have been approved or are in advanced clinical trials for adjuvant cancer treatment. Examples of these inhibitors

Address for correspondence: Mohamed S. A. Mohamed, MD. MSAM Clinic and Medical School Brandenburg, Brandenburg, Germany Phone: +4915201043716 E-mail: msamclinic@gmail.com ORCID: 0009-0003-4369-9763

Submitted: December 07, 2024 Revised: May 08, 2025 Accepted: May 10, 2025 Available Online: October 21, 2025

© (1)(8)



Table 1. Examples of anti-VEGF agents considered for clinical application		
Drug	Mechanism of action	
Axitinib (Inlyta®)	A tyrosine kinase inhibitor capable of inhibiting the angiogenic effects mediated by VEGF receptors 1–3, c-KIT, and PDGFR.	
Bevacizumab (Avastin®)	Monoclonal antibody against VEGF-A.	
Cabozantinib (Cometriq®)	Impedes MET (hepatocyte growth factor receptor protein), VEGFR, RET (receptor tyrosine kinase), GAS6 receptor (AXL), KIT), and Fms-like tyrosine kinase-3 (FLT-3).	
Lenvatinib mesylate (Lenvima®)	A multi-kinase inhibitor targeting VEGFR1, VEGFR2, and VEGFR3 kinases.	
Pazopanib (Votrient®)	A multi-kinase inhibitor that targets and inhibits the vascular endothelial growth factor receptor (VEGFR), platelet-derived growth factor receptor (PDGFR), c-KIT, and fibroblast growth factor receptor (FGFR).	
Ramucirumab (Cyramza®)	A direct competitive inhibitor of VEGFR2, exhibiting a high affinity for binding to the extracellular domain of VEGFR2, thereby preventing its interaction with the natural ligands (VEGF-A, VEGF-C, and VEGF-D).	
Regorafenib (Stivarga®)	Exhibits binary-targeted inhibitory activity against the tyrosine kinases VEGFR2 and TIE2.	
Sorafenib (Nexavar®)	A protein kinase inhibitor that demonstrates activity against VEGFR, PDGFR, and RAF kinases. Among the RAF kinases, sorafenib exhibits greater selectivity for C-Raf compared to B-Raf.	
Sunitinib (Sutent®)	A multitargeted tyrosine kinase inhibitor capable of binding to PDGF receptors (PDGF-Rs), VEGF receptors (VEGFRs), CD117 (c-KIT), RET, CD114, and CD135.	
Vandetanib (Caprelsa®)	Inhibits the tyrosine kinase activity of two concurrent pathways by targeting VEGFR-2 and the epidermal growth factor receptor (EGFR).	
Aflibercept (EYLEA™)	A soluble fusion protein that binds all isoforms of VEGF-A, as well as VEGF-B and placental growth factor, thereby inhibiting their receptor activation.	
Zivaflibercept (Zaltrap®)	A soluble decoy protein for the VEGF receptors, VEGFR-1 and VEGFR-2.	
Brolucizumab (Beovu®)	A 26 kDa single-chain monoclonal antibody fragment capable of inhibiting the activation of VEGF receptors.	
Ranibizumab (Lucentis®)	A recombinant humanized monoclonal antibody fragment targeting VEGF-A.	

are presented in Table 1. The success rates of these agents vary due to several factors. Table 2 and Table 3 summarize some reported clinical outcomes, revealing two key limitations of these agents: Limited success rates and hypertensive side effects.

Hypothesis (Aim of work)

The limitations reported in the experimental and clinical studies can be attributed to several potential factors, as illustrated in Figure 1:

Table 2. Repor	Table 2. Reported clinical success rates of some anti-angiogenic agents		
Drug	Reported findings		
Axitinib	In patients with cytokine-refractory metastatic renal cell carcinoma, Axitinib has the potential to yield an estimated 5-year survival rate of 20.6% [4].		
Bevacizumab	A total of 167 patients with recurrent glioblastoma were enrolled in a multicenter, phase II, randomized, noncomparative trial. Patients who experienced a first or second relapse with progression while on temozolomide were randomized to receive either bevacizumab (10 mg/kg) alone or in combination with irinotecan, administered in 2-week cycles. The objective response rates observed were 28% in the single-agent group and 38% in the combination group. Six-month progression-free survival rates were 43% for the bevacizumab monotherapy group and 50% for the combination group. The median overall survival was 9.2 months for the bevacizumab-only arm and 8.7 months for the combination arm. The most common side effects included hypertension, seizures, neutropenia, and fatigue [5].		
Cabozantinib	The phase 3 CheckMate 9ER trial randomly assigned patients with renal cell carcinoma to receive either cabozantinib in combination with nivolumab or sunitinib. The study reported an objective response rate (ORR) of 55.7% for the cabozantinib/nivolumab combination, with a complete response (CR) rate of 12.4%. In contrast, sunitinib demonstrated an ORR of 28.4% and a CR rate of 5.2%. The median duration of response (DOR) was 23.1 months for the cabozantinib nivolumab regimen, compared to 15.1 months for sunitinib [6].		
Lenvatinib	According to GlobalData, the success rate of the transition phase in the phase III trial evaluating lenvatinib mesylate in patients with colorectal cancer was 43% [7, 8].		
Pazopanib	In the SPIRE study, 211 patients with advanced soft tissue sarcomas were treated with pazopanib as a second-line or subsequent therapy. The median treatment duration was 3.1 months. The median progression-free survival was 3 months, while the median overall survival was 11.1 months. The overall clinical benefit rate across most histological subtypes was 46% [9, 10].		
Ramucirumab	The administration of Ramucirumab in 355 patients with gastro-esophageal cancer demonstrated a response rate of 4%. However, it also showed a disease stability rate of 45%, compared to 21% in the placebo group, yielding an overall disease control rate of 45% versus 23% in the placebo group [11].		

Table 2. Cont.	
Drug	Reported findings
Regorafenib	Patients with metastatic colorectal cancer treated with Regorafenib had a progression-free survival of 2.9 months (interquartile range: 2.2 to 4.4 months), an overall response rate of 4% (n=2), and a disease control rate of 40% (n=19) [12].
Sorafenib	The use of Sorafenib in advanced-stage hepatocellular carcinoma demonstrated the following outcomes: a median overall survival of 26.1 months, 6- and 12-month survival rates of 92.1% and 85%, respectively, a median time to radiological progression of 8 months, and a progression-free survival rate of 64.3% [13].
Sunitinib	Objective response rates of 47% for Sunitinib and 12% for IFN- α (p<0.001) were observed in patients with metastatic renal cell carcinoma. The primary Sunitinib-related adverse effects included hypertension (12%), fatigue (11%), diarrhea (9%), and hand-foot syndrome (9%) [14].
Vandetanib	The use of Vandetanib in patients with locally advanced or metastatic medullary thyroid carcinoma yielded a pooled complete response rate of 0.7% and a disease stabilization rate of 47%, as determined by the RECIST criteria [15].
Zivaflibercept	Patients with colorectal cancer treated with Zivaflibercept demonstrated a median overall survival of 13.5 months and a median progression-free survival of 6.9 months, in contrast to 12.06 months and 4.67 months, respectively, for those receiving a placebo. Similarly, the response rate for the Zivaflibercept plus FOLFIRI combination was 19.8%, compared to 11.1% for the FOLFIRI-only group [16].
Dovitinib	In a mutation-specific, single-arm, phase 2 study involving 80 cancer patients with colorectal, gastrointestinal stromal, or ovarian cancers, Dovitinib demonstrated a clinical benefit rate of 13.8% [17].
	In an open-label, randomized phase 3 clinical trial evaluating dovitinib as a third-line targeted treatment for patients with metastatic renal cell carcinoma, the drug resulted in an increase of 3.7 months in progression-free survival and 11.1 months in overall survival [18].

- Hypoxia and relative ischemia are commonly observed alongside the rapid growth of solid tumors [19].
- Hypoxic conditions result in a significant decrease in NOSTRIN (Nitric-Oxide Synthase Trafficking Inducer) levels [20].
- Under hypoxic conditions, hypoxia-inducible factor 1-alpha (HIF-1α) forms a dimeric complex with HIF-1β through nuclear translocation. This complex binds to the hypoxia response element (HRE), interacting with the coactivator p300, which subsequently enhances the expression of VEGF-A, matrix metalloproteinases (MMPs), angiopoietin, and platelet-derived growth factor (PDGF) [21].
- Low NOSTRIN levels are associated with increased activity
 of endothelial nitric oxide synthase III (eNOS) [22], which,
 in turn, elevates VEGF-A [23], thereby inducing the release
 of soluble VEGF receptor 1 (sVEGFR-1 or sflt-1) [24].
- The presence of soluble VEGF receptor 1 (sVEGFR-1) has been reported to enhance the vasoconstrictive activity of endothelin-1 (ET-1) [25].

Clinically, low NOSTRIN has been linked to tumor progression, prognosis, and metastasis [26, 27]. Elevated levels of eNOS and VEGFs have been similarly associated with tumor progression, prognosis, recurrence, and metastasis [28]. Furthermore, high endothelin-1 (ET-1) levels have been clinically correlated with tumor progression and metastasis [29].

Therefore, the inhibition of the proangiogenic and vasodilatory effects of the eNOS/VEGF axis by anti-VEGF agents may lead to inadequate control of angiogenesis, potentially resulting in hypertension. This could be attributed to the continued proangiogenic activity and the unopposed vasoconstrictive effects of the endothelin-1 axis. The objective of this work is to validate the aforementioned principles.

Role of eNOS/VEGF axis in angiogenesis

During the conversion of l-arginine to l-citrulline, endothelial nitric oxide synthase (eNOS) acts as a catalyst, leading to the production of nitric oxide (NO). NO plays a critical role in mediating the angiogenic activity of various factors, including vascular endothelial growth factor (VEGF). The activation of eNOS is partially regulated by the upstream Akt/protein kinase B signaling pathway [29]. The VEGF family consists of seven known members: VEGF-A, VEGF-B, VEGF-C, VEGF-D, placental growth factor (PIGF), non-human genome encoded VEGF-E, and snake venom VEGF (svVEGF) [15]. VEGF-A is vital for supporting the vascular endothelium and serves as a key regulator of angiogenesis, contributing to tumor growth, proliferation, invasion, metastasis, angiogenesis, and drug resistance [30]. VEGF-B is involved in promoting neuronal survival and cardiovascular development through angiogenesis in specific organs. The roles of VEGF-C and VEGF-D are particularly significant in tumor growth and metastasis, as they are implicated in VEGFR-3mediated lymphangiogenesis and lymphatic metastasis [30].

Role of endothelin -1 axis in angiogenesis

Endothelin-1 (ET-1) exerts a direct angiogenic effect on endothelial and peri-vascular cells [31]. It plays a crucial role in cell growth and proliferation, and its effects are mediated through the activation of the MAPK pathway [32]. Consequently, ET-1 is actively involved in tumor angiogenesis. Furthermore, ET-1 can enhance VEGF expression and promote angiogenesis via its endothelin A receptor (ETAR), integrin-linked kinase (ILK), Akt, and hypoxia-inducible factor-1α (HIF-1α) signaling pathways [33].

Materials and Methods

A systematic review of the literature was conducted in accordance with the PRISMA (Preferred Reporting Items for Systematic Reviews and Meta-Analyses) guidelines. The search

Table 3. Summa	ry of clinica	Table 3. Summary of clinical outcomes for anti-VEGF agents in solid tumors	ts in solid tumor	16			
Drug	Phase (trial)	Study population	Sample size (N)	ORR (%)	PFS (months)	OS (months)	Adverse events
Axitinib	Phase III	Metastatic RCC	Not specified	20.6 (5-yr survival)	Not specified	20.6 (5-yr)	Hypertension
Bevacizumab	Phase II	Recurrent glioblastoma Metastatic RCC	167 651	28–38 55.7	6-month PFS: 43–50%	9.2 Not specified	Hypertension, seizures, fatigue
Lenvatinib	Phase III	Colorectal cancer	Not specified	43	Not specified	Not specified	Not specified
Pazopanib	Phase II	Soft tissue sarcoma	211	Not specified	3.0	11.1	Not specified
Ramucirumab	Phase III	Gastro-esophageal cancer	355	4	Not specified	Not specified	Hypertension
Regorafenib	Phase III	Metastatic colorectal cancer	Unclear	4	2.9	Not specified	Hypertension
Sorafenib	Phase III	Advanced HCC	Not specified	Not specified	8.0	26.1	Hypertension
Sunitinib	Phase III	Metastatic RCC	Unclear	47	Not specified	Not specified	Hypertension
Vandetanib	Phase III	Medullary thyroid carcinoma	Unclear	0.7	Not specified	Not specified	Not specified
Ziv-aflibercept	Phase III	Colorectal cancer	Not specified	19.8	6.9	13.5	Hypertension
Dovitinib	Phase II	Various solid tumors	80	13.8	3.7	11.1	Not specified
VEGFR: Vascular endo	thelial growth f	VEGEB: Vascular endothelial growth factor receptor: ORB: Objective response rate: PFS: Progression-free survival: OS: Overall survival: RCC: Benal cell carcinoma: HCC: Hepatocellular carcinoma.	te: PFS: Progression-fre	e survival: OS: Overall surviv	al: RCC: Renal cell carcinoma: HCC:	: Hepatocellular carcir	oma.

strategy included queries in PubMed and Scopus using the following keywords and Boolean combinations: "Anti-VEGF therapy," "angiogenesis inhibitors," "VEGF antagonists," "endothelin-1," "cancer angiogenesis," and "clinical trials." The review was limited to English-language articles published between 2005 and 2024.

Inclusion criteria

- Peer-reviewed clinical trials or meta-analyses evaluating anti-angiogenic therapies.
- Studies reporting specific efficacy outcomes (e.g., ORR, PFS, OS) or adverse events, such as hypertension).
- Trials involving FDA- or EMA-approved anti-VEGF agents.

Exclusion criteria

- Non-clinical studies unless providing essential mechanistic insights.
- Conference abstracts without full datasets.
- Duplicate publications or interim analyses of the same trial.

After screening by title/abstract and applying inclusion/exclusion criteria, the selected studies were considered as sources for the informations included in this article.

In addition, HuH7 and HEK293T cells were sourced from affiliated research groups. The cells were harvested and washed with phosphate-buffered saline (PBS). Three independent biological replicates were performed, with 200,000 cells seeded into culture wells (6-well plates) and incubated overnight in 2 mL of supplemented medium at 37 °C in a humidified atmosphere with 5% CO₂ and ≥95% relative humidity. The medium used was DMEM, supplemented with 10% FBS (Gibco), 1X sodium pyruvate, 1X penicillin-streptomycin (Gibco), 1X Glutamax (Gibco), and 25 mM HEPES. The cells were subsequently treated with CoCl₂ (Sigma-Aldrich) according to the experimental protocol outlined below:

- Control non treated cells
- Cells treated with 200µM CoCl₂
- Cells treated with 300µM CoCl₂
- Cells treated with 400µM CoCl₂

Cells were incubated under the same conditions for an additional 72 hours before harvesting and subsequent processing. The impact of the treatments on HIF-1 α and its target proteins was evaluated through immunoblotting, which was performed according to standard laboratory protocols. Equal amounts of total protein (50 μ g per lane) were resolved on a 10% SDS-PAGE gel (Bio-Rad) and transferred to a nitrocellulose membrane via wet transfer. Membranes were blocked with 5% non-fat dry milk in TBST (Tris-buffered saline with 0.1% Tween-20) prior to antibody incubation. Primary antibodies specific to the target proteins were obtained from Proteintech, Germany. Band densities were analyzed using ImageJ software. An unpaired t-test was applied to compare the values of the experimental conditions to the control, with P-values less than 0.05 considered statistically significant.

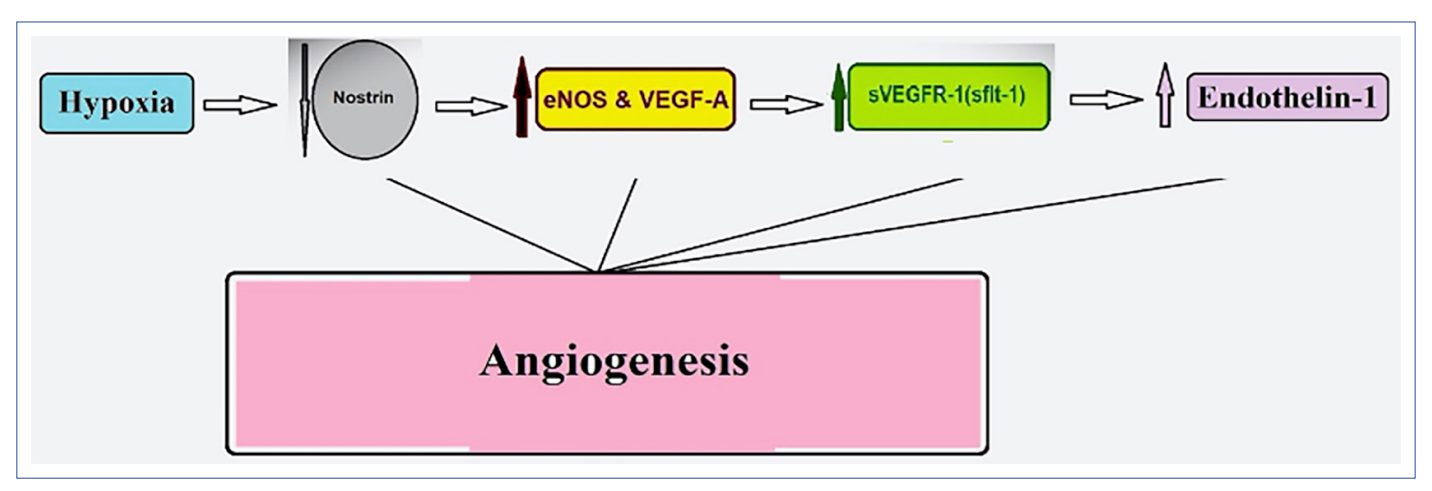


Figure 1. Diagrammatic representation of the article's hypothesis. Hypoxia is associated with decreased NOSTRIN and leads to increased eNOS, VEGF-A, sVEGFR-1 and ET-1.

eNOS: Nitric oxide synthase III; VEGF: Vascular endothelial growth factor; sVEGFR-1: Soluble VEGF receptor 1; ET-1: Endothelin-1; NOSTRIN: Nitric-Oxide Synthase Trafficking Inducer.

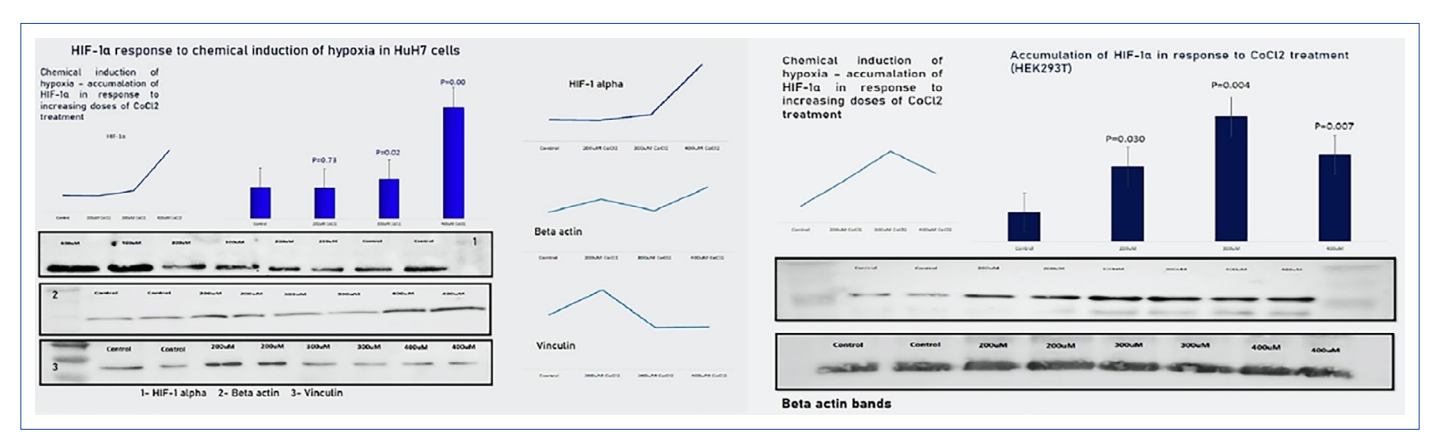


Figure 2. HIF-1α induction in HuH7 and HEK293T cells following treatment with various concentrations of CoCl₂. HIF-1α band intensities were normalized to their respective loading controls. Protein concentrations were estimated using the Bradford assay prior to gel loading. Equal amounts of total protein were loaded for each sample, and vinculin and β-actin were used as loading controls. Vinculin was favored over β-actin as a reference, given reports of β-actin's reactivity to hypoxia—an effect observed at the 400 μM treatment in HuH7 cells. CoCl₂ treatment induced dose-dependent changes in HIF-1α expression in HuH7 cells (p=0.73, 0.02, and 0.0001 for 200 μM, 300 μM, and 400 μM, respectively) and in HEK293T cells (p=0.03, 0.004, and 0.007 for 200 μM, 300 μM, and 400 μM, respectively). HIF-1α: Hypoxia-inducible factor 1-alpha.

Results

The chemical induction of hypoxia was successfully achieved, as evidenced by the upregulation of HIF-1 α (Fig. 2). In response to HIF-1 α activation, the secretion of eNOS, VEGF-A, sVEGFR1, and Endothelin-1 (ET-1) was elevated in a dose-dependent manner (Fig. 3). Similar experiments conducted on human umbilical vein endothelial cells (HUVECs) also demonstrated an increase in ET-1 secretion (Fig. 4).

Discussion

The selected target proteins are well-established effectors that play crucial roles in endothelial physiology and vascular pathology. These proteins serve as indicators of tissue hypoxia and are involved in the process of angiogenesis [31]. To mitigate potential variations that may arise in studies uti-

lizing physical hypoxia, such as differences in the type (e.g., sustained or intermittent), duration (e.g., short-term or long-term), or extent of hypoxia, this study employed the previously validated chemical induction of hypoxia through the use of $CoCl_2$, which promotes the accumulation of HIF-1 α and HIF-2 α under normoxic conditions [34].

This study demonstrates that the secretion of ET-1 and VEGF-A increases concurrently in response to hypoxia, prior to the statistical significance peak of HIF-1a. This observation suggests that both effectors may exhibit heightened sensitivity to hypoxia and/or play simultaneous leading roles in the tissue's response to hypoxia, particularly at the paracrine and/or remote levels.

The roles of eNOS, NO, and VEGF-A in angiogenesis have been extensively investigated and thoroughly documented. The majority of clinically approved anti-angiogenic therapies target this specific pathway (Table 1). VEGF-A stim-

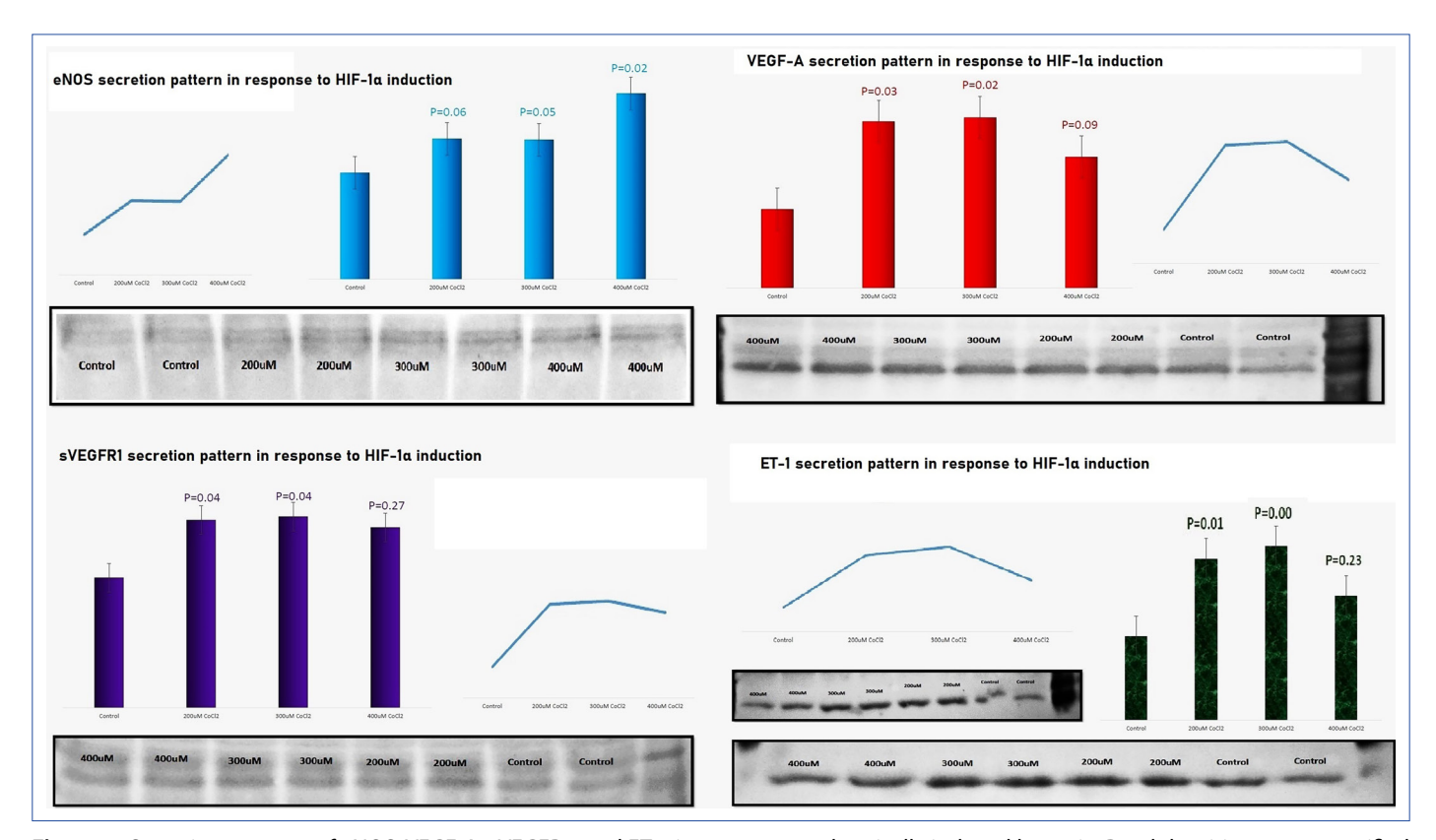


Figure 3. Secretion patterns of eNOS, VEGF-A, sVEGFR1, and ET-1 in response to chemically induced hypoxia. Band densities were quantified using ImageJ software. Each treatment group was compared independently to the control using an unpaired t-test. A P-value of less than 0.05 was considered statistically significant. No corrections for multiple comparisons were applied, as the values were analyzed independently. eNOS: Nitric oxide synthase III; VEGF: Vascular endothelial growth factor; sVEGFR-1: Soluble VEGF receptor 1; ET-1: Endothelin-1; NOSTRIN: Nitric-Oxide Synthase Trafficking Inducer.

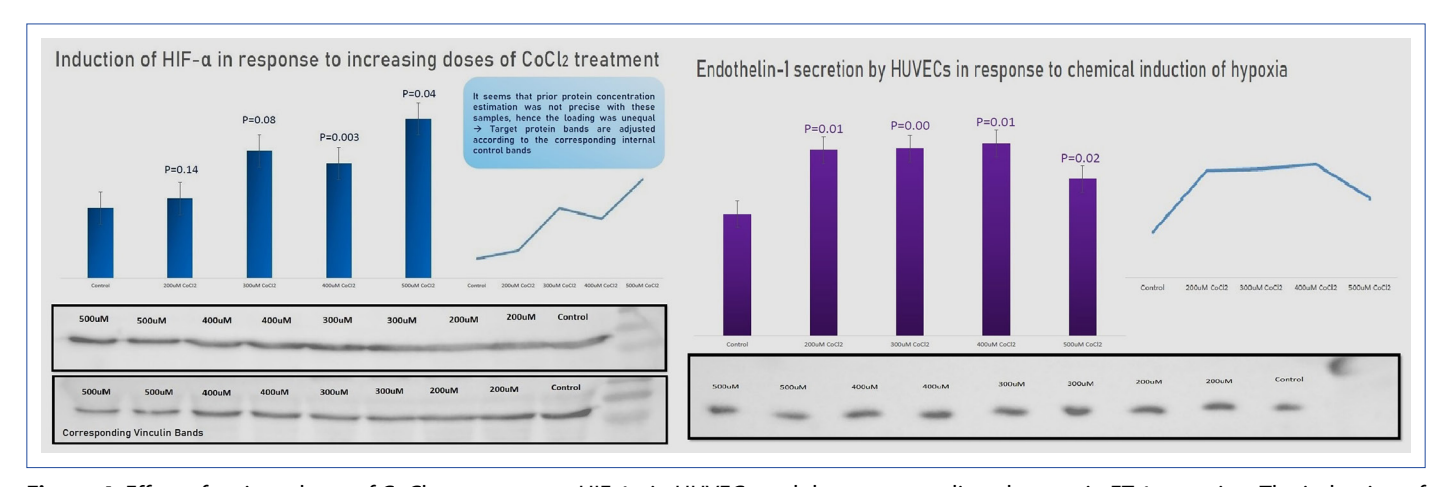


Figure 4. Effect of various doses of $CoCl_2$ treatment on HIF-1 α in HUVECs and the corresponding changes in ET-1 secretion. The induction of HIF-1 α was associated with corresponding increase in ET-1 secretion (p<0.05).

HIF-1a: Hypoxia-inducible factor 1-alpha.; ET-1: Endothelin-1; HUVECs: Human umbilical vein endothelial cells.

ulates eNOS expression and enhances NO production by vascular endothelial cells. A reduction in NO production impairs angiogenesis and decreases the vascular permeability typically induced by VEGF-A [35].

Similarly, the elevated secretion of ET-1 by cultured cells in response to hypoxia has been previously reported, [36] along with other contradictory findings. *In-vivo* preclinical and clinical

studies have also reported similar outcomes, with intermittent hypoxia linked to ET-1 overexpression in animal models [37–39], and chronic intermittent hypoxia, as observed in patients with obstructive sleep apnea, associated with the accumulation of HIF-1 α and elevated circulating ET-1 levels [40–42]. Increased circulating ET-1 levels have been associated with vascular complications and endothelial dysfunction in humans [43].

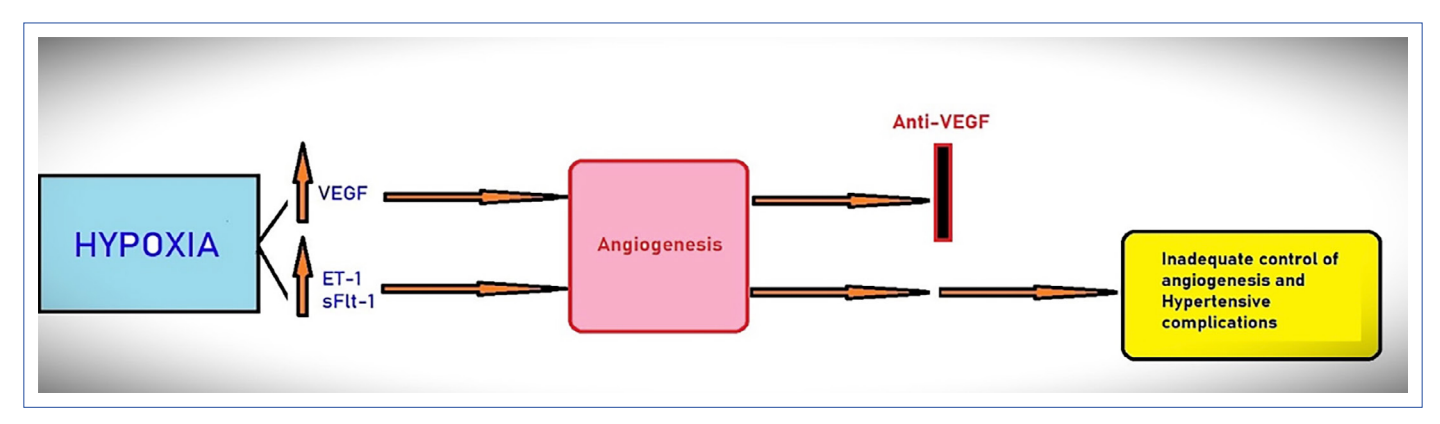


Figure 5. Diagrammatic representation of the main conclusion of the work: Anti-VEGF therapy may antagonize the effects of VEGF during hypoxia-induced angiogenesis; however, sVEGFR1 (sFlt-1) and ET-1 would remain elevated, which may explain the reported low success rates and hypertensive side effects.

VEGF: Vascular endothelial growth factor; sVEGFR-1: Soluble VEGF receptor 1; ET-1: Endothelin-1.

A recent study examined the impact of sustained and intermittent hypoxia (SH and IH, respectively) on HIF-1α, VEGF, and ET-1 in HepG2 cells (hepatocellular carcinoma cell line). The study found an overexpression of HIF-1α and VEGF in response to IH, but not to SH, whereas no such effect was observed for ET-1 [44]. While these findings may seem contradictory to those of the present study, several key considerations should be taken into account when interpreting these results; the hypoxia induction in the study was achieved physically through exposure to a low oxygen gas mixture. The cells employed were of cancerous origin, which may be associated with specific proangiogenic alterations that could make it challenging to detect additional induction of ET-1. In other words, cancerous cells may undergo a degree of hypoxia in culture, as indicated by their accelerated growth rates. As demonstrated in my experiments, ET-1 secretion increased with a 200 µM CoCl₂ treatment but tended to decrease at the 400 µM treatment, where HIF-1α exhibited its peak expression (Fig. 3). In addition, the primary findings of this study focus on ET-1 secretion, which may not directly correspond to changes in mRNA or protein expression levels. In the context of cancer-related angiogenesis, where localized relative hypoxia is a constant feature of the tumor microenvironment, multiple studies have documented elevated circulating levels of ET-1 [45]. Therefore, the results of the present study appear to reflect a more realistic scenario.

Hypoxia-induced VEGF also stimulates the production of its truncated soluble form, VEGFR1, via the VEGFR-2-MEK-PKC signaling pathway, [46] which functions as a regulatory mechanism to prevent excessive activity. The ultimate consequence of hypoxia is the activation of angiogenesis, [47] a process characterized by a balance between proangiogenic and anti-angiogenic factors. Soluble VEGFR1 is part of the endogenous anti-angiogenic factors that help protect against uncontrolled angiogenesis, although it may also be actively involved in angiogenesis [48, 49]. These findings align with the results of the current study, which demonstrated an increase in sVEGFR1 following chemical induction of hypoxia (Fig. 3). However, a study reporting contradictory findings indicated that hypoxia led to a reduction in sVEGFR1

expression. This discrepancy may be attributed to the fact that their experiments were conducted on human microvascular endothelial cells isolated from neonatal dermis [50].

Soluble VEGFR-1 plays a significant role in angiogenesis, where perivascular cells interact with its isoforms via GM3 ganglioside. This interaction impacts actin cytoskeleton dynamics by destabilizing pericyte-endothelial cell interactions and altering adhesion contacts with the basement membrane, thereby contributing to vessel sprouting [51]. Moreover, the presence of sVEGFR-1 has been shown to shift $\alpha 5\beta 1$ integrin signaling from a traditional adhesion pathway to a more dynamic one [52], while also enhancing its expression [53]. Consequently, the presence of sVEGFR-1 in the endothelial cell microenvironment during vessel sprouting is crucial [54]. These findings support the critical role of sVEGFR-1 in vessel sprouting and angiogenesis through mechanisms beyond VEGF binding [55], which aligns with the conclusions of the present study.

The intervention in the present study involved $CoCl_2$ treatment (chemical induction of HIF-1 α), and thus, the observed changes can be attributed to the activities of HIF-1 α . While the dependence of certain effectors on the upregulation or down-regulation of others may be somewhat less considered based on the variations in response to different treatments, though it cannot be completely excluded yet.

The aim of this article was to confirm the dual activation of the eNOS/VEGF and ET-1 axes in response to hypoxia, which has been experimentally demonstrated, as well as to investigate the persistence of ET-1 activation despite anti-VEGF therapy (Fig. 5). As previously mentioned, the concurrent or parallel pattern of changes in VEGF-A and ET-1 secretion in response to hypoxia may suggest independent responses of both effectors. However, the appropriate approach to fully address this issue would have involved the introduction of various anti-VEGF agents followed by a reassessment of the levels of both effectors. Due to significant resource limitations, this investigation has not yet been conducted; thus, this issue will be further discussed based on existing published literature and experimental findings.

The secretion of VEGF-A in response to hypoxia persists for as long as the hypoxic stimulus is present [56]. Hypoxia induces angiogenesis, which is the process of new vessel formation [57]. Although the precise sequence of events remains unclear, this process involves both vascular endothelial and smooth muscle cells. VEGF-A acts as a specific mitogen for vascular endothelial cells, promoting their proliferation, while ET-1 stimulates the proliferation of vascular smooth muscle cells [58]. Therefore, both effectors are expected to increase concurrently, as observed in my experiments. Furthermore, it is anticipated that each effector can influence the expression of the other [58, 59].

From a biological perspective, the reduction in ET-1 observed following anti-VEGF therapy, despite the persistence of hypoxia and/or the initial stimulus, should be limited to the inhibition of the additional induction caused by VEGF overexpression, as its actions are suppressed by the therapy [60]. However, the response to the initial stimulus may remain unaffected. Consequently, reports of decreased ET-1 levels after anti-VEGF therapy may reflect scenarios where the stimulus for abnormal angiogenesis is simultaneously eliminated during the therapy [61]. In contrast, when the pathology persists, increased ET-1 levels have been observed post-therapy [61]. Therefore, in response to hypoxia and tumor-associated angiogenesis, driven by relative hypoxia within the tumor microenvironment, a reduction in ET-1 due to anti-VEGF therapy cannot be anticipated. For instance, VEGF-A, which normally reduces ET-1 production by 29%, loses this capability when its VEGFR2 receptor is blocked by SU5416, resulting in a 16% increase in ET-1 production under therapy [62].

Nevertheless, the current study demonstrated a notable increase in the levels of sVEGFR1 in the culture medium following hypoxia induction (Fig. 3). Soluble VEGFR1 is an endogenous antagonist of VEGF, and pharmacological anti-VEGF monoclonal antibodies exhibit structural and functional similarities to it [63]. Despite the elevation of sVEGFR1 in the culture medium, a significant increase in ET-1 levels was also observed (Fig. 3).

Conclusion

In summary, the limited success rates of anti-VEGF agents as adjuvant therapies in cancer treatment may be attributed to the principles discussed above. Additionally, any hypertensive side effects associated with these agents may be linked to the unopposed increase in ET-1 (Fig. 5). To achieve effective angiogenesis control without inducing hypertension, a dual antagonism of VEGF and ET-1 may be considered. Preclinical and clinical studies are necessary to evaluate the efficacy of such a dual therapy. Furthermore, since the secretion of the four effectors (eNOS, VEGF-A, sVEGFR1, and ET-1) significantly increases in response to hypoxia, which is a hallmark of angiogenesis, their levels may serve as biomarkers for monitoring the efficacy of therapy in angiogenesis-related pathologies, both before and after treatment. Thus, the SHEHATA MARKER OF ANGIOGENESIS has been introduced as a biomarker panel and is planned for further clinical validation [64].

Informed Consent: Not applicable. This study did not involve human participants, and no new patient data were collected or used. All data are derived from previously published sources or the author's own experiments on commercial cell lines.

Conflict of Interest Statement: The author has no conflicts of interest to declare.

Funding: The author declared that this study received no financial support.

Use of Al for Writing Assistance: No Al technologies utilized.

Peer-review: Externally peer-reviewed.

References

- Larionova I, Kazakova E, Gerashchenko T, Kzhyshkowska J. New angiogenic regulators produced by TAMs: Perspective for targeting tumor angiogenesis. Cancers (Basel) 2021;13(13):3253.
 [CrossRef]
- 2. Lugano R, Ramachandran M, Dimberg A. Tumor angiogenesis: Causes, consequences, challenges and opportunities. Cell Mol Life Sci 2020;77(9):1745–70. [CrossRef]
- 3. Yu E, Kim H, Park H, Hong JH, Jin J, Song Y, et al. Targeting the VEGFR2 signaling pathway for angiogenesis and fibrosis regulation in neovascular age-related macular degeneration. Sci Rep 2024;14(1):25682. [CrossRef]
- 4. Rini Bl, de La Motte Rouge T, Harzstark AL, Michaelson MD, Liu G, Grünwald V, et al. Five-year survival in patients with cytokine-refractory metastatic renal cell carcinoma treated with axitinib. Clin Genitourin Cancer 2013;11(2):107–14. [CrossRef]
- 5. Friedman HS, Prados MD, Wen PY, Mikkelsen T, Schiff D, Abrey LE, et al. Bevacizumab alone and in combination with irinote-can in recurrent glioblastoma. J Clin Oncol 2009;27(28):4733–40. [CrossRef]
- Yakes FM, Chen J, Tan J, Yamaguchi K, Shi Y, Yu P, et al. Cabozantinib (XL184), a novel MET and VEGFR2 inhibitor, simultaneously suppresses metastasis, angiogenesis, and tumor growth. Mol Cancer Ther 2011;10(12):2298–308. [CrossRef]
- 7. Matsui J, Funahashi Y, Uenaka T, Watanabe T, Tsuruoka A, Asada M. Multi-kinase inhibitor E7080 suppresses lymph node and lung metastases of human mammary breast tumor MDA-MB-231 via inhibition of vascular endothelial growth factor-receptor (VEGF-R) 2 and VEGF-R3 kinase. Clin Cancer Res 2008;14(17):5459–65. [CrossRef]
- 8. Hao Z, Wang P. Lenvatinib in management of solid tumors. Oncologist 2020;25(2):e302–310. [CrossRef]
- 9. Zivi A, Cerbone L, Recine F, Sternberg CN. Safety and tolerability of pazopanib in the treatment of renal cell carcinoma. Expert Opin Drug Saf 2012;11(5):851–9. [CrossRef]
- 10. Verweij J, Sleijfer S. Pazopanib, a new therapy for metastatic soft tissue sarcoma. Expert Opin Pharmacother 2013;14(7):929–35. [CrossRef]
- 11. Fuchs CS, Tomasek J, Yong CJ, Dumitru F, Passalacqua R, Goswami C, et al.; REGARD Trial Investigators. Ramucirumab monotherapy for previously treated advanced gastric or gastro-oesophageal junction adenocarcinoma (REGARD): An international, randomised, multicentre, placebo-controlled, phase 3 trial. Lancet 2014;383(9911):31–9. [CrossRef]

- 12. Unseld M, Filip M, Seirl S, Gleiss A, Bianconi D, Kieler M, et al. Regorafenib therapy in metastatic colorectal cancer patients: Markers and outcome in an actual clinical setting. Neoplasma 2018;65(4):599–603. [CrossRef]
- Sacco R, Bargellini I, Ginanni B, Bertini M, Faggioni L, Federici G, et al. Long-term results of sorafenib in advanced-stage hepatocellular carcinoma: What can we learn from routine clinical practice? Expert Rev Anticancer Ther 2012;12(7):869–75. [CrossRef]
- 14. Choueiri TK, Powles T, Burotto M, Escudier B, Bourlon MT, Zurawski B, et al.; CheckMate 9ER Investigators. Nivolumab plus cabozantinib versus sunitinib for advanced renal-cell carcinoma. N Engl J Med 2021;384(9):829–41. [CrossRef]
- Trimboli P, Castellana M, Virili C, Giorgino F, Giovanella L. Efficacy of vandetanib in treating locally advanced or metastatic medullary thyroid carcinoma according to RECIST criteria: A systematic review and meta-analysis. Front Endocrinol (Lausanne) 2018;9:224. [CrossRef]
- 16. Van Cutsem E, Tabernero J, Lakomy R, Prenen H, Prausová J, Macarulla T, et al. Addition of aflibercept to fluorouracil, leucovorin, and irinotecan improves survival in a phase III randomized trial in patients with metastatic colorectal cancer previously treated with an oxaliplatin-based regimen. J Clin Oncol 2012;30(28):3499–506. [CrossRef]
- 17. Taylor MH, Alva AS, Larson T, Szpakowski S, Purkaystha D, Amin A, et al. A mutation-specific, single-arm, phase 2 study of dovitinib in patients with advanced malignancies. Oncotarget 2020;11(14):1235–43. [CrossRef]
- 18. Motzer RJ, Porta C, Vogelzang NJ, Sternberg CN, Szczylik C, Zolnierek J, et al. Dovitinib versus sorafenib for third-line targeted treatment of patients with metastatic renal cell carcinoma: An open-label, randomised phase 3 trial. Lancet Oncol 2014;15(3):286–96. [CrossRef]
- 19. Shaharudin NS, Surindar Singh GK, Kek TL, Sultan S. Targeting signaling pathways with andrographolide in cancer therapy (review). Mol Clin Oncol 2024;21(5):81. [CrossRef]
- 20. Wade BE, Zhao J, Ma J, Hart CM, Sutliff RL. Hypoxia-induced alterations in the lung ubiquitin proteasome system during pulmonary hypertension pathogenesis. Pulm Circ 2018;8(3):2045894018788267. [CrossRef]
- Ikeda H, Kakeya H. Targeting hypoxia-inducible factor 1 (HIF-1) signaling with natural products toward cancer chemotherapy. J Antibiot (Tokyo) 2021;74(10):687–95. [CrossRef]
- 22. Chakraborty S, Ain R. Nitric-oxide synthase trafficking inducer is a pleiotropic regulator of endothelial cell function and signaling. J Biol Chem 2017;292(16):6600–20. [CrossRef]
- 23. Yamamoto N, Oyaizu T, Enomoto M, Horie M, Yuasa M, Okawa A, et al. VEGF and bFGF induction by nitric oxide is associated with hyperbaric oxygen-induced angiogenesis and muscle regeneration. Sci Rep 2020;10(1):2744. [CrossRef]
- 24. Saito T, Takeda N, Amiya E, Nakao T, Abe H, Semba H, et al. VEGF-A induces its negative regulator, soluble form of VEGFR-1, by modulating its alternative splicing. FEBS Lett 2013;587(14):2179–85. [CrossRef]
- 25. Askarinejad A, Alizadehasl A, Jolfayi AG, Adimi S. Hypertension in cardio-oncology clinic: An update on etiology, assessment, and management. Cardiooncology 2023;9(1):46. [CrossRef]

- 26. Wang J, Yang S, He P, Schetter AJ, Gaedcke J, Ghadimi BM, et al. Endothelial nitric oxide synthase traffic inducer (NOSTRIN) is a negative regulator of disease aggressiveness in pancreatic cancer. Clin Cancer Res 2016;22(24):5992–6001. [CrossRef]
- 27. Paul M, Gope TK, Das P, Ain R. Nitric-oxide synthase trafficking inducer (NOSTRIN) is an emerging negative regulator of colon cancer progression. BMC Cancer 2022;22(1):594. [CrossRef]
- 28. Marisi G, Scarpi E, Passardi A, Nanni O, Ragazzini A, Valgiusti M, et al. Circulating VEGF and eNOS variations as predictors of outcome in metastatic colorectal cancer patients receiving bevacizumab. Sci Rep 2017;7(1):1293. [CrossRef]
- 29. Cianfrocca R, Rosanò L, Tocci P, Sestito R, Caprara V, Di Castro V, et al. Blocking endothelin-1-receptor/β-catenin circuit sensitizes to chemotherapy in colorectal cancer. Cell Death Differ 2017;24(10):1811–20. [CrossRef]
- 30. Di Francesco D, Bertani F, Fusaro L, Clemente N, Carton F, Talmon M, et al. Regenerative potential of a bovine ECM-derived hydrogel for biomedical applications. Biomolecules 2022;12(9):1222. [CrossRef]
- 31. Liu ZL, Chen HH, Zheng LL, Sun LP, Shi L. Angiogenic signaling pathways and anti-angiogenic therapy for cancer. Signal Transduct Target Ther 2023;8(1):198. [CrossRef]
- 32. Miyashita-Ishiwata M, El Sabeh M, Reschke LD, Afrin S, Borahay MA. Differential response to hypoxia in leiomyoma and myometrial cells. Life Sci 2022;290:120238. [CrossRef]
- 33. Wu MH, Huang CY, Lin JA, Wang SW, Peng CY, Cheng HC, et al. Endothelin-1 promotes vascular endothelial growth factor-dependent angiogenesis in human chondrosarcoma cells. Oncogene 2014;33(13):1725–35. [CrossRef]
- 34. Muñoz-Sánchez J, Chánez-Cárdenas ME. The use of cobalt chloride as a chemical hypoxia model. J Appl Toxicol 2019;39(4):556–70. [CrossRef]
- 35. Bosma EK, Darwesh S, Habani YI, Cammeraat M, Serrano Martinez P, van Breest Smallenburg ME, et al. Differential roles of eNOS in late effects of VEGF-A on hyperpermeability in different types of endothelial cells. Sci Rep 2023;13(1):21436. [CrossRef]
- 36. Kourembanas S, Marsden PA, McQuillan LP, Faller DV. Hypoxia induces endothelin gene expression and secretion in cultured human endothelium. J Clin Invest 1991;88(3):1054–7. [CrossRef]
- 37. Belaidi E, Morand J, Gras E, Pépin JL, Godin-Ribuot D. Targeting the ROS-HIF-1-endothelin axis as a therapeutic approach for the treatment of obstructive sleep apnea-related cardiovascular complications. Pharmacol Ther 2016;168:1–11. [CrossRef]
- 38. Beaudin AE, Waltz X, Hanly PJ, Poulin MJ. Impact of obstructive sleep apnoea and intermittent hypoxia on cardiovascular and cerebrovascular regulation. Exp Physiol 2017;102(7):743–63. [CrossRef]
- 39. Morales-Loredo H, Jones D, Barrera A, Mendiola PJ, Garcia J, Pace C, et al. A dual blocker of endothelin A/B receptors mitigates hypertension but not renal dysfunction in a rat model of chronic kidney disease and sleep apnea. Am J Physiol Renal Physiol 2019;316(5):F1041–52. [CrossRef]

- 40. Gjørup PH, Wessels J, Pedersen EB. Abnormally increased nitric oxide synthesis and increased endothelin-1 in plasma in patients with obstructive sleep apnoea. Scand J Clin Lab Invest 2008;68(5):375–85. [CrossRef]
- 41. Kosacka M, Brzecka A. Endothelin-1 and LOX-1 as markers of endothelial dysfunction in obstructive sleep apnea patients. Int J Environ Res Public Health 2021;18(3):1319. [CrossRef]
- 42. Schoen T, Aeschbacher S, Leuppi JD, Miedinger D, Werthmüller U, Estis J, et al. Subclinical sleep apnoea and plasma levels of endothelin-1 among young and healthy adults. Open Heart 2017;4(1):e000523. [CrossRef]
- 43. Radeau T, Lebel M, Houde I, Larivière R, Mauriège P, Kingma I, et al. Endothelin-1 levels and cardiovascular risk factors in renal transplant patients. Clin Biochem 2004;37(12):1072–8. [CrossRef]
- 44. Minoves M, Hazane-Puch F, Moriondo G, Boutin-Paradis A, Lemarié E, Pépin JL, et al. differential impact of intermittent vs. sustained hypoxia on HIF-1, VEGF and proliferation of HepG2 cells. Int J Mol Sci 2023;24(8):6875. [CrossRef]
- 45. Elbadry MM, Tharwat M, Mohammad EF, Abdo EF. Diagnostic accuracy of serum endothelin-1 in patients with HCC on top of liver cirrhosis. Egyptian Liver J 2020;10:1–7. [CrossRef]
- 46. Takahashi H, Shibuya M. The vascular endothelial growth factor (VEGF)/VEGF receptor system and its role under physiological and pathological conditions. Clin Sci (Lond) 2005;109(3):227–41. [CrossRef]
- 47. Fonódi M, Nagy L, Boratkó A. Role of protein phosphatases in tumor angiogenesis: Assessing PP1, PP2A, PP2B and PTPs activity. Int J Mol Sci 2024;25(13):6868. [CrossRef]
- 48. Kargozar S, Baino F, Hamzehlou S, Hamblin MR, Mozafari M. Nanotechnology for angiogenesis: Opportunities and challenges. Chem Soc Rev 2020;49:5008–57. [CrossRef]
- 49. Chappell JC, Mouillesseaux KP, Bautch VL. Flt-1 (vascular endothelial growth factor receptor-1) is essential for the vascular endothelial growth factor-notch feedback loop during angiogenesis. Arterioscler Thromb Vasc Biol 2013;33(8):1952–9. [CrossRef]
- 50. Ikeda T, Sun L, Tsuruoka N, Ishigaki Y, Yoshitomi Y, Yoshitake Y, et al. Hypoxia down-regulates sFlt-1 (sVEGFR-1) expression in human microvascular endothelial cells by a mechanism involving mRNA alternative processing. Biochem J 2011;436(2):399–407. [CrossRef]
- 51. Jin J, Sison K, Li C, Tian R, Wnuk M, Sung HK, et al. Soluble FLT1 binds lipid microdomains in podocytes to control cell morphology and glomerular barrier function. Cell 2012;151(2):384–99. [CrossRef]
- 52. Orecchia A, Mettouchi A, Uva P, Simon GC, Arcelli D, Avitabile S, et al. Endothelial cell adhesion to soluble vascular endothelial growth factor receptor-1 triggers a cell dynamic and angiogenic phenotype. FASEB J 2014;28(2):692–704. [CrossRef]

- 53. Etienne-Selloum N, Prades J, Bello-Roufai D, Boone M, Sevestre H, Trudel S, et al. Expression analysis of $\alpha 5$ integrin subunit reveals its upregulation as a negative prognostic biomarker for glioblastoma. Pharmaceuticals (Basel) 2021;14(9):882. [CrossRef]
- 54. Chappell JC, Cluceru JG, Nesmith JE, Mouillesseaux KP, Bradley VB, Hartland CM, et al. Flt-1 (VEGFR-1) coordinates discrete stages of blood vessel formation. Cardiovasc Res 2016;111:84–93. [CrossRef]
- 55. Failla CM, Carbo M, Morea V. Positive and negative regulation of angiogenesis by soluble vascular endothelial growth factor receptor-1. Int J Mol Sci 2018;19(5):1306. [CrossRef]
- 56. Yu R, Kim NS, Li Y, Jeong JY, Park SJ, Zhou B, et al. Vascular sema3E-plexin-D1 signaling reactivation promotes post-stroke recovery through VEGF downregulation in mice. Transl Stroke Res 2022;13(1):142–59. [CrossRef]
- 57. Hahne M, Schumann P, Mursell M, Strehl C, Hoff P, Buttgereit F, et al. Unraveling the role of hypoxia-inducible factor (HIF)-1α and HIF-2α in the adaption process of human microvascular endothelial cells (HMEC-1) to hypoxia: Redundant HIF-dependent regulation of macrophage migration inhibitory factor. Microvasc Res 2018;116:34–44. [CrossRef]
- 58. Matsuura A, Yamochi W, Hirata K, Kawashima S, Yokoyama M. Stimulatory interaction between vascular endothelial growth factor and endothelin-1 on each gene expression. Hypertension 1998;32(1):89–95. [CrossRef]
- 59. Lee KJ, Kim MK, Park YH, Seol HJ, Lim JE, Lee JN, et al. Vascular endothelial growth factor induces endothelin-1 production via matrix metalloproteinase-2 rather than endothelin-converting enzyme-1. Hypertens Pregnancy 2007;26(2):189–99. [CrossRef]
- 60. Lee JE, Kim JY, Jung JH, Shin DH, Park SW. Induction of vascular endothelial growth factor receptor expression in human umbilical vein endothelial cells after repeated bevacizumab treatment *in vitro*. Int J Ophthalmol 2017;10(7):1064–8.
- 61. Kida T, Flammer J, Oku H, Morishita S, Fukumoto M, Suzuki H, et al. Suppressed endothelin-1 by anti-VEGF therapy is important for patients with BRVO-related macular edema to improve their vision. EPMA J 2016;7(1):18. [CrossRef]
- 62. Star GP, Giovinazzo M, Lamoureux E, Langleben D. Effects of vascular endothelial growth factor on endothelin-1 production by human lung microvascular endothelial cells *in vitro*. Life Sci 2014;118:191–4. [CrossRef]
- 63. Fuh G, Wu P, Liang WC, Ultsch M, Lee CV, Moffat B, et al. Structure-function studies of two synthetic anti-vascular endothelial growth factor fabs and comparison with the avastin fab. J Biol Chem 2006;281(10):6625–31. [CrossRef]
- 64. Mohamed MSA. Shehata marker: A promising tool for assessing graft endothelial dysfunction and hypoxic injury. Int J Organ Transplant Med 2024;15(3):133–45. [CrossRef]

INTERNATIONAL JOURNAL OF

MEDICAL BIOCHEMISTRY

DOI: 10.14744/ijmb.2025.69346 Int J Med Biochem 2025;8(4):261–271

Research Article



Urokinase-type plasminogen activator and related microRNAs in hepatocellular carcinoma; a bioinformatic based study

Durmus Ayan² Gonul Seyda Seydel¹, Durmus Ayan²

¹Department of Health Care Services, Nigde Omer Halisdemir University, Nigde Zübeyde Hanım Vocational School of Health Service, Nigde, Türkiye

²Department of Medical Biochemistry, Nigde Omer Halisdemir University Faculty of Medicine, Nigde, Türkiye

Abstract

Objectives: Hepatocellular carcinoma (HCC) is one of the most prevalent cancers worldwide. Urokinase-type plasminogen activator (uPA), which is encoded by the PLAU gene, is a serine protease involved in the degradation of the extracellular matrix. Increasing evidence indicates that PLAU is overexpressed in various cancers and is associated with poor prognosis, making it a potential biomarker for cancer. However, its potential role in HCC remains unclear. Therefore, this study aimed to investigate the role of PLAU and related microRNAs in HCC using multiple bioinformatics tools. **Methods:** PLAU expression was evaluated using the TNMplot and GEPIA2 databases. Promoter methylation levels were assessed through UALCAN. Survival analysis (overall survival (OS) and recurrence-free survival (RFS) rates), was conducted using the Kaplan-Meier Plotter. Protein-protein interaction networks were examined with STRING. Target miRNAs were identified using TargetScan 8.0. Differential expression, survival analysis, and co-expression of miRNAs were investigated using ENCORI.

Results: PLAU expression was significantly upregulated in liver hepatocellular carcinoma (LIHC) compared to normal tissues (p<0.05). Promoter methylation level of PLAU was significantly increased (hypermethylation) in LIHC tissues (p=5.43×10⁻¹²). Elevated PLAU expression was not associated with OS (p=0.16) and RFS (p=0.28) rates. hsa-miR-181a-5p, hsa-miR-181b-5p, hsa-miR-181c-5p, and hsa-miR-181d-5p were positively correlated with PLAU in LIHC tissue (p<0.05). The hsa-miR-181a-5p and hsa-miR-181b-5p were up-regulated in LIHC (p<0.05).

Conclusion: In conclusion, our study highlights the potential role of PLAU and its related miRNAs (hsa-miR-181a-5p and hsa-miR-181b-5p) in HCC. However, elevated PLAU expression did not correlate with survival rates, indicating its involvement in tumor development but no prognostic significance. Further applicable studies are needed on this subject. **Keywords:** Bioinformatic analysis, hepatocellular carcinoma, DNA methylation, microRNA, PLAU, prognosis, urokinase-type plasminogen activator

How to cite this article: Seydel GS, Ayan D. Urokinase-type plasminogen activator and related microRNAs in hepatocellular carcinoma; a bioinformatic based study. Int J Med Biochem 2025;8(4):261–271.

epatocellular carcinoma (HCC), which constitutes approximately 90% of primary liver cancers, is one of the most prevalent cancers globally, ranking sixth in incidence and third in cancer-related mortality [1, 2]. HCC remains a significant global health concern, with rising incidence rates observed in both developed and developing countries [3, 4]. The

pathogenesis of HCC involves a complex array of molecular alterations, such as cell cycle dysregulation, immune modulation, DNA methylation changes, epithelial-mesenchymal transition (EMT), and microRNA (miRNA) dysregulation [5]. HCC is characterized by poor overall survival and a high recurrence rate [4]. Despite notable advances in surgical interventions,

Address for correspondence: Gonul Seyda Seydel, MD. Department of Health Care Services, Nigde Omer Halisdemir University, Nigde Zübeyde Hanım Vocational School of Health Service, Nigde, Türkiye

Phone: +90 553 351 45 91 E-mail: seydaseydel@hotmail.com ORCID: 0000-0001-9317-0719

Submitted: April 04, 2025 Revised: May 17, 2025 Accepted: May 21, 2025 Available Online: October 21, 2025

OPEN ACCESS This is an open access article under the CC BY-NC license (http://creativecommons.org/licenses/by-nc/4.0/).





targeted therapies, and imaging techniques, the overall survival rates remain low. Early-stage cases may benefit from surgical approaches such as hepatic resection, liver transplantation, and local/regional therapies, while options for advanced stages remain limited, with median survival of 6 to 8 months. Therefore, understanding the mechanisms underlying HCC and identifying new biomarkers is crucial for improving early diagnosis, prognosis, and treatment [4–6].

Urokinase-type plasminogen activator (uPA), encoded by the PLAU gene, is a serine protease that converts inactive plasminogen into active plasmin. This process plays a crucial role in the degradation of the extracellular matrix (ECM) and the basement membrane [7]. Such degradation facilitates cancer cell invasion and serves as a critical initial step in tumor progression. Numerous studies have demonstrated that uPA is integral to various stages of tumor progression, including tumor cell proliferation, migration, angiogenesis, and EMT [7–9]. Furthermore, research has shown that PLAU expression, and consequently uPA levels, are significantly elevated in tumor cells, with higher PLAU expression strongly correlating with poor prognosis [7, 8, 10–12]. Additionally, PLAU levels have been found to be markedly increased in HCC; however, the number of studies on this topic remains limited [13–16].

MiRNAs are small non-coding RNA molecules that regulate target gene expression by binding to specific mRNAs, serving as key modulators of post-transcriptional gene silencing. They play a crucial role in the initiation and progression of cancer and are considered potential biomarkers for cancer diagnosis and treatment [17, 18]. The role of PLAU in HCC, particularly its interaction with miRNAs, remains poorly understood. To date, no research has explored the relationship between PLAU and its associated miRNAs in HCC. Therefore, this study aimed to investigate the role of PLAU and related miRNAs in HCC using various bioinformatics tools.

Materials and Methods

Statement of ethics

Data for this study were retrieved from various publicly available databases; therefore, ethical approval was not necessary.

The analysis of differential gene expression of PLAU using the tnmplot database

The TNMplot database (http://www.tnmplot.com/, accessed on December 12, 2024) is an online tool designed for analyzing differential gene expression in tumor, normal, and metastatic tissues. This resource comprises 56,938 unique samples collected from the Gene Expression Omnibus (GEO), the Genotypic-Tissue Expression (GTEx), the Cancer Genome Atlas (TCGA), and the Therapeutically Applicable Research to Generate Effective Treatments (TARGET) databases [19]. We utilized the TNMplot database to investigate the differential gene expression of PLAU in various tumor tissues and normal tissues derived from the TCGA (adjacent normal) and GTEx (healthy normal) datasets.

The analysis of PLAU gene expression in LIHC using the GEPIA2 database

Gene Expression Profiling Interactive Analysis, version 2 (GEPIA2, http://gepia2.cancer-pku.cn, accessed on December 12, 2024), is a comprehensive bioinformatics tool designed for analyzing gene expression data derived from the TCGA and GTEx databases [20]. We used the GEPIA2 platform to analyze the expression levels of PLAU in liver hepatocellular carcinoma (LIHC) tumor tissues compared to adjacent normal tissues from TCGA and health normal tissues from the GTEx database, using the "Match TCGA normal and GTEx data" option. Additionally, PLAU expression was examined across different LIHC subtypes.

The analysis of gene expression and promoter methylation of PLAU using the UALCAN database

The University of ALabama at Birmingham CANcer (UALCAN, http://ualcan.path.uab.edu, accessed on December 12, 2024) is an interactive and comprehensive web-based resource for the analysis of cancer OMICS data, including gene expression and promoter methylation profiles derived from TCGA datasets [21]. In this study, the UALCAN platform was utilized to evaluate PLAU gene expression and promoter methylation levels in LIHC tissues compared to adjacent normal tissues. Gene expression analysis was performed across various clinicical characteristics, including race, gender, age, weight, and nodal metastasis status.

The survival analysis of PLAU in LIHC using the kaplanmeier plotter database

Kaplan-Meier plotter (KM plotter, http://kmplot.com/analysis, accessed on December 12, 2024) is a web-based database designed to explore the relationship between gene expression and prognosis across 21 different types of cancer using clinical data [22]. We utilized this database to investigate the overall survival (OS) and relapse-free survival (RFS) rates of PLAU in LIHC tissue.

The analysis of the protein-protein interaction network and biological process (Gene Ontology) enrichment analysis of PLAU using the STRING database

The Search Tool for the Retrieval of Interacting Genes/Proteins (STRING, https://string-db.org/, accessed on December 12, 2024) is a widely used online database for exploring and predicting protein-protein interaction (PPI). Its objective is to establish a comprehensive and objective global network that encompasses both physical and functional interactions between two or more proteins [23]. We utlized the STRING database to examine the PPI networks and the biological process (Gene Ontology) enrichment of PLAU.

The analysis of target miRNAs using the TargetScan 8.0 database

TargetScan 8.0 (https://www.targetscan.org/vert_80/, accessed on December 12, 2024) is a web resource utilized for predicting the target genes of miRNAs [24]. TargetScan

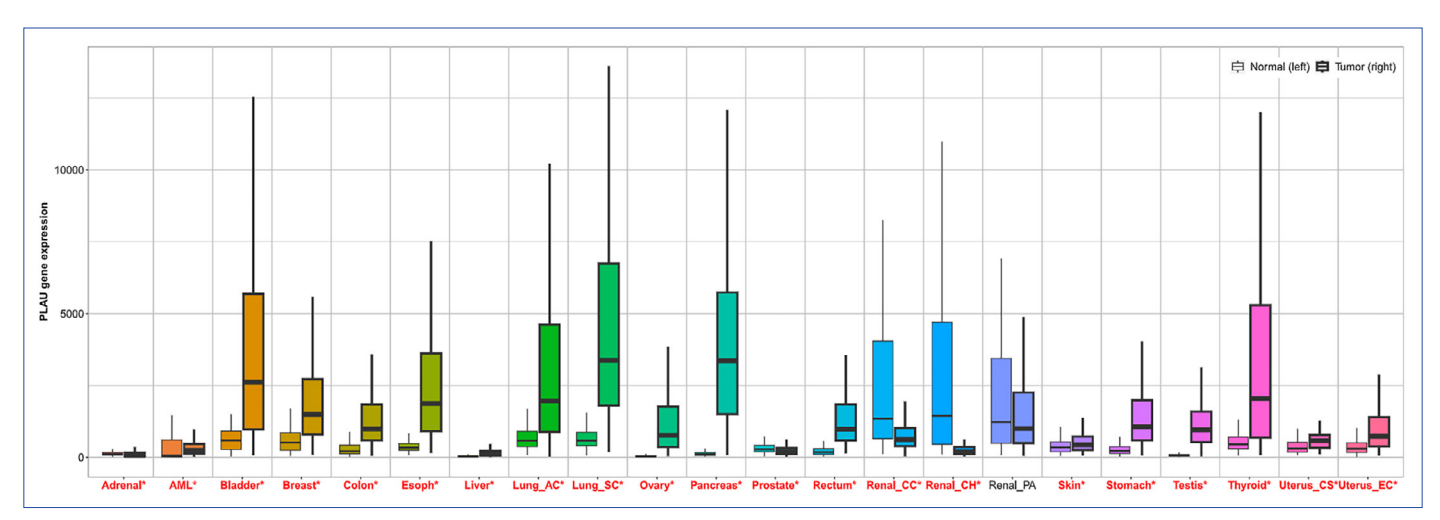


Figure 1. Box plots illustrating the differential PLAU expression analysis in normal (left) and tumor (right) tissues in TNMplot database. Significant differences are indicated in red, with *p<0.05.

predicts the biological targets of miRNAs by identifying conserved 8mer, 7mer, and 6mer sites that align with the seed region of each miRNA [25]. Furthermore, it provides predictions that encompass poorly conserved sites and nonconserved miRNAs. The tool also identifies sites with seed region mismatches that are compensated by conserved 3' pairing [26]. In mammals, predictions are prioritized based on their estimated targeting efficacy, which is determined using a biochemical model of miRNA-mediated repression. This model has been extended to all miRNA sequences through the application of a convolutional neural network [24]. We used this database to identify the target miRNAs of PLAU.

The analysis of differential expression, survival analysis, and co-expression of miRNAs using the ENCORI database

The Encyclopedia of RNA Interactomes (ENCORI, https://rnasysu.com/encori/panCancer.php, accessed on December 12, 2024) Pan-Cancer analysis platform is a comprehensive tool developed to decode Pan-Cancer Networks of long noncoding RNAs (IncRNAs), miRNAs, pseudogenes, small nucleolar RNAs (snoRNAs), RNA-binding proteins (RBPs), and all protein-coding genes by analysing their expression profiles across 32 different cancer types [27]. We performed the this database to analyze differential expression, survival analysis, and co-expression of miRNAs in LIHC and normal tissues.

Statistical analysis

All statistical analyses were conducted using the default or recommended settings of each database. In the TNMplot database, the Mann–Whitney U test was used, and p<0.05 was considered statistically significant. In the GEPIA2 database, differential expression analysis was performed using |log2 fold change| >1 and p-value <0.01 as cut-off criteria. The data were log2 (TPM+1) transformed, and a one-way ANOVA was applied for comparisons. Additionally, pathological stage analysis was conducted using the same platform. In the UALCAN database, a Student's t-test was employed with statistical signifi-

cance defined as p<0.05. In the Kaplan–Meier Plotter, survival analysis was performed using log-rank p-values to compare high and low expression groups in LIHC, with auto-selected best cutoff, and significance was set at p<0.05. In the STRING database, p<0.05 was considered statistically significant for PPI network analysis, and FDR<0.05 was used for biological process enrichment analysis. In the ENCORI database, expression levels were presented as log2(RPM+0.01).

Results

The differential gene expression of the PLAU in various tumor tissues

We conducted a pan-cancer analysis of the TNMplot database to evaluate the expression of PLAU across 22 different tumor types. The results demonstrated that PLAU was significantly expressed in 21 out of the 22 tumor tissues analyzed. As shown in Figure 1, PLAU expression was significantly upregulated in the adrenal, acute myeloid leukemia (AML), bladder, breast, colon, esophagus, liver, lung adenocarcinoma (lung-AC), lung squamous cell carcinoma (lung-SC), ovary, pancreas, rectum, skin, stomach, testis, thyroid, and both subtypes of uterine carcinoma (uterus-CS and uterus-EC) when compared to normal tissues. In contrast, PLAU expression was downregulated in prostate, renal clear cell carcinoma (renal-CC), and renal chromophobe carcinoma (renal-CH) tumor tissues (p<0.05). There was no statistically significant difference in PLAU expression in renal papillary adenocarcinoma (renal-PA) (p>0.05).

The gene expression level of PLAU in LIHC

We examined the expression levels of PLAU in LIHC tissues (n=369) compared to normal tissues (n=160) using GEPIA2. The results indicated that PLAU expression was significantly upregulated in LIHC compared to normal tissues (p<0.01) (Fig. 2a). Box plot of the subtypes revealed that PLAU levels were upregulated in LIHC tissues compared to normal tissues in both iCluster_1 and iCluster_2 (p<0.01). However, no signifi-

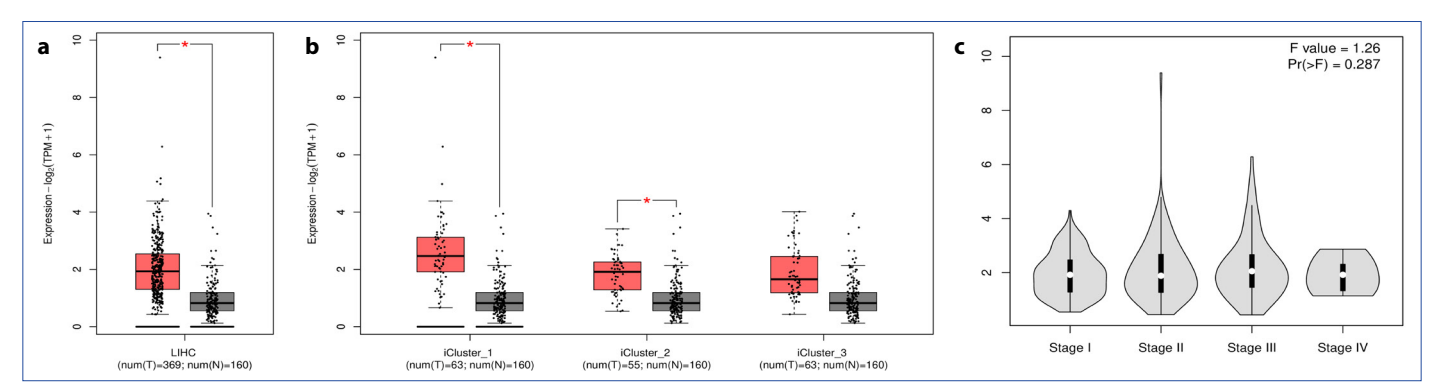


Figure 2. PLAU expression in LIHC tissue. (a) The box plot illustrating PLAU expression levels in LIHC (red) compared to normal tissues (gray) in GEPIA2 database. (b) The box plot showing PLAU expression levels at different iCluster groups in GEPIA2 database (c) The violin plot depicting PLAU expression levels at different stages of LIHC in GEPIA2 database.

Significant differences are indicated in red, with *p<0.01. LIHC: Liver hepatocellular carcinoma.

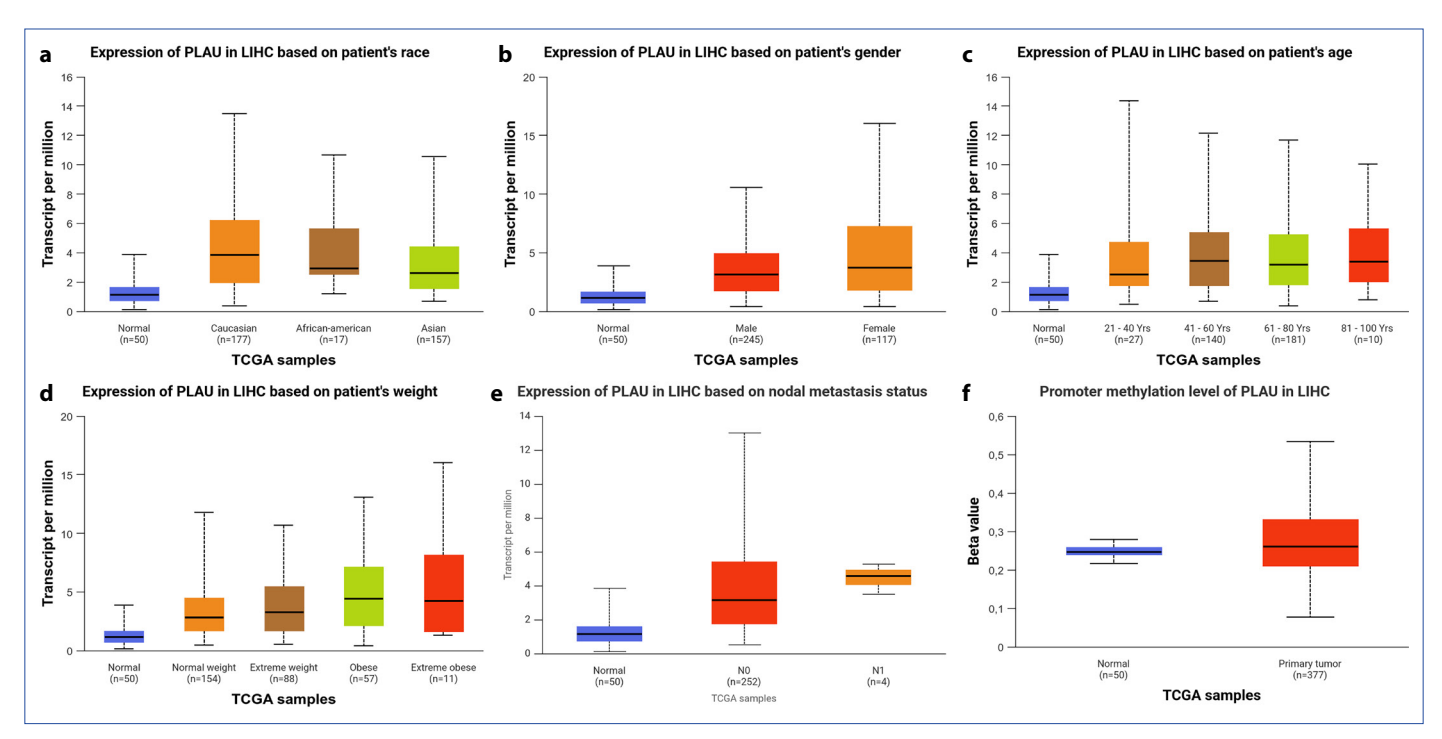


Figure 3. Box plots illustrating the gene expression and promoter methylation levels of PLAU in LIHC tissues compared to adjacent normal tissues using the UALCAN database. PLAU expression levels are shown based on (a) race, (b) gender, (d) age, (d) weight, and (e) nodal metastasis status. (f) Promoter methylation levels of PLAU.

TCGA: The cancer genome atlas.

cant difference was observed in iCluster_3 (Fig. 2b). Additionally, violin plot of the pathological stages showed no statistically significant differences among stages I, II, III, and IV of LIHC (F=1.26; Pr(>F)=0.287) (Fig. 2c).

The gene expression and promoter methylation level of PLAU in LIHC

The expression of PLAU in LIHC was analyzed based on patients' race, gender, age, weight and nodal metastasis status using TCGA data via the UALCAN platform. The results indicated that PLAU expression was significantly upregulated in tumor tissues compared to adjacent normal tissues in Cau-

casian (p= 4.1×10^{-15}) and African-American (p=0.016) patients, while no statistically significant difference was observed in Asian patients (p=0.089). Additionally, there were no significant differences in PLAU expression among racial groups (Caucasian vs. African-American: p=0.991; Caucasian vs. Asian: p=0.341; African-American vs. Asian: p=0.355) (Fig. 3a). PLAU expression was significantly upregulated in both male (p=0.0362) and female (p= 7.05×10^{-11}) patients compared to adjacent normal tissues. However, there was no statistically significant difference in PLAU expression between male and female patients (p=0.342) (Fig. 3b). Age-stratified analysis showed significant upregulation of PLAU expression in the 21–40

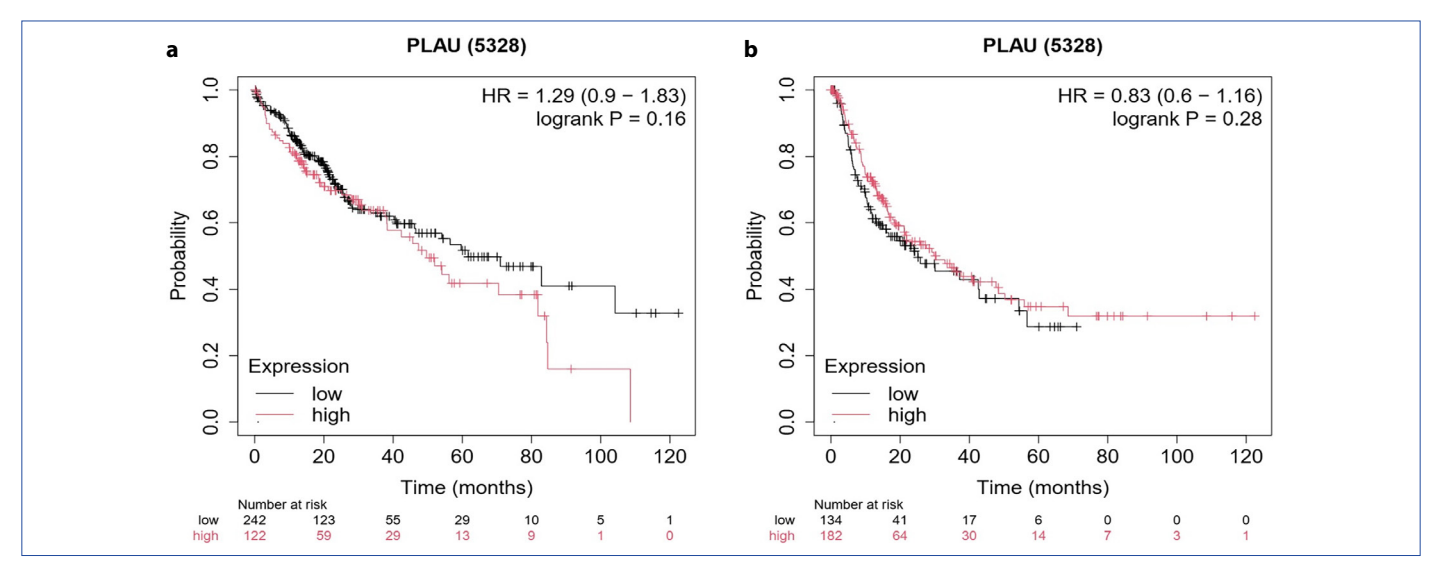


Figure 4. The survival analysis of PLAU in LIHC in the Kaplan-Meier plotter database. (a) Overall survival rates. (b) Relapse-free survival rates. HR: Hazard ratio; LIHC: Liver hepatocellular carcinoma.

 $(p=1.48\times10^{-3})$, 61–80 $(p=1.20\times10^{-12})$, and 81–100 (p=0.040)year groups. No significant upregulation was observed in the 41–60 group (p=0.087). Additionally, no significant differences were found among age groups (all p>0.05) (Fig. 3c). Regarding weight groups, PLAU expression was significantly upregulated in tumors from patients classified as extreme weight $(p=6.38\times10^{-8})$, obese $(p=2.38\times10^{-6})$, and extreme obese (p=0.027), whereas no significant upregulation was observed in the normal weight group (p=0.079). Additionally, no significant differences were found among the tumor weight groups (all p>0.05) (Fig. 3d). PLAU expression was significantly upregulated in patients without regional lymph node metastasis (N0) compared to adjacent normal tissues (p=0.032). However, no significant differences were observed in patients with limited lymph node involvement (N1, defined as metastasis in 1 to 3 axiallry lymph nodes) compared to adjacent normal tissues (p>0.05), nor between the NO and N1 groups (p>0.05) (Fig. 3e). Additionally, promoter methylation levels of PLAU were investigated in LIHC using the UALCAN database. The results demonstrated that promoter methylation was significantly increased (hypermethylation) in LIHC tissues (n=377) compared to adjacent normal tissues (n=50), with median beta values of 0.26 and 0.247, respectively (p= 5.43×10^{-12}) (Fig. 3f).

The survival analysis of PLAU in LIHC

We examined the association between PLAU expression and the OS and RFS rates in LIHC. The analysis revealed that PLAU expression was not significantly associated with OS in LIHC patients (HR=1.29, 95% CI: 0.90–1.83, p=0.16) (Fig. 4a). The median survival rates for cohorts with low and high PLAU expression were 61.7 months and 49.7 months, respectively. PLAU expression was not significantly associated with RFS in LIHC patients (HR=0.83, 95% CI: 0.60–1.16, p=0.28) (Fig. 4b). The median survival rates for cohorts with low and high PLAU expression were 25.14 months and 30.4 months, respectively.

The analysis of protein-protein interactions and biological process enrichment of PLAU

The protein-protein interactions and biological process enrichment of PLAU were analyzed using the STRING database. The resulting PPI network comprises 11 nodes and 41 edges, with an average node degree of 7.45, an average local clustering coefficient of 0.856, and an expected number of edges of 12. The PPI enrichment p-value was 9.26×10-11. The results demonstrated that PLAU interacts with serine protease inhibitor 1 (SERPIN1), serine protease inhibitor 2 (SERPIN2), serine protease inhibitor A5 (SERPIN5), serine protease inhibitor EB2 (SERPINEB2), plasminogen activator urokinase receptor (PLAUR), plasminogen (PLG), matrix metalloproteinase-9 (MMP9), vitronectin (VTN), cathepsin B (CTSB), insulin like growth factor 2 receptor (IGF2R) (Fig. 5a). Furthermore, the biological process enrichment analysis revealed that the interactions are associated with several biological processes, including the regulation of blood coagulation, fibrinolysis, plasminogen activation, and proteolysis (Fig. 5b).

The analysis of target miRNA

The miRNAs associated with PLAU were analyzed using the TargetScan 8.0 database. We identified five conserved miRNAs: hsa-miR-181a-5p, hsa-miR-181b-5p, hsa-miR-181c-5p, hsa-miR-181d-5p, and hsa-miR-4262.

The analysis of differential expression, survival, and coexpression of miRNAs

ENCORI analysis was conducted to compare the differential expression, survival analysis, and co-expression of hsa-miR-181a-5p, hsa-miR-181b-5p, hsa-miR-181c-5p, hsa-miR-181d-5p, and hsa-miR-4262 between LIHC (n=370) and normal tissues (n=50). The results indicated that hsa-miR-181a-5p and hsa-miR-181b-5p were significantly upregulated in LIHC

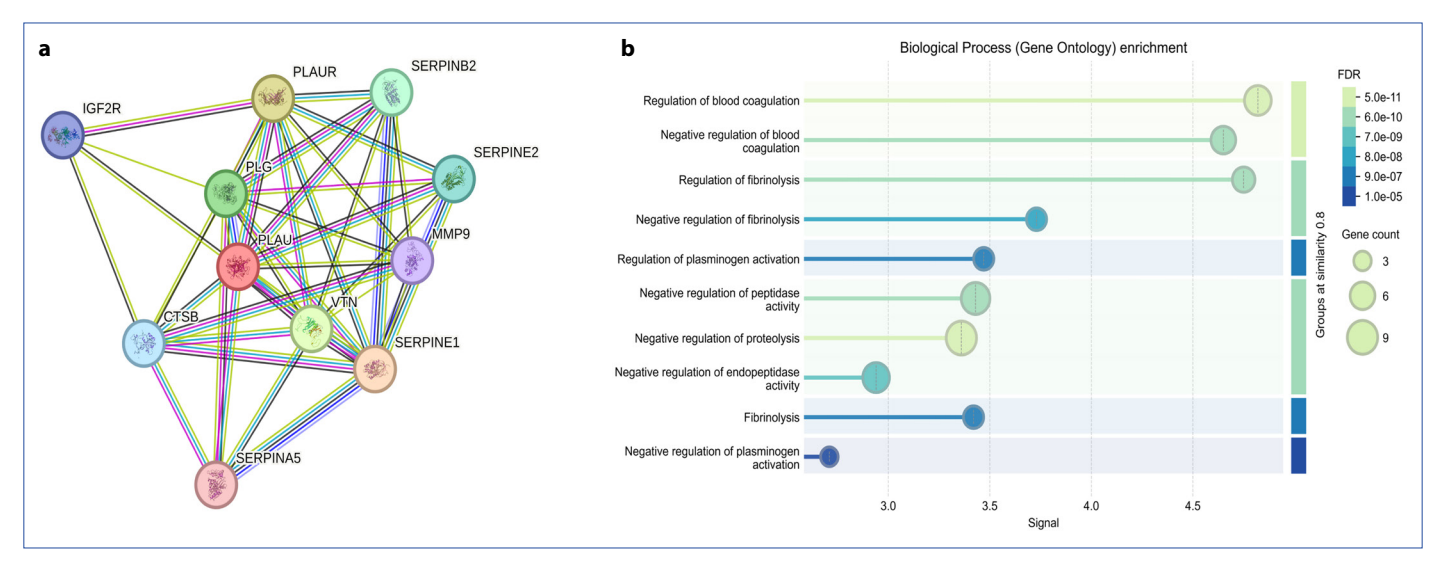


Figure 5. Interaction network of PLAU in the STRING database. (a) Protein-protein interactions of PLAU. (b) Biological process (Gene Ontology) enrichment analysis for PLAU.

FDR: False discovery rate.

tissues compared to normal tissues (p<0.05) (Table 1; Fig. 6a). None of the miRNAs showed a statistically significant association with OS in LIHC tissues (Fig. 6b). According to the co-expression analysis, hsa-miR-181a-5p, hsa-miR-181b-5p, hsa-miR-181c-5p, and hsa-miR-181d-5p were positively correlated with PLAU in LIHC tissues (p=3.60×10⁻¹⁴, 1.64×10⁻¹⁷, p=1.47×10⁻²³, and p=3.79×10⁻²¹, respectively) (Fig. 6c).

Discussion

The role of PLAU in HCC, particularly its relationship with miRNAs, remains unclear. This study is the first to investigate PLAU's involvement in HCC and its interaction with miRNAs through bioinformatic analysis. The urokinase-type plasminogen activator is an extracellular proteolytic enzyme that plays a pivotal role in remodeling tumor microenvironment and the progression of cancer [8]. Recently, uPA has garnered significant attention due to its involvement in tumor growth, metastasis, and angiogenesis, as well as its overexpression in various cancers. Elevated levels of uPA have been linked to poor prognosis, highlighting its potential as a valuable diagnostic, prognostic, and therapeutic biomarker [7, 8, 10]. Numerous strategies have been developed to target the uPA system by modulating its expression and activity in cancer

[7, 10, 28]. However, research on the role of PLAU in HCC remains limited [13–16]. In the present study, we first assessed the differential expression of PLAU across 22 different tumor types using the TNMplot database. Our findings demonstrated that PLAU was significantly expressed in the majority of tumor types (21 out of 22), with expression levels varying according to the specific cancer type. Consistent with previous research, our analysis confirmed that PLAU is consistently overexpressed in multiple cancers [12, 13, 15]. Subsequently, we analyzed PLAU expression using the GEPIA2 database to investigate its levels in LIHC tissue. The results revealed that PLAU expression was significantly upregulated in LIHC tissues compared to normal tissues, consistent with previous studies [13, 15]. Additionally, we examined PLAU expression across different iCluster groups using the GEPIA2 database. Significant differences were observed in iCluster_1 (proliferative/stem cell-like) and iCluster 2 (intermediate/immune-active), while no significant difference was found in iCluster_3 (non-proliferative/metabolic). This may suggest a potential subtype-specific role of PLAU in the tumor biology of LIHC. Furthermore, we assessed the expression of the PLAU gene across different stages of cancer using the same database. The results indicated that PLAU expression did not show a

:DNA -	Fold shows a	_	Falsa diasawawa wata
miRNAs	Fold change	р	False discovery rate
hsa-miR-181a-5p	1.37	0.044	0.14
hsa-miR-181b-5p	1.76	0.00091	0.0055
hsa-miR-181c-5p	1.19	0.94	0.96
hsa-miR-181d-5p	1.52	0.39	0.72
hsa-miR-4262	1.0	0.71	0.78

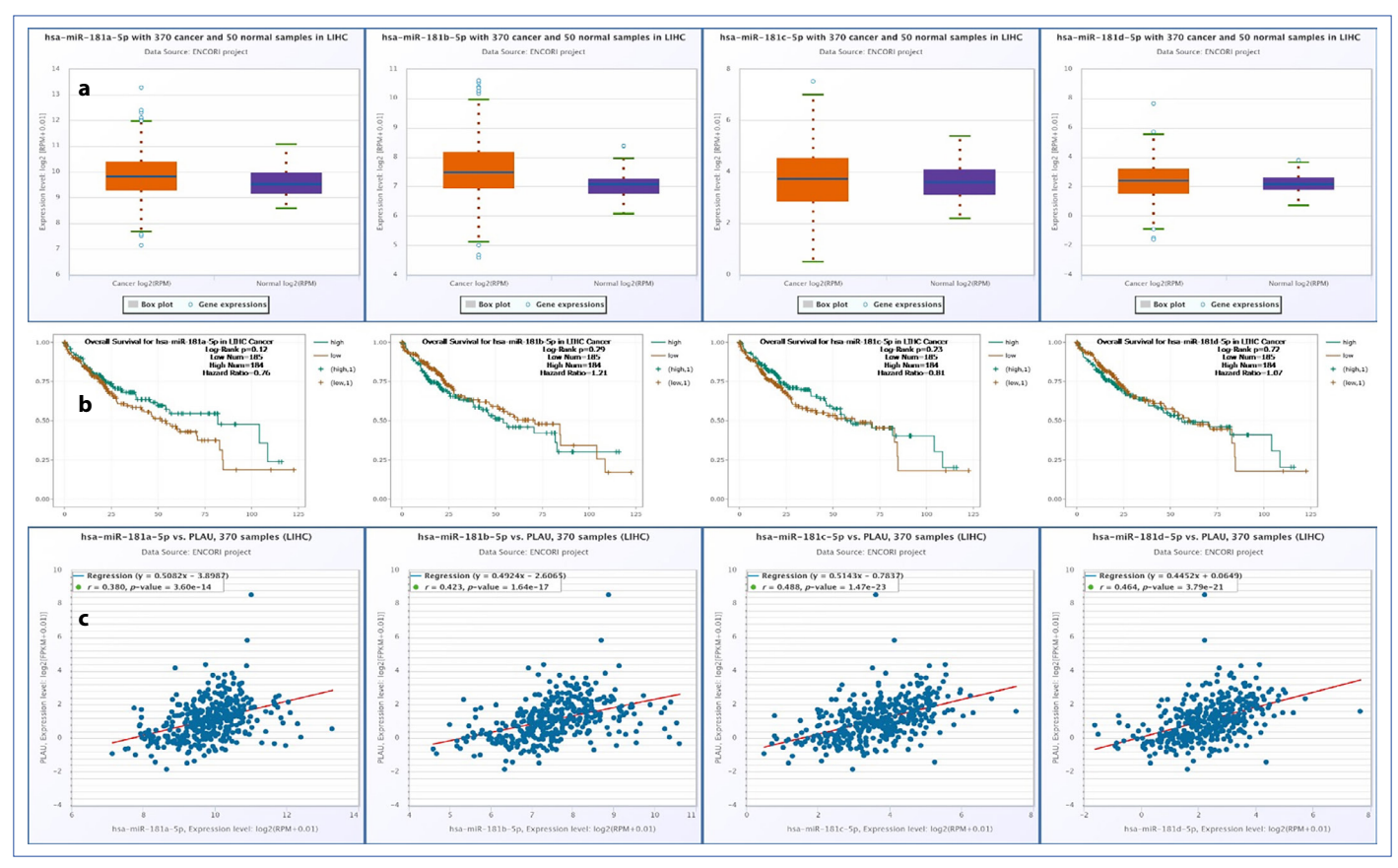


Figure 6. (a) The differential expression of hsa-miR-181a-5p, hsa-miR-181b-5p hsa-miR-181c-5p, and hsa-miR-181d-5p in LIHC in the ENCORI database. (b) Overall survival rates of hsa-miR-181a-5p, hsa-miR-181b-5p hsa-miR-181c-5p, and hsa-miR-181d-5p in LIHC in the ENCORI database. (c) Correlation between hsa-miR-181a-5p, hsa-miR-181b-5p hsa-miR-181c-5p, and hsa-miR-181d-5p expressions and PLAU expression in LIHC in the ENCORI database.

LIHC: Liver hepatocellular carcinoma.

statistically significant difference among stages I, II, III, and IV of LIHC. This suggests that PLAU expression remains relatively stable throughout disease progression, implying that its expression may not be stage-dependent. These findings underscore the need for further research into the functional role of PLAU in HCC subtypes. To our knowledge, this is the first study to explore this specific subject.

To further explore the clinical relevance of PLAU in LIHC, its expression was evaluated across various demographic and clinical subgroups. PLAU expression was significantly upregulated in Caucasian and African-American patients with LIHC, while no significant increase was observed in Asian patients. Moreover, no significant differences were found among the racial groups. These findings may suggest that PLAU plays a role in LIHC tumorigenesis in certain racial populations. PLAU expression was also significantly upregulated in both male and female patients with LIHC. However, no significant difference was observed between the sexes, suggesting that PLAU overexpression occurs independently of sex. Age-stratified analysis showed significant upregulation in the 21–40, 61–80, and 81–100 age groups, but not in the 41–60 group. Nonetheless, the lack of intergroup differences suggests that PLAU overex-

pression is not strongly age-dependent. Similarly, elevated PLAU expression in patients with extreme weight, obesity, and extreme obesity, but not in those with normal weight, was observed. However, the absence of significant variation among weight groups indicates a limited association with body weight. Notably, PLAU overexpression in patients without nodal metastasis (N0) suggests a potential role in early tumorigenesis. However, the absence of significant expression differences in N1 patients or between N0 and N1 groups, suggesting PLAU may not contribute to lymphatic spread in LIHC. Numerous studies suggest that uPA may serve as a prognostic marker, with elevated PLAU expression associated with poor prognosis in HCC [13-15]. Wu et al. [15] reported that high PLAU expression was associated with poorer OS. Tsai et al. [14] found that elevated serum uPA levels were linked to poorer OS in HCC patients after resection. Furthermore, Niu et al. [13] demonstrated that high uPA expression correlated with poor prognosis, indicating its potential role as a prognostic biomarker in HCC. Despite these findings, our analysis using the KM Plotter database did not reveal a statistically significant correlation between PLAU expression and OS or RFS in LIHC patients. The discrepancies between our findings and

those of previous studies may be attributed to differences in sample sizes, methodologies, or the specific databases utilized for analysis. Additionally, the heterogeneity of PLAU expression across different tumor stages, etiologies, and molecular subtypes of HCC may influence prognostic outcomes. Further validation studies are necessary to clarify the prognostic value of PLAU expression in LIHC.

HCC is commonly associated with genetic and epigenetic aberrations [29]. DNA methylation, an important epigenetic modification, plays a critical role in regulating gene expression. Aberrant DNA methylation is a hallmark of cancer, closely linked to the onset, development, and progression of cancer, and it holds potential as a biomarker for diagnosis and prognosis [30, 31]. Specifically, the epigenetic modification of the PLAU gene through DNA methylation has been implicated in cancer development [7]. Numerous studies have demonstrated that the promoter region of PLAU undergoes hypomethylation, which is linked to increased PLAU expression and contributes to its oncogenic effects [28, 30, 32, 33]. Pakneshan et al. [32] found that DNA hypomethylation at the PLAU promoter correlates with elevated expression in aggressive breast cancer, suggesting its potential as an early bimarker. Similarly, Wu et al. [30] reported an inverse relationship between PLAU promoter methylation and gene expression in differentiated thyroid cancer. Additionally, Huo et al. [28] identified a link between PLAU overexpression and DNA hypomethylation in head and neck squamous cell carcinoma, highlighting its role as an independent diagnostic and prognostic biomarker. In the present study, we examined the methylation of the PLAU promoter using the UALCAN database to investigate its role in LIHC. Contrary to existing literature, we found that the PLAU promoter was hypermethylated in LIHC tissues. While hypermethylation is typically linked to gene silencing, our results indicated increased PLAU expression, contradicting the conventional view that DNA methylation always suppresses gene expression [8, 31, 34]. Recent studies have highlighted instances where promoter hypermethylation correlates with increased expression, suggesting a more complex role for DNA methylation [31, 35–37]. Spainhour et al. [35] analyzed data from the TCGA and found that promoter methylation exhibited a positive correlation with gene expression, contrary to the expected negative correlation. This growing evidence suggests a potential link between hypermethylation and increased transcriptional activity. Several hypotheses have been proposed to clarify the molecular mechanisms underlying gene activation from hypermethylated promoters. These mechanisms include the binding of repressive transcription factors, interactions with distal elements, and expression from alternative promoters [31]. Our findings also offer new insights into the intricate relationship between methylation and transcriptional regulation. Further research is necessary to clarify the molecular mechanisms involved in gene activation in hypermethylated promoters and to understand the functional consequences of this epigenetic modification.

The uPA is a key protease that converts plasminogen into plasmin, playing a crucial role in fibrinolysis and coagulation [38]. Our PPI networks and enrichment analysis revealed that PLAU interacts with several proteins, including SERPIN1, SERPIN2, SERPIN5, SERPINEB2, PLAUR, PLG, MMP9, VTN, CTSB, and IGF2R. These interactions are involved in blood coagulation, fibrinolysis, plasminogen activation, and proteolysis. These findings highlight PLAU as a central regulator of the plasminogen system, contributing to tumor progression through proteolytic activity and ECM degradation. The interaction between PLAU and coagulation-related proteins suggests a dynamic crosstalk between fibrinolysis and tumor microenvironment remodeling, supporting the hypothesis that dysregulated hemostasis contributes to cancer progression [39]. While uPA is not a direct coagulation factor, it plays an essential role in the fibrinolytic system. Dysregulation of coagulation and proteolysis has been strongly linked to cancer progression, with proteases promoting tumor invasion and metastasis [38]. Further research is needed to elucidate the precise roles of PLAU-related proteins and to explore whether targeting PLAU or its associated pathways could offer novel therapeutic strategies for cancer treatment.

The miRNAs regulate key cellular processes such as proliferation, differentiation, and apoptosis. Their dysregulation is linked to various diseases, including cancer, where they play a complex role in tumor development and progression [17, 40]. To further investigate the mechanisms underlying PLAU upregulation in LIHC tissue, we conducted a bioinformatics analysis to predict miRNAs targeting PLAU. Our analysis identified hsa-miR-181a-5p and hsa-miR-181b-3p as upregulated in LIHC, showing a significant positive correlation with PLAU expression. Notably, no prior studies have explored the relationship between these miRNAs and PLAU in HCC. Recently, there has been growing interest in the roles of the miR-181 family in cancer. Research suggests that the miR-181 family members can act as either oncogenes or tumor suppressors, depending on the cellular context, and influence major pathways by targeting multiple genes [40-44]. Hsa-miR-181a-5p, a highly conserved microRNA, regulates crucial tumor-related processes, including proliferation, apoptosis, autophagy, angiogenesis, EMT, and migration [40]. Extensive studies have reported both upregulated and downregulated expression levels of hsa-miR-181a-5p across various tumor types [43-47]. These conflicting findings highlight the complexity of miRNAs, as their functions can vary significantly across tumor types. Hsa-miR-181a-5p has also been studied in HCC. Korhan et al. [44] demonstrated that hsa-miR-181a-5p is downregulated in HCC and directly targets c-Met, thereby inhibiting cell motility, invasion, and branching morphogenesis. Similarly, Bi et al. [45] reported that hsa-miR-181a-5p is downregulated in HCC and inversely correlated with Early Growth Response Factor 1 (Egr1) expression. Notably, overexpression of hsa-miR-181a-5p suppressed Egr1, inhibiting the TGF-β1/Smad pathway and reducing proliferation. Conversely, Chang et al. [48] found that IncRNA-XIST enhances the expression of the tumor suppressor gene PTEN by inhibiting hsa-miR-181a-5p. Restoration of hsa-miR-181a-5p expression

was shown to promote HCC cell proliferation and invasion. Yaday et al. [49] demonstrated that free fatty acid-induced hsamiR-181a-5p promotes apoptosis in hepatic cells by targeting and downregulating X-linked inhibitor of apoptosis protein and B-cell lymphoma 2, both of which are anti-apoptotic proteins. Numerous studies have shown that hsa-miR-181b-5p is overexpressed in various cancers, including HCC, where it promotes tumor progression through multiple signaling pathways [41, 42, 50]. Wang et al. [42] demonstrated that TGF-β signaling upregulates hsa-miR-181b in NASH-associated hepatocarcinogenesis by targeting tissue inhibitor of metalloproteinases 3 (TIMP3), leading to ECM degradation and tumor growth. These findings highlight the significance of the TGF-β/miR-181b/ TIMP3 axis in hepatocarcinogenesis and its potential as a therapeutic target. Similarly, Yu et al. [50] found that cSMARCA5 suppresses HCC progression by sponging miR-181b-5p, thereby restoring TIMP3 expression. Our findings align with these studies. In conclusion, hsa-miR-181a-5p and hsa-miR-181b-5p play important roles in HCC progression by acting through multiple signaling pathways. Our study demonstrated that the upregulation of these miRNAs and their positive correlation with PLAU may be a shared mechanism promoting tumor progression. This highlights the potential of targeting PLAU and hsa-miR-181a/hsa-miR-181b as a therapeutic strategy in HCC. Further research is required to clarify the roles and regulatory mechanisms of hsa-miR-181a-5p and hsa-miR-181b-5p in HCC.

Conclusion

To our knowledge, our study is the first to examine the relationship between PLAU and miRNAs in HCC using several bioinformatic databases. This study indicates that PLAU may play a significant role in HCC development through epigenetic modification and miRNA interactions. The positive correlation with hsa-miR-181a-5p and hsa-miR-181b-5p suggest a complex regulatory network influencing tumor development. However, the lack of association with OS and RFS suggests that while PLAU may contribute to tumor development, its prognostic significance in HCC remains uncertain. Further investigation into their functional interplay and regulatory mechanisms is essential to understand their role in HCC pathogenesis better.

Informed Consent: Informed consent was obtained from all participants.

Conflict of Interest Statement: The authors have no conflicts of interest to declare.

Funding: The authors declared that this study received no financial support.

Use of Al for Writing Assistance: No Al technologies utilized.

Authorship Contributions: Concept – G.S.S., D.A.; Design – G.S.S., D.A.; Supervision – G.S.S., D.A.; Funding – G.S.S., D.A.; Materials – G.S.S., D.A.; Data collection and/or processing – G.S.S., D.A.; Data analysis and/or interpretation – G.S.S., D.A.; Literature search – G.S.S., D.A.; Writing – G.S.S.; Critical review – G.S.S., D.A.

Peer-review: Externally peer-reviewed.

References

- 1. Chakraborty E, Sarkar D. Emerging therapies for hepatocellular carcinoma (HCC). Cancers 2022;14(11):2798. [CrossRef]
- Sung H, Ferlay J, Siegel RL, Laversanne M, Soerjomataram I, Jemal A, et al. Global cancer statistics 2020: GLOBOCAN estimates of incidence and mortality worldwide for 36 cancers in 185 countries. CA Cancer J Clin 2021;71(3):209–49. [CrossRef]
- 3. Llovet JM, Kelley RK, Villanueva A, Singal AG, Pikarsky E, Roayaie S, et al. Hepatocellular carcinoma. Nat Rev Dis Primers 2021;7(1):6. [CrossRef]
- 4. Raja A, Haq F. Molecular classification of hepatocellular carcinoma: Prognostic importance and clinical applications. J Cancer Res Clin Oncol 2022;148(1):15–29. [CrossRef]
- 5. Chidambaranathan-Reghupaty S, Fisher PB, Sarkar D. Hepatocellular carcinoma (HCC): Epidemiology, etiology and molecular classification. Adv Cancer Res 2021;149:1–61. [CrossRef]
- 6. Akkız H. Emerging role of cancer-associated fibroblasts in progression and treatment of hepatocellular carcinoma. Int J Mol Sci 2023;24(4):3941. [CrossRef]
- 7. Su SC, Lin CW, Yang WE, Fan WL, Yang SF. The urokinase-type plasminogen activator (uPA) system as a biomarker and therapeutic target in human malignancies. Expert Opin Ther Targets 2016;20(5):551–66. [CrossRef]
- 8. Mahmood N, Mihalcioiu C, Rabbani SA. Multifaceted role of the urokinase-type plasminogen activator (uPA) and its receptor (uPAR): Diagnostic, prognostic, and therapeutic applications. Front Oncol 2018;8:24. [CrossRef]
- 9. Mekkawy AH, Pourgholami MH, Morris DL. Involvement of urokinase-type plasminogen activator system in cancer: An overview. Med Res Rev 2014;34(5):918–56. [CrossRef]
- 10. Masucci MT, Minopoli M, Di Carluccio G, Motti ML, Carriero MV. Therapeutic strategies targeting urokinase and its receptor in cancer. Cancers 2022;14(3):498. [CrossRef]
- 11. Ma J, Qi G, Xu J, Ni H, Xu W, Ru G, et al. Overexpression of forkhead box M1 and urokinase-type plasminogen activator in gastric cancer is associated with cancer progression and poor prognosis. Oncol Lett 2017;14(6):7288–96. [CrossRef]
- Hosen SMZ, Uddin MN, Xu Z, Buckley BJ, Perera C, Pang TCY, et al. Metastatic phenotype and immunosuppressive tumour microenvironment in pancreatic ductal adenocarcinoma: Key role of the urokinase plasminogen activator (PLAU). Front Immunol 2022;13:1060957. [CrossRef]
- 13. Niu FY, Jin C, Ma L, Shi YX, Li XS, Jiang P, et al. Urokinase plasminogen activator predicts poor prognosis in hepatocellular carcinoma. J Gastrointest Oncol 2021;12(4):1851–9. [CrossRef]
- 14. Tsai MC, Yen YH, Chang KC, Hung CH, Chen CH, Lin MT, et al. Elevated levels of serum urokinase plasminogen activator predict poor prognosis in hepatocellular carcinoma after resection. BMC Cancer 2019;19(1):1169. [CrossRef]
- 15. Wu J, Sun M, Li Z, Shen Y, Wu Y, Zhang H, et al. Effect of urokinase-type plasminogen activator combined with clinical stage and Barcelona Clinic Liver Cancer stage on the prognosis of patients with hepatocellular carcinoma. J Gastrointest Oncol 2023;14(3):1434–50. [CrossRef]

- Zhao X, Liu Z, Ren Z, Wang H, Wang Z, Zhai J, et al. Triptolide inhibits pancreatic cancer cell proliferation and migration via down-regulating PLAU based on network pharmacology of Tripterygium wilfordii Hook F. Eur J Pharmacol 2020;880:173225. [CrossRef]
- 17. Babaei K, Shams S, Keymoradzadeh A, Vahidi S, Hamami P, Khaksar R, et al. An insight of microRNAs performance in carcinogenesis and tumorigenesis; an overview of cancer therapy. Life Sci 2020;240:117077. [CrossRef]
- 18. Qiu P, Guo Q, Yao Q, Chen J, Lin J. Hsa-mir-3163 and CCNB1 may be potential biomarkers and therapeutic targets for androgen receptor positive triple-negative breast cancer. PLoS One 2021;16(11):e0254283. [CrossRef]
- 19. Bartha Á, Győrffy B. TNMplot.com: A web tool for the comparison of gene expression in normal, tumor and metastatic tissues. Int J Mol Sci 2021;22(5):2622. [CrossRef]
- 20. Tang Z, Kang B, Li C, Chen T, Zhang Z. GEPIA2: An enhanced web server for large-scale expression profiling and interactive analysis. Nucleic Acids Res 2019;47(W1):W556–60. [CrossRef]
- 21. Chandrashekar DS, Karthikeyan SK, Korla PK, Patel H, Shovon AR, Athar M, et al. UALCAN: An update to the integrated cancer data analysis platform. Neoplasia 2022;25:18–27. [CrossRef]
- 22. Menyhart O, Nagy A, Gyorffy B. Determining consistent prognostic biomarkers of overall survival and vascular invasion in hepatocellular carcinoma. R Soc Open Sci 2018;5(122):181006. [CrossRef]
- 23. Szklarczyk D, Kirsch R, Koutrouli M, Nastou K, Mehryary F, Hachilif R, et al. The STRING database in 2023: Protein-protein association networks and functional enrichment analyses for any sequenced genome of interest. Nucleic Acids Res 2023;51(D1):D638–46. [CrossRef]
- 24. McGeary SE, Lin KS, Shi CY, Pham TM, Bisaria N, Kelley GM, et al. The biochemical basis of microRNA targeting efficacy. Science 2019;366(6472):eaav1741. [CrossRef]
- 25. Lewis BP, Burge CB, Bartel DP. Conserved seed pairing, often flanked by adenosines, indicates that thousands of human genes are microRNA targets. Cell 2005;120(1):15–20. [CrossRef]
- 26. Friedman RC, Farh KK, Burge CB, Bartel DP. Most mammalian mRNAs are conserved targets of microRNAs. Genome Res 2009;19(1):92–105. [CrossRef]
- 27. Li JH, Liu S, Zhou H, Qu LH, Yang JH. starBase v2.0: Decoding miRNA-ceRNA, miRNA-ncRNA and protein-RNA interaction networks from large-scale CLIP-Seq data. Nucleic Acids Res 2014;42:D92–7. [CrossRef]
- 28. Huo Z, Li X, Zhou J, Fan Y, Wang Z, Zhang Z. Hypomethylation and downregulation of miR-23b-3p are associated with upregulated PLAU: A diagnostic and prognostic biomarker in head and neck squamous cell carcinoma. Cancer Cell Int 2021;21(1):564. [CrossRef]
- 29. Nagaraju GP, Dariya B, Kasa P, Peela S, El-Rayes BF. Epigenetics in hepatocellular carcinoma. Semin Cancer Biol 2022;86(Pt 3):622–32. [CrossRef]
- 30. Wu M, Wei B, Duan SL, Liu M, Ou-Yang DJ, Huang P, et al. Methylation-driven gene plau as a potential prognostic marker for differential thyroid carcinoma. Front Cell Dev Biol 2022;10:819484. [CrossRef]

- 31. Smith J, Sen S, Weeks RJ, Eccles MR, Chatterjee A. Promoter DNA hypermethylation and paradoxical gene activation. Trends Cancer 2020;6(5):392–406. [CrossRef]
- 32. Pakneshan P, Têtu B, Rabbani SA. Demethylation of urokinase promoter as a prognostic marker in patients with breast carcinoma. Clin Cancer Res 2004;10(9):3035–41. [CrossRef]
- 33. Guo Y, Pakneshan P, Gladu J, Slack A, Szyf M, Rabbani SA. Regulation of DNA methylation in human breast cancer effect on the urokinase-type plasminogen activator gene production and tumor invasion. J Biol Chem 2002;277(44):41571–9. [CrossRef]
- 34. Chen QW, Zhu XY, Li YY, Meng ZQ. Epigenetic regulation and cancer (review). Oncol Rep 2014;31(2):523–32. [CrossRef]
- 35. Spainhour JC, Lim HS, Yi SV, Qiu P. Correlation patterns between DNA methylation and gene expression in the cancer genome atlas. Cancer Inform 2019;18:1176935119828776. [CrossRef]
- 36. Rauluseviciute I, Drabløs F, Rye MB. DNA hypermethylation associated with upregulated gene expression in prostate cancer demonstrates the diversity of epigenetic regulation. BMC Med Genomics 2020;13(1):6. [CrossRef]
- 37. Chatterjee A, Stockwell PA, Rodger EJ, Parry MF, Eccles MR. Scan_tcga tools for integrated epigenomic and transcriptomic analysis of tumor subgroups. Epigenomics 2016;8(10):1315–30. [CrossRef]
- 38. Azam A, Klisic A, Mercantepe F, Faseeh H, Mercantepe T, Rafaqat S. Role of coagulation factors in hepatocellular carcinoma: A literature review. Life 2024;15(1):34. [CrossRef]
- 39. Bharadwaj AG, Holloway RW, Miller VA, Waisman DM. Plasmin and plasminogen system in the tumor microenvironment: Implications for cancer diagnosis, prognosis, and therapy. Cancers 2021;13(8):1838. [CrossRef]
- 40. Li J, Shen J, Zhao Y, Du F, Li M, Wu X, et al. Role of miR-181a-5p in cancer (review). Int J Oncol 2023;63(4):108. [CrossRef]
- 41. Fu X, He Y, Song J, Wang L, Guo P, Cao J. MiRNA-181b-5p modulates cell proliferation, cell cycle, and apoptosis by targeting SSX2IP in acute lymphoblastic leukemia. Turk J Haematol 2022;39(3):160–9. [CrossRef]
- 42. Wang B, Hsu SH, Majumder S, Kutay H, Huang W, Jacob ST, et al. TGFbeta-mediated upregulation of hepatic miR-181b promotes hepatocarcinogenesis by targeting TIMP3. Oncogene 2010;29(12):1787–97. [CrossRef]
- 43. Shi L, Cheng Z, Zhang J, Li R, Zhao P, Fu Z, et al. hsa-mir-181a and hsa-mir-181b function as tumor suppressors in human glioma cells. Brain Res 2008;1236:185–93. [CrossRef]
- 44. Korhan P, Erdal E, Atabey N. MiR-181a-5p is downregulated in hepatocellular carcinoma and suppresses motility, invasion and branching-morphogenesis by directly targeting c-Met. Biochem Biophys Res Commun 2014;450(4):1304–12. [CrossRef]
- 45. Bi JG, Zheng JF, Li Q, Bao SY, Yu XF, Xu P, et al. MicroRNA-181a-5p suppresses cell proliferation by targeting Egr1 and inhibiting Egr1/TGF-β/Smad pathway in hepatocellular carcinoma. Int J Biochem Cell Biol 2019;106:107–16. [CrossRef]
- 46. Fei J, Li Y, Zhu X, Luo X. miR-181a post-transcriptionally down-regulates oncogenic RalA and contributes to growth inhibition and apoptosis in chronic myelogenous leukemia (CML). PLoS One 2012;7(3):e32834. [CrossRef]

- 47. Shin KH, Bae SD, Hong HS, Kim RH, Kang MK, Park NH. miR-181a shows tumor suppressive effect against oral squamous cell carcinoma cells by downregulating K-ras. Biochem Biophys Res Commun 2011;404:896–902. [CrossRef]
- 48. Chang S, Chen B, Wang X, Wu K, Sun Y. Long non-coding RNA XIST regulates PTEN expression by sponging miR-181a and promotes hepatocellular carcinoma progression. BMC Cancer 2017;17(1):248. [CrossRef]
- 49. Yadav AK, Sata TN, Verma D, Mishra AK, Sah AK, Hossain MM, et al. Free fatty acid-induced miR-181a-5p stimulates apoptosis by targeting XIAP and Bcl2 in hepatic cells. Life Sci 2022;301:120625. [CrossRef]
- 50. Yu J, Xu QG, Wang ZG, Yang Y, Zhang L, Ma JZ, et al. Circular RNA cSMARCA5 inhibits growth and metastasis in hepatocellular carcinoma. J Hepatol 2018;68(6):1214–22. [CrossRef]

INTERNATIONAL JOURNAL OF

MEDICAL BIOCHEMISTRY

DOI: 10.14744/ijmb.2025.60973 Int J Med Biochem 2025;8(4):272–281

Research Article



Tau protein expression and phosphorylation in a glucoserepressed yeast model: Insights into the cancer-alzheimer's disease link

Merve Yilmazer, Semian Karaer Uzuner

Department of Molecular Biology and Genetics, Istanbul University Faculty of Science, Istanbul, Türkiye

Abstract

Objectives: The microtubule-associated protein tau, responsible for stabilizing microtubules, plays a role in the pathology of neurodegenerative diseases called tauopathies, including Alzheimer's disease. In Alzheimer's disease, neurofibrillary tangle formation is observed as a result of tau hyperphosphorylation. Although it is known that tau protein plays a role in many cellular processes, all of its functions have not yet been elucidated. The inverse relationship between Alzheimer's disease and cancer has been a topic of research that has attracted attention in recent years. In addition, the role of tau protein in cancer has also gained importance with the determination of its direct relationship with DNA. In particular, the negative correlation between Alzheimer's disease and cancer points to two extremes of a common mechanism. Discovering a common molecule or pathway will allow understanding the cause of both diseases and developing treatments.

Methods: In this study, we obtained a cell model that mimics cancer metabolism by creating aerobic glycolysis-like conditions with glucose repression in *S. pombe* cells heterologously expressing human tau protein. We examined tau protein expression and phosphorylation (S262, S396 and S404) and various cellular processes (glucose metabolism, stress response, ER stress, autophagy, 20S proteosome activity, intracellular oxidation) at the molecular level in model cells.

Results: Under aerobic glycolysis-like conditions, we observed an approximately 2-fold increase in tau protein expression. In addition to this increase, we determined that the amount of phosphorylation at S396 residue of tau protein was decreased, while phosphorylation at S262 and S404 residues was increased.

Conclusion: These findings suggest a potential divergence in tau regulation under altered metabolic conditions, warranting further investigation.

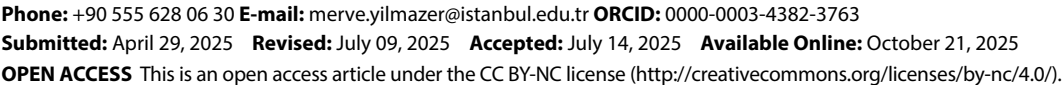
Keywords: Cancer, glucose repression, heterologous expression, tauopathy, tau protein

How to cite this article: Yilmazer M, Uzuner SK. Tau protein expression and phosphorylation in a glucose-repressed yeast model: Insights into the cancer-alzheimer's disease link. Int J Med Biochem 2025;8(4):272–281.

Microtubules play a role in morphogenesis, cell division, intracellular transport of macromolecules and organelles, and motility [1]. These processes occur through dynamic restructuring of microtubules mediated by microtubule-associated proteins such as tau. Tau protein is responsible for the stabilization of microtubules [2]. There is great interest in tau protein because it plays a major role in neurodegenerative diseases referred to as tauopathies, including Alzheimer's disease

(AD) [3]. There is increasing evidence that tau protein, in addition to its microtubule stabilizing function, is implicated in many significant signaling pathways, including proliferation, morphogenesis, and cell differentiation [4]. A lesser-known property of tau is its ability to bind to cancer-associated protein kinases. This suggests that tau has a potential role in regulating microtubule-independent cellular pathways [3]. It has also been determined that tau protein can bind to nu-

Address for correspondence: Merve Yilmazer, MD. Department of Molecular Biology and Genetics, Istanbul University Faculty of Science, Istanbul, Türkiye







cleic acids [5]. Tau has been suggested to be a DNA protector, specifically by preventing stress-induced DNA breaks [6, 7].

Over 55 million individuals globally suffer from dementia, with AD constituting 60-70% of these instances. The global prevalence of Alzheimer's disease is projected to surpass 138 million by 2050 [8]. Another leading disease with a high mortality rate is cancer. Approximately 10 million deaths attributed to cancer were reported globally in 2020, along with 19.3 million newly diagnosed cases of cancer. [9, 10]. In AD, alterations in behavior and cognitive impairments linked to neurodegeneration typically manifest around a decade following the beginning of protein pathy. Its two characteristic features are AB plaques, and neurofibrillary tangles caused by tau hyperphosphorylation [11]. Cancer is a disease in which some cells uncontrolled divide by genetic mutations and they spread to other parts of the body. Brown and colleagues define cancer as a disease characterized by the uncontrolled multiplication of altered cells that undergo evolution through natural selection [12]. Multiple epidemiological studies indicate a negative correlation between cancer and AD [13]. This intriguing correlation is limited to certain types of cancer and neurodegenerative diseases. However, the underlying mechanisms of the two diseases are very different. While cancers evade cell death, neurodegeneration leads to cell death. As a result, it is possible that people with a neurodegenerative disease might have a lower likelihood of developing specific kinds of cancer, and the opposite might also be true [14]. Even though the underlying physiological processes of cancer and AD have been extensively researched, they are not yet distinctly understood [10].

Dysregulation of cellular energy metabolism is one of the hallmarks of cancer [15]. The Warburg effect refers to the transition from aerobic respiration to aerobic glycolysis, resulting in the production of lactate from glucose as the end-product. Warburg reported that even when oxygen is sufficient in an environment, cancer cells generally use glucose via glycolysis rather than oxidative phosphorylation [16]. Cancer cells typically exhibit increased glycolysis and diminished oxidative phosphorylation. While this long-term metabolic reprogramming is known as the Warburg effect, the short-term, reversible alteration of this metabolic process is known as the Crabtree effect [17]. The Warburg effect provides an advantage for cancer cells to survive and progress. In order to achieve high aerobic glycolysis rates, some types of cancer cells are induced to possess specific isoforms of glycolytic enzymes [18]. This metabolic adaptation helps cancer cells to proliferate and become more invasive. The relationship between high glucose and cancer development is still being investigated [19].

Glucose is the preferred carbon source for most living cells, and glucose metabolism provides the energy necessary for cell survival [20]. In yeast, glucose can induce the expression of various genes encoding some glucose transporters, ribosomal proteins, and glycolytic enzymes, by a process known as glucose induction. At the same time, the expression of numerous genes involved in respiration, gluconeogenesis, and the

utilization of alternative carbon sources can be suppressed, in the process named glucose repression. Yeasts are easy to use as models in studies examining glucose perception and signal transduction because of their similarity to complex multicellular eukaryotes in terms of glucose metabolism. Although yeast cells can use a wide variety of carbon sources, the presence of abundant glucose suppresses the utilization of alternative carbon sources, cellular respiration, and gluconeogenesis [21]. Schizosaccharomyces pombe, the fission yeast, is a single-celled model organism that can be used in studies on glucose sensing, intracellular signaling, and signal response processes. It shows high similarity with multicellular eukaryotic organisms in terms of molecular processes [22, 23].

Genes involved in various processes in human have orthologs in *S. pombe*, and *S. pombe* has 1514 orthologous transcripts (proteins and ncRNAs) associated with human diseases [24, 25]. Phosphorylation of tau protein, which plays a role in various diseases, is carried out by glycogen synthase kinase 3 beta (GSK-3 β), cyclin-dependent kinase 5 (CDK-5), and cAMP-dependent protein kinase A (PKA) and the orthologous of the human GSK3 β gene, which is the major kinase in the phosphorylation of tau protein, exists in the *S. pombe* genome [26–28]. Moreover, in our previous studies, we showed that human tau protein is phosphorylated in the *S. pombe* model, and we detailed several cellular processes [29, 30].

In this study, based on the inverse correlation seen in cancer and neurodegenerative diseases, we investigated the relationship between tau protein and the aerobic fermentation process observed in cancer, which we mimicked by glucose repression metabolism in yeast. We hypothesize that one of the factors affecting the dysregulation of glucose metabolism in neurodegenerative diseases and cancer may be the tau protein, which stands out with its role in microtubule stabilization and has a potential effect on glucose metabolism. In the present study, the conditions of glucose repression in S. pombe were referred to as "aerobic glycolysis-like state". For this purpose, we cultured *S. pombe* cells heterologously producing human tau protein under high glucose conditions (5%) to create glucose-repression and mimicked aerobic fermentation in cancer cells. We studied various processes at the molecular level in model cells with aerobic glycolysis-like metabolism in the presence of tau protein. In our model cells, a decrease in stress response was seen, as in cancer cells. We determined that under aerobic glycolysis-like conditions, the expression of tau protein in cells increased approximately 2-fold. Additionally, we observed a decrease in the phosphorylation level at the S396 site of tau protein and an increase in the phosphorylation levels at the S404 and S262 regions. Contrary to expectations under aerobic glycolysis-like conditions, the increase in tau level and the decrease in hexokinase, which plays a role in glycolysis, suggested that tau protein has a greater role in glucose metabolism than is known. The findings suggest that the inverse relationship between neurodegenerative diseases and cancer may be due to differences in the phosphorylation level of tau protein, which plays a role in

Table 1. Primer sequences used in real-time PCR						
Gene	Forward Primer	Reverse Primer	Tm (°C)			
gpdh	5' ggtgacaaccactcctccat 3'	5' tcaacaacacggtgggagta 3'	55			
mapt	5' caagtgtggctcaaaggataat 3'	5' ggtttatgatggatgttgcctaa 3'	55			
hxk2	5' caacaaggactttgcccaat 3'	5' aaggtgtcgctctcctttga 3'	55			
fbp1	5' gtatggtgcttcggctcatt 3'	5' ttcatgtttcgatgggtcaa 3'	55			
sod1	5' attggccgtaccattgtcat 3'	5' gacaccacaagcgttacgtg 3'	55			
ctt1	5' atcctcaatccgaccacttg 3'	5' aacgtcggtaatttcgtcca 3'	55			
ire1	5' attctcgacattcttcgggt 3'	5' aacttgtgaatccgtctggt 3'	55			
atg14	5' tcaccctagtttactctcaaca 3'	5' cggcaaatgtccataaaaactc 3'	55			
gsk3	5' gatgcttctcctcgtcatt 3'	5' catcaagtttcacgggtaaag 3'	55			
pp2a	5' tattgttatcgctgtggtaatc 3'	5' ggtgtccttcgagctatt 3'	55			

the molecular mechanisms of both diseases, or to an as-yet-unknown function of tau protein in glucose metabolism.

Materials and Methods

Yeast strain and culture conditions

In the present study, we used *S. pombe* cells (pMS-mapt) that produce human tau protein, which we obtained in our previous study [29]. pMS-mapt cells are auxotrophic for guanine and carry the human *MAPT* gene in the pSGP572 plasmid. pSGP572 contains the *ura4* marker gene, and the *GFP* gene at the 3'-terminal in the cloning site. So, the tau protein produced is a fusion protein with GFP. The *MAPT* and *GFP* genes are under the control of the *nmt* promoter, which is an inducible promoter and is repressed by thiamine [31].

In this study, we investigated the relationship between aerobic fermentation conditions and tau protein. Firstly, tau protein production was induced in pMS-mapt cells [24], then these cells were grown under different glucose conditions. For this purpose, cells were grown in standard EMM (1% glucose) medium containing thiamine (15 μ M) and guanine (50 mg/L) at 30°C for 24 hours. Then, the cells were washed with PBS and cultured in standard thiamine-free EMM medium with guanine for 20 hours. After incubation, cells were washed with PBS and cultured in EMM containing different concentrations of glucose (3% and 5%) at 30°C for 4 hours.

Cell densities of pMS-mapt cells were measured spectrophotometrically at 600nm wavelength for 32 hours, and their growth under different conditions were compared. Cells grown under different glucose concentration conditions were examined under the microscope.

Gene expression analysis

After cells collected, total RNA isolation was performed by using "Thermo Scientific GeneJET RNA Purification Kit", according to the manufacturer's instructions with a minor modification. Cells in PBS were mechanically homogenized by using glass beads. After RNA isolation, cDNA was synthesized from 2 µg of total RNA by using a "Roche Transcriptor High Fidelity cDNA Synthesis Kit", according to the manufacturer's instructions.

We examined the expression level of genes related to various cellular mechanisms, including glucose metabolism (hxk2, fbp1), stress response (sod1, ctt1), ER stress (ire1), autophagy (atg14), and regulators of tau phosphorylation (gsk3, pp2a). Additionally, mapt gene expression was also examined.

Real-Time PCR was performed using "ThermoScientific Applied Biosystems PowerUp SYBR™ Green PCR Master Mix" kit and the primers, which we used in our previous study, listed in Table 1 [24]. Pairs of primers were designed using the "IDT PrimerQuest Tool". S. pombe gapdh gene was used as the reference gene. We applied the Pfaffl equation to analyse the relative expression levels of genes and we used gapdh gene expression levels for normalization [32]. All experiments were performed in three biological and technical replicates.

Immunoblotting analysis

Protein extraction from cells grown under different glucose concentration conditions was performed according to the method of Forsburg and Rhind (2006) with minor modifications [31]. The cells were mechanically homogenized by vigorous shaking using glass beads and lysis buffer (150 mM NaCl, 1mM PMSF, 0.5% (w/v) Nonidet-P40, 5 mM EDTA 50 mM Tris). SMART™ bicinchoninic acid (BCA) protein assay kit (iNtRON Biotechnology) was used to quantify total protein. Equal amounts of protein (30 µg/well) was loaded on 10% SDS-PAGE, and transferred to PVDF membrane (Thermo Fisher Scientific). After blocking, the membrane blots were incubated overnight with the following primary antibodies: Anti-tau rabbit IgG (1/1000 dilution, Tau Rabbit mAb, Abclonal) and anti-phospho-tau (Ser396) rabbit IgG (E178) (1/1000 dilution, ab32057, Abcam), phospho-tau S404 Rabbit mAb (1/1000 dilution, AP1378 Abclonal) and phospho-tau S262 Rabbit pAb (1/1000 dilution, AP0397 Abclonal). Anti-GAPDH mouse IgG (1/2500 dilution, MA5-15738 Invitrogen) was used as internal control. The washed membranes were incubated with HRP-linked secondary antibody (1/5000 dilution anti-rabbit HRP Goat Anti-Rabbit IgG, Abclonal). Following washing, the blots were visualized using SuperSignal West Pico PLUS ECL reagent (Thermo Fisher Scientific). Immunoblots (heterologous MAPT protein levels) were imaged

using the ChemiDoc XRS system (BioRad). We performed quantification by using ImageLab 6.0.1 software (Bio-Rad).

Measurement of 20S proteasome activity

We determined 20S proteasome activity as suggested by Reinheckel et al. [33]. After protein extraction from grown cells under stated conditions, we diluted protein concentration to 50 μ g/mL with assay buffer (50 mM Tris, 20 mM KCl, 0.5M DTT, 5 mM CH3(COO)2). To measure peptidase activity, we added 99 μ L assay buffer and 1 μ L Suc-Leu-Leu-Val-Tyr-AMC (Sigma) (stock 40 mM) to 100 μ L of diluted protein sample. After 1 h incubation at 37°C, the reaction was stopped by adding an equal volume of cold ethanol and 1.6 mL of 125 mM sodium borate buffer (Na2B4O7.10H2O, pH 9.0). Then, we measured 20S proteasome activity by a spectrofluorometer plate reader (ex: 390nm, em: 470 nm).

Determination of intracellular oxidation level

We determined the intracellular oxidation level as recommended by Inoue et al. [34]. In this method, intracellular oxidation level is measured by conversion of DCFH-DA (2',7' dichlorofluorescein diacetate) to the fluorescent compound 2',7'-dichlorofluorescein. pMS-mapt cells grown in EMM media containing guanine and different glucose concentrations (3%, 5%) were centrifuged for 5 minutes at 3000 g, and cells were dissolved in 1 mL EMM media with guanine. 40 µM DHCF-DA (Sigma) solution dissolved in ethanol was added and incubated at 30°C for 1 h, and the samples were washed with PBS. We kinetically measured intracellular oxidation level with a spectrofluorometer plate reader (Bio-tek FLx800) with excitation and emission wavelengths of 490 and 524 nm.

Imaging by microscopy

S. pombe cells grown under the stated conditions were fixed using 10% formaldehyde, and the cells were washed with PBS. Then, cells were examined under the microscopy (Olympus BX53).

Statistical data

We expressed all of our data as mean±SD. We used GraphPad Prism 9 software for statistical comparisons based on Student's t-test. The value of p<0.05 was considered statistically significant.

Results

Microscopic examination of the cells

We examined pMS-mapt cells grown under different glucose concentrations under the microscope, and observed morphological differences in cells grown under aerobic glycolysis-like conditions for 4 hours (Fig. 1a). Additionally, the absorbance graph of cell cultures measured every two hours at 600 nm wavelength for 32 hours is given in Figure 1b.

Aerobic glycolysis-like conditions

When pMS-mapt cells grown under standard glucose concentration conditions were compared with cells under aerobic

glycolysis-like conditions, a 3.58-fold decrease in the expression of the *hxk2* gene, which encodes the hexokinase 2 enzyme that plays a role in glycolysis in glucose metabolism, was observed under aerobic glycolysis-like conditions. A 4.52-fold decrease was observed in the expression of the *fbp1* gene, which encodes the fructose-1,6-bisphosphatase 1 enzyme that plays a role in gluconeogenesis under aerobic glycolysis-like conditions (Fig. 2).

Tau protein and its phosphorylation

When the expression of tau protein in cells grown under standard and aerobic glycolysis-like conditions was examined by western blot analysis, an increase in total tau was observed under repression conditions, consistent with gene expression analysis. However, it was determined that the phosphorylation level in the S396 region of the tau protein was lower in cells grown under aerobic glycolysis-like conditions, while the phosphorylation level in the S262 and S404 regions of the tau protein was higher in cells grown under aerobic glycolysis-like conditions (Fig. 3a).

Under aerobic glycolysis-like conditions, *MAPT* gene expression increased 2.68-fold. However, the expression of the *gsk3* gene, which is responsible for the phosphorylation of tau protein and encodes the glycogen synthase kinase 3 enzyme, decreased 2.67-fold. In addition, the expression of the *pp2a* gene, which encodes the protein phosphatase 2a enzyme that removes phosphate groups from the tau protein, decreased 2.78-fold (Fig. 3b).

Cellular stress response

When the intracellular oxidation level was examined, a significant 1.86-fold increase was observed under aerobic glycolysis-like conditions (Fig. 4a). The expression of *sod1* and *ctt1* genes, which encode superoxide dismutase and catalase enzymes that play a role in the stress response in the cell, decreased 1.68 and 3.39 times, respectively (Fig. 4b).

Under aerobic glycolysis-like conditions, 20S proteasome activity, one of the pathways responsible for the degradation of proteins in the cell, was found to be 10% higher than standard conditions (Fig. 5a). When the expression of the *atg14* gene, which is related to autophagy, another degradation pathway, was examined, no significant change was observed under aerobic glycolysis-like conditions. The expression of the *ire1* gene, a marker of endoplasmic reticulum stress, decreased 2.14-fold under glucose suppression conditions. (Fig. 5b).

Discussion

In recent years, interest in the relationship between Alzheimer's disease and cancer has increased. There are studies showing that the risk of developing cancer decreases in Alzheimer's patients and, conversely, the risk of developing AD decreases in cancer patients [10, 13, 35, 36]. In their study, Musicco and colleagues reported that the risk of cancer was

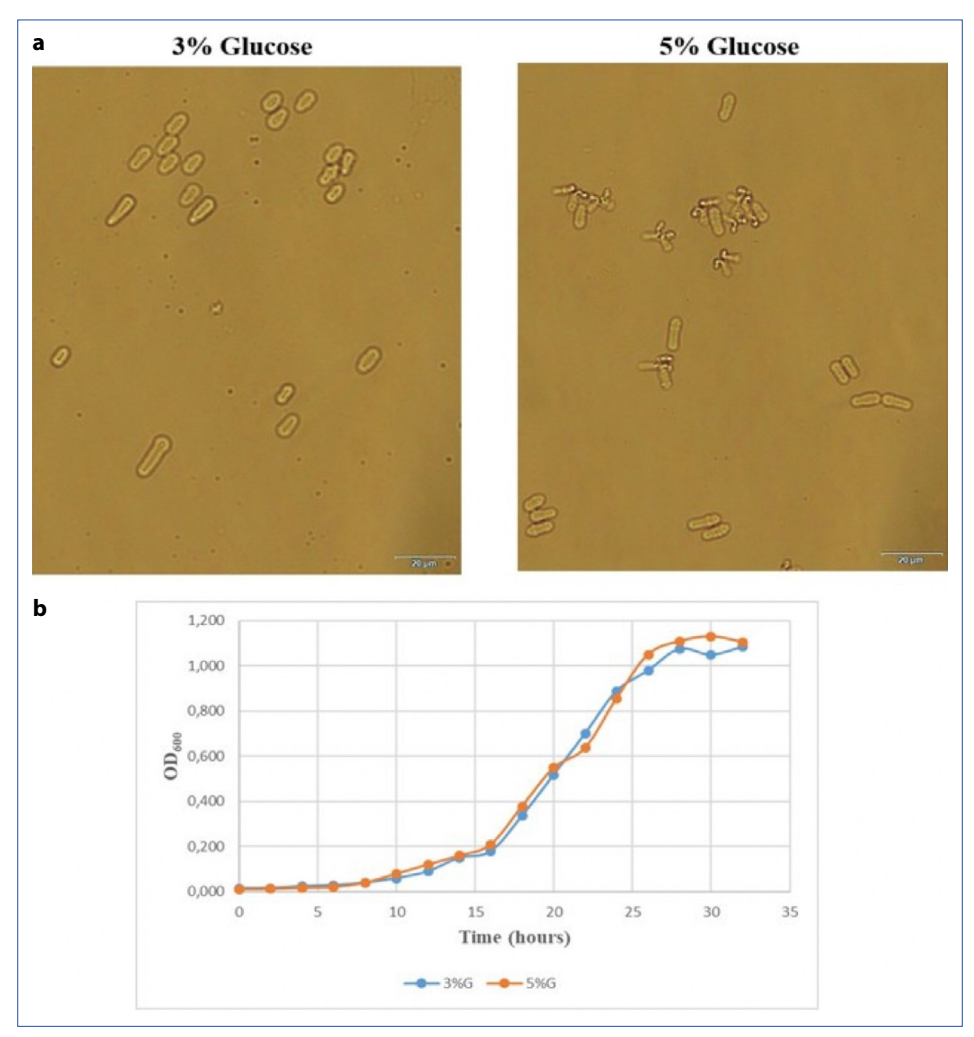


Figure 1. Growth and imaging of pMS-mapt cells under different conditions. (a) Microscope images of pMS-mapt cells grown under different glucose concentrations (40X magnification and bar represents 20 μ m). (b) Growth curves of pMS-mapt cells grown under different glucose concentrations.

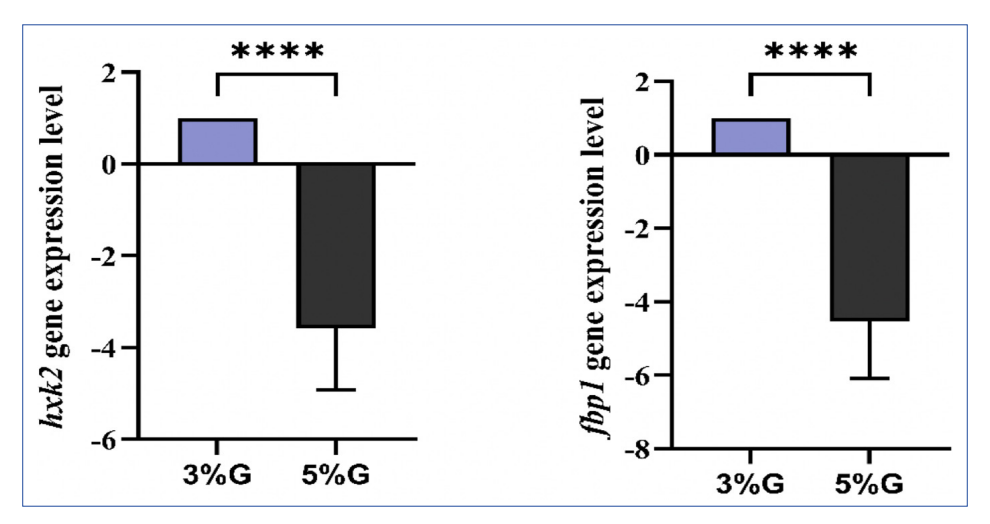


Figure 2. Expression levels of *hxk2* and *fbp1* genes related to glucose metabolism in pMS-mapt cells grown at different glucose (G) concentrations (3%G, 5%G).

Data (mean \pm SD) was derived from three independent experiments and analyzed using unpaired Student's t-test (****p<0.0001).

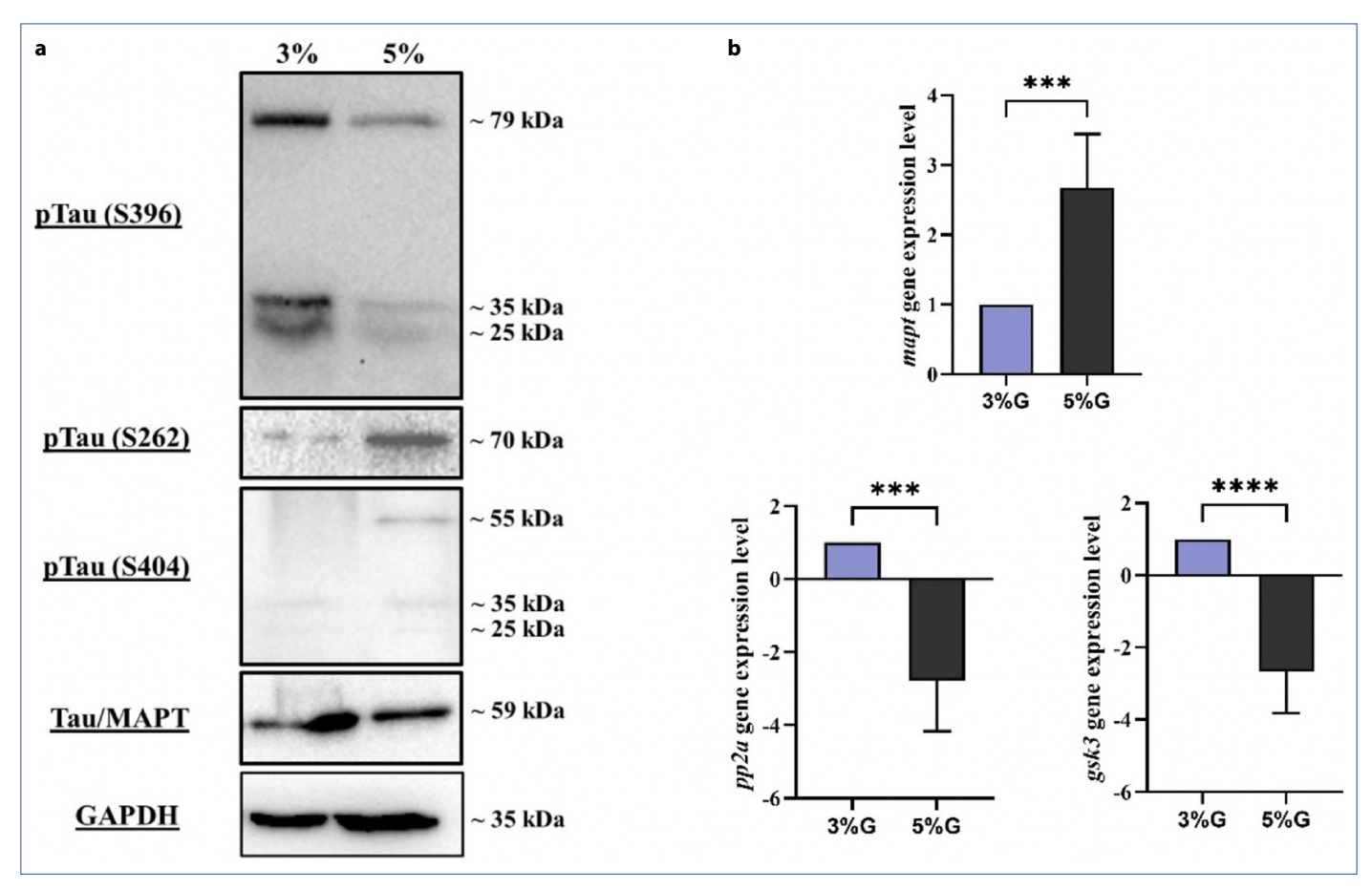


Figure 3. Indication of tau protein expression and phosphorylation in pMS-mapt cells grown under different conditions. (a) Membrane images as a result of western blot of total tau and phosphorylated tau protein (S262, S396 and S404) in pMS-mapt cells. (b) Expression levels of the *MAPT* gene encoding tau protein and the *gsk3* and *pp2a* genes encoding glycogen synthase kinase 3 and protein phosphatase 2a, which are responsible for the phosphorylation and dephosphorylation of tau protein.

Data (mean±SD) was derived from three independent experiments and analyzed using unpaired Student's t-test (***p<0.001; ****p<0.0001). SD: Standard deviation.

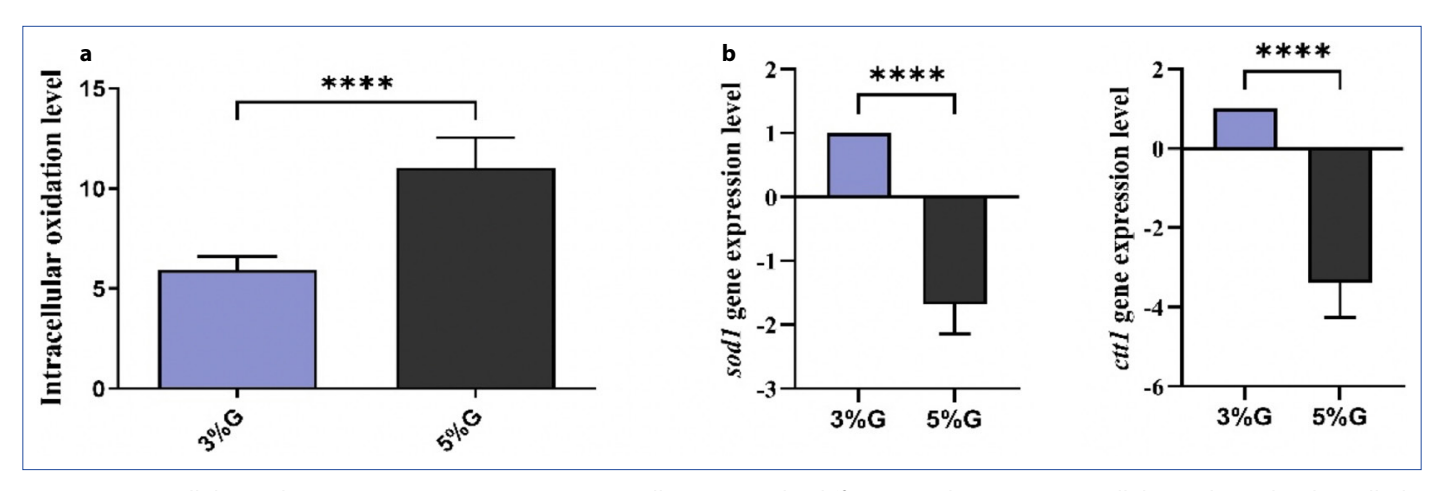


Figure 4. Intracellular oxidative stress response in pMS-mapt cells grown under different conditions. (a) Intracellular oxidation level in cells (b) Expression levels of stress response genes *sod1* and *ctt1*.

Data (mean±SD) was derived from three independent experiments and analyzed using unpaired Student's t-test (****p<0.0001).

halved in AD patients and the risk of AD in cancer patients was reduced by 35% [37]. Although the pathophysiological mechanisms of both cancer and AD have been widely stud-

ied, they have not been elucidated. However, an inverse relationship between them is noticed. It has been determined that patients with AD have a 61% lower risk of cancer [10].

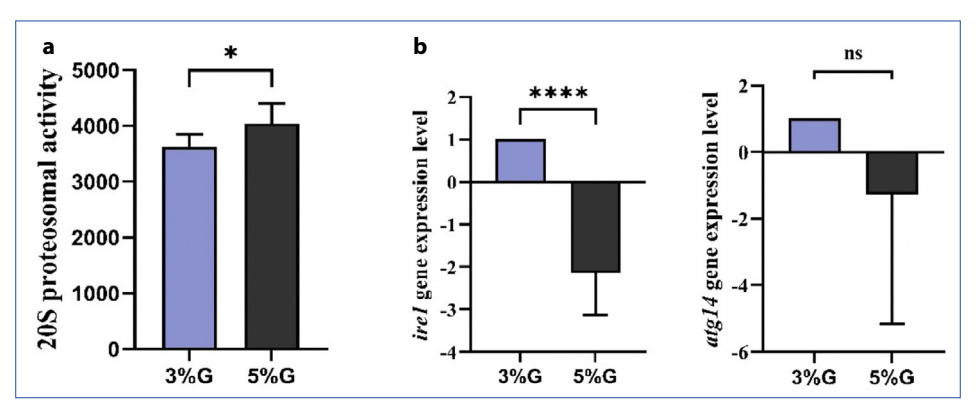


Figure 5.20S proteasome activity in pMS-mapt cells grown under different conditions. (a) 20S proteasome activity in cells (b) Expression levels of ire1 genes, which play a role in ER stress response, and atq14 genes, which play a role in autophagy.

Data (mean±SD) was derived from three independent experiments and analyzed using unpaired Student's t-test (*p<0.05; ****p<0.0001). ns: Non-significant.

Tau protein is recognized for its involvement in neurodegenerative disorders. Research indicates that Tau may contribute to the advancement of several tumors and the resistance to cancer therapies [3]. Numerous studies have documented abnormal levels of tau in cancer cells of the brain, breast, stomach, and prostate [38]. Moreover, the level of tau expression has been associated with resistance to anti-microtubule drugs in cancer [39, 40]. Gargini and colleagues showed that higher levels of MAPT were inversely correlated with glioma aggressiveness [41].

Aerobic glycolysis (Warburg effect) is observed in cancer cells under high glucose conditions. In some types of cancer, glycolytic enzymes are stimulated to achieve high rates of aerobic glycolysis [18]. Glycolysis is promoted, and this metabolic adjustment enables cancer cells to reproduce and invade more rapidly. This strengthens the competition between cancer cells with normal cells [19].

Yeasts also prefer fermentation despite the presence of oxygen, similar to cancer cells, when there is plenty of glucose in the environment. Additionally, the expression of numerous genes that play a role in gluconeogenesis and respiration, the use of alternative carbon sources, and stress response pathways are suppressed in cells [21, 41].

There are both similarities and differences between aerobic glycolysis, where cancer cells turn to glycolysis even in the presence of oxygen (the Warburg effect), and processes where yeast cells prefer fermentation over cellular respiration in the presence of high glucose and oxygen (the Crabtree effect). In both cancer cells and yeast, this fermentative metabolism is associated with rapid growth and proliferation [17]. In both processes, fermentation occurs in an oxygenated environment; however, the end products are lactate (resulting from aerobic glycolysis) or ethanol (resulting from fermentation). Additionally, aerobic glycolysis and fermentation, glycolysis is rapid, and mitochondrial respiration is repressed. Besides their similarities, one of the most important differences is that the Warburg effect is permanent in cancer cells, but in yeast, when glucose is depleted in the environment, aerobic respiration be-

gins [42]. Santos and Hartman (2019) mimicked the Warburg effect by repressing respiration in the presence of glucose in *S. cerevisiae*. They examined the effects of doxorubicin used in chemotherapy in a yeast model and reported that glucose-repressed yeasts could be a suitable model for cancer research [43]. Although yeast, a single-celled organism, cannot fully provide the Warburg effect, it has the potential to elucidate cancer mechanisms due to the similarities between the processes.

In *S. pombe*, glucose is sensed by G protein-coupled receptor (GPCR), and signal transduction occurs via cAMP-dependent protein kinase A (PKA) [22, 44]. Glucose repression signaling represses *fbp1* gene expression via activation of the cAMP-dependent PKA pathway [45]. In our study, under aerobic glycolysis-like conditions, the expression of the *fbp1* gene encoding the fructose-1,6-bisphosphatase-1 enzyme that plays a role in gluconeogenesis was repressed.

Hexokinase-2 enzyme is encoded by the *hxk2* gene and is a rate-limiting enzyme that functions in the first step of the glycolytic cascade [19]. Hxk2 is an important enzyme in glucose repression. Under high glucose conditions, PKA causes hyperphosphorylation of Rgt1, followed by expression of the *hxk2* gene [46, 47]. In our study, transcription of the *hxk2* gene was unexpectedly decreased under aerobic glycolysis-like conditions in pMS-mapt cells. This may be due to the increase in the expression of the *MAPT* gene.

When total tau and the phosphorylation status of tau in the S262, S396, and S404 regions were examined by immunoblot analysis, aerobic glycolysis-like caused an increase in the expression of tau protein, while a decrease in phosphorylation was observed at S396 residue. Tau phosphorylation at S396 and S404 residue is one of the earliest events in AD [48, 49]. We observed that under aerobic glycolysis-like conditions, the increase in *MAPT* gene expression in cells is consistent with the increase in tau protein. However, under aerobic glycolysis-like conditions, higher phosphorylation occurred at residues S262 and S404 of tau protein. Tau phosphorylation at sites such as Ser262 in the proline-rich region and Ser396/404 at the edges of the microtubule binding

site induces conformational change of tau protein and weakens the binding of tau protein to microtubules [50]. Full-length tau has 85 potential phosphorylation sites [51]. Since only three phosphorylation sites (S262, S396, and S404) were analyzed in the present study, our interpretation remains limited. Future studies should include additional AD-relevant phosphorylation sites to better assess tau modification patterns.

Glycogen synthase kinase-3 (GSK3) is a protein kinase composed of GSK3α and GSK3β subunits that phosphorylates a large number of substrates. Increased GSK3 expression has been seen in the brains of AD patients and models. GSK3 directly promotes tau phosphorylation, modulates amyloid precursor protein (APP) breakage, results in AB production, and either directly or indirectly incites neuroinflammation and oxidative injury [52]. In our study, under aerobic glycolysis-like conditions, the expression of the qsk3 gene, which encodes GSK3, which phosphorylates tau protein, was reduced in cells, and the decrease in the phosphorylation level of tau protein was associated with this decrease in the expression of the gsk3 gene. PP2A, a serine/threonine protein phosphatase, is a tumor suppressor [53] and regulates the cell cycle by interacting with more than 300 cell cycle-related substrates [54]. Expression of protein phosphatase 2A (PP2A) is reduced in both cancer and neurodegenerative diseases. A decrease in PP2A-Aa subunit expression to approximately 50% of the normal level induces tumor formation, while a decrease in PP2A-Aa expression by more than 63% results in apoptosis [14]. Similar to cancer conditions, we observed that decreased expression of the pp2a gene in pMS-mapt cells under aerobic glycolysis-like conditions.

It was seen that the cells were both smaller and had different cellular shapes compared to cells in normal conditions. However, these differently shaped cells are not dead cells, because the cells were observed to reproduce for 32 hours.

Under glucose repression conditions, the stress response in the cell is repressed [22, 55, 56]. We also observed a decrease in the gene expression of stress response genes sod1 and ctt1, as expected. Suppression of stress response genes in pMSmapt cells resulted in an increase in the level of intracellular oxidation. ER stress and unfolded protein response (UPR) are molecular events in the development of AD. Failure of these mechanisms results in the formation of pathological structures such as neurofibrillary tangles formed by hyperphosphorylated tau. ER stress is an imbalance between protein synthesis and ER protein folding capacity. This results in the accumulation of misfolded proteins in the ER. As a result of ER stress, unfolded proteins are proteasomally degraded [57–59]. In the present study, we observed that the expression of the ire1 gene, which is involved in the ER stress response, was reduced under aerobic glycolysis-like conditions. A decrease in autophagy is an expected result due to decreased ER stress in pMS-mapt cells, and this may explain the decrease in atg14 gene expression. No significant change in 20S proteasome activity was observed under aerobic glycolysis-like conditions in pMS-mapt cells. Decreases in ER stress response and autophagy are the expected results under repression conditions.

Several studies on diabetes and tau protein suggest a role of tau protein, particularly in regulating glucose homeostasis. In some studies, Alzheimer's disease has been referred to as type III diabetes. However, the relationship between impaired glucose signaling and tau has not yet been elucidated [60]. One of the limitations of this study is that the effect of insulin, one of the most important components of glucose metabolism, could not be demonstrated in model cells. Another limitation is that the DNA protection function of tau protein has not been examined in our model. Emerging evidence for tau's functions in P53 regulation and DNA repair suggests that it is associated with cancer. Studies have shown that the MAPT gene is a potential factor in many types of cancer. However, the role of tau in cancer is still unclear. Whether tau is positively or negatively associated with cancer type may be because it plays a role in different cellular processes [7].

In the present study, aerobic fermentation metabolism in cancer was mimicked by creating glucose repression conditions in the tau protein-producing S. pombe model organism. Under aerobic glycolysis-like conditions, we observed an increase in tau protein expression and a decrease in its phosphorylation. In contrast, it is the increase in tau phosphorylation that causes pathology in tauopathies. Thus, under cancer-mimicking conditions, a situation in tau phosphorylation that was opposite to that in neurodegeneration was observed. The fact that a different response than expected occurred also in glucose metabolism in these tauproducing cells suggests that tau protein may be a common component that plays a greater role in the mechanisms underlying the diseases than thought. In our study, we examined only one phosphorylation site, and although this is not sufficient for a definitive conclusion, it provides data on the change of phosphorylation status. In future studies, target phosphorylation sites in Alzheimer's disease should be examined in more detail in cancer. Based on previous studies and our findings, tau protein may play a more important and multifunctional role in cellular mechanisms than thought. Therefore, the cellular mechanisms in which tau protein is involved and the molecular components it interacts with should be investigated in more detail.

Conclusion

More detailed studies are needed to understand the molecular and cellular mechanisms related to the different or common features between cancer and neurodegeneration. Both diseases are common and have high mortality rates. Most studies investigating the relationship between cancer and neurodegenerative diseases demonstrate the potential for one disease to protect against the other. At this point, it is of great importance to determine the mechanism that brings together two opposing processes, such as uncontrolled cell proliferation and degeneration, and the intermediary molecules involved in this mechanism. Understanding the underlying mechanisms linking AD and cancer will enable the development of prevention strategies and treatment for both diseases.

Informed Consent: Informed consent was obtained from all participants.

Conflict of Interest Statement: The authors declare that there are no competing interests associated with the manuscript.

Funding: The authors declared that this study received no financial support.

Use of AI for Writing Assistance: No AI technologies utilized.

Authorship Contributions: Concept – M.Y., S.K.U.; Design – M.Y., S.K.U.; Supervision – S.K.U.; Funding – M.Y., S.K.U.; Materials – M.Y., S.K.U.; Data collection and/or processing – M.Y.; Data analysis and/or interpretation – M.Y.; Literature search – M.Y., S.K.U.; Writing – M.Y.; Critical review – M.Y.

Peer-review: Externally peer-reviewed.

References

- 1. Mitchison T, Kirschner M. Dynamic instability of microtubule growth. Nature 1984;312(5991):237–42. [CrossRef]
- 2. Drubin DG, Kirschner MW. Tau protein function in living cells. J Cell Biol 1986;103(6):2739–46. [CrossRef]
- 3. Hedna R, Kovacic H, Pagano A, Peyrot V, Robin M, Devred F, et al. Tau protein as therapeutic target for cancer? Focus on glioblastoma. Cancers 2022;14(21):5386. [CrossRef]
- 4. Cirillo L, Gotta M, Meraldi P. The elephant in the room: The role of microtubules in cancer. Cell Div Mach Dis 2017;1002:93–124. [CrossRef]
- Galas MC, Bonnefoy E, Buee L, Lefebvre B. Emerging connections between tau and nucleic acids. Tau Biol 2020;1184:135–43. [CrossRef]
- 6. Rico T, Denechaud M, Caillierez R, Comptdaer T, Adriaenssens E, Buée L, et al. Cancer cells upregulate tau to gain resistance to DNA damaging agents. Cancers 2022;15(1):116. [CrossRef]
- 7. Callari M, Sola M, Magrin C, Rinaldi A, Bolis M, Paganetti P, et al. Cancer-specific association between Tau (MAPT) and cellular pathways, clinical outcome, and drug response. Sci Data 2023;10(1):637. [CrossRef]
- Gauthier S, Webster C, Servaes S, Morais JA, Rosa-Neto P. World Alzheimer Report 2022: Life after diagnosis: Navigating treatment, care and support. London: Alzheimer's Disease International; 2022.
- Sung H, Ferlay J, Siegel RL, Laversanne M, Soerjomataram I, Jemal A, et al. Global cancer statistics 2020: GLOBOCAN estimates of incidence and mortality worldwide for 36 cancers in 185 countries. CA Cancer J Clin 2021;71(3):209–49. [CrossRef]
- Zabłocka A, Kazana W, Sochocka M, Stańczykiewicz B, Janusz M, Leszek J, et al. Inverse correlation between Alzheimer's disease and cancer: Short overview. Mol Neurobiol 2021;58(12):6335–49. [CrossRef]
- Maccioni RB, Navarrete LP, González A, González-Canacer A, Guzmán-Martínez L, Cortés N. Inflammation: A major target for compounds to control Alzheimer's disease. J Alzheimer Dis 2020;76(4):1199–213. [CrossRef]
- 12. Brown JS, Amend SR, Austin RH, Gatenby RA, Hammarlund EU, Pienta KJ. Updating the definition of cancer. Mol Cancer Res 2023;21(11):1142–47. [CrossRef]

- 13. Lanni C, Masi M, Racchi M, Govoni S. Cancer and Alzheimer's disease inverse relationship: An age-associated diverging derailment of shared pathways. Mol Psychiatry 2021;26(1):280–95. [CrossRef]
- 14. Seo J, Park M. Molecular crosstalk between cancer and neurodegenerative diseases. Cell Mol Life Sci 2020;77(14):2659–80. [CrossRef]
- 15. Hanahan D, Weinberg RA. Hallmarks of cancer: The next generation. Cell 2011;144(5):646–74. [CrossRef]
- 16. Warburg O. On the origin of cancer cells. Science 1956;123(3191):309–14. [CrossRef]
- 17. Diaz-Ruiz R, Rigoulet M, Devin A. The Warburg and Crabtree effects: On the origin of cancer cell energy metabolism and of yeast glucose repression. Biochim Biophys Acta Bioenerg 2011;1807(6):568–76. [CrossRef]
- 18. Vander Heiden MG, Cantley LC, Thompson CB. Understanding the Warburg effect: The metabolic requirements of cell proliferation. Science 2009;324(5930):1029–33. [CrossRef]
- 19. Supabphol S, Seubwai W, Wongkham S, Saengboonmee C. High glucose: An emerging association between diabetes mellitus and cancer progression. J Mol Med 2021;99(9):1175–93. [CrossRef]
- 20. Takeda K, Starzynski C, Mori A, Yanagida M. The critical glucose concentration for respiration-independent proliferation of fission yeast, schizosaccharomyces pombe. Mitochondrion 2015;22:91–5. [CrossRef]
- 21. Kayikci Ö, Nielsen J. Glucose repression in saccharomyces cerevisiae. FEMS Yeast Res 2015;15(6):fov068. [CrossRef]
- 22. Hoffman CS. Glucose sensing via the protein kinase A pathway in schizosaccharomyces pombe. Biochem Soc Trans 2005;33(1):257–60. [CrossRef]
- 23. Hoffman CS, Wood V, Fantes PA. An ancient yeast for young geneticists: A primer on the schizosaccharomyces pombe model system. Genetics 2015;201(2):403–23. [CrossRef]
- 24. Harris MA, Rutherford KM, Hayles J, Lock A, Bähler J, Oliver SG, et al. Fission stories: Using PomBase to understand schizosaccharomyces pombe biology. Genetics 2022;220(4):iyab222. [CrossRef]
- 25. Acs-Szabo L, Papp LA, Miklos I. Understanding the molecular mechanisms of human diseases: The benefits of fission yeasts. Microb Cell 2024;11:288. [CrossRef]
- 26. Avila J. Tau kinases and phosphatases. J Cell Mol Med 2008;12(1):258. [CrossRef]
- 27. Ma Y, Kato T, Furuyashiki T. Genetic interactions among AMPK catalytic subunit Ssp2 and glycogen synthase kinases Gsk3 and Gsk31 in Schizosaccharomyces pombe. Kobe J Med Sci 2016;62(3):E70.
- 28. Yılmazer M, Uzuner SK. Effects of glucose on the cellular respiration in fission yeast expressing human GSK3B gene. Trakya Univ J Nat Sci 2024;25(1):1–10. [CrossRef]
- 29. Yilmazer M, Uzuner S. Heterologous expression of tau protein in fission yeast as a disease model. Fresen Environ Bull 2020;29(10):9218–25.
- 30. Yılmazer M, Şengelen A, Aksüt Y, Palabıyık B, Önay-Uçar E, Karaer Uzuner S. Glucose starvation induces tau phosphorylation leading to cellular stress response in fission yeast. Arch Microbiol 2025;207(7):1–16. [CrossRef]

- 31. Forsburg SL, Rhin N. Basic methods for fission yeast. Yeast 2006;23(3):173–83. [CrossRef]
- 32. Pfaffl MW. A new mathematical model for relative quantification in real-time RT-PCR. Nucleic Acids Res 2001;29(9):e45. [CrossRef]
- 33. Reinheckel T, Grune T, Davies KJ. The measurement of protein degradation in response to oxidative. In Walker JM, Keyse SM, eds. Methods in Molecular Biology Vol 99. Stress Stress Response: Methods and Protocols. Totowa: Humana Press; 2000
- 34. Inoue Y, Matsuda T, Sugiyama KI, Izawa S, Kimura A. Genetic analysis of glutathione peroxidase in oxidative stress response of saccharomyces cerevisiae. J Biol Chem 1999;274(38):27002–9. [CrossRef]
- 35. Li JM, Liu C, Hu X, Cai Y, Ma C, Luo XG, et al. Inverse correlation between Alzheimer's disease and cancer: Implication for a strong impact of regenerative propensity on neurodegeneration? BMC Neurol 2014;14:1–7. [CrossRef]
- Alexandre-Silva V, Cominetti MR. Unraveling the dual role of ADAM10: Bridging the gap between cancer and Alzheimer's disease. Mech Ageing Dev 2024;219:111928. [CrossRef]
- 37. Musicco M, Adorni F, Di Santo S, Prinelli F, Pettenati C, Caltagirone C, et al. Inverse occurrence of cancer and Alzheimer disease: A population-based incidence study. Neurology 2013;81(4):322–28. [CrossRef]
- 38. Souter S, Lee G. Microtubule-associated protein tau in human prostate cancer cells: Isoforms, phosphorylation, and interactions. J Cell Biochem 2009;108(3):555–64. [CrossRef]
- 39. Rouzier R, Rajan R, Wagner P, Hess KR, Gold DL, Stec J, et al. Microtubule-associated protein tau: A marker of paclitaxel sensitivity in breast cancer. Proc Natl Acad Sci U S A 2005;102(23):8315–20. [CrossRef]
- 40. Pusztai L, Jeong JH, Gong Y, Ross JS, Kim C, Paik S, et al. Evaluation of microtubule-associated protein-Tau expression as a prognostic and predictive marker in the NSABP-B 28 randomized clinical trial. J Clin Oncol 2009;27(26):4287–92. [CrossRef]
- 41. Gargini R, Segura-Collar B, Herránz B, García-Escudero V, Romero-Bravo A, Núñez FJ, et al. The IDH-TAU-EGFR triad defines the neovascular landscape of diffuse gliomas. Sci Transl Med 2020;12(527):eaax1501. [CrossRef]
- 42. Diaz-Ruiz R, Uribe-Carvajal S, Devin A, Rigoulet M. Tumor cell energy metabolism and its common features with yeast metabolism. Biochim Biophys Acta 2009;1796:252–65. [CrossRef]
- 43. Santos SM, Hartman JL. A yeast phenomic model for the influence of Warburg metabolism on genetic buffering of doxorubicin. Cancer Metab 2019;7:1–42. [CrossRef]
- 44. Rolland F, Winderickx J, Thevelein JM. Glucose-sensing and-signalling mechanisms in yeast. FEMS Yeast Res 2002;2(2):183–201. [CrossRef]
- 45. Hoffman CS, Winston F. Glucose repression of transcription of the Schizosaccharomyces pombe fbp1 gene occurs by a cAMP signaling pathway. Genes Dev 1991;5(4):561–71. [CrossRef]

- 46. Palomino A, Herrero P, Moreno F. Tpk3 and Snf1 protein kinases regulate Rgt1 association with saccharomyces cerevisiae HXK2 promoter. Nucleic Acids Res 2006;34(5):1427–38. [CrossRef]
- 47. Nair A, Sarma SJ. The impact of carbon and nitrogen catabolite repression in microorganisms. Microbiol Res 2021;251:126831. [CrossRef]
- 48. Mondragón-Rodríguez S, Perry G, Luna-Muñoz J, Acevedo-Aquino MC, Williams S. Phosphorylation of tau protein at sites Ser 396-404 is one of the earliest events in Alzheimer's disease and Down syndrome. Neuropathol Appl Neurobiol 2014;40(2):121–35. [CrossRef]
- 49. Regalado-Reyes M, Furcila D, Hernández F, Ávila J, DeFelipe J, León-Espinosa G. Phospho-tau changes in the human CA1 during Alzheimer's disease progression. J Alzheimer Dis 2019;69(1):277–88. [CrossRef]
- 50. Liu Y, Yan D, Wang Y, Zhang X, Wang N, Jiao Y, et al. Subchronic exposure to acrylamide caused behaviour disorders and related pathological and molecular changes in rat cerebellum. Toxicol Lett 2021;340:23–32. [CrossRef]
- 51. Xia Y, Prokop S, Giasson BI. "Don't Phos Over Tau": Recent developments in clinical biomarkers and therapies targeting tau phosphorylation in Alzheimer's disease and other tauopathies. Mol Neurodegener 2021;16(1):37. [CrossRef]
- 52. Zhao J, Wei M, Guo M, Wang M, Niu H, Xu T, et al. GSK3: A potential target and pending issues for treatment of Alzheimer's disease. CNS Neurosci Ther 2024;30(7):e14818. [CrossRef]
- 53. Westermarck J, Hahn WC. Multiple pathways regulated by the tumor suppressor PP2A in transformation. Trends Mol Med 2008;14(4):152–60. [CrossRef]
- 54. Wlodarchak N, Xing Y. PP2A as a master regulator of the cell cycle. Crit Rev Biochem Mol Biol 2016;51(3):162–84. [CrossRef]
- 55. Carlson M. Glucose repression in yeast. Curr Opin Microbiol 1999;2(2):202–7. [CrossRef]
- 56. Palabiyik B, Ghods FJ, Uzuner SK. Role of glucose repression in the oxidative stress response of schizosaccharomyces pombe: analysis of transcript levels of fbp1, hxk2, sod1 and ctt1 genes in sty1, atf1 and pap1 knock-out mutants. Turk J Biol 2016;40(4):815–25. [CrossRef]
- 57. Dufey E, Sepúlveda D, Rojas-Rivera D, Hetz C. Cellular mechanisms of endoplasmic reticulum stress signaling in health and disease. 1. An overview. Am J Physiol Cell Physiol 2014;307(7):C582–94. [CrossRef]
- 58. Hetz C, Saxena S. ER stress and the unfolded protein response in neurodegeneration. Nat Rev Neurol 2017;13(8):477–91.
- 59. González A, Calfío C, Churruca M, Maccioni RB. Glucose metabolism and AD: evidence for a potential diabetes type 3. Alzheimers Res Ther 2022;14(1):56. [CrossRef]
- 60. Shieh JCC, Huang PT, Lin YF. Alzheimer's disease and diabetes: Insulin signaling as the bridge linking two pathologies. Mol Neurobiol 2020;57(4):1966–77. [CrossRef]

INTERNATIONAL JOURNAL OF

MEDICAL BIOCHEMISTRY

DOI: 10.14744/ijmb.2025.32656 Int J Med Biochem 2025;8(4):282–291

Research Article



Adaptive mitochondrial modules: Going with the flow of cancer-specific metabolic rewiring

Mehmet Taha Yildiz

Department of Child Development, University of Health Sciences, Hamidiye Faculty of Health Sciences, Istanbul, Türkiye

Abstract

Objectives: Mitochondrial gene networks constitute a fundamental subsystem of cellular homeostasis, integrating bioenergetic, metabolic, and signaling functions. In cancer, the rewiring of these networks represents a critical mechanism of metabolic adaptation, enabling tumor cells to sustain growth and survival under diverse microenvironmental constraints. To systematically characterize these alterations, we analyzed transcriptomic data from The Cancer Genome Atlas (TCGA) with a specific focus on mitochondrial genes, aiming to uncover cancer-type-specific patterns of differential expression and their potential biological implications.

Methods: Transcriptomic data from The Cancer Genome Atlas (TCGA) were analysed to identify differential expression patterns in mitochondrial genes. Weighted Gene Co-expression Network Analysis (WGCNA) was applied to detect co-expressed gene modules. The biological relevance of these modules was assessed through functional enrichment analysis and survival modelling using Cox regression and Kaplan–Meier estimations. Dimensionality reduction techniques including PCA and UMAP were used to evaluate module-driven clustering patterns across cancer types.

Results: Seven mitochondrial gene modules were identified, six of which demonstrated significant associations with specific cancer types. Modules ME2, ME4, ME5, ME6, and ME7 were associated with improved overall survival, while ME3 correlated with poorer prognosis. Functional enrichment analyses revealed distinct mitochondrial processes including oxidative phosphorylation, apoptosis, fatty acid β -oxidation, and ketone body metabolism. Dimensionality reduction analyses supported the presence of module-specific expression patterns with cancer-type-dependent clustering.

Conclusion: The observed cancer-type-specific expression and prognostic associations of mitochondrial gene networks reflect their central involvement in the metabolic flexibility of tumors. By underscoring the clinical and biological significance of mitochondrial subsystems, these findings suggest that they may serve not only as prognostic markers but also as promising targets for therapeutic modulation.

Keywords: Cancer metabolism, co-expression modules, gene expression profiling, gene co-expression networks, mitochondrial genes, systems biology

How to cite this article: Yildiz MT. Adaptive mitochondrial modules: Going with the flow of cancer-specific metabolic rewiring. Int J Med Biochem 2025;8(4):282–291.

Biological systems are intrinsically complex, dynamic, and deeply interconnected. To maintain cellular homeostasis, they rely on multilayered regulatory networks that combine structural redundancy with exceptional adaptive flexibility [1, 2]. This adaptability may allow cancer cells to emerge as reorganized—yet still coordinated—deviations from the original regulatory architecture. Even in the disease state, internal logic

and systemic coordination may persist through altered but non-random arrangements of regulatory configurations [3].

Understanding these transformations is particularly challenging due to the high-dimensional, non-linear, and interdependent nature of molecular interactions. Numerous molecular components operate simultaneously and influence one another in non-linear ways, making it difficult to isolate individual

Address for correspondence: Mehmet Taha Yildiz, MD. Department of Child Development, University of Health Sciences, Hamidiye Faculty of Health Sciences, Istanbul, Türkiye

Phone: +90 554 227 43 48 E-mail: mtaha.yildiz@sbu.edu.tr ORCID: 0000-0003-4768-0333

Submitted: July 11, 2025 **Revised:** September 02, 2025 **Accepted:** September 03, 2025 **Available Online:** October 21, 2025 **OPEN ACCESS** This is an open access article under the CC BY-NC license (http://creativecommons.org/licenses/by-nc/4.0/).





effects or predict system-wide behavior. This complexity poses significant challenges for both computational modeling and biological interpretation, especially when attempting to capture the emergent properties of the system as a whole [4–6].

One rational strategy to navigate this complexity is to focus on key functional groups of genes or proteins (regulatory nodes) that coordinate specific biochemical pathways or molecular processes. These groups are critical for cellular survival and proliferation and may be maintained or repurposed by cancer cells to sustain viability, differentiation, and growth [7, 8]. Among these, mitochondria are pivotal due to their roles in metabolic reprogramming, redox signaling, and apoptotic regulation [9]. Beyond these functions, while mitochondrial functions are modulated by nuclear-encoded proteins (1,138 genes), their compact genome (37 genes), defined metabolic pathways, and membrane-bound localization render them a relatively self-contained and tractable subsystem for dissecting cancer's regulatory rewiring [10–14].

Given these considerations, we hypothesize that differential mitochondrial gene expression patterns can reveal cancer-type-specific prognostic modules. Their regulatory roles are not fixed but dynamically adapted to meet the context-specific demands of diverse tumor types. This plasticity may underlie resistance to single-agent therapies, as tumors exploit the flexibility of these mitochondrial subsystems—groups of interacting genes or proteins performing coordinated functions—to sustain survival under therapeutic pressure [15–20].

In this study, we adopt a systems biology approach to investigate mitochondrial gene networks as a model regulatory subsystem—a group of interacting genes or proteins that jointly perform a functional role. Our aim is to identify adaptive mitochondrial modules that contribute to cancer-type-specific regulatory reorganization, with a particular focus on their prognostic significance and functional diversity across tumors.

Materials and Methods

Ethical considerations

This study was conducted exclusively using publicly available data from The Cancer Genome Atlas (TCGA) project (https:// www.cancer.gov/tcga). All data were fully deidentified and used in accordance with the TCGA publication guidelines and data access policies. No new human or animal data were collected or generated by the authors. Therefore, this research is exempt from institutional review board (IRB) approval under current regulations [21]. All procedures performed in this study complied with the ethical standards of the TCGA consortium and with the 1964 Helsinki Declaration and its later amendments. The study complies with the U.S. Department of Health and Human Services policy for the protection of human research subjects (45 CFR 46). The TCGA provides an invaluable and ethically curated resource for studying cancer biology at the molecular level, enabling reproducible and large-scale in silico analyses [22, 23].

Study design and overview

To investigate mitochondrial gene regulatory networks across diverse cancer types, we used a systems biology framework that combines co-expression network analysis, module—phenotype association, and mechanistic enrichment. Our middle-out strategy—anchored at the module level where eigengenes represent the dominant expression pattern of co-expressed genes—links gene-level perturbations to higher-order phenotypes. This design enables the detection of biologically meaningful modules first and their subsequent association with phenotypes, balancing molecular detail with system-level interpretation.

This integrative analysis was conducted in three key phases; first, we analysed RNA-seq data from TCGA to identify tumor-specific co-expression modules (Fig. 1, steps 1 to 3). Second, we correlated these modules with clinical outcomes including survival and molecular subtypes (Fig. 1, steps 4 to 6). Third, we performed pathway enrichment analysis using pathway enrichment results obtained via Enrichr-KG which integrates GO, KEGG and Reactome databases to annotate mechanistic functions (Fig. 1, step 7) [24]. This integrative strategy enabled systematic mapping of mitochondrial regulatory programs in cancer while maintaining biological interpretability.

Data acquisition and preprocessing

RNA-seq data and clinical metadata were retrieved from TCGA using the GDCRNATools R package [25]. Raw HTSeq count data and corresponding clinical metadata were downloaded for 23 cancer types. Only cancer types with ≥ 2 matched Solid Tissue Normal samples were retained, excluding other tissue types and technical duplicates. This filtering yielded 17 cancer types: BLCA, BRCA, CESC, COAD, ESCA, GBM, HNSC, KICH, KIRC, KIRP, LIHC, LUAD, PRAD, READ, STAD, THCA, UCEC. Normalization was performed using the Trimmed Mean of M-values (TMM) method, followed by voom transformation, as implemented in the GDCRNATools package. Only genes annotated as mitochondrial in the MitoCarta3.0 [26] human gene set (n=1,138) were included, resulting in expression profiles for 7,874 samples (7,202 Primary Tumor, 672 Solid Tissue Normal). Sample counts per cancer type ranged from 91 (KICH) to 1,208 (BRCA).

Delta expression matrix calculation

To quantify tumor-specific transcriptional alterations, a delta expression matrix was constructed by subtracting the mean expression of each gene in Solid Tissue Normal samples from Primary Tumor expression values, separately within each cancer type. Sample types were assigned using clinical metadata. The final matrix contained 1,138 mitochondrial genes (rows) and 7,202 tumor samples (columns). All identifiers were checked for dimensional consistency prior to further analysis. A limitation of this approach is the small number of normal samples in a few cancer types, which may reduce the robustness of the differential expression scores.

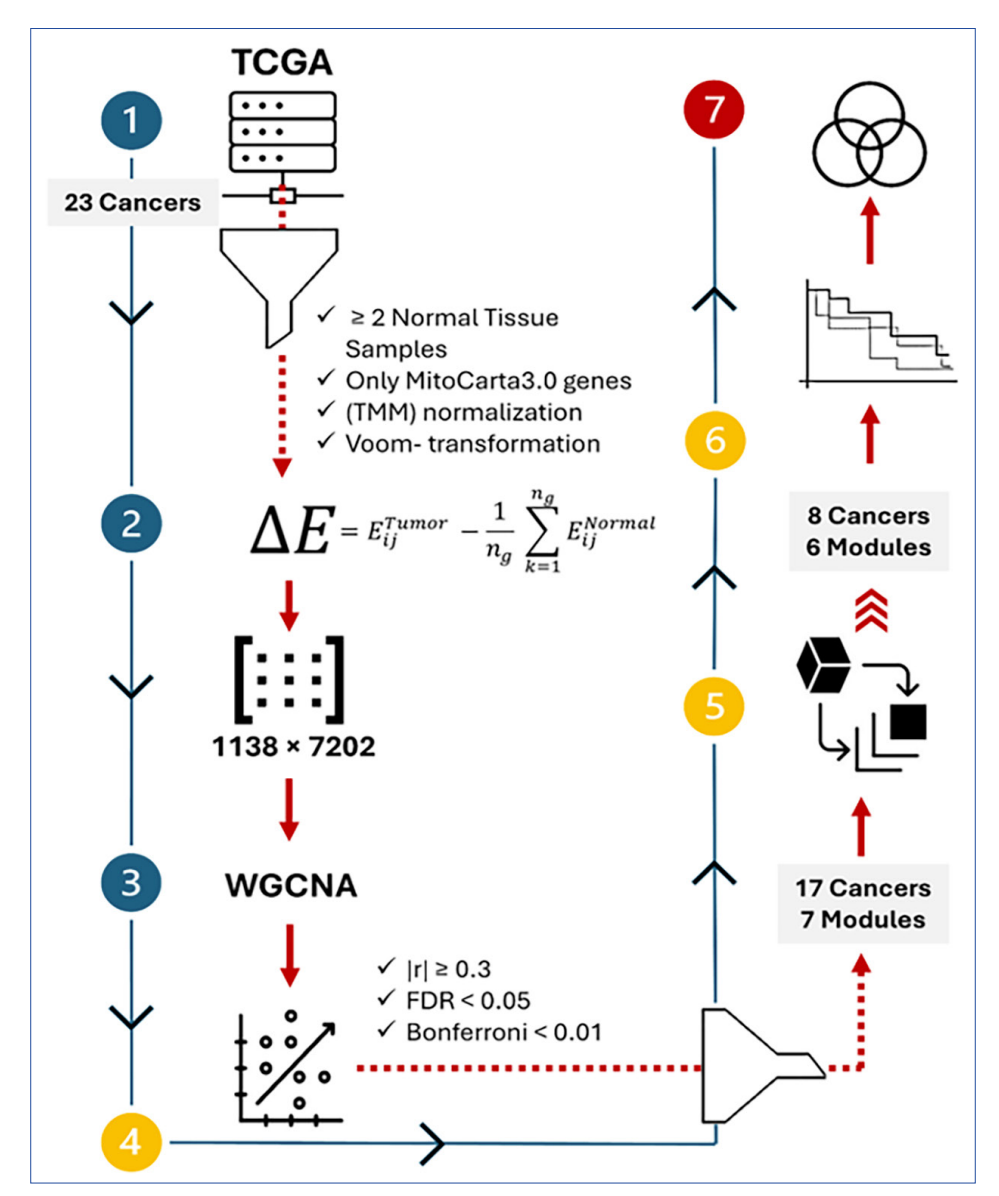


Figure 1. Schematic overview of the module-based cancer analysis pipeline. The workflow consists of seven main steps: (1) acquisition and preprocessing of gene expression and phenotype data, (2) calculation of delta expression, (3) construction of a gene co-expression network and module detection via WGCNA tool, (4) correlation analysis between modules and cancer types, (5) dimensionality reduction and visualization of module-trait relationships, (6) survival analysis based on module expression, and (7) functional enrichment analysis to infer biological relevance. Funnel icons represent filtering steps, with specific exclusion criteria indicated adjacent to each filter. WGCNA: Weighted Gene Co-expression Network Analysis.

Co-expression network construction and module detection

Weighted Gene Co-expression Network Analysis (WGCNA) was performed on the delta expression matrix to identify modules of co-expressed mitochondrial genes [27]. A soft-thresholding power of β =4 was selected based on scale-free topology and mean connectivity criteria (R^2 =0.89), as illustrated in Appendix 1a-b. The resulting adjacency matrix was used to compute the topological overlap matrix (TOM), followed by hierarchical clustering and dynamic tree cutting, which identified seven distinct co-expression modules (Appendix 1c).

To evaluate module stability, the dataset was randomly split into reference (70%) and test (30%) subsets, and module preservation was assessed across 20 permutations using both Z-summary and median rank statistics, with higher Z-summary and lower median rank values indicating stronger and more biologically coherent preservation; median rank values supported the hierarchy suggested by Z-summary, hub genes were identified based on intra-module connectivity (Appendix 2). The Topological Overlap Matrix (TOM) was used to compute kWithin values, and genes with kWithin >1 SD above the

module mean were designated as hub genes. These genes were retained for downstream functional analyses.

Module-cancer type correlation analysis

Cancer type metadata was one-hot encoded to match the sample order in the module eigengene (ME) matrix. Pearson correlations between MEs and binary cancer-type variables were computed to identify module—cancer associations, with significance assessed via Student's t-distribution. Multiple testing correction was performed using both False Discovery Rate (FDR) and Bonferroni methods. Correlations with $|r| \ge 0.3$ and adjusted p-values <0.05 and FDR<0.01 (Bonferroni) were considered significant (Appendix 2).

Dimensionality reduction and visualization of moduletrait relationships

To explore module–cancer associations, dimensionality reduction was applied to delta expression data restricted to genes within significant modules. Principal Component Analysis (PCA) was used to project samples into lower-dimensional space while preserving variance. Clustering patterns by cancer type were visualized along the first two principal components, and cluster quality was assessed using silhouette scores. To capture nonlinear structure, UMAP and t-SNE were also performed, both supporting PCA-derived groupings and revealing distinct cancer type separations based on module gene expression.

Functional enrichment analysis

Functional enrichment analysis was conducted for each module using the Enrichr-KG platform, which integrates curated databases such as WikiPathways, Reactome, KEGG, and Gene Ontology [24]. Enrichment was based on the statistical overrepresentation of module genes within known pathways, assessed via adjusted p-values. Only modules significantly correlated with cancer types were included to focus on biologically relevant gene networks. Significant terms were summarized and visualized to aid interpretation of predominant functional themes within each module.

Survival analysis

The prognostic relevance of mitochondrial gene co-expression modules was assessed using Kaplan-Meier survival curves and univariate Cox proportional hazards models based on module eigengene expression. Module scores were matched with clinical survival data (time-to-event and event status) from 7,202 tumor samples with complete metadata. Samples were dichotomized into "High" and "Low" groups by the median eigengene value per module. While median-based grouping is common practice, it may lead to some information loss, which should be considered when interpreting results. Survival differences were evaluated with log-rank tests, and hazard ratios (HR) with 95% confidence intervals were estimated via Cox models. P-values were adjusted for multiple testing using the Benjamini-Hochberg false discovery rate (FDR) method (Appendix 2). This approach provided robust prognostic assessment across cancer types while avoiding assumptions related to continuous variable modeling.

Table 1. Mitochondrial gene co-expression modules and preservation statistics

Module	Gene count	Z -summary	Median rank
ME1	443	28.85	2
ME3	107	16.54	4
ME2	162	13.89	7
ME4	99	13.29	5
ME6	58	12.27	2
ME5	72	10.13	5
ME7	46	9.85	4

Preservation was assessed using Z-summary, a composite statistic reflecting module stability across datasets, and median rank metrics over 20 permutations. Higher Z-summary and lower median rank values indicate stronger and more biologically coherent module preservation across cancer types.

Software and tools

All analyses were performed using R version 4.4.1 (2024-06-14) on Windows 11 x64. Key R packages included GDCRNATools (v1.18.0), WGCNA (v1.73), survival (v3.8-3), survminer (v0.5.0), dynamicTree-Cut (v1.63-1), fastcluster (v1.2.6), ggplot2 (v3.5.2), ggpubr (v0.6.0), tidyverse (v2.0.0), umap (v0.2.10.0), and Rtsne (v0.17).

Results

Module preservation and structural robustness

WGCNA identified seven mitochondrial gene co-expression modules (ME1–ME7), ranging from 46 to 443 genes in size (Table 1). Genes not assigned to any module (ME0) were grouped into the gray module and excluded from downstream analyses. Module preservation was evaluated using Z-summary and median rank statistics across 20 permutations. Four modules—ME1, ME3, ME2, and ME4—showed strong preservation. ME6 and ME5 also met the threshold for high preservation, while ME7 demonstrated moderate stability. Median rank values supported the Z-summary-based hierarchy of module robustness. Collectively, these results indicate that the identified modules represent reproducible and biologically coherent co-expression structures among mitochondrial genes across cancer types.

Module-cancer type associations

To evaluate the biological relevance of mitochondrial gene modules across cancer types, we assessed the correlations between module eigengenes and tumor labels. Six of the seven modules (ME2–ME7) showed statistically significant associations with at least one cancer type (Fig. 2). In total, twelve significant module–cancer type pairs were identified, involving eight distinct cancer types. Full correlation coefficients and adjusted p-values are presented in Table 2. The strongest positive associations were observed for ME6 with KIRC and ME5 with THCA, while ME7 exhibited the most pronounced negative correlation with LIHC.

These findings suggest that mitochondrial gene co-expression patterns vary systematically across cancer types, potentially reflecting tumor-specific mitochondrial reprogramming. Based on significance filtering, a refined dataset was

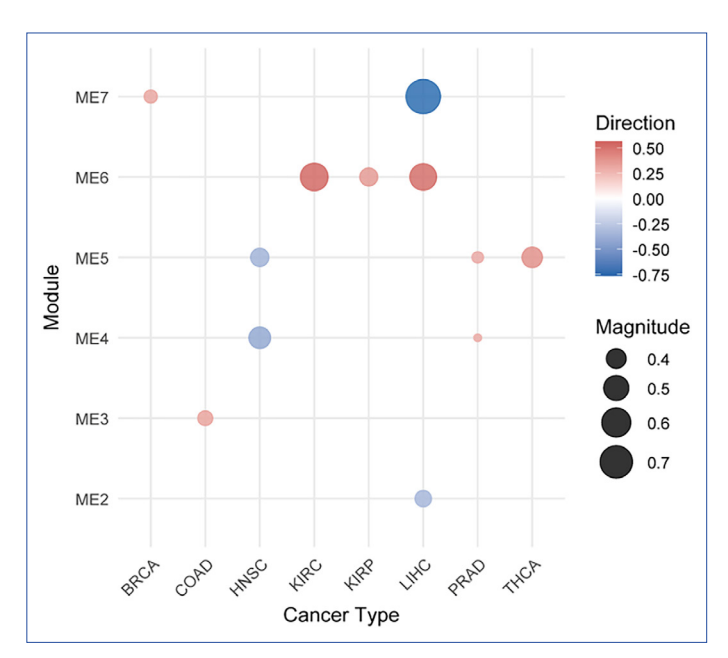


Figure 2. Module-cancer correlations. Bubble plot showing correlations between gene expression modules (ME2–ME7) and cancer types after significance filtering. Bubble size reflects the absolute correlation, while color indicates direction (red: positive, blue: negative).

generated comprising six modules (ME2 to ME7) and eight cancer types (BRCA, LIHC, COAD, KIRC, KIRP, HNSC, PRAD, and THCA). This subset included 544 genes and 4,269 tumor samples and was used for subsequent clustering, survival, and functional enrichment analyses. To provide a comprehensive overview, we included the full module–cancer correlation matrix, the module-level delta expression heatmap, and eigengene distributions across cancer types, shown in Appendix 3, 4, and 5, respectively.

Dimensionality reduction and clustering of module activity

To assess whether mitochondrial module activity could stratify tumors by type, we applied PCA, UMAP, and t-SNE to the expression profiles of 544 genes across 4,269 tumor samples. PCA accounted for a moderate portion of variance but yielded limited clustering performance for most cancer types (Fig. 3a). In contrast, both UMAP and t-SNE revealed clearer separation, with UMAP achieving the highest overall cluster quality and strongest within-type cohesion across several cancer types, notably PRAD, LIHC, and HNSC (Fig. 3b, c).

These findings indicate that non-linear dimensionality reduction techniques better capture the underlying mitochondrial expression patterns that differentiate tumor types.

Survival associations of mitochondrial modules

Univariate Cox proportional hazards analysis demonstrated significant associations between mitochondrial gene co-expression modules and overall survival across 7,202 tumor samples. Modules ME5, ME7, ME4, ME6, and ME2 were associated with improved prognosis, with hazard ratios ranging from approximately 0.40 to 0.79 (all adjusted p<0.001). Converse-

Table 2. Prognostic mitochondrial gene modules and their cancer-type-specific associations

Module	Cancer	Survival effect (HR)
ME5	HNSC (-), PRAD (+), THCA (+)	0.40 (protective)
ME7	BRCA (+), LIHC (-)	0.46 (protective)
ME4	HNSC (-), PRAD (+)	0.47 (protective)
ME6	KIRC (+), KIRP (+), LIHC (+)	0.72 (protective)
ME2	LIHC (-)	0.79 (protective)
ME3	COAD (+)	1.25 (risk increasing)
Cancer	Modules	Survival effect (HR)
BRCA	ME7 (+)	0.46 (protective)
COAD	ME3 (+)	1.25 (risk increasing)
HNSC	ME4 (-), ME5 (-)	0.47, 0.40 (protective)
KIRC	ME6 (+)	0.72 (protective)
KIRP	ME6 (+)	0.72 (protective)
LIHC	ME7 (-), ME2 (-), ME6 (+)	0.46 ,0.79, 0.72 (protective)
PRAD	ME4 (+), ME5 (+)	0.47 ,0.40 (protective)
THCA	ME5 (+)	0.40 (protective)

Mitochondrial modules (ME2–ME7) showing significant associations with specific cancer types and corresponding hazard ratios (HR) from survival analysis are summarized. The top section lists each module and its correlated cancer types; the bottom section takes a cancer-centric view, indicating associated modules and their prognostic effects. Modules with HR < 1 indicate protective associations, while HR>1 suggests increased risk.

ly, ME3 showed a significant association with poorer survival (HR>1, adjusted p<0.001). These findings were consistently supported by Kaplan–Meier survival analyses (Fig. 4) and further quantified by module-specific hazard ratios calculated from scaled eigengene expression.

Functional signatures of mitochondrial modules

Each identified module represents a coordinated gene program reflecting distinct aspects of mitochondrial biology. Functional enrichment analyses revealed that modules are associated with specific mitochondrial processes as follows.

ME2 (Aminoacyl-tRNA and mitochondrial protein synthesis)

ME2 is enriched in mitochondrial aminoacyl-tRNA synthetases and components involved in mitochondrial translation, with pathway enrichments in Aminoacyl-tRNA biosynthesis, Mitochondrial tRNA Aminoacylation, and Translation. It also includes genes related to the TCA cycle, suggesting a link between protein synthesis and central carbon metabolism. Functionally, ME2 likely regulates mitochondrial translational capacity critical for bioenergetic demands. Its expression is negatively correlated with tumor presence and positively associated with better overall survival in liver hepatocellular carcinoma (LIHC), indicating that preserved mitochondrial translation supports favorable prognosis in metabolically active tumors. Disease association analysis highlights links to mitochondrial disorders such as lactic acidosis, reflecting mitochondrial dysfunction that may underlie LIHC metabolic reprogramming.

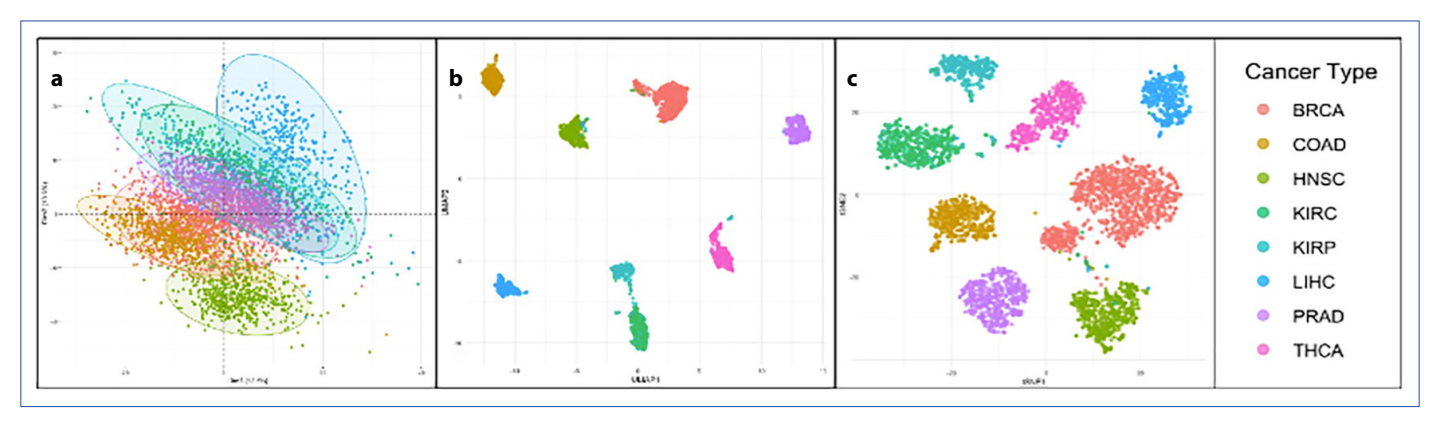


Figure 3. Dimensionality reduction analysis of module–trait relationships. (a) PCA, (b) UMAP, and (c) t-SNE plots illustrate the distribution of samples based on module eigengene expression profiles. Each point represents a sample, and colors correspond to different types of cancer as indicated in the legend. These visualizations highlight the clustering patterns and potential separability of cancer types based on module-level expression signatures.

PCA: Principal component analysis; UMAP: Uniform Manifold Approximation and Projection; t-SNE: t-Distributed Stochastic Neighbor Embedding.

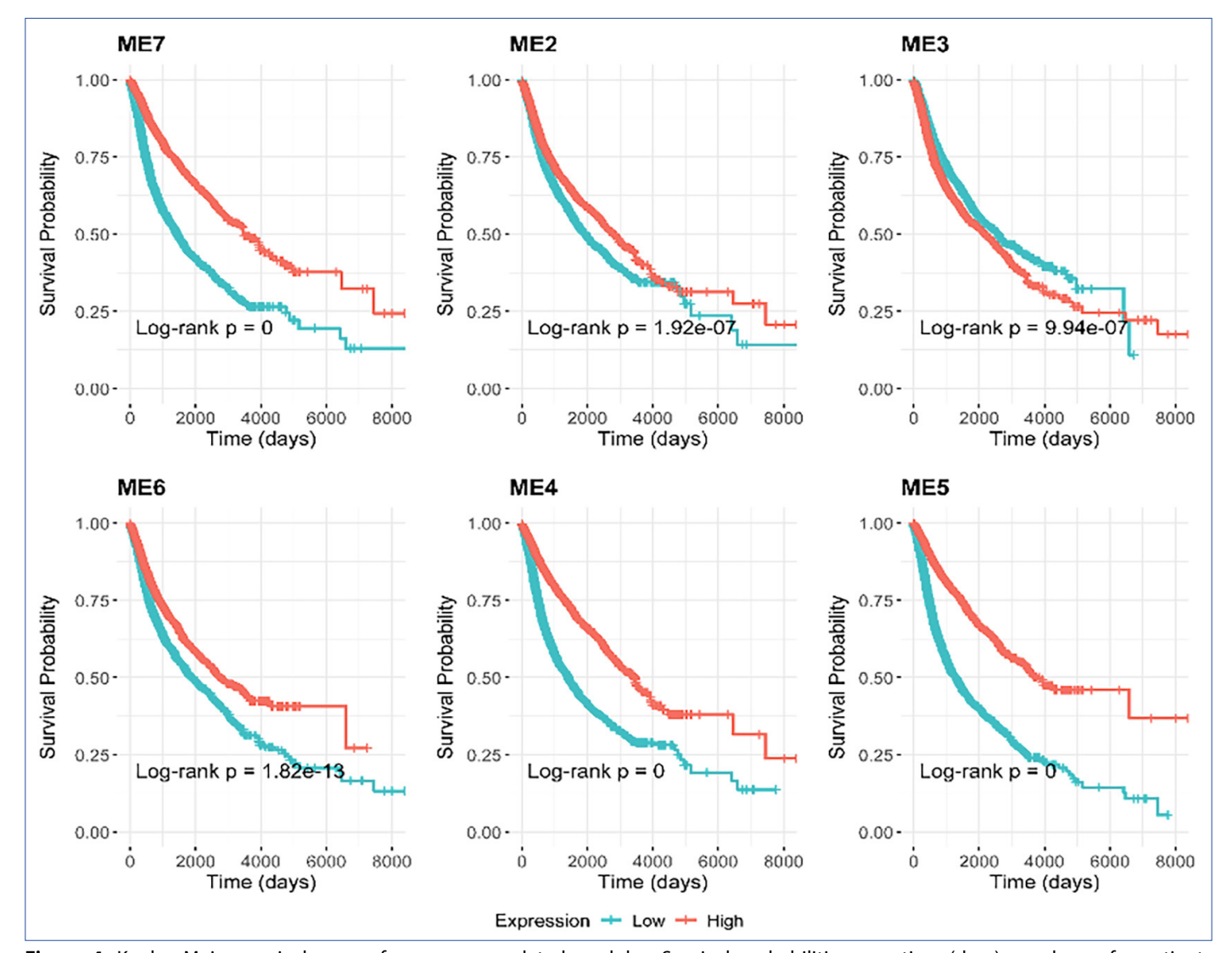


Figure 4. Kaplan-Meier survival curves for cancer correlated modules. Survival probabilities over time (days) are shown for patients stratified by high (red) versus low (blue) module expression. All differences between groups were statistically significant based on log-rank tests (adjusted p<0.001).

ME3 (Oxidative phosphorylation and mitochondrial translation initiation)

ME3 is enriched in genes related to mitochondrial translation initiation, oxidative phosphorylation (OXPHOS), and respiratory complex assembly, reflecting a coordinated bioenergetic program essential for ATP production. Key enriched pathways include Oxidative Phosphorylation, Respiratory Electron Transport, and Mitochondrial Translation Initiation. Clinically, ME3 expression positively correlates with tumor presence and poorer overall survival in colon adenocarcinoma (COAD), suggesting that elevated mitochondrial energy metabolism is associated with tumor aggressiveness. This module likely represents a mitochondrial bioenergetic signature contributing to cancer progression in COAD.

ME4 (Fatty acid β -oxidation and branched-chain amino acid catabolism)

ME4 is enriched for genes involved in mitochondrial fatty acid β -oxidation and branched-chain amino acid (BCAA) catabolism, with pathway enrichments highlighting lipid degradation, acyl-CoA metabolism, and peroxisomal lipid processing. Key enzymes in valine, leucine, and isoleucine degradation underscore ME4's role in maintaining mitochondrial energy homeostasis through versatile substrate utilization, especially under metabolic stress or nutrient scarcity.

ME5 (Apoptosis, mitochondrial dynamics, and calcium homeostasis)

ME5 is enriched in genes regulating intrinsic apoptosis, mitochondrial dynamics, and calcium transport, with key pathways including Apoptosis, Neurodegeneration, and Mitochondrial Calcium Ion Transport. This module likely coordinates mitochondrial quality control and stress responses. Clinically, ME5 expression is reduced in head and neck squamous cell carcinoma (HNSC), correlating with tumor presence and poorer prognosis, whereas in prostate adenocarcinoma (PRAD) and thyroid carcinoma (THCA), higher ME5 levels associated with better survival despite positive tumor correlation. These findings suggest a protective role of ME5 across cancers, with context-dependent transcriptional regulation reflecting mitochondrial integrity and apoptosis pathways.

ME6 (Lipid biosynthesis, Acyl-CoA metabolism, and amino acid conjugation)

ME6 is enriched in genes regulating fatty acid biosynthesis, acyl-CoA metabolism, glycine conjugation, and pathways related to detoxification and amino acid catabolism. Key pathways include Fatty Acid Beta-Oxidation, Peroxisome function, and Amino Acid Metabolism, indicating a role in lipid catabolism and mitochondrial–peroxisomal crosstalk. Clinically, ME6 expression positively correlates with tumor presence in kidney cancers (KIRC, KIRP) and liver hepatocellular carcinoma (LIHC), and associates with improved overall survival, suggesting a protective metabolic program that may limit tumor progression. This contrasts with modules

like ME7, characterized by downregulation of mitochondrial translation and negative correlation with tumors such as LIHC. While ME6 reflects an active metabolic state supporting fatty acid oxidation and detoxification linked to better prognosis, ME7 indicates mitochondrial dysfunction or repression of mitochondrial protein synthesis associated with more aggressive tumor behavior. Together, these differences highlight the complex and diverse mitochondrial adaptations across cancer types that shape tumor biology and patient outcomes.

ME7 (Ketone body metabolism, urea cycle, and sulfur amino acid turnover)

ME7 is enriched in genes involved in ketone body metabolism, urea cycle, and sulfur amino acid metabolism. Pathway annotations highlight ketone metabolism, nitrogen metabolism, and sulfur relay systems, suggesting roles in metabolic reprogramming during fasting or nutrient fluctuations, integrating nitrogen detoxification, energy substrate switching, and redox buffering. Functionally, ME7 is composed mainly of mitochondrial ribosomal proteins and oxidative phosphorylation components, reflecting a core mitochondrial translational and bioenergetic program essential for maintaining a balanced proteome, apoptosis regulation, and ATP production. Clinically, ME7 expression correlates positively with overall survival (HR=0.46), indicating preserved mitochondrial function may suppress tumor progression. ME7 shows cancer-type specific expression patterns: Upregulated in breast cancer (BRCA) and downregulated in liver hepatocellular carcinoma (LIHC). These findings may reflect tissue-specific metabolic reprogramming. In BRCA tumors, the retention of mitochondrial translation and apoptotic signaling is associated with better prognosis, whereas LIHC exhibits metabolic dedifferentiation and hypoxic adaptation. The loss of ME7 module expression in LIHC further supports a shift toward aggressive tumor phenotypes. Downregulation of ME7 in LIHC mirrors disruption of mitochondrial metabolic pathways including amino acid and nitrogen metabolism, supporting aggressive tumor phenotypes. Conversely, ME7 upregulation in BRCA aligns with preserved mitochondrial function and metabolic flexibility, promoting controlled tumor growth and apoptosis. Overall, ME7 represents a mitochondria-centered tumor suppressive module whose context-dependent expression is prognostically informative, underscoring the interplay between mitochondrial translation, apoptosis, and metabolic adaptation in cancer biology.

Discussion

Our integrative analysis of mitochondrial-related gene expression modules across multiple cancer types reveals distinct module-cancer specificity patterns with significant prognostic implications as summarized in Table 2. Modules ME2, ME4, ME5, ME6, and ME7 generally demonstrate protective effects on overall survival, whereas ME3 shows a risk-increasing effect, highlighting the heterogeneous roles

of mitochondrial functions in cancer progression. Notably, ME2 exhibits a strong protective association uniquely in liver hepatocellular carcinoma (LIHC), consistent with its role in mitochondrial aminoacyl-tRNA synthetase function and bioenergetic regulation. ME3, conversely, correlates positively with tumor presence and worse prognosis specifically in colon adenocarcinoma (COAD), reflecting heightened oxidative phosphorylation activity potentially driving tumor aggressiveness. Modules ME4 and ME5 show complex, cancer-specific correlation directions, protective in some cancers (e.g., HNSC) but positively correlated in others (e.g., PRAD, THCA), indicating context-dependent mitochondrial pathway engagement. Modules ME6 and ME7 also display strong protective effects with positive correlations in kidney cancers (KIRC, KIRP) and breast cancer (BRCA), respectively, supporting the notion that mitochondrial functional states may influence survival in a tumor-type-specific manner.

Overall, our results emphasize the potential of mitochondrial functional modules as robust prognostic biomarkers and promising therapeutic targets across diverse cancer types. For instance, ME2's strong protective association specifically in liver hepatocellular carcinoma (LIHC) highlights how preserving mitochondrial translational capacity may suppress tumor progression in metabolically demanding tumors. Conversely, the risk-increasing profile of ME3 in (COAD) suggests that elevated mitochondrial oxidative phosphorylation activity contributes to tumor aggressiveness in this cancer type. These cancer-specific patterns suggest that mitochondrial dysfunction and metabolic rewiring may vary across tumors, reflecting distinct bioenergetic adaptations. This modular perspective may inform metabolic precision oncology, where therapeutic strategies can be tailored based on the dominant mitochondrial module dysregulated in a patient's tumor. Such an approach may enhance treatment efficacy by addressing cancer-specific metabolic dependencies, as exemplified by ME2-associated modules in LIHC potentially benefiting from therapies that restore mitochondrial translation and bioenergetics, while ME3-associated pathways in COAD might be targeted by inhibitors of oxidative phosphorylation. Therefore, integrating mitochondrial module profiling into clinical decision-making offers a promising avenue for developing more effective, personalized cancer treatments grounded in tumor metabolic phenotyping.

Furthermore, when stratifying tumors by their estimated metabolic phenotypes, we observed a striking pattern: Nearly all tumors classified as HGLO (High Glycolysis, Low OXPHOS (Oxidative Phosphorylation)— meaning they rely mainly on glycolysis and have suppressed mitochondrial respiration—belonged to the subset of cancers that showed no significant correlation with mitochondrial gene modules. In contrast, all tumors classified as HGHO (High Glycolysis, High OXPHOS)—which maintain both glycolytic and mitochondrial activity— were exclusively found among cancers with strong and consistent correlations with mitochondrial modules.

This distribution aligns with prior pan-cancer metabolic classifications [28], and suggests that mitochondrial module engagement may be shaped by the tumor's dominant metabolic strategy. Specifically, tumors with suppressed oxidative phosphorylation (HGLO) may show lower activity of mitochondrial gene modules, which can reduce ATP production and alter redox balance, explaining the lack of correlation. Conversely, tumors with active mitochondrial metabolism (HGHO) rely more on mitochondrial energy production and biosynthetic pathways, resulting in enhanced energy production and robust module engagement. These findings support the view that mitochondrial module expression may be both cancer-type specific and metabolically contextual and highlight the importance of integrating metabolic phenotyping into mitochondrial biomarker interpretation.

Our findings align with the evolving paradigm of mitochondria as dynamic cancer regulators. While early studies focused on the Warburg effect, we now recognize their pleiotropic roles in metabolic reprogramming, ROS signaling, and apoptosis [7, 13, 29, 30]. Notably, our results supports that mitochondrial adaptations are highly context-dependent across tumor types [13, 31]. These modules—particularly in translation and bioenergetics—may explain observed therapeutic resistance [7, 32], suggesting that targeting mitochondrial plasticity requires personalized approaches. Consequently, stratifying tumors by mitochondrial module expression profiles may thus provide a framework for metabolic subtyping and inform therapeutic strategies targeting mitochondrial vulnerabilities. Although key mitochondrial modules with prognostic and subtype-specific relevance were identified, functional validation is needed to clarify their causal roles. Integrating additional data such as mutations, epigenetics, and metabolomics could deepen mechanistic insights. Future studies should assess the potential of these modules as predictive biomarkers for patient stratification and therapies targeting metabolic vulnerabilities.

Interestingly, the cancer-type-specific behavior of mitochondrial modules may reflect a form of adaptive pleiotropy, a concept previously described in microbial systems [33–35]. In such contexts, early adaptive mutations often occur in global regulators, leading to broad transcriptomic shifts that influence multiple traits simultaneously [36]. Analogous regulatory dynamics may underlie the divergent prognostic roles of modules like ME2 and ME7 across tumor types. The lack of module association in HGLO tumors may further support this interpretation, consistent with stress-induced mitochondrial suppression. These observations suggest that mitochondrial modules may operate within regulatory architectures that favor coordinated multi-trait adaptation, reinforcing their role as context-sensitive hubs in cancer evolution [37-39]. In summary, our findings support the concept of adaptive mitochondrial modules that 'go with the flow' of cancer-specific metabolic rewiring, highlighting their potential as context-sensitive biomarkers and therapeutic targets.

Online Appendix Files: https://jag.journalagent.com/ijmb/abs_files/IJMB-32656/IJMB-32656_(3)_IJMB-32656_Appendix.pdf

Informed Consent: Informed consent was obtained from all participants.

Conflict of Interest Statement: The authors have no conflicts of interest to declare.

Funding: The authors declared that this study received no financial support.

Use of AI for Writing Assistance: No AI technologies utilized.

Peer-review: Externally peer-reviewed.

References

- Huitzil S, Huepe C. Life's building blocks: The modular path to multiscale complexity. Front Syst Biol 2024;4:1417800. [CrossRef]
- Daves J. Exploring biological systems: Complexity, dynamics, and interact. Available at: https://www.scholarsresearchlibrary.com/articles/exploring-biological-systems-complexity-dynamics-and-interactions-108015.html. Accessed Aug 29, 2025.
- 3. Axenie C, Bauer R, Martínez MR. The multiple dimensions of networks in cancer: A perspective. Symmetry 2021;13(9):1559. [CrossRef]
- 4. Alon U. Network motifs: Theory and experimental approaches. Nat Rev Genet. 2007;8(6):450–61. [CrossRef]
- 5. Kitano H. Systems biology: A brief overview. Science 2002;295(5560):1662–4. [CrossRef]
- 6. Tyson JJ, Chen KC, Novak B. Sniffers, buzzers, toggles and blinkers: Dynamics of regulatory and signaling pathways in the cell. Curr Opin Cell Biol 2003;15(2):221–31. [CrossRef]
- 7. Weinberg SE, Chandel NS. Targeting mitochondria metabolism for cancer therapy. Nat Chem Biol 2015;11(1):9–15. [CrossRef]
- 8. Zong WX, Rabinowitz JD, White E. Mitochondria and cancer. Mol Cell 2016;61(5):667–76. [CrossRef]
- Porporato PE, Filigheddu N, Pedro JMBS, Kroemer G, Galluzzi L. Mitochondrial metabolism and cancer. Cell Res 2018;28(3):265–80. [CrossRef]
- 10. Cantó C. Mitochondrial dynamics: Shaping metabolic adaptation. Int Rev Cell Mol Biol 2018;340:129–67. [CrossRef]
- 11. Nunnari J, Suomalainen A. Mitochondria: in sickness and in health. Cell 2012;148(6):1145–59. [CrossRef]
- 12. Vyas S, Zaganjor E, Haigis MC. Mitochondria and cancer. Cell 2016;166(3):555–66. [CrossRef]
- 13. Wallace DC. Mitochondria and cancer. Nat Rev Cancer 2012;12(10):685–98. [CrossRef]
- 14. Zhao Q, Wang J, Levichkin IV, Stasinopoulos S, Ryan MT, Hoogenraad NJ. A mitochondrial specific stress response in mammalian cells. EMBO J 2002;21(17):4411–9. [CrossRef]
- 15. Asghar U, Witkiewicz AK, Turner NC, Knudsen ES. The history and future of targeting cyclin-dependent kinases in cancer therapy. Nat Rev Drug Discov 2015;14(2):130–46. [CrossRef]
- 16. Hanahan D, Weinberg RA. Hallmarks of cancer: The next generation. Cell 2011;144(5):646–74. [CrossRef]
- 17. Kitano H. Cancer as a robust system: Implications for anticancer therapy. Nat Rev Cancer 2004;4(3):227–35. [CrossRef]

- 18. Malumbres M. Cyclin-dependent kinases. Genome Biol 2014;15(6):122. [CrossRef]
- 19. Shapiro Gl. Cyclin-dependent kinase pathways as targets for cancer treatment. J Clin Oncol 2006;24(11):1770–83. [CrossRef]
- 20. Vasan K, Werner M, Chandel NS. Mitochondrial metabolism as a target for cancer therapy. Cell Metab 2020;32(3):341–52. [CrossRef]
- 21. The Cancer Genome Atlas Program (TCGA) NCI. 2022. Available at: https://www.cancer.gov/ccg/research/genome-sequencing/tcga. Accessed Sep 16, 2025.
- 22. Tomczak K, Czerwińska P, Wiznerowicz M. The Cancer Genome Atlas (TCGA): An immeasurable source of knowledge. Contemp Oncol (Pozn) 2015;19(1A):A68–77. [CrossRef]
- 23. Grossman RL, Heath AP, Ferretti V, Varmus HE, Lowy DR, Kibbe WA, et al. Toward a shared vision for cancer genomic data. N Engl J Med 2016;375(12):1109–12. [CrossRef]
- 24. Evangelista JE, Xie Z, Marino GB, Nguyen N, Clarke DJB, Ma'ayan A. Enrichr-KG: bridging enrichment analysis across multiple libraries. Nucleic Acids Res 2023;51(W1):W168–79. [CrossRef]
- 25. Li R, Qu H, Wang S, Wei J, Zhang L, Ma R, et al. GDCRNATools: An R/Bioconductor package for integrative analysis of IncRNA, miRNA and mRNA data in GDC. Bioinformatics 2018;34(14):2515–7. [CrossRef]
- 26. Rath S, Sharma R, Gupta R, Ast T, Chan C, Durham TJ, et al. MitoCarta3.0: An updated mitochondrial proteome now with sub-organelle localization and pathway annotations. Nucleic Acids Res 2021;49(D1):D1541–7. [CrossRef]
- 27. Langfelder P, Horvath S. WGCNA: An R package for weighted correlation network analysis. BMC Bioinformatics 2008;9:559. [CrossRef]
- 28. Hoadley KA, Yau C, Hinoue T, Wolf DM, Lazar AJ, Drill E, et al. Cell-of-origin patterns dominate the molecular classification of 10,000 tumors from 33 types of cancer. Cell 2018;173(2):291–304.e6.
- 29. Vander Heiden MG, Cantley LC, Thompson CB. Understanding the Warburg effect: The metabolic requirements of cell proliferation. Science 2009;324(5930):1029–33. [CrossRef]
- 30. Warburg O. On the origin of cancer cells. Science 1956;123(3191):309–14. [CrossRef]
- 31. Chandel NS. Evolution of mitochondria as signaling organelles. Cell Metab 2015;22(2):204–6. [CrossRef]
- 32. Liberti MV, Locasale JW. The Warburg effect: How does it benefit cancer cells? Trends Biochem Sci 2016;41(3):211–8. [CrossRef]
- 33. Deyell M, Opuu V, Griffiths AD, Tans SJ, Nghe P. Global regulators enable bacterial adaptation to a phenotypic trade-off. iScience 202;28(1):111521. [CrossRef]
- 34. Wagner GP, Zhang J. The pleiotropic structure of the genotype-phenotype map: The evolvability of complex organisms. Nat Rev Genet 2011;12(3):204–13. [CrossRef]
- 35. Couce A. Regulatory networks may evolve to favor adaptive foresight. PLoS Biol 2024;22(12):e3002922. [CrossRef]
- 36. Kinsler G, Geiler-Samerotte K, Petrov D. A genotype-phenotype-fitness map reveals local modularity and global pleiotropy of adaptation. bioRxiv 2020;2020: 2020.06.25.172197. [CrossRef]

- 37. Avolio R, Matassa DS, Criscuolo D, Landriscina M, Esposito F. Modulation of mitochondrial metabolic reprogramming and oxidative stress to overcome chemoresistance in cancer. Biomolecules 2020;10(1):135. [CrossRef]
- 38. Pendleton KE, Wang K, Echeverria GV. Rewiring of mitochondrial metabolism in therapy-resistant cancers:
- Permanent and plastic adaptations. Front Cell Dev Biol 2023;11:1254313. [CrossRef]
- 39. Berner MJ, Wall SW, Echeverria GV. Deregulation of mitochondrial gene expression in cancer: Mechanisms and therapeutic opportunities. Br J Cancer 2024;131(9):1415–24. [CrossRef]

INTERNATIONAL JOURNAL OF

MEDICAL BIOCHEMISTRY

DOI: 10.14744/ijmb.2025.02438 Int J Med Biochem 2025;8(4):292-299

Research Article



Can cinnamon reduce endoplasmic reticulum stress in diabetic nephropathy?: An experimental rat model

- 🗓 Berrin Oztas¹, 🗓 Fatma Ceyla Eraldemir¹, 🗓 Sezgi Akbal², 🕦 Esra Acar³, 🗓 Fatih Hunc¹, Melda Yardimoglu Yilmaz²
- ¹Department of Medical Biochemistry, Kocaeli University Faculty of Medicine, Kocaeli, Türkiye
- ²Department of Histology and Embryology, Kocaeli University Faculty of Medicine, Kocaeli, Türkiye

Abstract

Objectives: The aim was to investigate the effects of cinnamon on the kidney tissue serum endoplasmic reticulum (ER) stress marker, reticulone (RTN)1A, receptor for advanced glycation end products (RAGE) and the lipid peroxidation indicator, malondialdehyde (MDA) in an experimental diabetes mellitus (DM) rat model.

Methods: Twenty-eight male Wistar Albino rats (six months old and weighing 350-400 g) were divided equally into four groups: 1) Control group - citrate buffer (0.2 M, pH 4.4; ip); 2) Cinnamon group - cinnamon (600 mg/kg/day, orogastric tube); 3) DM group -STZ (35 mg/kg, ip); and 4) DM + cinnamon group; Cinnamon and STZ were given at the same doses and route as in Groups 2 and 3, respectively. At the end of the 12-week experiment period, serum, urine and kidney tissue samples were taken from all groups. Serum RTN 1A, RAGE, MDA, urea, blood urea nitrogen (BUN), creatinine levels andkidney tissue RTN 1A, RAGE and MDA levels were measured.

Results: Our biochemical results showed that there was a statistically significant decrease in RAGE and MDA levels in the DM + cinnamon group compared to the DM group (p<0.05). In addition, the decrease in serum urea, BUN, and creatinine levels in the DM + cinnamon group was also remarkable (p<0.05). Althought histologically no widespread necrosis was observed, cortical interstitial vascular dilatation was observed in DM+cinnamon group.

Conclusion: Cinnamon was effective in reducing markers of oxidative stress and ER stress including RAGE and MDA, in kidney tissue in an animal model of diabetic nephropathy.

Keywords: Cinnamon, diabetic nephropathy, endoplasmic reticulum stress, malondialdehyde, receptor for advanced glycation end products, reticulon 1A

How to cite this article: Oztas B, Eraldemir FC, Akbal S, Acar E, Hunc F, Yardimoglu Yilmaz M. Can cinnamon reduce endoplasmic reticulum stress in diabetic nephropathy?: An experimental rat model. Int J Med Biochem 2025;8(4):292-299.

iabetic nephropathy (DN) is a major cause of end-stage renal disease worldwide. Between 20 and 40% of diabetic patients develop DN [1]. DN is characterized by thickening of the glomerular and basement membranes, renal inflammation, tubular interstitial fibrosis, and progressive decrease in kidney function. Proteinuria and microalbuminuria are important markers for evaluating the progression of DN [2, 3].

Chronic hyperglycemia is the main cause of metabolic, biochemical and vascular abnormalities in DN. Oxidative stress (OS) caused by increased levels of reactive oxygen species

(ROS) in the cell, triggered by chronic hyperglycemia, due to mitochondrial dysfunctional cellular respiration and nicotinamide adenine dinucleotide phosphate (NADPH) oxidase (NOX) activity, can lead to DN [4-6]. As a result of OS, critical cellular components, especially protein, lipid, and DNA, are damaged and can lead to podocyte damage, endothelial cell dysfunction, mesangial cell damage, microalbuminuria, and apoptosis in the kidney [7]. Hyperglycemic states can also trigger an unfolded protein response (UPR) by inducing ER stress [5]. It has been suggested that hyperglycemia, protein-





³Department of Biochemistry, Kocaeli Health and Technology University Faculty of Pharmacy, Kocaeli, Türkiye

uria, and increased advanced glycation end products (AGEs) and free fatty acids in DN can trigger UPR in kidney cells, and chronic increased UPR response may result in cell death and increased kidney damage [6–8].

It is thought that the accumulation of AGEs has an important place in the pathophysiology of DN by contributing to the deterioration of ER homeostasis. AGEs show their abnormal effects by binding to their receptor, RAGE. Binding of AGEs with RAGE induces signal transduction and activates ROS production through dysregulation of NOX activity in endothelial cells. ER stress is induced not only in hyperglycemic states but also by hypoxia or oxidative stress, and UPR is triggered [9–11].

Reticulone 1 (RTN1)A is another molecule thought to contribute to ER stress-mediated kidney damage in DN [12]. Reticulones (RTNs) are proteins located in the ER membrane of the cell. There are three human RTN1 isoforms: RTN1A, RTN1B, RTN1C [13]. The human RTN1A protein consists of 776 amino acids, with a hydrophobic region in the ER membrane and hydrophilic regions extending out of the membrane (N-terminal and C-terminal) [14]. Increased expression of RTN1A has been reported to be associated with the progression of DN and the severity of kidney damage, but its mechanism is not yet clear [12, 15]. Increased expression of RTN1A in tubular epithelial cells induces apoptosis through the activation of ER stress [16]. Generally, agents that induce apoptosis at low doses induce necrosis at higher doses. Depending on the severity of exposure to the stimulus, apoptosis and cell necrosis may follow each other, both of which may copresent in most pathological conditions [17]. In this case, RTN1A cell content, indicated by increased renal expression, may be detected in the blood.

Cinnamon is widely consumed around the world as a spice and dietary supplement. The bark of cinnamon is peeled and dried from the body of a small tropical tree. Although there are about 250 types of cinnamon grown in the world, there are two types of cinnamon spices that humans consume: Cinnamomum (C.) zeylanicum and C. cassia [18]. Cinnamon has been shown to modulate glucose and lipid metabolism [19] and has shown pharmacological functions including inhibition of OS, and anti-inflammatory, antihypertensive, and antimicrobial effects [20, 21]. There are also studies suggesting that cinnamon is both preventive of the development of DN and protective against its progression by inhibiting the formation of AGEs [22, 23]. To date, no studies have investigated the impact of cinnamon on diabetic nephropathy (DN) in relation to RTN1A, an established marker of endoplasmic reticulum (ER) stress. In this study, we hypothesized that cinnamon would affect RTN1A, RAGE, and the lipid peroxidation indicator, MDA, in an animal model of DN.

Materials and Methods

Animals

Twenty-eight male Wistar Albino rats, six months old and weighing 350–400 g, were used. All rats were adapted for one week before the experimental procedure. During the adaptation and

treatment periods, all the animals were housed in cages at room temperature (22±2 °C) and humidity (55±5%), and maintained under standard conditions with 12-hour light/dark cycles. They were fed a standard pellet diet and tap water ad libitum throughout the study. The study protocol was approved by the Institutional Animal Care and Ethical Committee of the University. (Approval Number: KOU HADYEK 2/1-2020). The study was designed in accordance with the Helsinki Declaration.

Experimental protocol

After the adaptation period, the rats were divided into four equally sized groups (n=7/group). These groups were: 1) the control group, which received the citrate buffer placebo (0.2 M, pH 4.4; Sigma Aldrich Co., St. Louis, MO., USA) intraperitoneally (i.p), in a single dose. 2) the cinnamon group which received cinnamon (stem barks of C. Zeylanicum (Ceylon cinnamon), 600 mg/kg/day) via orogastric tube suspended in distilled water, as previously described [24]; 3) the diabetes mellitus (DM) group, which received streptozotocin (STZ, Cat. No. S0130, Sigma Aldrich, St Louis, MO, USA) at a dose of 35 mg/kg dissolved in 0.2 M pH 4.4 citrate buffer i.p., was given as a single dose, as previously described [25]; And 4) the DM + cinnamon group: Diabetic rats were given cinnamon (600 mg/kg/day, orogastric tube) for 10 weeks.

Three days after STZ injection, rats with blood glucose levels of ≥300 mg/dL measured by glucometer (Accu-Chek, Roche, Basel, Switzerland) were considered diabetic and selected for the study [25]. This measurement was used solely as an inclusion criterion and was not part of the follow-up data. The experiment was continued for 12 weeks, including a two-week adaptation period [26]. Blood glucose levels were monitored at baseline and at the end of the first, third, and tenth weeks following STZ administration. Cinnamon was administered simultaneously with the STZ injection.

Collection of blood, urine and tissue samples

Spot urine samples of rats in all groups were collected into Eppendorf tubes and stored at -40 °C until tested. At the end of the experimental period, intracardiac blood was collected from rats in all groups under general anesthesia with 75 mg/kg ketamine + 15 mg/kg xylazine (90 + 12 mg/kg, i.p. single dose). Blood taken into a plain tube was centrifuged at 3500 g for 15 minutes and stored at -40°C for biochemical analysis. Kidneys were perfused via abdominal aorta with 100 ml of phosphate buffered saline (PBS). Right kidney tissues were weighed, and 1/10 weight/volume PBS (0.1 M and pH 7.4) was added, and the tissues were homogenized. The homogenates were centrifuged at 3500 g for 15 minutes; the supernatants were separated, taken into Eppendorf tubes, and stored at -40°C until analysis. Left kidney tissues were fixed with Bouin for 48 hours and prepared for routine light microscopy.

Biochemical measurements

In all groups, urea and creatinine levels of serum and urine were measured with an automated chemistry analyzer (AU

Table 1. Serum RTN1A, RAGE and MDA levels in all groups						
Parameter	Control group (n=7)	Cinnamon group (n=7)	DM group (n=7)	DM+cinnamon group (n=7)		
δRTN1A (pg/mL)	307.34±87.67	327.91±74.40	428.28±204.44	336.50±23.68		
ΨRAGE (ng/mL)	168.74±4.27	179.98±3.76*	186.19±4.75*	181.26±3.44*		
δMDA (nmol/mL)	0.76±0.25	0.86±0.13	1.48±0.68* ^{&}	0.96±0.07		

The values are expressed as mean±standard deviation (SD). ⁶: p values are calculated with Mann-Whitney U test; *: p values are calculated with independent sample test; *: Compared with Control group; p<0.05, ⁸: Compared with Cinnamon group; p<0.05. RTN1A: Reticulone 1 (RTN1)A; RAGE: Receptor for advanced glycation end products; MDA: Malondialdehyde; DM: Diabetes mellitus.

Table 2. Renal tissue RTN1A, RAGE and MDA levels in all groups						
Parameters Control group Cinnamon group DM group DM+cinnar (n=7) (n=7) (n=7) group (n=7)						
^ψ RTN1A (pg/mg protein)	31.50±3.24	32.53±3.17	48.92±7.86*&	36.45±4.99		
^δ RAGE (ng/mg protein)	29.58±1.84	30.69±1.29	48.72±8.48* ^{&}	33.45±3.06 ^{&+}		
δMDA (nmol/mg protein)	0.14±0.04	0.15±0.01	0.33±0.09* ^{&}	0.18±0.10 ^{&+}		

The values are expressed as mean±standard deviation (SD), $^{\circ}$: p values are calculated with independent sample test; $^{\circ}$: p values are calculated with Mann-Whitney U test; * : Compared with Control group, p<0.05; $^{\circ}$: Compared with DM group, p<0.05.

5800, Beckman Coulter Inc., Brea, CA, USA). Rat RTN1A and rat RAGE concentrations in kidney tissue and serum were measured by rat-specific ELISA (Cat. No: 201-11-4817 and Cat. No: 201-11-4438, Sunred Biological Technology Co., Shanghai, China). Serum and kidney tissue malondialdehyde (MDA) concentrations were measured using the method of Buege and Aust [27]. Protein concentrations of tissues were determined by the method of Lowry et al. [28].

Light microscope procedures

Sections were trimmed into 20 µm sections up to the beginning of the kidney tissue using a Leica SM2000 R microtome (Leica microsystems, Wetzlar, Germany). When the tissue was reached, serial sections of 4-6 µm were taken. Five preparations were made by skipping ten sections from each kidney. The sections were taken from a hot water bath set at 450°C and mounted on standard glass slides. Then, the sections were stained with either hematoxylin and eosin (H&E) or periodic acid Schiff (PAS). The microscopic structure of kidney tissue was routinely evaluated with H&E. The development of diabetic nephropathy in rats was evaluated according to histopathological criteria. Histologically, necrotic changes in the renal cortex were quantified according to 5 parameters: 1. Interstitial Edema, 2. Epithelial Changes, 3. Tubular Degeneration, 4. Capillary Congestion, 5. Leukocyte Infiltration. PAS stains glomerular capillaries, mesangium, basement membranes of tubules, and Bowman capsules as positive (+). Examination using PAS thus allows for evaluation of the thickness of the basement membrane and possible defects in renal structures. Renal sections from all groups stained with H&E and PAS, were examined under an Olympus Light Microscope (Olympus CX41RF, Olympus Corporation, Tokyo, Japan) and photographed with an Olympus DP26 (Olympus Corporation, Tokyo, Japan) camera.

Statistical analysis

Statistical analyses were performed using SPSS version 20.0 (IBM Corp., Armonk, NY, USA) and GraphPad Prism 10 (GraphPad Software Inc.; San Diego, CA, USA). Normality of data distribution was assessed using the Shapiro–Wilk test. Descriptive statistics were expressed as mean±standard deviation (SD) for normally distributed variables. Independent sample t test was employed for normally distributed data, for non-parametric variables, Mann-Whitney U test was performed.

In addition, two-way ANOVA followed by Tukey's post hoc multiple comparison test was conducted to evaluate changes in glucose levels across four time points. All tests were two-tailed, and a p value < 0.05 was considered statistically significant.

Results

Effects of cinnamon on serum RTN1A, RAGE and MDA levels

The effects of cinnamon on serum RTN1A, RAGE and MDA levels in this diabetic rat model are shown in Table 1. In the DM group, serum RAGE and MDA levels significantly increased compared to the control group (p<0.05). No statistically significant difference was found between the DM + Cinnamon group and the DM group in terms of any parameter.

Effect of cinnamon on kidney tissue RTN1A, RAGE and MDA levels.

The effects of cinnamon on kidney tissue RTN1A, RAGE, and MDA levels in this diabetic rat model are shown in Table 2. In the DM group, RTN1A, RAGE, and MDA levels were significantly increased compared to the control group (p<0.05). In the DM + Cinnamon group compared to the DM group, a statistically significant decrease was found in RAGE and MDA levels (p<0.05).

T-1-1-2 Fff4-f-:	DIINI	v albumin and creatinine levels in all groups
Iania 3 Figet of cinnamon on seriim iirea	KIIN and creatining and iirinar	v ainiimin and creatinine levels in all drolins
Table 3. Effect of chillianion on serain area	Don and creatinine, and armai	y dibdillill dild credtillile levels ill dil giodps

			<u>* </u>		<u> </u>
	Parameters	Control group (n=7)	Cinnamon group (n=7)	DM group (n=7)	DM+cinnamon group (n=7)
Serum	δUrea (mg/dL)	38.83±2.07	36.65±5.32	57.88±8.55* ^{&}	39.59±2.27+
	δBUN (mg/dL)	18.42±1.13	16.43±2.99	29.58±7.99 ^{&}	17.43±2.99+
	^ψ Creatinine (mg/dL)	0.34±0.04	0.29±0.08	0.47±0.06*&	0.38±0.06+
Urine	^δ Albumin (mg/dL)	2.69±1.13	4.26±1.45	21.85±15.47*&	22.33±19.48*+
	$^{\delta}$ Creatinine(mg/dL)	28.92±10.79	23.32±8.97*	25.84±6.72*	36.15±12.60*

The values are expressed as mean \pm standard deviation (SD). $^{\delta}$: p values are calculated with Mann-Whitney U test; $^{\psi}$: p values are calculated with independent sample test; * : Compared with Control group; p<0.05; $^{\delta}$: Compared with DM group; p<0.05. BUN: Blood urea nitrogen; DM: Diabetes mellitus.

Table 4. Blood glucose concentrations (mean±SD, mg/dL) in control and experimental groups of rats measured at baseline and at 1, 3, and 10 weeks following STZ injection

Experimental groups	Baseline	1st week after STZ injection	3 rd week after STZ injection	10 th week after STZ injection
Control group	86.6±12.8	81.6±14.2	87.2±13.4	85.4±14.7
Cinnamon group	86.7±9.4	79.6±9.6	88.6±7.2	85.4±8.7
DM group	85.4±6.9	403.6±31.6	410.5±26.2	420.6±21.6
DM+cinnamon group	87.6±8.7	352.8±28.7	342.8±24.6	345.6±26.1
Group comparison	Baseline	1 st week	3 rd week	10 th week
Control vs. cinnamon	NS	NS	NS	NS
Control vs. DM	NS	p<0.001	p<0.001	p<0.001
Control vs. DM+cinnamon	NS	p<0.001	p<0.001	p<0.001
Cinnamon vs. DM	NS	p<0.001	p<0.001	p<0.001
Cinnamon vs. DM+cinnamon	NS	p<0.001	p<0.001	p<0.001
DM vs. DM+cinnamon	NS	p<0.001	p<0.001	p<0.001

The values are expressed as mean±standard deviation (SD). Results of two-way ANOVA followed by Tukey's post hoc multiple comparison test. SD: Standard deviation; STZ: Streptozotocin; DM: Diabetes mellitus; NS: Non-significant.

Effect of cinnamon on serum and urine parameters

Serum urea, BUN, and creatinine, and urine albumin and creatinine levels in the four groups are shown in Table 3. DM group: Serum urea, BUN, creatinine and urinary albumin levels significantly increased compared to the control group, while urinary creatinine levels decreased (p<0.05). Serum urea, BUN, and creatinine levels were significantly decreased in the DM + Cinnamon group compared to the DM group (p<0.05).

Blood glucose levels were analyzed after the STZ injection, at the 1st, 3rd, and 10th weeks, and it was determined that diabetes developed in the rats. Two-way ANOVA with Tukey's post-hoc multiple comparison test demonstrated that baseline glucose values did not differ among groups. From week 1 onward, diabetic (DM) animals exhibited markedly elevated glucose levels compared with controls (p<0.001). Cinnamon supplementation in DM animals produced a significant, progressive reduction in glucose concentrations versus DM alone (week 1: –50.8; week 3: –67.7; week 10: –75.0 units; all p<0.001), while no differences were observed between Control and Cinnamon groups at any time point (Table 4).

Histological evaluation

Normal parenchymal morphology of glomeruli, Bowman's capsular spaces, and tubules were observed in the kidney sections of the Control group under light microscopy. Tubules and arterioles were observed in the areas between the glomeruli. Larger arteries and vessels were traced at the interface between cortex and medulla. Only tubules and blood vessels were observed in the medulla. PAS staining revealed that the basement membranes in the tubules the Bowman capsule surrounding the glomeruli were thin (Fig. 1a-d). Similar morphological findings were observed in the Cinnamon group (Fig. 1e-h).

Granulo-vacuolar epithelial cell degeneration areas, and desquamation in tubules, hyaline cast, and leukocytic infiltration were observed in the DM and DM + cinnamon groups (Fig. 1i-p). PAS staining enabled examination of basement membrane thickness of renal tubules and Bowman capsules. PAS (+) areas in both the DM and DM + cinnamon group kidney sections, and PAS (+) staining in glomerulo-basement membranes were increased in comparison to tissues obtained from control animals (Fig. 1d, h, l, p).

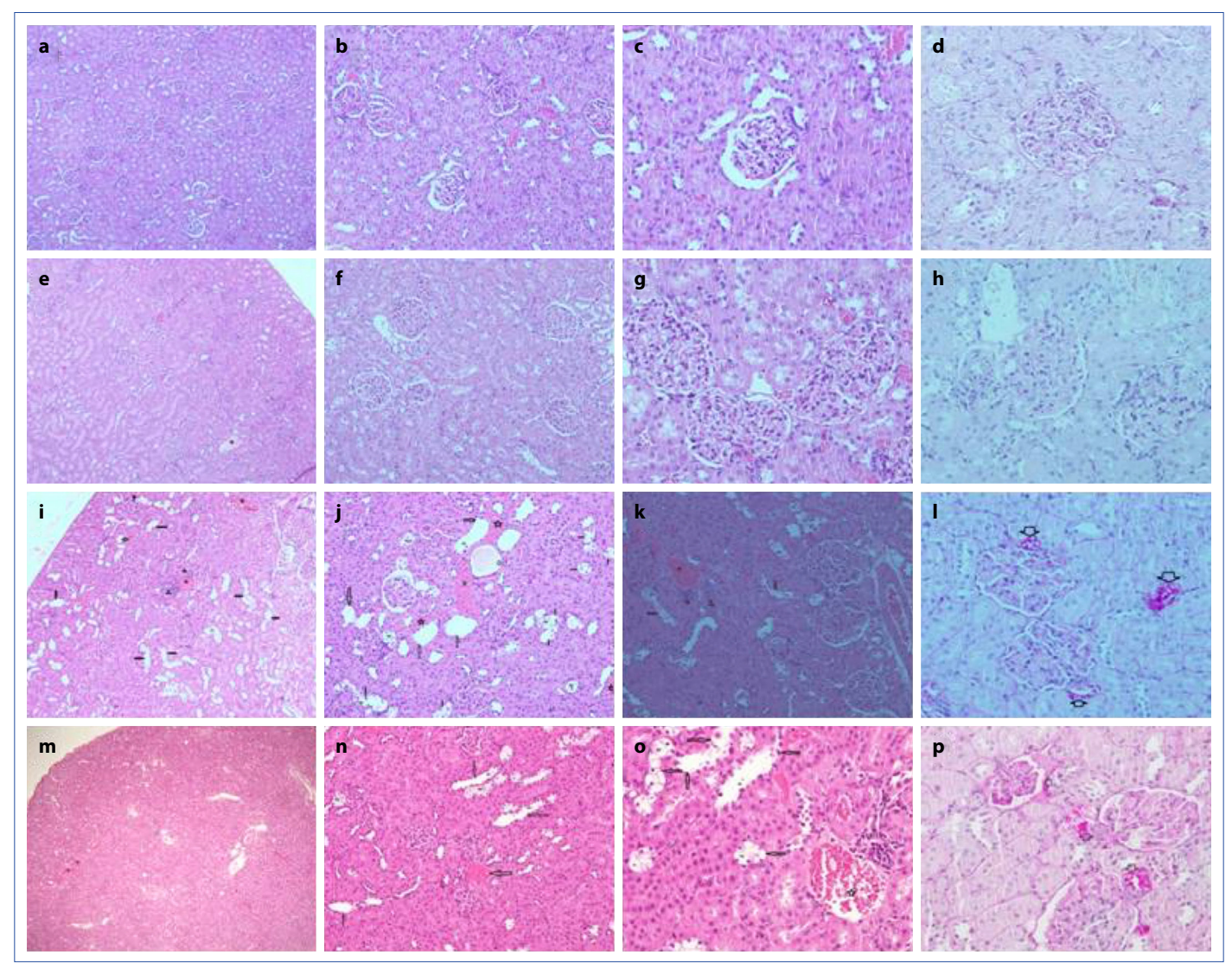


Figure 1. Photomicrographs of diabetic rats showing the effects of cinnamomum zeylanicum treatment on renal histology.

Histopathological changes were more prominent in the DM group (Fig. 1i-l) compared to the DM + cinnamon group (Fig. 1 m-p). Although no widespread necrosis was observed, cortical interstitial vascular dilatation was observed in the DM+cinnamon group, (Fig. 1m-o).

These histological results suggest that cinnamon ingestion in the DM + cinnamon group did not completely eliminate microscopic renal damage. However, renal damage was not as common as in the DM group.

Discussion

This study demonstrates that cinnamon supplementation has significant effects on endoplasmic reticulum (ER) stress and oxidative stress (OS) in diabetic nephropathy (DN). In particular, RAGE and MDA levels in renal tissue were found to be significantly lower in the DM + cinnamon group compared with the DM group, suggesting an improvement in stress-related molecular pathways. Histologically, renal tissue damage such as tubu-

lar degeneration, leukocytic infiltration, vascular dilatation, and PAS(+) thickening of the glomerular basement membrane was observed in the diabetic groups; however, the severity of these changes was less pronounced in the DM + cinnamon group. Overall, these findings indicate that cinnamon intake reduced necrotic areas and alleviated renal damage in diabetic rats.

DN is one of the major microvascular complications of DM. The formation of AGEs, associated with hyperglycemia, is thought to play a central role in the pathophysiology of DN [29]. RAGE, a transmembrane receptor belonging to the immunoglobulin superfamily and found in almost all cell types in the kidney, plays key roles in innate immunity and inflammatory processes [30, 31]. It has been shown that increased AGEs due to DM stimulate RAGE expression in the kidneys [32]. It is thought that RAGE activation induces OS, ER stress, and UPR activation by stimulating NOX-mediated ROS production, causing inflammation, glomerular hypertrophy, podocyte damage and renal fibrosis. NOXs are sources of ROS, induced ER stress in kidney cells, and NOX

activity is induced by hyperglycemia, aggregation of AGEs, and activation of protein kinase C (PKC) [33]. UPR consists of three main signaling pathways initiated by the activation of three ER membrane receptors: Activating transcription factor 6 (ATF 6), enzyme 1 α that requires inositol (IRE1 α), and pancreatic ER eIF2a kinase (PERK) [34]. These UPR-transducer proteins form the inflammatory signal cascade and regulate the expression of pro-inflammatory gene products through nuclear factor- κ B (NF- κ B) as well as other ER stress-inducible transcription factors that modulate ER functions [35]. Consistent with our study, Neto et al. [36] also concluded that cinnamaldehyde treatment reduced ER stress.

An interaction between ER stress and OS has been shown during the development and progression of DN [37]. OS can cause chronic inflammation in kidney tissue, tubule-interstitial fibrosis, and renal hypertrophy. It may also contribute to thickening of tubular and glomerular membranes, podocyte dysfunction, and development of apoptosis [38]. OS caused by chronic hyperglycemia can lead to metabolic and cellular disorders, including lipid peroxidation, protein oxidation, and DNA damage. Non-enzymatic glycosylation of endogenous antioxidants may also contribute to increased OS. Consequently, an imbalance between pro-oxidant and antioxidant processes in DN results in an increase in ROS [39]. The mechanisms of ROS formation in chronic hyperglycemia include oxidative phosphorylation of glucose, which may inhibit regeneration of reduced glutathione and increase superoxide production due to excessive consumption of NADPH in the polyol pathway, AGEs production, mitochondrial respiratory processes, and separation of NOX [40]. In a study investigating the effects of cinnamon on DN, it was reported that procyanidin-B2, one of the active metabolites of cinnamon, inhibited the accumulation of AGEs in diabetic rat kidney, caused a decrease in urinary albumin and creatinine levels, and that it had a curative effect on AGEs-mediated pathogenesis of DN. Recent reports have shown that accumulation of AGEs induced apoptosis through ER stress in various cell types, including glomerular mesangial cells [41, 42]. In agreement with these studies, our results suggest that cinnamon has a protective effect against ER stress by reducing the RAGE level.

Recent studies have suggested that RTN1A analysis plays a critical role in the development of renal tubular cell damage and renal fibrosis [16]. In our study, RTN1A levels in kidney tissue were significantly higher in the DM group compared to the control groups. However, there was no lowering effect of cinnamon on RTN1A levels. These results may be due to the dose, and duration of the cinnamon applied to the experimental groups. The increased expression of RTN1A was associated with progression of DN and the severity of kidney damage [15]. RTN1A has been shown to contribute to both glomerular and tubular cell damage in DN through regulation of ER stress. Fan et al. [6] showed that RTN1A interacts with PERK through its N-terminal and C-terminal domains, and mutation of these PERK domains prevents ER

stress [12]. PERK is known as an important UPR sensor in ER and is activated by phosphorylation under ER stress. Over-expression of RTN1A is thought to increase PERK phosphorylation in kidney cells, leading to the expression of the C/EBP homologous protein (CHOP), a transcription factor that is activated during ER stress [43].

Cinnamon is thought to modulate the production of antioxidant glutathione and phase II detoxifying enzymes, and can prevent the initiation and progression of DN by removing ROS through the activation of nuclear factor erythroid 2-related factor 2 (Nrf2) [44, 45]. In agreement with these studies, in our study, the concentrations of the lipid peroxidation product, MDA, in the DM + cinnamon group were significantly lower than in the DM group. Similarly, Mishra et al. [46] showed that cinnamon reduces lipid peroxidation products and increases antioxidant capacity in a dose-dependent manner (5, 10, 20 mg/kg; i.p.) in the DN model.

In our study, cinnamon administration markedly improved serum markers of renal dysfunction, including serum urea, BUN, and creatinine, in diabetic rats. These findings are consistent with previous experimental studies demonstrating that cinnamon or its active components, such as cinnamal-dehyde, reduce serum urea and creatinine levels and ameliorate renal histopathology in STZ-induced diabetic models [47–49]. This effect of cinnamon may be attributed to its antioxidant and anti-inflammatory properties, which alleviate oxidative stress and metabolic disturbances commonly associated with diabetic nephropathy [50].

However, despite the improvements in serum biochemical parameters, urinary albumin excretion remained elevated in the cinnamon-treated diabetic group compared with the DM group. This finding contradicts some studies reporting that cinnamon or its bioactive fractions reduced albuminuria in diabetic rats [23, 51], but it may indicate that the impact of cinnamon on glomerular permeability depends on the formulation, dose, and duration of treatment. Our results suggest that, at the dose and duration applied in our study, cinnamon ameliorated metabolic and oxidative stress–related damage but showed limited ability to reduce proteinuria.

We have shown both biochemical and histopathological changes in kidney tissues in diabetic animals supplemented with cinnamon. Our histological results suggested that cinnamon ingestion in the DM cinnamon group did not eliminate completely microscopic renal damage. However, it should be kept in mind that biochemical changes are likely to be detectable before histopathological changes are evident using basic light microscopy. Therefore, we believe that further studies are warranted using different cinnamon doses and different measures of ER stress and OS in DN models. In addition, performing histological evaluations by more sensitive methods, such as electron microscopy, may allow us to both observe the damage in more depth and show the possible protective effect of cinnamon in more detail.

Conclusion

These data suggest that cinnamon exerts a protective effect against DN in STZ-induced diabetic rats by reducing the ER stress response and OS. Cinnamon may have a role as an additional supportive agent in preventing the development of diabetic complications, especially those caused by the AGEs and the OS-mediated pathologies such as diabetic nephropathy. However, larger prospective animal studies followed by clinical trials would be necessary to confirm and expand upon these findings.

Ethics Committee Approval: The study was approved by the Kocaeli University Institutional Animal Care Local Ethics Committee (no: 2/1-2020, date: 27/02/2020).

Informed Consent: Informed consent was obtained from all participants.

Conflict of Interest Statement: The authors have declared that no competing interests exist.

Funding: This study was supported by Kocaeli University Scientific Research Project Coordination Unit (project code: 2017/063 HD).

Use of AI for Writing Assistance: No AI technologies utilized.

Authorship Contributions: Concept – B.O., F.C.E., S.A., E.A., F.H., M.Y.Y.; Design – F.C.E., M.Y.Y.; Materials – B.O., F.C.E., S.A., E.A.; Data collection and/or processing – F.C.E., S.A., M.Y.Y.; Data analysis and/or interpretation – E.A., F.H.; Writing – B.O.; Critical review – B.O., F.C.E., S.A., E.A., F.H., M.Y.Y.

Peer-review: Externally peer-reviewed.

References

- 1. American Diabetes Association Professional Practice Committee. 11. Chronic kidney disease and risk management: Standards of care in diabetes 2024. Diabetes Care 2024;47(Suppl 1):S219–30. [CrossRef]
- Liu H, Feng J, Tang L. Early renal structural changes and potential biomarkers in diabetic nephropathy. Front Physiol 2022;13:1020443. [CrossRef]
- 3. Qi C, Mao X, Zhang Z, Wu H. Classification and differential diagnosis of diabetic nephropathy. J Diabetes Res 2017;2017:8637138. [CrossRef]
- 4. Forbes JM, Cooper ME. Mechanisms of diabetic complications. Physiol Rev 2013;93:137–88. [CrossRef]
- Ni L, Yuan C, Wu X. Endoplasmic reticulum stress in diabetic nephrology: Regulation, pathological role, and therapeutic potential. Oxid Med Cell Longev 2021;2021:7277966. [CrossRef]
- Fan Y, Lee K, Wang N, He JC. The role of endoplasmic reticulum stress in diabetic nephropathy. Curr Diab Rep 2017;17:17. [CrossRef]
- Lindenmeyer MT, Rastaldi MP, Ikehata M, Neusser MA, Kretzler M, Cohen CD, et al. Proteinuria and hyperglycemia induce endoplasmic reticulum stress. J Am Soc Nephrol 2008;19:2225– 36. [CrossRef]
- 8. Cybulsky AV, Papillon J, Guillemette J, Navarro Betancourt JR, Chung CF, Iwawaki T, et al. Deletion of IRE1α in podocytes exacerbates diabetic nephropathy in mice. Sci Rep 2024;14(1):11718. [CrossRef]

9. Matsui T, Higashimoto Y, Nishino Y, Nakamura N, Fukami K, Yamagishi SI. RAGE-aptamer blocks the development and progression of experimental diabetic nephropathy. Diabetes 2017;66:1683–95. [CrossRef]

- 10. Kislinger T, Fu C, Huber B, Qu W, Taguchi A, Du Yan S, et al. N(epsilon)-(carboxymethyl)lysine adducts of proteins are ligands for receptor for advanced glycation end products that activate cell signaling pathways and modulate gene expression. J Biol Chem 1999;274:31740–9. [CrossRef]
- 11. Inagi R. Inhibitors of advanced glycation and endoplasmic reticulum stress. Methods Enzymol 2011;491:361–80. [CrossRef]
- 12. Xie Y, E J, Cai H, Zhong F, Xiao W, Gordon RE, et al. Reticulon-1A mediates diabetic kidney disease progression through endoplasmic reticulum-mitochondrial contacts in tubular epithelial cells. Kidney Int 2022;102(2):293–306. [CrossRef]
- 13. GrandPré T, Nakamura F, Vartanian T, Strittmatter SM. Identification of the Nogo inhibitor of axon regeneration as a reticulon protein. Nature 2000;403:439–44. [CrossRef]
- 14. Yang YS, Strittmatter SM. The reticulons: A family of proteins with diverse functions. Genome Biol 2007;8:234. [CrossRef]
- 15. Xiao W, Fan Y, Wang N, Chuang PY, Lee K, He JC. Knockdown of RTN1A attenuates ER stress and kidney injury in albumin overload-induced nephropathy. Am J Physiol Renal Physiol 2016;310:F409–15. [CrossRef]
- 16. Min L, Chen Y, Chen Y, Zhong F, Ni Z, Gu L, et al. RTN1A mediates diabetes-induced AKI-to-CKD transition. JCI Insight 2024;9(24):e185826. [CrossRef]
- 17. Priante G, Gianesello L, Ceol M, Del Prete D, Anglani F. Cell death in the kidney. Int J Mol Sci 2019;20(14):3598. [CrossRef]
- 18. Shang C, Lin H, Fang X, Wang Y, Jiang Z, Qu Y, et al. Beneficial effects of cinnamon and its extracts in the management of cardiovascular diseases and diabetes. Food Funct 2021;12(24):12194–12220. [CrossRef]
- Khan A, Safdar M, Ali Khan MM, Khattak KN, Anderson RA. Cinnamon improves glucose and lipids of people with type 2 diabetes. Diabetes Care 2003;26:3215–18. [CrossRef]
- 20. Li AL, Li GH, Li YR, Wu XY, Ren DM, Lou HX, et al. Lignan and flavonoid support the prevention of cinnamon against oxidative stress related diseases. Phytomedicine 2019;53:143–53. [CrossRef]
- 21. Pagliari S, Forcella M, Lonati E, Sacco G, Romaniello F, Rovellini P, et al. Antioxidant and anti-inflammatory effect of cinnamon (Cinnamomum verum J Presl) bark extract after *in vitro* digestion simulation. Foods 2023;12(3):452. [CrossRef]
- 22. Saraswat M, Reddy PY, Muthenna P, Reddy GB. Prevention of non-enzymic glycation of proteins by dietary agents: Prospects for alleviating diabetic complications. Br J Nutr 2009;101(11):1714–21. [CrossRef]
- 23. Muthenna P, Raghu G, Kumar PA, Surekha MV, Reddy GB. Effect of cinnamon and its procyanidin-B2 enriched fraction on diabetic nephropathy in rats. Chem Biol Interact 2014;222:68–76. [CrossRef]
- 24. Ranasinghe P, Perera S, Gunatilake M, Abeywardene E, Gunapala N, Premakumara S, et al. Effects of cinnamomum zeylanicum (ceylon cinnamon) on blood glucose and lipids in a diabetic and healthy rat model. Pharmacognosy Res 2012;4(2):73–9. [CrossRef]

- 25. Srinivasan K, Viswanad B, Asrat L, Kaul CL, Ramarao P. Combination of high-fat diet-fed and low-dose streptozotocin-treated rat: A model for type 2 diabetes and pharmacological screening. Pharmacol Res 2005;52(4):313–20. [CrossRef]
- 26. Al-Rasheed NM, Al-Rasheed NM, Bassiouni YA, Hasan IH, Al-Amin MA, Al-Ajmi HN, et al. Simvastatin ameliorates diabetic nephropathy by attenuating oxidative stress and apoptosis in a rat model of streptozotocin-induced type 1 diabetes. Biomed Pharmacother 2018;105:290–8. [CrossRef]
- 27. Buege JA, Aust SD. Microsomal lipid peroxidation. Methods Enzymol 1978;52:302–10. [CrossRef]
- 28. Lowry OH, Rosebrough NJ, Farr AL, Randall RJ. Protein measurement with the Folin phenol reagent. J Biol Chem 1951;193(1):265–75. [CrossRef]
- 29. Sanajou D, Ghorbani Haghjo A, Argani H, Aslani S. AGE-RAGE axis blockade in diabetic nephropathy: Current status and future directions. Eur J Pharmacol 2018;833:158–64. [CrossRef]
- 30. Kawakami R, Katsuki S, Travers R, Romero DC, Becker-Greene D, Passos LSA, et al. S100A9-RAGE axis accelerates formation of macrophage-mediated extracellular vesicle microcalcification in diabetes mellitus. Arterioscler Thromb Vasc Biol 2020;40(8):1838–53. [CrossRef]
- 31. Neeper M, Schmidt AM, Brett J, Yan SD, Wang F, Pan YC, et al. Cloning and expression of a cell surface receptor for advanced glycosylation end products of proteins. J Biol Chem 1992;267(21):14998–5004. [CrossRef]
- Yang L, Liang B, Li J, Zhang X, Chen H, Sun J, et al. Dapagliflozin alleviates advanced glycation end product induced podocyte injury through AMPK/mTOR mediated autophagy pathway. Cell Signal 2022;90:110206. [CrossRef]
- Pathomthongtaweechai N, Chutipongtanate S. AGE/RAGE signaling-mediated endoplasmic reticulum stress and future prospects in non-coding RNA therapeutics for diabetic nephropathy. Biomed Pharmacother 2020;131:110655. [CrossRef]
- 34. Cao SS, Kaufman RJ. Unfolded protein response. Curr Biol 2012;22:R622–6. [CrossRef]
- 35. Wang M, Kaufman RJ. Protein misfolding in the endoplasmic reticulum as a conduit to human disease. Nature 2016;529:326–35. [CrossRef]
- 36. Neto JGO, Boechat SK, Romão JS, Pazos-Moura CC, Oliveira KJ. Treatment with cinnamaldehyde reduces the visceral adiposity and regulates lipid metabolism, autophagy and endoplasmic reticulum stress in the liver of a rat model of early obesity. J Nutr Biochem 2020;77:108321. [CrossRef]
- 37. Victor P, Umapathy D, George L, Juttada U, Ganesh GV, Amin KN, et al. Crosstalk between endoplasmic reticulum stress and oxidative stress in the progression of diabetic nephropathy. Cell Stress Chaperones 2021;26:311–21. [CrossRef]
- 38. Miranda-Díaz AG, Pazarín-Villaseñor L, Yanowsky-Escatell FG, Andrade-Sierra J. Oxidative stress in diabetic nephropathy with early chronic kidney disease. J Diabetes Res 2016;2016:7047238. [CrossRef]

- 39. Khanra R, Dewanjee S, Dua TK, Sahu R, Gangopadhyay M, De Feo V, et al. Abroma augusta L (Malvaceae) leaf extract attenuates diabetes induced nephropathy and cardiomyopathy via inhibition of oxidative stress and inflammatory response. J Transl Med 2015;13:6. [CrossRef]
- 40. Singh DK, Winocour P, Farrington K. Oxidative stress in early diabetic nephropathy: Fueling the fire. Nat Rev Endocrinol 2011;7:176–84. [CrossRef]
- 41. Chiang CK, Wang CC, Lu TF, Huang KH, Sheu ML, Liu SH, et al. Involvement of endoplasmic reticulum stress, autophagy, and apoptosis in advanced glycation end products-induced glomerular mesangial cell injury. Sci Rep 2016;6:34167. [CrossRef]
- 42. Suzuki R, Fujiwara Y, Saito M, Arakawa S, Shirakawa JI, Yamanaka M, et al. Intracellular accumulation of advanced glycation end products induces osteoblast apoptosis via endoplasmic reticulum stress. J Bone Miner Res Off J Am Soc Bone Miner Res 2020;35:1992–2003. [CrossRef]
- 43. Liu CY, Kaufman RJ. The unfolded protein response. J Cell Sci 2003;116:1861–2. [CrossRef]
- 44. Huang TC, Chung YL, Wu ML, Chuang SM. Cinnamaldehyde enhances Nrf2 nuclear translocation to upregulate phase II detoxifying enzyme expression in HepG2 cells. J Agric Food Chem 2011;59:5164–71. [CrossRef]
- 45. Zheng H, Whitman SA, Wu W, Wondrak GT, Wong PK, Fang D, et al. Therapeutic potential of Nrf2 activators in streptozoto-cin-induced diabetic nephropathy. Diabetes 2011;60:3055–66. [CrossRef]
- 46. Mishra A, Bhatti R, Singh A, Singh Ishar MP. Ameliorative effect of the cinnamon oil from Cinnamomum zeylanicum upon early stage diabetic nephropathy. Planta Med 2010;76:412–7. [CrossRef]
- 47. Huang YC, Chen BH. A comparative study on improving streptozotocin-induced type 2 diabetes in rats by hydrosol, extract and nanoemulsion prepared from cinnamon leaves. Antioxidants (Basel) 2022 Dec 23;12(1):29. [CrossRef]
- 48. Ghazal NA, Agamia YT, Meky BK, Assem NM, Abdel-Rehim WM, Shaker SA. Cinnamaldehyde ameliorates STZ-induced diabetes through modulation of autophagic process in adipocyte and hepatic tissues on rats. Sci Rep 2024;14(1):10053. [CrossRef]
- 49. Kouame K, Peter AI, Akang EN, Moodley R, Naidu EC, Azu OO. Histological and biochemical effects of Cinnamomum cassia nanoparticles in kidneys of diabetic Sprague-Dawley rats. Bosn J Basic Med Sci 2019;19(2):138–45. [CrossRef]
- 50. Moreira LSG, Brum ISDC, de Vargas Reis DCM, Trugilho L, Chermut TR, Esgalhado M, et al. Cinnamon: An aromatic condiment applicable to chronic kidney disease. Kidney Res Clin Pract 2023;42(1):24–26. [CrossRef]
- 51. Fatima N, Khan MI, Jawed H, Qureshi U, Ul-Haq Z, Hafizur RM, et al. Cinnamaldehyde ameliorates diabetes-induced biochemical impairments and AGEs macromolecules in a pre-clinical model of diabetic nephropathy. BMC Pharmacol Toxicol 2024;25(1):85. [CrossRef]

INTERNATIONAL JOURNAL OF

MEDICAL BIOCHEMISTRY

DOI: 10.14744/ijmb.2025.60590 Int J Med Biochem 2025;8(4):300–305

Research Article



Platelet-normalized biomarkers as diagnostic and prognostic indicators in crimean-congo hemorrhagic fever

Serkan Bolat¹, D Seyit Ali Buyuktuna²

¹Department of Medical Biochemistry, Sivas Cumhuriyet University Faculty of Medicine, Sivas, Türkiye

²Department of Infectious Diseases and Clinical Microbiology, Sivas Cumhuriyet University Faculty of Medicine, Sivas, Türkiye

Abstract

Objectives: Crimean-congo hemorrhagic fever (CCHF) is a viral disease characterized by thrombocytopenia and systemic inflammation. In this study, we evaluated the role of platelet-normalizing biomarkers as diagnostic and prognostic indicators of CCHF.

Methods: This study included 60 patients with CCHF and 30 age-/sex-matched healthy controls. Biochemical parameters, including aspartate aminotransferase, alanine aminotransferase (ALT), gamma-glutamyl transferase, alkaline phosphatase, C-reactive protein and interleukin-6 (IL-6) levels were measured using photometric or electrochemiluminescence methods (Roche Cobas 8000, c702 and e801). Coagulation parameters' levels; activated partial thromboplastin time, international normalized ratio, fibrinogen, and D-dimer were determined using Roche Cobas t511. These parameters were expressed as ratios to platelet count (Plt). Comparisons were performed between the CCHF cohort and control group. Subgroup analyses evaluated associations with intensive care unit (ICU) admission and mortality risk.

Results: Statistically significant differences were observed between CCHF patients and healthy controls in all parameters (p<0.05). Patients admitted to the ICU or those who did not survive exhibited a significant increase in all plate-let-normalized ratios (p<0.05), except ALT/Plt. ROC analysis revealed that IL-6/Plt (AUC=0.998, cut-off>0.018, sensitivity=98.3%, specificity=100%) and D-dimer/Plt (AUC=0.992, cut-off>0.002, sensitivity=95%, specificity=96.7%) had the highest diagnostic accuracy for CCHF. Furthermore, IL-6/Plt and D-dimer/Plt ratios also showed high predictive accuracy for predicting the need for ICU admission and mortality risk.

Conclusion: Platelet-normalized biomarkers, particularly IL-6/Plt and D-dimer/Plt, demonstrate strong diagnostic and prognostic potential for CCHF. Their inclusion in clinical protocols could improve early detection, risk assessment and treatment decisions for CCHF patients.

Keywords: Biomarkers, Crimean-congo hemorrhagic fever, inflammation, mortality prediction, platelet indices

How to cite this article: Bolat S, Buyuktuna SA. Platelet-normalized biomarkers as diagnostic and prognostic indicators in Crime-an-congo hemorrhagic fever. Int J Med Biochem 2025;8(4):300–305.

Crimean-congo hemorrhagic fever (CCHF) is a serious viral disease caused by Crimean-congo hemorrhagic fever virus, a member of the Nairoviridae family [1, 2]. CCHF is endemic in several regions, including Africa, the Middle East, Asia and Southeast Europe, and there has been a notable increase in its incidence over the past decade [3]. The disease is characterized by a range of symptoms, including high fever, muscle pain, vomiting and severe hemorrhagic manifestations, and can lead to a mortality rate ranging from 5% to 30%, depending on the outbreak and region [4].

One of the hallmarks of CCHF is thrombocytopenia, a critical indicator of disease severity and progression [5]. Thrombocytopenia in CCHF is often accompanied by life-threatening conditions such as petechiae, ecchymosis, and gastrointestinal bleeding. The pathogenesis of CCHF involves a complex interaction between the virus and the host. Infection triggers an inflammatory response that can develop into a cytokine storm, a hyper-inflammatory condition characterized by excessive release of pro-inflammatory cytokines. This cytokine storm is associated with severe tissue damage and can cause hemorrhag-

Address for correspondence: Serkan Bolat, MD. Department of Medical Biochemistry, Sivas Cumhuriyet University Faculty of Medicine, Sivas, Türkiye

Phone: +90 507 439 00 28 **E-mail:** drsbolat@gmail.com **ORCID:** 0000-0002-8669-8782

Submitted: February 18, 2025 Accepted: May 11, 2025 Available Online: October 21, 2025

OPEN ACCESS This is an open access article under the CC BY-NC license (http://creativecommons.org/licenses/by-nc/4.0/).





ic symptoms observed in CCHF patients [6, 7]. Studies have

shown that CCHF virus can target immune cells, leading to their activation and subsequent cytokine release, which can exacerbate the inflammatory response [6, 8]. The resulting cytokine storm can lead to multiple organ failure, which is a common cause of death in severe cases of CCHF. Liver damage in CCHF is often evaluated through biomarkers such as alanine aminotransferase (ALT) and aspartate aminotransferase (AST), which are indicators of hepatocellular damage. High levels of these enzymes have been consistently reported in CCHF patients, reflecting the degree of liver involvement during infection [9]. Platelet indices are increasingly recognized as potential biomarkers for disease severity and prognosis in a variety of infectious and inflammatory conditions [10, 11]. However, the utility of platelet and liver enzymes, inflammatory markers, and coagulation parameters in assessing the inflammatory and coagulopathic response in CCHF has not been adequately studied. In this study, it aims to determine whether these ratios provide clinically meaningful information about disease progression and severity, potentially improving risk stratification and guiding therapeutic interventions. For this purpose, aspartate aminotransferase to platelet ratio (AST/Plt), alanine aminotransferase to platelet ratio (ALT/Plt), gamma-glutamyl transferase to platelet ratio (GGT/Plt), alkaline phosphatase to platelet ratio (ALP/Plt), C-reactive protein to platelet ratio (CRP/ Plt), interleukin-6 to platelet ratio (IL-6/Plt), activated partial thromboplastin time to platelet ratio (APTT/Plt), international normalized ratio to platelet ratio (INR/Plt), fibrinogen to platelet ratio (Fibrinogen/Plt), and D-dimer to platelet ratio (D-dimer/Plt) were evaluated in CCHF patients and healthy controls.

Materials and Methods

Patients

The study included 60 patients aged over 18 years who were admitted to the Infectious Diseases Clinic between March and October 2022 with a preliminary diagnosis of Crimean-congo hemorrhagic fever (CCHF). The diagnosis of CCHF was subsequently confirmed using PCR or serological methods. Additionally, a control group consisting of 30 age-/sex-matched healthy people, with no history of chronic disease or drug use, was included for comparison.

The minimum total sample size required to detect a moderate effect size (Cohen's d=0.65) at a significance level (α) of 5%, with 80% statistical power (1 – β) and a group allocation ratio (N1/N2) of 2, was calculated to be 90. While enlarging the sample size may enhance the detection of statistically significant differences between groups, such differences risk being clinically irrelevant. To prioritize the identification of biologically and clinically meaningful effects, a moderate effect size was selected a priori, balancing statistical sensitivity and practical significance. Power analysis indicated that a total sample size (n=90) would minimize the possibility of overinterpreting insignificant differences and provide sufficient power for the study. All human research protocols were in compliance with

relevant national regulations, institutional policies, and the principles outlined in the Declaration of Helsinki. The study was approved by the Institutional Review Board (Ethical Committee approval No: 2025-01/62, Date: 16/01/2025). Informed consent was obtained from all participants involved in the study.

Laboratory analyses

Platelet count, AST, ALT, GGT, ALP, CRP, IL-6, INR, APTT, fibrinogen, and D-dimer levels were measured in both patient and control groups. Additionally, data regarding the need for intensive care unit (ICU) and the survival status of patients were recorded. Laboratory tests for AST, ALT, GGT, ALP, and CRP were conducted using photometric methods on a Roche Cobas c702 analyzer (Roche Diagnostics, Germany), while IL-6 levels were assessed using an electrochemiluminescence method on a Roche Cobas e801 analyzer. Complete blood count tests were performed using a Sysmex XN-1000 (Sysmex Corporation, Japan) analyzer, and coagulation tests were conducted on a Roche Cobas t511 analyzer.

Statistical analysis

New indices were derived by dividing the laboratory data by platelet count. These indices were compared between the patient and control groups and, within the patient group, based on the need for intensive care and survival status. The assumption of normality was assessed using the Shapiro-Wilk test. The non-parametric Mann-Whitney U test was used for comparisons between two groups. Furthermore, receiver operating characteristic (ROC) analyses were conducted to evaluate the performance of the indices in predicting CCHF diagnosis and disease prognosis, including the need for intensive care and survival status. The area under the curve (AUC), sensitivity, and specificity were calculated. Data were analyzed using SPSS software (IBM Corp., SPSS Statistics for Windows, Version 23.0, USA), and GraphPad Prism version 8.3.0 (GraphPad Software, www.graphpad.com, USA) was employed for data visualization. A significance level of p<0.05 was considered for all statistical tests.

Results

Statistically significant differences were observed between CCHF patients and healthy controls in all parameters studied. All indices were higher in patients than in healthy controls (Table 1, Fig. 1).

INR/Plt, APTT/Plt, D-dimer/Plt, fibrinogen/Plt AST/Plt, GGT/Plt and ALP/Plt, CRP/Plt and IL-6/Plt values of patients admitted to ICU were significantly increased in the ICU group, however, ALT/Plt (p=0.068) was not statistically significant between the groups (Table 2). Similar results were obtained for patients who did not survive.

IL-6/Plt (AUC=0.998), D-dimer/Plt (AUC=0.992), and AST/Plt (AUC=0.990) had the highest predictive values in the ROC analysis to predict the diagnosis of CCHF, with sensitivity and specificity reaching nearly 100% at cut-off values (>0.018, >0.002, and >0.162, respectively). The highest probability

Parameters	Gro	pups	р
	Control (n=30)	Patient (n=60)	
INR/Plt	0.004 (0.004–0.005)	0.012 (0.009–0.02)	<0.00
APTT/Plt	0.118 (0.099-0.146)	0.409 (0.268-0.628)	<0.001
D-dimer/Plt	0.001 (0.001-0.001)	0.033 (0.011–0.112)	<0.001
Fibrinogen/Plt	1.14 (0.923–1.373)	3.358 (2.287–4.821)	<0.001
AST/Plt	0.074 (0.06-0.093)	1.311 (0.38–4.991)	<0.001
ALT/Plt	0.077 (0.063-0.097)	0.568 (0.295-2.162)	<0.001
GGT/Plt	0.07 (0.047-0.121)	0.587 (0.25–1.137)	<0.001
ALP/Plt	0.304 (0.241-0.336)	0.981 (0.589–1.554)	<0.001
CRP/Plt	0.005 (0.002-0.009)	0.156 (0.046-0.477)	<0.001
IL-6/Plt	0.007 (0.006-0.009)	0.26 (0.15–1.142)	<0.001

Continuous variables are expressed as median and quartiles (Q1-Q3). Groups were compared using the Mann-Whitney U test. Significant p-values are shown in bold. CCHF: Crimean-congo hemorrhagic fever; INR: International normalized ratio; Plt: Platelet; APTT: Activated partial thromboplastin time; AST: Aspartate aminotransferase; ALT: Alanine aminotransferase; GGT: Gamma-glutamyl transferase; ALP: Alkaline phosphatase; CRP: C-reactive protein; IL-6: Interleukin-6.

Parameters	Intensive care u	р	
	No (n=53)	Yes (n=7)	
INR/Plt	0.012 (0.009–0.016)	0.038 (0.029–0.048)	<0.00
APTT/Plt	0.368 (0.259-0.544)	1.364 (0.824–1.524)	<0.00
D-dimer/Plt	0.021 (0.01-0.06)	1.273 (0.824–1.524)	<0.00
Fibrinogen/Plt	3.2 (2.186-4.548)	6.048 (4.452-7.182)	0.005
AST/Plt	0.745 (0.348-3.365)	5.818 (2.843-6.071)	0.006
ALT/Plt	0.551 (0.288–1.895)	1.394 (0.832–3.129)	0.068
GGT/Plt	0.472 (0.244-0.947)	1.524 (0.686–13.581)	0.009
ALP/Plt	0.875 (0.584–1.275)	2.636 (1.69–3.452)	<0.00
CRP/Plt	0.132 (0.036-0.286)	2.806 (0.686-5.952)	<0.00
IL-6/Plt	0.24 (0.124-0.688)	7.182 (2.706–15.806)	<0.00

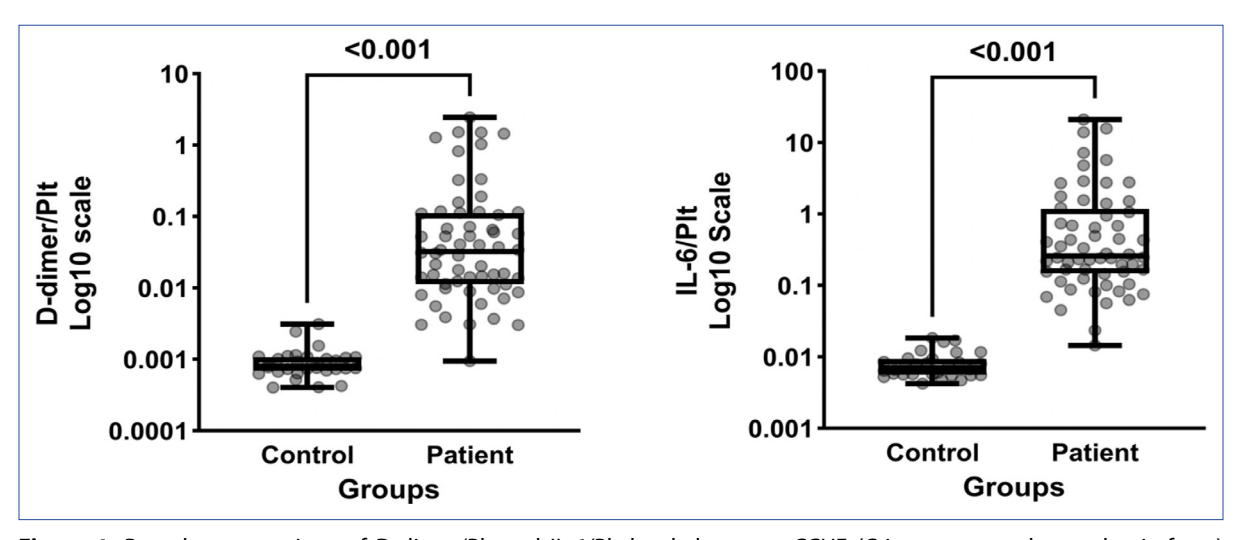


Figure 1. Box-plot comparison of D-dimer/Plt and IL-6/Plt levels between CCHF (Crimean-congo hemorrhagic fever) patients and healthy controls.

Table 3. ROC ana	Table 3. ROC analysis results for predicting the CCHF diagnosis						
Parameters	Cut-off value	AUC	Sensitivity (%)	Specificity (%)	LR (+)	LR (-)	
INR/Plt	>0.007	0.973	90 (79.5–96.2)	96.7 (82.8–99.9)	27 (3.92–185)	0.1 (0.048-0.22)	
APTT/Plt	>0.196	0.958	93.3 (83.8-98.2)	96.7 (82.8-99.9)	28 (4.07-192)	0.069 (0.027-0.18)	
D-dimer/Plt	>0.002	0.992	98.3 (91.1–100)	96.7 (82.8-99.9)	29.5 (4.29-202)	0.017 (0.003-0.12)	
Fibrinogen/Plt	>2.03	0.970	88.3 (77.4–95.2)	100 (88.4-100)		0.12 (0.058-0.23)	
AST/Plt	>0.162	0.990	96.7 (88.5-99.6)	100 (88.4-100)		0.033 (0.009-0.13)	
ALT/Plt	>0.162	0.957	90 (79.5-96.2)	96.7 (82.8-99.9)	27 (3.92–185)	0.1 (0.048-0.22)	
GGT/Plt	>0.188	0.930	86.7 (75.4–94.1)	93.3 (77.9–99.2)	13 (3.40-49.8)	0.14 (0.074-0.27)	
ALP/Plt	>0.434	0.976	95 (86.1–99.0)	93.3 (77.9–99.2)	14.3 (3.73-54.4)	0.054 (0.018-0.16)	
CRP/Plt	>0.014	0.978	93.3 (83.8-98.2)	100 (88.4–100)		0.067 (0.026-0.17)	
IL-6/Plt	>0.018	0.998	98.3 (91.1–100)	100 (88.4–100)		0.017 (0.002-0.12)	

ROC: Receiver operating characteristic; CCHF: Crimean-congo hemorrhagic fever; AUC: Area under the curve; LR: Likelihood ratio; INR: International normalized ratio; Plt: Platelet; APTT: Activated partial thromboplastin time; AST: Aspartate aminotransferase; ALT: Alanine aminotransferase; GGT: Gamma-glutamyl transferase; ALP: Alkaline phosphatase; CRP: C-reactive protein; IL-6: Interleukin-6.

Table 4. ROC analysis results for predicting the intensive care unit requirements of CCHF patients						
Parameters	Cut-off value	AUC	Sensitivity (%)	Specificity (%)	LR (+)	LR (-)
INR/Plt	>0.025	0.895	85.7 (42.1–99.6)	94.3 (84.3-98.8)	15.1 (4.84–47.4)	0.15 (0.025-0.93)
APTT/Plt	>0.762	0.895	85.7 (42.1–99.6)	92.5 (81.8-97.9)	11.4 (4.22-30.6)	0.15 (0.025-0.95)
D-dimer/Plt	>0.118	0.978	100 (59.0-100)	92.5 (81.8-97.9)	13.3 (5.16-34.0)	0
Fibrinogen/Plt	>4.43	0.819	85.7 (42.1–99.6)	73.6 (59.7–84.7)	3.24 (1.89-5.58)	0.19 (0.031-1.20)
AST/Plt	>1.94	0.814	85.7 (42.1–99.6)	66.0 (51.7–78.5)	2.52 (1.56-4.09)	0.22 (0.035-1.34)
ALT/Plt	>0.569	0.714	100 (59.0-100)	58.5 (44.1–71.9)	2.41 (1.75-3.32)	0
GGT/Plt	>0.590	0.798	100 (59.0-100)	58.5 (44.1–71.9)	2.41 (1.75-3.32)	0
ALP/Plt	>1.23	0.900	100 (59.0-100)	73.6 (59.7–84.7)	3.79 (2.42-5.93)	0
CRP/Plt	>0.529	0.914	85.7 (42.1–99.6)	88.7 (77.0–95.7)	7.57 (3.36–17.1)	0.16 (0.026-0.99)
IL-6/Plt	>1.77	0.946	85.7 (42.1–99.6)	92.5 (81.8–97.9)	11.4 (4.22–30.6)	0.15 (0.025-0.95)

rates for positive outcomes were observed for D-dimer/Plt (LR+=29.5) and APTT/Plt (LR+=28) (Table 3, Fig. 2).

In the ROC analysis to estimate ICU requirements, D-dimer/Plt (AUC=0.978, cut-off >0.118) and IL-6/Plt (AUC=0.946, cut-off >1.77) showed the highest predictive accuracy with sensitivity

and specificity exceeding 85% in most cases. The highest positivity rates were observed for INR/Plt (LR+=15.1) and D-dimer/Plt (LR+=13.3) (Table 4, Fig. 2).

Similar to the results in patients admitted to the ICU, ROC analysis to estimate mortality risk exhibited high predictive accura-

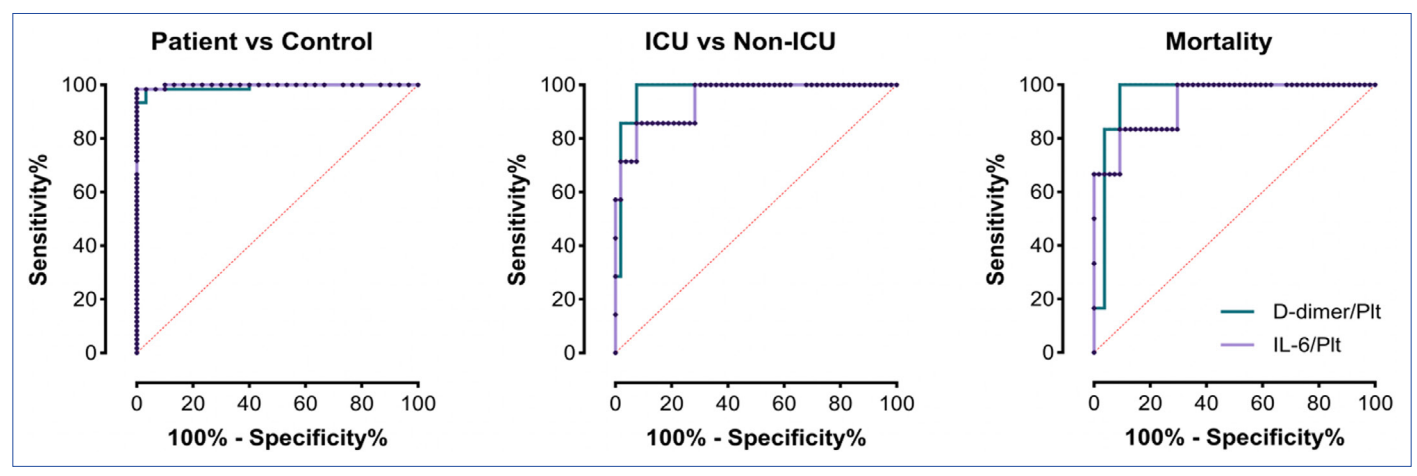


Figure 2. Diagnostic accuracy of D-dimer/Plt and IL-6/Plt levels in CCHF (Crimean-congo hemorrhagic fever) prediction, ICU (intensive care unit) requirements and mortality risk.

cy with sensitivity and specificity exceeding 80% for D-dimer/Plt (AUC=0.960, cut-off >0.118) and IL-6/Plt (AUC=0.935, cut-off >1.77) (Fig. 2). The highest positivity rates were observed for INR/Plt (LR+=11.3) and D-dimer/Plt (LR+=10.8).

Discussion

Viral hemorrhagic fevers are a group of serious, often fatal illnesses caused by several different families of viruses. Among these illnesses is CCHF, which is characterized by systemic inflammation, vascular instability, and coagulation abnormalities, frequently leading to hemorrhage, multiple organ failure, and death [12]. Thrombocytopenia is an important feature of CCHF and plays a critical role in the prognosis of the disease. Platelet count below 20,000/µL has been associated with severe bleeding and poor outcomes [13]. An important factor that plays a role in the pathogenesis of CCHF is uncontrolled immune response and cytokine storm [14]. IL-6 is an important proinflammatory cytokine involved in the acute phase response and has been widely studied as a biomarker of disease severity in a variety of infectious and inflammatory conditions [15]. Studies have reported increased levels of IL-6 in patients with CCHF [14, 16]. In a study conducted in Türkiye, serum IL-6 levels were found to be high in CCHF patients and positively correlated with disease severity [16]. Another study highlighted that high levels of IL-6 are associated with disseminated intravascular coagulation (DIC) in CCHF patients, and high levels of IL-6 are observed in fatal cases [3]. Our results in this study show that the IL-6/Plt ratio is significantly higher in CCHF patients compared to healthy controls. We think that thrombocytopenia and an increased level of IL-6 reflect the complex interplay between viral infection, immune activation, and clotting disorders. The elevation of IL-6/Plt level showed high diagnostic accuracy with an AUC of 0.998, specificity of 100%, and sensitivity of 98.3%. These findings suggest that IL-6/Plt ratio is a valuable biomarker in the early detection of CCHF.

Understanding the mechanisms underlying this finding in CCHF is also important for developing targeted therapies to improve the management and outcomes of this life-threatening disease and to mitigate its impact in CCHF.

D-dimers are produced as a result of the breakdown of cross-linked fibrin by plasmin during the fibrinolysis process. D-dimer is elevated in conditions associated with coagulation activation and fibrinolysis, such as DIC. High levels of D-dimers indicate activation of coagulation and fibrinolytic systems, which are hallmarks of viral hemorrhagic fever. In CCHF, elevated D-dimer levels are a common finding and are closely related to disease severity and outcomes. Many studies have documented elevated D-dimer levels in CCHF patients. Büyüktuna et al. [17] found that D-dimer levels were significantly higher in severe CCHF cases compared to mild and moderate groups. Similarly, Ergönül et al. [18] reported that D-dimer levels were strongly associated with coagulopathy and bleeding severity in CCHF patients [18]. Our findings demonstrate that

the D-dimer/Plt ratio is significantly higher among patients requiring ICU care and in those who did not survive, compared with non-ICU and surviving patients. Notably, the high AUC, sensitivity, and specificity values (AUC=0.978 for ICU requirement and AUC=0.960 for mortality) underscore the potential of the D-dimer/platelet ratio as a reliable biomarker for predicting both critical care needs and mortality risk.

This study has some limitations. First, the sample size (60 patients and 30 controls) may restrict the statistical power of subgroup analyses, particularly for rare outcomes like ICU requirement or mortality risk. Second, the single-center design introduces potential selection bias. Third, the cross-sectional nature of the study limits causal inference. Future multicenter studies with larger cohorts are needed to validate these findings.

Conclusion

Our findings highlight the diagnostic and prognostic value of platelet-based ratios in CCHF. A significantly higher IL-6/ Plt ratio in patients compared to healthy controls indicates that it can be used as an early detection biomarker with its high sensitivity and specificity. Furthermore, the D-dimer/platelet ratio was found to be higher among patients requiring intensive care and non-survivors, underscoring its potential role in predicting both critical care needs and mortality risk. These results reflect the complex interaction between viral infection, immune activation, and coagulation disorders, highlighting the importance of thrombocytopenia and inflammatory cytokines in the pathophysiology of CCHF. Going forward, mechanistic investigations focusing on the specific pathways by which IL-6 and D-dimer affect coagulation and immune responses in CCHF could guide the development of targeted therapies. The incorporation of these biomarkers into existing clinical protocols can improve early diagnosis, risk stratification, and therapeutic decision-making, ultimately improving patient outcomes in this life-threatening disease.

Ethics Committee Approval: The study was approved by the Sivas Cumhuriyet University Non-interventional Clinical Research Ethics Committee (no: 2025-01/62, date: 16/01/2025).

Informed Consent: Informed consent was obtained from all participants.

Conflict of Interest Statement: All authors declared no conflict of interest.

Funding: The authors declared that this study received no financial support.

Use of Al for Writing Assistance: No Al technologies utilized.

Authorship Contributions: Concept – S.B., S.A.B.; Design – S.B.; Supervision – S.A.B.; Materials – S.A.B.; Data collection and/or processing – S.A.B.; Data analysis and/or interpretation – S.B.; Literature search – S.A.B.; Writing – S.B.; Critical review – S.A.B.

Peer-review: Externally peer-reviewed.

References

- Baysal AÇ, Kıymaz YÇ, Şahin NÖ, Bakır M. Investigation of long noncoding RNA-NRAV and long noncoding RNA-lethe expression in Crimean-Congo hemorrhagic fever. J Med Virol 2024;96(12):e70142. Erratum in: J Med Virol 2025;97(2):e70245. [CrossRef]
- Khan ST, Hashim H, Hamid W, Mehmood S, Qamar F. Crimean-Congo hemorrhagic fever--Distribution, diagnosis, treatment and control measures. Lahore Garrison Univ J Life Sci 2017;1:152–67. [CrossRef]
- 3. Hawman DW, Feldmann H. Crimean-Congo haemorrhagic fever virus. Nat Rev Microbiol 2023;21(7):463–77. [CrossRef]
- Büyüktuna SA, Doğan HO. Diagnosis, prognosis and clinical trial in Crimean-Congo hemorrhagic fever. In: Human Viruses: Diseases, Treatments and Vaccines: The New Insights. Springer International Publishing; 2021. p. 207–19. [CrossRef]
- Yilmaz H, Yilmaz G, Kostakoğlu U, Yaman H, Örem A, Köksal İ. The prognostic significance of serum troponin T levels in Crimean-Congo hemorrhagic fever patients. J Med Virol 2017;89(3):408–12. [CrossRef]
- Frank MG, Weaver G, Raabe V; State of the Clinical Science Working Group of the National Emerging Pathogens Training and Education Center's Special Pathogens Research Network. Crimean Congo hemorrhagic fever virus for clinicians-Virology, pathogenesis, and pathology. Emerg Infect Dis 2024;30(5):847–53. [CrossRef]
- Akinci E, Bodur H, Sunbul M, Leblebicioglu H. Prognostic factors, pathophysiology and novel biomarkers in Crimean-Congo hemorrhagic fever. Antiviral Res 2016;132:233–43. [CrossRef]
- Welch SR, Ritter JM, McElroy AK, Harmon JR, Coleman-Mc-Cray JD, Scholte FEM, et al. Fluorescent Crimean-Congo hemorrhagic fever virus illuminates tissue tropism patterns and identifies early mononuclear phagocytic cell targets in Ifnar-/mice. PLoS Pathog 2019;15(12):e1008183. [CrossRef]

- Rathore SS, Manju AH, Wen Q, Sondhi M, Pydi R, Haddad I, et al. Crimean-Congo haemorrhagic fever-induced liver injury: A systematic review and meta-analysis. Int J Clin Pract 2021;75(11):e14775. [CrossRef]
- 10. Viswanathan S, Saravanakumari V. Are platelet indices useful in diagnosis of tropical acute febrile illnesses? J Local Global Health Sci 2016;2016:3. [CrossRef]
- 11. Incir S, Calti HK, Palaoglu KE. The role of immature granulocytes and inflammatory hemogram indices in the inflammation. Int J Med Biochem 2020;3:125–30. [CrossRef]
- 12. Muzammil K, Rayyani S, Abbas Sahib A, Gholizadeh O, Naji Sameer H, Jwad Kazem T, et al. Recenta in Crimean-Congo hemorrhagic fever virus detection, treatment, and vaccination: Overview of current status and challenges. Biol Proced Online 2024;26(1):20. [CrossRef]
- 13. Doğan HO, Büyüktuna SA, Kapancik S, Bakir S. Evaluation of the associations between endothelial dysfunction, inflammation and coagulation in Crimean-Congo hemorrhagic fever patients. Arch Virol 2018;163(3):609–16. [CrossRef]
- 14. Doğan K, Bolat S, Öksüz C, Büyüktuna SA. Leukotriene metabolism and proiflammatory cytokines in Crimean Congo hemorrhagic fever. J Med Virol 2023;95(1):e28199. [CrossRef]
- 15. McElvaney OJ, Curley GF, Rose-John S, McElvaney NG. Interleukin-6: Obstacles to targeting a complex cytokine in critical illness. Lancet Respir Med 2021;9(6):643–54. [CrossRef]
- 16. Onuk S, Sipahioglu H, Beştepe Dursun Z, Eren E, Aslan Sırakaya H, Kuzugüden S, et al. The relationship between cytokine concentrations and severity scoring index for Crimean-Congo hemorrhagic fever. Cureus 2023;15(2):e34882. [CrossRef]
- 17. Büyüktuna SA, Yerlitaş Sİ, Zararsız GE, Doğan K, Kablan D, Bağcı G, et al. Exploring free amino acid profiles in Crimean-Congo hemorrhagic fever patients: Implications for disease progression. J Med Virol 2024;96(5):e29637. [CrossRef]
- 18. Ergönül O. Crimean-Congo haemorrhagic fever. Lancet Infect Dis 2006;6(4):203–14. [CrossRef]

INTERNATIONAL JOURNAL OF

MEDICAL BIOCHEMISTRY

DOI: 10.14744/ijmb.2025.90582 Int J Med Biochem 2025;8(4):306–311

Research Article



Determination of analytical performances of NT-proBNP and aPTT tests with three methods

Dilek Yegin

Central Laboratory, Bursa City Hospital, Bursa, Türkiye

Abstract

Objectives: This study aimed to evaluate the analytical performances of N-terminal pro-B-type natriuretic peptide (NT-proBNP), which has not been investigated before, and activated partial thromboplastin time (aPTT), which has been the subject of little research, using the six sigma methodology and to calculate the quality goal index values of low-performing parameters. It was aimed to evaluate the analytical process with three methods by presenting this performance with Operation specification charts, which have been done in few other studies.

Methods: Three consecutive months of internal quality control data obtained from NT-proBNP and aPTT tests, twice daily, and data obtained from a monthly external quality control program were used. Sigma values were calculated using the calculation of Sigma=(Total allowable error-bias)/(Coefficient of variation) and shown with Operation specification charts (OPSpecs). Quality goal index (QGI) was calculated for those with sigma <6.

Results: The sigma values for levels 1 and 2 of the NT-proBNP test were calculated as 5.06 and 5.65, and the performance status was determined as very good. The sigma values for levels 1 and 2 of the aPTT test were calculated as 4.28 and 3.56, respectively, and this was evaluated as moderate and good performance. The Quality goal index values (QGI) for levels 1 and 2 of the NT-proBNP test were calculated as 0.11 and 0.12, respectively. The Quality goal index (QGI) values for levels 1 and 2 of the aPTT test were calculated as 0.90 and 0.75, respectively.

Conclusion: Both tests had moderate, good and very good performance. It is of great importance to increase quality standards in laboratory tests. In this direction, continuous improvement-oriented initiatives should be implemented to make analytical processes more competent.

Keywords: aPTT, NT-proBNP, OPSpecs, quality goal index, six sigma

How to cite this article: Yeğin D. Determination of analytical performances of NT-proBNP and aPTT tests with three methods. Int J Med Biochem 2025;8(4):306–311.

The entire testing process in clinical laboratories is divided into three stages: Preanalytical, analytical, and postanalytical. Research indicates that error rates are estimated to range from 30–75% in the preanalytical stage, 4–30% in the analytical stage, and 9–55% in the postanalytical stage [1]. Laboratories need to assess their process performance based on scientifically established quality standards. This assessment involves analyzing the rate of sample errors and rejections during the preanalytical phase, evaluating the accuracy and precision of test results in the analytical phase, and monitoring the reporting of critical values as well as test turn around times in the postanalytical phase [2]. Among

these stages, analytical quality alone is not sufficient as a standalone quality requirement; however, other quality parameters hold no significance unless analytical quality is achieved. Laboratories must ensure accurate test results before addressing other quality criteria [3].

The Six Sigma approach is a technique applied in quality control and process enhancement. It aims to detect defects and minimize mistakes and variations [4]. Six sigma quality management is not just a tool for defining process performance; it is also a methodology aimed at reducing the error rate within the process. In automated analytical systems, it is important to determine the situations where precision error, accuracy error,





or both errors occur together, which are among the test-specific reasons, in order to ensure the quality improvement of tests. These performance data can also be evaluated by calculating the quality goal index (QGI) [5]. The six sigma method allows for an objective assessment of performance. The sigma level of a process can be determined by using specific equations. The sigma value indicates the frequency of potential errors. A low sigma value suggests that the process is more likely to produce errors. Ideal or world-class performance should have a minimum of 6 sigma values, which translates to fewer than three or four errors per million products [6].

In this study, the research was planned by prioritizing the feedback from clinicians to the laboratory regarding the tests. Considering this situation, it was aimed to evaluate the analytical performances of N-terminal pro-B-type natriuretic peptide (NT-proBNP), which has not been investigated before, and activated partial thromboplastin time (aPTT), which is a subject of little research, using the six sigma methodology and to calculate the quality target index (QGI) values of the parameters showing low performance. It was aimed to evaluate the analytical process with three methods by presenting this performance with Operation Specification Charts (OPSpecs charts), which have been done in few other studies.

Materials and Methods

The study was approved by the Bursa City Hospital Scientific Research Ethics Committee (no: 2024-21/23, date: 11/12/2024), following the principles of the Declaration of Helsinki.

For the six sigma methodology calculations, three consecutive months of NT-proBNP tests performed on the Cobas 8000 Modular Analyzer System (Cobas, Mannheim, Germany) and aPTT tests performed on the Cobas t 711 (Roche Diagnostics Mannheim, Germany) coagulation analyzer, two-level internal quality control (IQC) data per day and data obtained from the monthly external quality control (RIQAS, UK) program were used retrospectively. All stages of the study were carried out conformity the Helsinki Declaration.

Calculation of sigma values of tests

To calculate sigma values; The mean, standard deviation (SD), coefficient of variation (CV%), bias (%) and total analytical error calculations of the tests must be made. The calculations were made as follows:

CV values (%) = $(SD/Mean of IQC data) \times 100$

For CVmean (mean %CV) values, 2-level internal quality control results were used.

 $CVmean = (CV1^2 + CV2^2)\frac{1}{2}$

The bias (%) values were calculated using the formula provided below:

Bias (%) = [(IQC data mean of our laboratory-target mean of IQC data)/target mean of IQC data]×100.

The total analytical error for each parameter and control level was determined using the formula outlined below: Total analytical error = Bias+(1.65x CVmean)

Sigma values were calculated for each parameter and each control level.

Sigma = (TEa-Bias)/CV formula was used [7].

Evaluation of analytical performance of tests using OPSpecs charts

OPSpecs charts can also be used as quality planning and performance evaluation tools in clinical laboratories [8]. In the study, sigma levels of the tests were shown on OPSpecs charts.

Calculation of quality goal indices of tests

The Quality Goal Index (QGI) is a recent parameter that reflects the extent to which both accuracy and precision align with the applicable quality targets and helps identify which factor may be responsible for the issue [9]. Quality goal index calculation;

QGI = Bias/(1.5×CV) formula was used [10].

Statistical analysis

All calculations were made using Microsoft Office Excel 2021 software.

Results

In the study, two levels, three-month average %CV, %Bias values, %TEa ratios of NT-proBNP and aPTT tests are shown (Table 1). The mean, standard deviation (SD), and coefficient of variation (CV%) of the tests were calculated using internal quality control data collected over a 3-month period.

In the study, the sigma value of Level 1 for the NT-proBNP test was calculated as 5.06 and the sigma value of Level 2 was calculated as 5.65. For the aPTT test, the sigma value of Level 1 was calculated as 4.28 and the sigma value of Level 2 was cal-

Table 1. CV%, Bias%, total analytical error and TEa values of NT-proBNP and aPTT tests							
Parameter	CV (%)		CVmean	Bias (%)	Total analytical error	TEa (%)	CLIA 2025
	Level 1	Level 2					
NT-proBNP	5.74	5.13	7.70	0.98	16.19	30	
aPTT	2.66	3.20	4.15	3.61	11.91	15	

CV: Coefficient of variation; TEa: Total allowable error; NT-proBNP: N-terminal pro-B-type natriuretic peptide; aPTT: Activated partial thromboplastin time; CLIA 2025: Clinical laboratory improvement amendments 2025.

Table 2. Sigma values of NT-proBNP and aPTT tests, performance status of these values and recommended control rules

Parameter	Sigma		Per	Recommended internal control rules		
	Level 1	Level 2	Level 1	Level 2	Level 1	Level 2
NT-proBNP	5.06	5.65	Very good or excellent, individual quality control rules apply	Very good or excellent, individual quality control rules apply	1 _{2.5S}	1 _{2.5S}
аРТТ	4.28	3.56	Good, multiple quality control rules are applied	Medium requires quality control procedure. More than 1 analytical run and multiple measurements per run	1 _{2.55}	$1_{3s}/2_{2s}/R_{4s}/4_{1S}$

NT-proBNP: N-terminal pro-B-type natriuretic peptide; aPTT: Activated partial thromboplastin time.

Table 3. Recommended control rules based on sigma values

Sigma	Performance description	Recommended control rules	R (number of measurements)	N (number of controls)
<3 sigma	Bad, quality improvement plan should be implemented	$1_{3s}/2_{2s}/R_{4s}/4_{1S}$	2 or 4	R=2 for N=4 R=4 for N=2
≥3-<4 sigma	It is fit for purpose but more than one quality study should be done and multiple rules should be used	$1_{3s}/2_{2s}/R_{4s}/4_{1S}$	1 or 2	R=1 for N=4 R=2 for N=2
≥4-<6 sigma	Fit for purpose	1 _{2.55}	1	2
≥6 sigma	World class	1 _{3s}	1	2

Table 4. Performance criteria according to sigma values

Performance criteria
Unacceptable, not valid as a measurement procedure
Bad, quality improvement plan should be implemented
Medium requires Quality Control (QC) procedure. More than 1 analytical run and multiple measurements per run
Good, multiple quality control rules are applied
Very good or excellent, individual quality control rules apply
world class

culated as 3.56. According to these measured sigma values, performance statuses and recommended control rules according to these performances are shown (Table 2).

The quality control Westgard rules used depending on the sigma metric value of the analytes are shown [7] (Table 3).

The performance criteria created depending on the sigma metric value of the analytes are shown [7, 11] (Table 4).

In this study, sigma values of NT-proBNP and aPTT tests are shown with OPSpecs charts [12] (Fig. 1). The sigma of the line closest to the operation point we obtained gives our process sigma level.

The criteria for interpreting the quality goal index ratios of analytes are as follows; <0.8 QGI: Indicates that there is precision error, 0.8–1.2 QGI: Indicates that there is precision and accuracy error, and >1.2 QGI: Indicates that there is accuracy error. In this study, the quality goal indices of the

tests have been calculated and the error types corresponding to these results are shown (Table 5).

Discussion

The six sigma methodology, in addition to identifying the causes of errors, provides recommendations on control measures. The sigma method, which can be applied to every step of the total testing process, is used to evaluate laboratory performance [13]. In this research, the analytical performance of NT-proBNP and aPTT parameters was assessed using the six sigma approach, QGI, and OPSpecs charts.

No study was found in the literature review on the NT-proBNP test. However, a study was found on the BNP (brain natriuretic peptide) test. Accordingly: Üstündag et al. [14] calculated sigma values for the BNP test using the six sigma methodology. They reported that sigma values varied between 0.76 and 2.06 at dif-

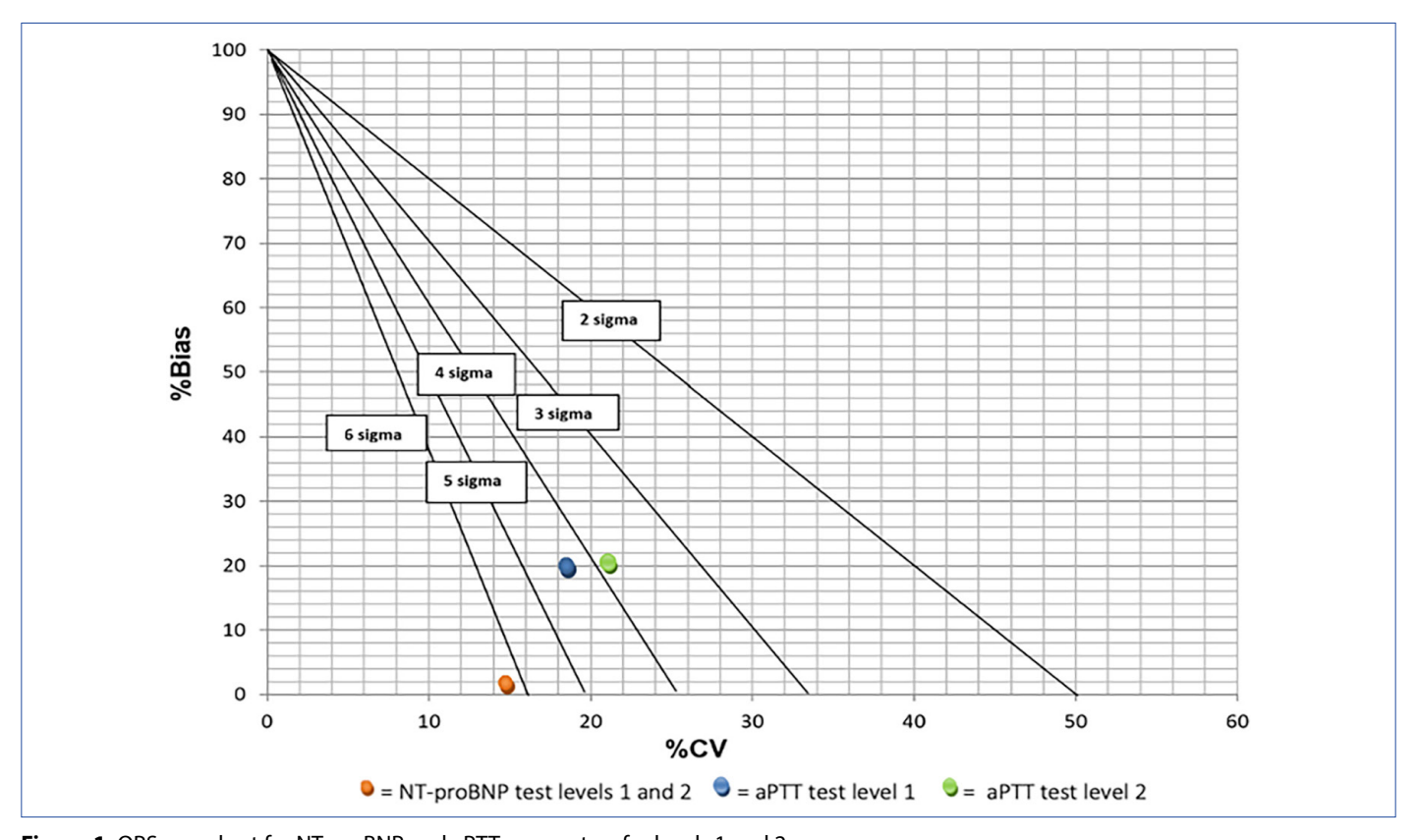


Figure 1. OPSpecs chart for NT-proBNP and aPTT parameters for levels 1 and 2.

CV: Coefficient of variation; aPTT: Activated partial thromboplastin time; OPSpecs: Operation Specification Charts; NT-proBNP: N-terminal pro-B-type natriuretic peptide.

study was uncertainty according to the calculated QGI levels. Studies evaluating aPTT performance are as follows. El-Neanaey et al. [15] calculated sigma values of aPTT tests in a study they conducted and found sigma values of the test to be >3 at normal and pathological levels, according to their findings. Hollestelle et al. [16] showed that sigma values for aPTT in two laboratories were higher than 3. Aksit et al. [17] found level 1 and level 2 sigma values for aPTT to be 5.27 and 4.31, respectively. Üğe et al. [11] calculated the normal and high level sigma values of the aPTT test as 4.51 and 4.31, respectively. They reported that they found the QGI calculation for the aPTT test as 0.41 and 0.36, respectively, at normal and high levels.

ferent quality control levels and that the problem in the BNP

Total allowable error (TEa) refers to the maximum acceptable difference between the actual concentration of an analyte

and the value reported by the laboratory, ensuring the result is considered accurate and trustworthy [18]. The TEa values for NT-proBNP and aPTT parameters were sourced from the CLIA 2025 database [19]. In this study, the total analytical error rate for the NT-proBNP test was determined to be 16.19, which is below the permissible total error rate set by CLIA (30%). Likewise, the total analytical error rate for the aPTT test was calculated as 11.91, which is also lower than the CLIA allowable total error rate of 15% (Table 1).

Since the sigma values of the NT-proBNP test in this study were calculated as 5.06 and 5.65 for levels 1 and 2, respectively, its performance was evaluated as very good or excellent and it was recommended to apply single quality control rules in the form of the 12.5S rule. Since the sigma value of the level 1 control for the aPTT test was found to be 4.28, its performance was; It was evaluated as good and the 12.5S

Parameter	Sigma		QGI		Performance	
	Level 1	Level 2	Level 1	Level 2	Level 1	Level 2
NT-proBNP	5.06	5.65	0.11	0.12	Precision error	Precision error
aPTT	4.28	3.56	0.90	0.75	Precision and accuracy error	Precision error

NT-proBNP: N-terminal pro-B-type natriuretic peptide; aPTT: Activated partial thromboplastin time; QGI: Quality goal index.

rule was recommended to be applied as multiple quality control rules. The sigma value of the level 2 control of the aPTT test was found to be 3.56, accordingly its performance was evaluated as moderate and it was recommended to perform multiple analytical runs as 13s /22s/R4s/41S and multiple measurements per run (Table 2, 3).

The sigma values calculated in this study were calculated as 5.06 for level 1 of the NT-proBNP test and 5.65 for level 2. For the aPTT test, it was calculated as 4.28 for level 1 and 3.56 for level 2. When evaluated in terms of performance criteria according to sigma values, a sigma value less than 3 is an indicator of a poor performance procedure. Good performance is shown by a sigma level higher than 3 [20] (Table 4).

OPSpecs charts describe the deviations from the allowable precision and accuracy for a method and specify the internal quality control rules required to monitor the performance of the method. The inaccuracy plot is shown on the y-axis, while the imprecision plot is represented on the x-axis. The operating point is the combination of the deviations in both precision and accuracy [21]. The sigma values are plotted on the OPSpecs charts (Fig. 1). OPSpecs charts assist in evaluating the quality of an analytical process by offering a sigma value. For each sigma metric, the appropriate Westgard rule (along with the optimal number of QC levels) can be selected to maximize error detection while minimizing false rejections. It is evident that the sigma metric can be enhanced in two ways: By decreasing bias or by reducing the CV [12].

The quality goal index (QGI), introduced by Westgard, incorporates both repeatability (precision) and accuracy elements. It is used to pinpoint the source of error in measurements with a sigma value less than 6. A QGI score of <0.8 indicates that precision needs to be improved, a QGI score of >1.2 indicates that accuracy needs to be improved, and a QGI score between 0.8 and 1.2 indicates that both precision and accuracy need to be improved [19]. For the NT-proBNP test, the QGI values were determined to be 0.11 and 0.12 for levels 1 and 2, respectively. Similarly, the QGI values for the aPTT test were calculated as 0.90 and 0.75 for levels 1 and 2, respectively. The QGI values for the NT-proBNP test point to precision errors at both levels, while the aPTT test values indicate precision and accuracy errors at level 1 and accuracy errors at level 2 (Table 5). These results highlight the need for improvements in both precision and accuracy.

Conclusion

The process performance of laboratories should be evaluated in accordance with internationally accepted scientific quality criteria. In order to ensure higher accuracy, reliability and repeatability, it is of great importance to increase quality standards in laboratory tests. In this direction, continuous improvement-oriented initiatives should be implemented to make analytical processes more effective.

Ethics Committee Approval: The study was approved by the Bursa City Hospital Scientific Research Ethics Committee (no: 2024-21/23, date: 11/12/2024).

Informed Consent: Informed consent was obtained from all participants.

Conflict of Interest Statement: The authors have no conflicts of interest to declare.

Funding: The authors declared that this study received no financial support.

Use of AI for Writing Assistance: No AI technologies utilized.

Peer-review: Externally peer-reviewed.

References

- 1. Jayasinha Y. Decreasing turnaround time and increasing patient satisfaction in a safety net hospital-based pediatrics clinic using lean six sigma methodologies. Qual Manag Health Care 2016;25(1):38–43. [CrossRef]
- 2. Llopis MA, Trujillo G, Llovet MI, Tarrés E, Ibarz M, Biosca C, et al. Quality indicators and specifications for key analytical-extranalytical processes in the clinical laboratory. Five years' experience using the Six Sigma concept. Clin Chem Lab Med 2011;49(3):463–70. [CrossRef]
- 3. Westgard S, Bayat H, Westgard JO. Mistaken assumptions drive new Six Sigma model off the road. Biochem Med (Zagreb) 2019;29(1):010903. [CrossRef]
- 4. Ilin M, Bohlen J. Six Sigma Method. Treasure Island (FL): StatPearls Publishing; 2025.
- 5. Kang F, Zhang C, Wang W, Wang Z. Sigma metric analysis for performance of creatinine with fresh frozen serum. Scand J Clin Lab Invest 2015;76(1):40–4. [CrossRef]
- 6. Nevalainen D, Berte L, Kraft C, Leigh E, Picaso L, Morgan T. Evaluating laboratory performance on quality indicators with the six sigma scale. Arch Pathol Lab Med 2000;124(4):516–9. [CrossRef]
- 7. Çevlik T, Haklar G. The performance evaluation in complete blood count: sigma values and quality goal indexes. Turk Klin Biyokim Derg 2023;21(1):13–22. [Article in Turkish]
- 8. Westgard JO. A Six Sigma Design Tool. Available at: https://westgard.com/lessons/advanced-quality-management-six-sigma/lesson68.html. Accessed Feb 2, 2025.
- 9. Öztürk KN, Günay NE, Koçer D. Six Sigma and analytical process in biochemistry laboratory of Kayseri City Hospital. Turk Klin Biyokim Derg 2024;22(2):72–82. [Article in Turkish]
- Panchal KR, Vaghasiya ND, Vasava SH, Patel DS. Achieving high standards in clinical biochemistry: Integrating Six Sigma, quality goal index (QGI), and operating specifications (OPSpecs) for targeted quality enhancement. Cureus 2024;16(11):e74693.
 [CrossRef]
- 11. Üğe M. Six sigma management and evulation in coagulation tests. DEU Tip Derg 2022;36(1):1–8. [Article in Turkish]
- 12. Westgard. Normalized Opspecs calculator. Available at: https://westgard.com/normalized-opspecs-calculator.html. Accessed Feb 2, 2025.

- 13. Korkmaz Ş. Evaluation of analytical phase performance by using six sigma method. Turk Klin Biyokim Derg 2019;17(3):126–33. [Article in Turkish]
- 14. Ustundag Y, Huysal K, Eris C, Duger S, Esmedere ES, Yavuz S. Evaluation of sigma value and quality goal index for brain natriuretic peptide test. Int J Med Biochem 2020;3(3):178–82. [CrossRef]
- 15. El-Neanaey AW, AbdEllatif NM, Abdel Haleem Abo Elwafa R. Evaluation of sigma metric approach for monitoring the performance of automated analyzers in hematology unit of Alexandria Main University Hospital. Int J Lab Hematol 2021;00:1–6.
- 16. Hollestelle MJ, Ruinemans-Koerts J, Idema RN, Meijer P, de Maat MPM. Determination of sigma score based on biological variation for haemostasis assays: Fit-for-purpose for daily practice? Clin Chem Lab Med 2019;57(8):1235–41. [CrossRef]

- 17. Aksit M, Colak A, Basok Bl, Zeytinli AM, Fidan M, Kazar M, et al. Evaluation of analytical quality of coagulation parameters by sigmametric methodology. Int J Med Biochem 2023;6(2):84–9. [CrossRef]
- 18. Panda CR, Kumari S, Mangaraj M, Nayak S. The evaluation of the quality performance of biochemical analytes in clinical biochemistry laboratory using Six Sigma matrices. Cureus 2023;15(12):e51386. [CrossRef]
- 19. Westgard. Clia & quality. Available at: https://westgard.com/clia-a-quality/quality-requirements/2024-clia-requirements. html. Accessed Feb 2, 2025.
- 20. Feldhammer M, Brown M, Colby J, Bryksin J, Milstid B, Nichols JH. A survey of sigma metrics across three academic medical centers. J Appl Lab Med 2021;6(5):1264–75. [CrossRef]
- 21. Schoenmakers CH, Naus AJ, Vermeer HJ, van Loon D, Steen G. Practical application of sigma metrics QC procedures in clinical chemistry. Clin Chem Lab Med 2011;49(11):1837–43. [CrossRef]

INTERNATIONAL JOURNAL OF

MEDICAL BIOCHEMISTRY

DOI: 10.14744/ijmb.2025.03779 Int J Med Biochem 2025;8(4):312–317

Research Article



Adult references intervals for thyroid hormones using beckman coulter from Türkiye

Department of Biochemistry, Kocaeli University Faculty of Medicine, Kocaeli, Türkiye

Abstract

Objectives: In this study, we aimed to establish reliable reference intervals (RIs) for free triiodothyronine (fT3), free thyroxine (fT4), and thyroid stimulating hormone (TSH) in our population using the Beckman Coulter UniCel Dxl 800. **Methods:** We followed the Clinical Laboratory Standards Institute (CLSI) C28-A3 guidelines to calculate RIs through both direct (DRM) and indirect methods (IDM) and compared them with the RIs provided by Beckman Coulter UniCel Dxl 800 Access® immunoassay system. High sensitive (h)TSH reagent used for TSH analyses. For DM, we excluded anti thyroid peroxidase (anti-TPO) or antithyroglobulin (anti-TG) positive samples, outliers, and samples with insufficient serum, resulting in final sample sizes of 420 for TSH, 411 for fT4, and 407 for fT3. For IDM, anti-TPO or anti-TG-positive samples, repeated samples, and outliers were excluded, resulting in final sample sizes of 2874 for TSH, 2072 for fT4, and 1163 for fT3. **Results:** Our study included 450 participants (225 females, 225 males) over the age of eighteen for DRM and utilized data from the Laboratory Information System (LIS) between March 1, 2018, and February 28, 2020, for IDM. After excluding certain samples and outliers, the final sample sizes were determined. The reference intervals (RIs) for TSH, fT4, and fT3 were 0.42-4.18 mIU/L, 0.41-4.45 mIU/L, 0.57-1.08 ng/dL, 0.63-1.14 ng/dL, 2.62-4.01 pg/mL, and 2.72-4.41 pg/mL for DRM and IDM, respectively.

Conclusion: In conclusion, the RI that we will use for thyroid hormones in our laboratory is different from that provided by the manufacturer.

Keywords: Reference intervals, thyroid diseases, thyrotropin, thyroxine, triiodothyronine

How to cite this article: Sahin I, Eraldemir FC, Oztas B, Yildirim Şik B, Kir HM. Adult references intervals for thyroid hormones using beckman coulter from Türkiye. Int J Med Biochem 2025;8(4):312–317.

The clinical manifestations of thyroid diseases, especially subclinical hypothyroidism (SCH) or subclinical hyperthyroidism, are not specific. SCH is a more commonly encountered condition [1], and the disease ranges between euthyroidism and overt hypothyroidism [2–4].

The symptoms associated with hypothyroidism typically include general and mental fatigue and cognitive difficulties, referred to as brain fog, which involve problems with concentration, motivation, memory, and reasoning, thereby impairing an individual's quality of life [3]. These patients are often prone to high levels of anxiety, anddepression [4]. All of these symptoms prompt clinicians to inquire about other diseases, and the symptoms are not specific to the thyroid.

Due to the nonspecific nature of clinical symptoms, the diagnosis of thyroid dysfunction relies on laboratory results. The most sensitive and specific indicator of systemic thyroid function is thyroid-stimulating hormone (TSH). Changes in serum TSH levels act as an 'early warning system' while attempting to maintain thyroid hormone levels within healthy ranges. Thus, SCH is diagnosed by elevated TSH levels above the reference interval (RI) accompanied by normal levels of free thyroxine (fT4) and free triiodothyronine (fT3) [2].

However, reliable RIs are crucial for interpreting TSH measurements. Reporting test results with well-defined RIs is critical for correct interpretation, especially when diagnosing subclinical thyroid dysfunction [5–7].

Address for correspondence: Fatma Ceyla Eraldemir, MD. Department of Biochemistry, Kocaeli University Faculty of Medicine, Kocaeli, Türkiye Phone: +90 262 303 72 56 E-mail: ceyla.eraldemir@kocaeli.edu.tr ORCID: 0000-0001-9410-8554

Submitted: February 17, 2025 Revised: June 02, 2025 Accepted: June 03, 2025 Available Online: October 21, 2025

OPEN ACCESS This is an open access article under the CC BY-NC license (http://creativecommons.org/licenses/by-nc/4.0/).





For instance, a recent study was conducted in a region of China considered to have sufficient iodine levels to determine the reference intervals (RIs) for thyroid hormones using the Abbott Architect analyzer. In this study, the RIs obtained from the healthy population were inconsistent with the RIs provided by the manufacturer [8].

The laboratories typically use the RIs provided in kit inserts. However, RIs can vary depending on socioeconomic status, geographic location, exposure to environmental factors, and race. For these reasons, it is recommended by the Clinical and Laboratory Standards Institute (CLSI) and The International Federation of Clinical Chemistry (IFCC) that thesuitability of the RI provided in kit inserts for the regional population be tested or that each laboratory establish its own reference ranges [7].

Especially when developing clinical guidelines for thyroidal diseases, the RIs used should be tailored to accommodate differences in the analyzer platform on which the test will be performed. Since TSH levels are used as the basis for initiating thyroid hormone therapy and adjusting treatment doses for thyroidal diseases, the use of device- and population-specific RIs ensures that the most accurate decisions are made in managing the disease [6, 9].

The aim of this study was to calculate the RIs for fT3, fT4 and TSH using both the direct method (DRM) and the indirect method (IDM) according to the Clinical Laboratory Standards Institute (CLSI) C28-A3 guidelines and to compare them with the RIs provided by the Beckman Coulter Dxl 800 [10].

Materials and Methods

This study aimed to determine the reference intervals (RIs) for fT3, fT4, and TSH in patients with DRM and IDM. All procedures performed in studies involving human participants were in accordance with the ethical standards of national research committee and with the 1964 Helsinki declaration and its later amendments or comparable ethical standards for patient with DRM. Chief medical officer's approval was received for retrospective data (patient with IDM). This study was conducted with the approval of the Kocaeli University Ethical Committee (No: KOU GOAEK 2019/196, Date: 08/05/2019).

Reference individuals for DRM were selected among volunteers who visited our hospital's Central Laboratory Blood Collection Unit and Primary Health Care Centers in our province. Volunteers who agreed to participate were administered a questionnaire with exclusion criteria.

The questionnaire included questions about family history of thyroid disease, recent history of illness, presence of chronic disease, recent blood transfusion or donation, pregnancy and breastfeeding, drug addiction, surgery in the last 3 months, fasting for 8–12 hours, and obesity, weight gain or loss, loss of appetite, smoking (>20/day), alcohol abuse, hypotension or hypertension, vitamin use, oral contraceptive use, fatigue, irritability, insomnia, exhaustion, muscle weakness, intolerance to cold or heat, dull mood, difficulty remembering, and trem-

or. Individuals who were considered unsuitable for the study according to the exclusion criteria were excluded. Informed consent was obtained from individuals eligible to participate in the study. Blood samples were collected between 08:30 and 10:00, after the participants had fasted for 8–12 hours. Samples were collected using red-capped biochemistry tubes without anticoagulants or any other active substances (Plain tube, BD vacutainet, lot number 8306831). Samples were allowed to clot for 1 hour and then centrifuged at $1800 \times g$ for 15 minutes to obtain the serum. Equal numbers of male and female reference individuals were carefully selected to ensure age and gender homogeneity. An equal number of individuals of both genders were included in each age group (1st group: 18-28 years, 2^{nd} group: 29-38 years, 3^{rd} group: 39-48 years, 4^{th} group: 49-58 years, 5^{th} group: 59 years and older).

Although participants were assumed to be healthy in terms of thyroid function, adhere to exclusion criteria, and have no history of thyroid dysfunction in themselves or their families, it is known that subclinical thyroid dysfunction may still exist. To overcome this issue and identify and exclude these individuals, thyroid antibody (TAb), anti-thyroid peroxidase (anti-TPO) and antithyroglobulin (anti-TG) antibody tests were conducted on reference individuals. Individuals with anti-TPO>9 IU/mL or anti-TG>4 IU/mL results, i.e., all individuals with positive antibody tests, were excluded from the study. Therefore, the study began with 450 individuals to ensure that results were obtained from at least 400 individuals for calculation purposes.

For IDM, data were downloaded from the Laboratory Information System (LIS) for patients who underwent simultaneous fT3, fT4, and TSH tests between March 01, 2018, and February 28, 2020. According to the CLSI's EP28-A3C guidelines, patients from oncology and intensive care units were not included in the study. Since individuals with multiple test results are likely to be healthy, the latest result in the LIS was included in the study [6].

In our study, serum fT3, fT4, TSH, anti-TPO and anti-TG data obtained from both DRM and IDM groups were analyzed with various reagents using chemiluminescence method on Beckman Coulter UniCel Dxl 800 Access® immunoassay system (Beckman- CLIA, Brea, CA, USA). Access provides standardization to the World Health Organization 3rd International Standard (IS) for human TSH analysis (IRP 81/565). In our study, the TSH 3rd IS method was used for TSH analysis and hypersensitive TSH (hTSH) test results were obtained. The Access TSH (3rd IS) assay provides high functional sensitivity and precision. Calibration of anti-TPO (Access calibrator ref: A18227) and anti-TG (Access calibrator ref: A36920) were conducted using original calibrators and controls provided by Beckman Coulter. Internal quality controls were performed three times daily with SeronormTM Immunoassays (207005 Liq L-1 12×3 mL, 207105 Liq L-2 12×3 mL, and 207205 Liq L-3 12×3 mL) for all tests (Sero AS, Hvalstad, Norway). External quality controls were performed monthly using the External

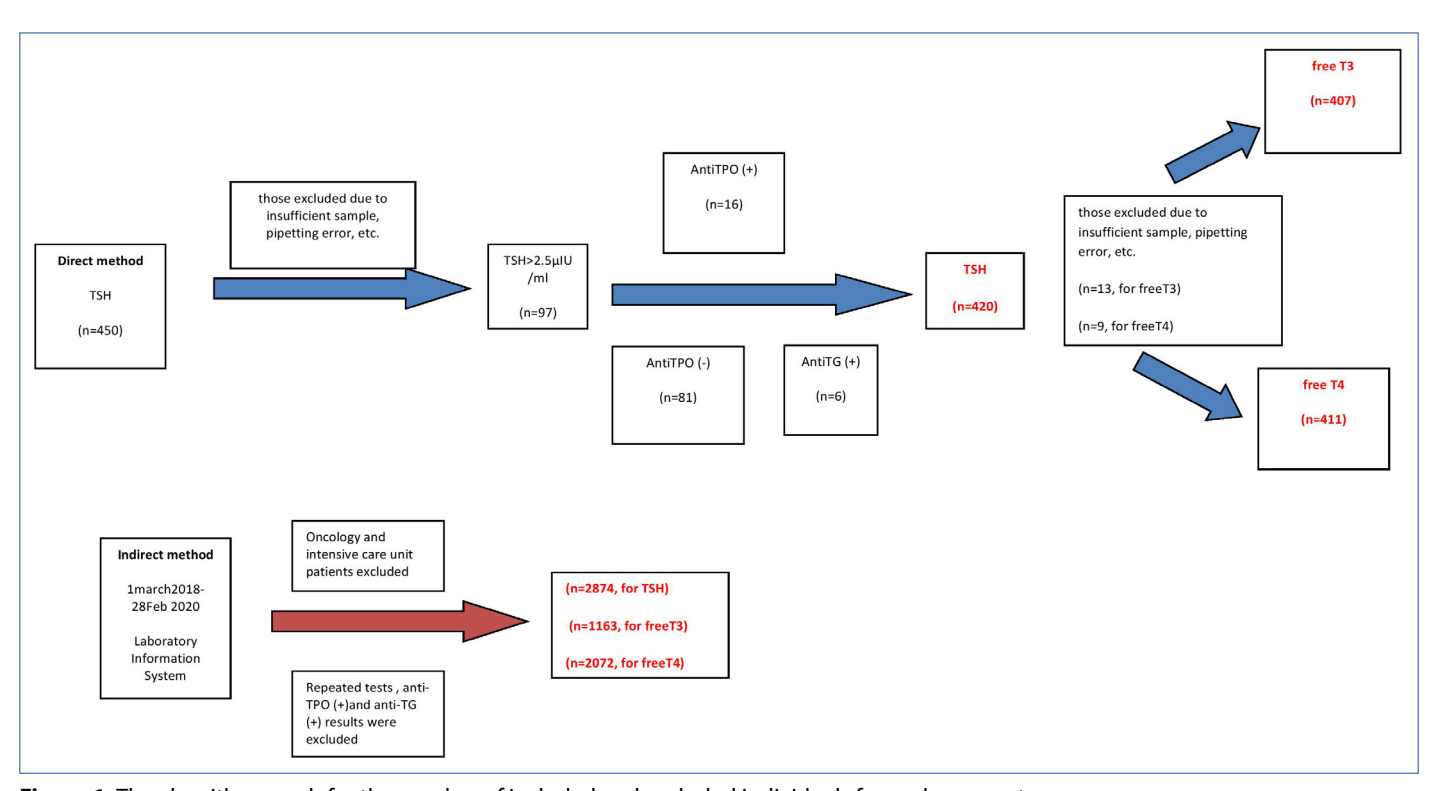


Figure 1. The algorithm graph for the number of included and excluded individuals for each parameter. TSH: Thyroid stimulating hormone; fT4: Free thyroxine; fT3: Triiodothyronine; anti-TPO: Anti-thyroid peroxidase; anti-TG: Antithyroglobulin.

Quality Assurance Services (EQAS) Immunoassay Program. No outlier values were found in TSH, fT3 and fT4 evaluations in the EQAS reports of our laboratory.

At the end of the study, the data obtained from the DRM and IDM were transferred to the IBM SPSS Statistics 24.0 program. The histograms of the data were evaluated. The normality of the data was assessed using the Kolmogorov–Smirnov test. Outliers values were identified through histogram evaluation and by applying the Dixon method. After removing outlier values, the distribution of the remaining data was re- evaluated as visual. Independent sample t tests were conducted to determine whether there were significant differences between sexes for tests showing a normal distribution, while the Mann–Whitney U test was used for tests not conforming to a normal distribution.

The reference intervals for tests showing a normal distribution were calculated using the standard deviation (SD) (lower limit: mean - $1.96 \times SD$, upper limit: mean + $1.96 \times SD$). For tests not showing a normal distribution, the reference interval boundary values were found using the formula lower value = $0.025 \times (n+1)$ and upper value = $0.975 \times (n+1)$, where 'n' represents the number of data points (noninteger values were rounded to the nearest integer).

Results

After excluding inadequate samples or pipetting errors resulting in failure to obtain results, as well as data from individuals with positive Anti-TPO or Anti-TG test results and identified

outliers, the following number of data points were obtained for hTSH: 420, fT3: 407, and fT4: 411 from the reference individual group formed by DRM. For IDM, following exclusion of samples according to CLSI's EP28-A3C guidelines and after removing outliers, the following number of data points were obtained for hTSH: 2874, sT3: 1163, and sT4: 2072 from the LIS. The algorithm graph for the number of included and excluded individuals for each parameter is shown in Figure 1.

When testing for normality, data with a significance level (p value) greater than 0.05 in the Kolmogorov–Smirnov test indicated a normal distribution, while those with a significance level less than 0.05 indicated a nonnormal distribution. Statistical evaluations of the data obtained from the DRM and IDM in our study revealed that the fT3 test results exhibited a normal distribution, while the hTSH and fT4 test results did not. For fT3, which showed a normal distribution, an independent sample t test was conducted to assess the significance of sex differences. The groups had a homogeneous distribution, and there was a statistically significant difference between DRM (for fT3 patients with DRM, p<0.001; for fT3 patients with IDM, p<0.001).

When examining the significance of sex differences for hTSH and fT4, which were not normally distributed, a statistically significant difference was found for both tests (for DRM, hTSH p<0.001, fT4 p=0.033; for IDM, hTSH p=0.024, fT4 p<0.001). Based on this information, RIs were calculated. The RIs at the 95% confidence intervals obtained without sex differences from the DRM and IDM data, as well as the RIs recommended

Table 1. The reference intervals obtained through direct and indirect methods for TSH, fT4, fT3, and the reference intervals provided by the manufacturer

		DRM		MRI		IDM	
Test	Unit	LL	UL	LL	UL	LL	UL
fT3	pg/mL	2.62	4.01	2.5	3.9	2.72	4.41
fT4	ng/dL	0.57	1.08	0.61	1.12	0.63	1.14
hTSH	mIU/L	0.42	4.18	0.34	5.60	0.41	4.45

hTSH: High sensitive thyroid stimulating hormone; fT4: Free thyroxine; fT3: Triiodothyronine; DRM: Direct method; MRI: The reference intervals provided by the manufacturer; IDM: Indirect method, LL: Lower limit; UL: Upper limit.

Table 2. The presentation of reference intervals obtained through DRM and IDM according to genders

Test Gende			DI	RM	IC	М
	Gender	Unit	2.5 th percentile	97.5 th percentile	2.5 th percentile	97.5 th percentile
fT3	Female	pg/mL	2.54	3.99	2.62	4.29
	Male	pg/mL	2.72	4.15	2.88	4.49
fT4	Female	ng/dL	0.57	1.09	0.63	1.12
	Male	ng/dL	0.58	1.08	0.65	1.15
hTSH	Female	mIU/L	0.52	4.33	0.42	4.43
	Male	mIU/L	0.41	3.95	0.40	4.57

by the manufacturer, are presented in Table 1. The RIs obtained at the 95% confidence intervals with sex differences between the DRM and IDM groups are presented in Table 2.

Discussion

In our study, we found that gender-specific RIs were narrower than the RIs determined by DRM and IDM in all cases and that the RIs we obtained differed from those provided by the manufacturer.

For hTSH in our study, we obtained narrower RIs in females with DRM (0.52–4.33 mIU/L) than in those with IDM (0.42–4.43 mIU/L). In males, we found the RI to be particularly lower at the upper limit compared to the IDM (0.41–3.95 mIU/L for DRM versus 0.40–4.57 mIU/L for IDM). The RI provided by the manufacturer for hTSH without sex differentiation was 0.34–5.60 mIU/L. In a multicenter study conducted in Italy with IDM using the same kit and autoanalyzer as our study (Access TSH 3rd IS, using UniCel DxI), the hTSH RI without sex differences was found to be different from that in our study (0.36–5.28 mIU/L) [10].

In an RI determination study conducted with DRM in a different region of Turkey in 2010 using the same device as ours (Beckman Unicel DxI, although the generation of the kit was not emphasized), a TSH RI of 0.41–4.25 mIU/L was found [11]. Despite using the same brand of kit and autoanalyzer, there are some differences in the RIs found among regions.

In fact, according to data obtained from the Global lodine Network in 2021, Turkey appears to be among the countries with sufficient iodine intake [12]. However, there may still be differences in dietary habits among regions. Therefore, determining RIs for a specific region or city's population is important. In particular, determining RIs with DRM ensures more reliable RI determination [13].

In a region of China reported to have sufficient iodine levels, the RIs for TSH determined with DRM using the Abbott Architect autoanalyzer were 0.67–4.62 mIU/L for males and 0.72–5.15 mIU/L for females. The RIs obtained for this study without sex differences were 0.70–4.93 mIU/L. The RI provided by the manufacturer for TSH without sex differences was 0.35–4.94 mIU/L. In particular, there was a significant difference in the lower limit of the RI compared to what was provided by the manufacturer in this study [8].

In a study conducted with IDM using the Siemens Advia Centaur XP analyzer, the RIs for TSH were found to be 0.71–4.92 mIU/L, which differs from the manufacturer's recommended TSH range (0.55–4.78 mIU/L) [14].

In another study conducted in the United Kingdom in 2017 with DRM, researchers determined RIs for TSH and fT4 through the four most commonly used analytical platforms in their country. As seen in this study, it is obvious that the same RI cannot be used for thyroid hormones analyzed on all analytical platforms and different RIs should be used. In this study, the Beckman Unicel DxI RI for TSH was found to be 0.57–3.60 mIU/L [15].

According to the guidelines of the European and American Thyroid Associations, the serum TSH level is the most reliable test for the diagnosis of all forms of hypothyroidism and hyperthyroidism [16–18]. However, it should be noted which analytical platform the test is performed on when creating guidelines [9, 15]. Additionally, the region where the RI will be applied is also important. Reporting patient test results with RIs not determined according to regional populations may lead to the di-

agnosis of thyroid dysfunction in many individuals who do not have thyroid dysfunction, resulting in unnecessary medication use. Similarly, it may also lead to the misclassification of many individuals with thyroid dysfunction as healthy individuals. Considering the possible harmful effects of unnecessary medication use or the vital risks of not treating patients who require treatment, it is essential for each laboratory to determine its own RI to minimize these critical issues for every individual [7]. In our study, the RIs obtained for fT4 differed between DRM and IDM for females (0.57–1.09 ng/dL with DRM and 0.63–1.12 ng/dL with IDM) and males (0.58-1.08 ng/dL with DRM and 0.65-1.15 ng/dL with IDM), especially at the lower limit. The RIs obtained with both methods were also different from the values provided by the manufacturer (0.61–1.12 ng/dL). In a study conducted in a different region of Turkey with the same autoanalyzer as ours in 2010, the RI for fT4 with DRM was also different from ours (0.61–1.06 ng/dL) [11].

Another study conducted with IDM on the Siemens Advia Centaur XP analyzer showed apparent differences in RIs for fT4, with ranges of 12.2–20.1 pmol/L for males and 11.9–18.9 pmol/L for females, compared to the manufacturer's RI of 11.5–22.7 pmol/L [14]. In a study conducted in the UK in 2017 with 261 participants from the same region, different RIs were obtained for fT4 patients with DRM using four different analyzers. One of the analyzers used in this study was the same as that used in our study, and the RI for fT4 (7.9–13.0 pmol/L) was different from that used in our study [15].

As observed, different populations and different analyzers yielded different results. However, another factor to consider may be the units used. Unit differences can also lead to problems in result interpretation.

In our study, the RIs for fT3 differed between DRM and IDM, with ranges of 2.54–3.99 pg/mL for females and 2.62–4.29 pg/mL for males with DRM and 2.72–4.15 pg/mL for females and 2.88–4.49 pg/mL for males with IDM. The manufacturer's kit insert indicated a range of 2.5–3.9 pg/mL, and particularly, the upper limits of the RIs we established for males differed from those of the manufacturer.

In an RI determination study conducted with DRM in another region of our country, the RI for fT3 was found to be 2.62–3.84 pg/mL, although separate RIs for sex were not determined [11].

With IDM on the Siemens Advia Centaur XP analyzer, the RIs for fT3 were 3.9–6.0 pmol/L, while the manufacturer recommended 3.5–6.5 pmol/L for fT3. The RIs for fT3 were notably different for males (4.3–6.2 pmol/L) and females (3.8–5.5 pmol/L) [14].

The CLSI and IFCC have recommended that RI determination studies be conducted either with DRM or, if not feasible, with IDM. Therefore, many laboratories tend to prefer IDM due to concerns such as cost, time, and labor.

In our study, the RIs determined for fT3, fT4, and TSH using DRM and IDM showed statistically significant differences between sexes. As a result, separate RI values were provided for each gender in our study, as in previous similar studies [18]. The population in our study comprised individuals aged be-

tween 18 and 88 years. In our DRM-based RI determination study, care was taken to ensure an equal number of male and female reference individuals in each age group. Despite attempts to establish age-specific RIs by setting age boundaries, a definitive age cutoff could not be reached, and statistically significant differences were not obtained; therefore, age-specific RIs could not be determined. Our results were in line with the recommendation in the CLSI's EP28-A3c guidelines, emphasizing the necessity for each laboratory to establish its own RI. When comparing the RIs determined by both DRM and IDM with those provided by the manufacturer, although the RIs for fT3 and fT4 were close, the RIs we established had a narrower range. For the TSH test, while the lower limit of our RI was similar to that set by the manufacturer, there was a significant difference between the upper limit set by the manufacturer (5.60 mIU/L) and ours (DRM: 4.18 mIU/L, IDM: 4.45 mIU/L).

Subclinical thyroid dysfunction is defined by fT4 levels within the RI and TSH levels outside the RI. Studies have demonstrated an association between SCH and increased risks of hypertension, hyperlipidemia, atherosclerosis, and coronary artery disease, while subclinical hyperthyroidism has been linked to increased risks of atrial fibrillation and coronary artery disease [19].

Due to the greater number of reference individuals obtained with the IDM than with the DRM, we may have obtained wider RIs with the IDM. Additionally, the reliability of the health status of the reference individuals determined with DRM may not be ensured with IDM; therefore, we believe that the RI determined with DRM is more sensitive.

Conclusion

In conclusion, using the RI determined by us instead of the RI provided by the manufacturer for the TSH test revealed that many individuals considered normal in terms of thyroid function may actually have SCH. Therefore, we are of the opinion that the manufacturer's RI may not be suitable for our region, and it would be more appropriate to use the RI determined by our laboratory instead of the RI provided by the manufacturer.

Ethics Committee Approval: The study was approved by the Kocaeli University Non-interventional Clinical Research Ethics Committee (no: 2019/196, date: 08/05/2019).

Informed Consent: Informed consent was obtained from all participants.

Conflict of Interest Statement: The authors have no conflicts of interest to declare.

Funding: This thesis project was supported by KOU BAP (Project number THD-2020-2140).

Use of Al for Writing Assistance: No Al technologies utilized.

Authorship Contributions: Concept – F.C.E., I.S.; Design – F.C.E., I.S., H.M.K.; Supervision – I.S., F.C.E.; Funding – F.C.E., I.S.; Materials – F.C.E., I.S.; Data collection and/or processing – I.S., B.O., B.Y.S.; Data analysis and/or interpretation – H.M.K., F.C.E., B.O.; Literature search – B.O., B.Y.S., I.S.; Writing – I.S., F.C.E., H.M.K.; Critical review – H.M.K., F.C.E.

Peer-review: Externally peer-reviewed.

References

- Vanderpump MP. Epidemiology of thyroid disorders. In Luster M, Duntas LH, Wartofsky L, Eds. The Thyroid and Its Diseases: A Comprehensive Guide for the Clinician. Cham: Springer International Publishing; 2019. p. 75–85. [CrossRef]
- Urgatz B, Razvi S. Subclinical hypothyroidism, outcomes and management guidelines: A narrative review and update of recent literature. Curr Med Res Opin. 2023;39(3):351–65. [Cross-Ref]
- 3. Samuels MH, Bernstein LJ. Brain fog in hypothyroidism: What is it, how is it measured, and what can be done about it. Thyroid 2022;32(7):752–63. [CrossRef]
- Stern M, Finch A, Haskard-Zolnierek KB, Howard K, Deason RG. Cognitive decline in midlife: Changes in memory and cognition related to hypothyroidism. J Health Psychol 2023;28(4):388–401. [CrossRef]
- Okosieme O, Gilbert J, Abraham P, Boelaert K, Dayan C, Gurnell M, et al. Management of primary hypothyroidism: Statement by the British Thyroid Association Executive Committee. Clin Endocrinol 2016;84(6):799–808. [CrossRef]
- Ozarda Y. Establishing and using reference intervals. Turk J Biochem 2020;45(1):1–10. [CrossRef]
- Clinical and Laboratory Standards Institute. Measurement Procedure Comparison and Bias Estimation Using Patient Samples. Approved Guideline-Third Edition. CLSI document EP09-A3. Wayne (PA): CLSI; 2013.
- 8. Lu Y, Zhang WX, Li DH, Wei LH, Zhang YJ, Shi FN, et al. Thyroid hormone reference intervals among healthy individuals in Lanzhou, China. Endocrinol Metab. 2023;38(3):347. [CrossRef]
- Yoo WS. Clinical implications of different TSH reference intervals between TSH kits for the management of subclinical hypothyroidism. Endocrinol Metab 2024;39(1):188–9. [CrossRef]
- Clerico A, Trenti T, Aloe R, Dittadi R, Rizzardi S, Migliardi M, et al. A multicenter study for the evaluation of the reference interval for TSH in Italy (ELAS TSH Italian Study). Clin Chem Lab Med 2018;57:259–67. [CrossRef]

- 11. Çavuşoğlu AÇ, Bilgili S, Erkızan Ö, Arıcan H, Karaca B. Thyroid hormone reference intervals and the prevalence of thyroid antibodies. Turk J Med Sci 2014;40:665–72.
- 12. IGN IG. Global scorecard of iodine nutrition in 2021 in the general population based on school-age children (SAC). Available at: https://ign.org/app/uploads/2023/04/IGN_Global_Scorecard_2021_7_May_2021.pdf. Accessed Sep 15, 2025.
- Clinical and Laboratory Standards Institute. Defining, establishing, and verifying reference intervals in the clinical laboratory. Approved Guideline-Third Edition. CLSI document C28-A3c. Wayne (PA): CLSI; 2010.
- 14. Zou Y, Wang D, Cheng X, Ma C, Lin S, Hu Y, et al. Reference intervals for thyroid-associated hormones and the prevalence of thyroid diseases in the Chinese population. Ann Lab Med 2021;41(1):77–85. [CrossRef]
- 15. Barth JH, Luvai A, Jassam N, Mbagaya W, Kilpatrick ES, Narayanan D, et al. Comparison of method-related reference intervals for thyroid hormones: studies from a prospective reference population and a literature review. Ann Clin Biochem 2018;55:107–12. [CrossRef]
- Durante C, Hegedüs L, Czarniecka A, Paschke R, Russ G, Schmitt F, et al. 2023 European Thyroid Association clinical practice guidelines for thyroid nodule management. Eur Thyroid J 2023;12(5):e230067. [CrossRef]
- 17. Jonklaas J, Bianco AC, Cappola AR, Celi FS, Fliers E, Heuer H, et al. Evidence-based use of levothyroxine/liothyronine combinations in treating hypothyroidism: A consensus document. Eur Thyroid J 2021;10(1):10–38. [CrossRef]
- 18. Baskin HJ, Cobin RH, Duick DS, Gharib H, Guttler RB, Kaplan MM, et al. American Association of Clinical Endocrinologists medical guidelines for clinical practice for the evaluation and treatment of hyperthyroidism and hypothyroidism. Endocr Pract 2002;8(6):457–69. [CrossRef]
- 19. Rodondi N, Bauer DC, Gussekloo J. Risk of coronary heart disease and mortality for adults with subclinical hypothyroidism. JAMA 2010;304(22):2481–2. [CrossRef]

INTERNATIONAL JOURNAL OF

MEDICAL BIOCHEMISTRY

DOI: 10.14744/ijmb.2025.24186 Int J Med Biochem 2025;8(4):318–325

Research Article



Evaluation of the analytical performance of the access vitamin B12 II assay with the new calibrator

D Ozlem Cakir Madenci, Alper Kutukcu

Department of Biochemistry Laboratory, Dr. Lutfi Kirdar Kartal City Hospital, Istanbul, Türkiye

Abstract

Objectives: We aimed to compare the analytical performance of the Access Vitamin B12 assay with the new B12 II calibrator to the current Access and Abbott assays and determined the method-specific reference interval.

Methods: The new B12 II was assessed for imprecision, accuracy, analytical sensitivity, linearity, and carryover. Bland-Altman, Passing Bablok, and concordance correlation coefficient (CCC) analyses were performed on 650 samples. Vitamin B12 tests were performed using the UniCel DxI 800 (Beckman Coulter, USA), and Alinity i System (Abbott Laboratories, Abbott Park, IL, USA) analyzers.

Results: The Access new B12 II assay demonstrated acceptable analytical performance; however, its reference range (138-787 pg/mL) was lower than the manufacturer's recommendation. The Access Vitamin B12 assay showed significant negative differences of 45.8% and 37.0% relative to the Abbott and new B12 II assays, respectively, while the new B12 II assay showed a smaller difference of 9.4% against Abbott. Significant proportional and constant errors were observed between Access and new B12 II (slope: 0.780, intercept: -21.95) and Access and Abbott (slope: 0.707, intercept: -18.95). Abbott and new B12 II demonstrated lower proportional and constant errors (slope: 0.902, intercept: 6.388). Concordance analysis indicated poor agreement of the Access assay with both Abbott and new B12 II (CCC: 0.806, 0.879), whereas Abbott and new B12 II demonstrated substantial agreement (CCC: 0.958).

Conclusion: The new B12 II assay demonstrated appropriate analytical performance and improved consistency with the Abbott assay. The reference interval we established differed from the manufacturer's suggested range, highlighting the importance of determining population-based reference intervals.

Keywords: Calibration, reference standards, vitamin B12, vitamin B12 deficiency

How to cite this article: Madenci OC, Kutukcu A. Evaluation of the analytical performance of the access vitamin B12 II assay with the new calibrator. Int J Med Biochem 2025;8(4):318–325.

Vitamin B12, or cobalamin, is a water-soluble vitamin that is critical for key physiological processes, including DNA synthesis, fatty acid metabolism, and myelin production. It is predominantly obtained from animal-derived sources such as red meat, dairy products, and eggs [1]. Absorption of vitamin B12 occurs in the terminal ileum and requires intrinsic factor, a glycoprotein secreted by parietal cells in the stomach. Disruptions in this absorption mechanism—resulting from dietary insufficiency, malabsorption syndromes, or intrinsic factor de-

ficiency—can lead to significant clinical consequences, including hematologic abnormalities and neurological dysfunction. Although excess vitamin B12 is stored in the liver, prolonged disruption in B12 absorption—due to factors such as dietary insufficiency, malabsorption, or a deficiency of intrinsic factor—can deplete liver stores, resulting in a deficiency [1–3].

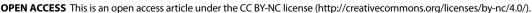
Vitamin B12 deficiency is a significant global health problem and vitamin B12 levels naturally decline with age [4, 5]. Subclinical B12 deficiency is notably more prevalent among the

The abstract was presented as poster in 26th IFCC-EFLM EUROMEDLAB Congress of Clinical Chemistry and Laboratory Medicine in Brussel, May 18–22, 2025.

Address for correspondence: Ozlem Cakir Madenci, MD. Department of Biochemistry Laboratory, Dr. Lutfi Kirdar Kartal City Hospital, Istanbul, Türkiye

Phone: +90 554 936 96 60 E-mail: ocakirmadenci@gmail.com ORCID: 0000-0001-9343-0234

Submitted: June 19, 2025 Revised: August 14, 2025 Accepted: August 21, 2025 Available Online: October 21, 2025







elderly, with reported prevalence rates ranging from 6% to 40% [6–9]. However, younger populations are also at an elevated risk of vitamin B12 deficiency and high-risk groups include vegetarians [10], individuals with gastrointestinal disorders [11], those suffering from depression [12], heavy drinkers [13], and individuals with renal dysfunction [11].

Despite its high prevalence, diagnosing vitamin B12 deficiency remains complex due to inconsistencies in assay methods and the absence of universally accepted reference standards [11]. At present, no definitive reference method exists for investigating suspected vitamin B12 deficiency. Diagnosis is primarily based on measuring serum or plasma vitamin B12 concentrations [14–16]. According to the World Health Organization (WHO), a serum level greater than 221 pmol/L (300 pg/mL) indicates adequate vitamin B12 status, while levels between 148–221 pmol/L (200–300 pg/mL) are considered low. A serum level below 200 pg/mL is classified as vitamin B12 deficiency [17, 18]. However, the lack of standardized reference materials and methods has prevented the establishment of uniformity in current measurement techniques. This results in variability between different vitamin B12 assays [19].

In December 2024, Beckman Coulter launched the Access Vitamin B12 II Calibrators for use with the Access Vitamin B12 assay (new B12 II) on Access Immunoassay Systems. These calibrators offer enhanced precision and accuracy in vitamin B12 detection, with a total imprecision of ≤12.0% across the measuring range. Standardized to the WHO International Standards (IS 03/178), the calibrators ensure greater confidence in patient test results. The analyte in the Access Vitamin new B12 II Calibrators (REF D06116) is traceable to the manufacturer's working calibrators, in accordance with the traceability guidelines outlined in EN ISO 17511. The Access Vitamin B12 assay demonstrated an average recovery rate of 111% compared to the WHO IS 03/178 assigned value of 480 pg/mL [20]. While the initial claims highlight improved diagnostic reliability, independent validation is necessary to confirm these advancements and assess the analytical performance against existing methods.

In this study, we aimed to evaluate the analytical performance of the Access Vitamin B12 assay using the newly introduced new B12 II calibrators, focusing on imprecision, accuracy, LoB, LoD, LoQ, linearity, and carryover. Additionally, we compared the new B12 II to the current Access Vitamin B12 assay on the DXI 800 system and the Abbott Vitamin B12 assay on the Alinity i System.

Materials and Methods

Study design and subjects

To conduct the analytical performance studies for the new B12 II assay, remnant serum samples from patients who visited our hospital for various reasons and had blood drawn and sent to the laboratory were utilized. For the method comparison study, samples were selected from patients aged 18 to 99 years who had Vitamin B12 tests requested from the outpa-

tient clinics of our hospital. A total of 650 patient samples (350 females and 300 males) with sufficient volume for additional Vitamin B12 testing were included in the study. The initial Vitamin B12 concentrations, as determined by the current Access Vitamin B12 assay, ranged from 63 to 1,491 pg/mL. These selected samples were reanalyzed on the same day using the new B12 II assay on the DXI 800 analyzer and the Abbott Vitamin B12 assay on the Alinity i System. The samples were carefully chosen to ensure their concentrations were within the analytical ranges of the alternative systems and represented a broad distribution of Vitamin B12 levels.

Blood Sampling

Blood samples were collected in the morning, between 8:00 and 10:00 AM, following an overnight fast. Venous blood was drawn from the antecubital vein into 5 mL Greiner Bio-One GmbH Samplix®. Blood samples were centrifuged at 2000 x g for 10 minutes. All studies were done according to the Clinical & Laboratory Standards Institute (CLSI) Evaluation Protocols (EP) specific to each parameter. Measurements were performed in the biochemistry laboratory of Dr. Lütfi Kırdar Kartal City Hospital between December 2024 and January 2025. This study was approved by the Ethical Committee of our institution (No: 2025/010.99/12/34, Date: 24/01/2025). This study was conducted in accordance with the principles of the Declaration of Helsinki.

Method

Serum Vitamin B12 analysis was performed using both the Dxl 800 Unicel and the Alinity i Systems. Both methods are based on competitive protein binding, utilizing chemiluminescence immunoassay (CLIA) as the detection method. In the Dxl 800 Unicel (Beckman Coulter, USA), chemiluminescence is generated from enzymatic reactions, while the Alinity i System (Abbott Laboratories, Abbott Park, IL, USA) employs chemiluminescence microparticle immunoassay (CMIA).

Assay performance studies

Imprecision

Imprecision (both within-run and within-laboratory) was analyzed using control samples with four different vitamin B12 concentrations: 185.2, 374.7, 608.7, and 804.8 pg/mL. Two commercial controls were tested at these concentration levels to calculate imprecision, expressed as CV%. Precision evaluation followed the Clinical and Laboratory Standards Institute (CLSI) EP15-Ed3-IG1 guidelines, involving measurements over five consecutive days, with five replicates performed each day [21]. The predefined acceptable imprecision limit was set at CV ≤12%.

Accuracy

Two samples from the Randox International Quality Assessment Scheme (RIQAS) monthly immunoassay external quality control program were used to assess accuracy. These samples, taken from Cycle 22, were tested using new B12 II in a single

	Access Vitamin B12 assay	New access Vitamin B12 II assay	Abbott Vitamin B12 assay
Test name	VitB12	B12II	Alinity i system B12
Imprecion (total CV %)	CV<12% across measuring range	CV<12% across measuring range	CV<7.9 % across measuring range
Analytical sensitivity	LoB (not given)	LoB<78	LoB<83
(pg/mL)	LoD<50	LoD<105	LoD<109
	LoQ<50	LoQ<105	LoQ<148
Linearity (pg/mL)	50–1.500	105–2.100	148–2000
Reference intervals (pg/mL)	180–914	222-1.439	187–883

analytical run. The percentage deviation from the reported target mean was calculated using the formula: ((Measured value – target mean) / target mean) × 100. The acceptable accuracy limit set by RIQAS was 16.9%.

Analytic sensitivity

Studies were conducted in accordance with CLSI EP17 guidelines [22]. The limit of blank (LoB) was determined by analyzing 20 replicates of the manufacturer's zero calibrator and calculated using the formula:

LoB = Mean (blank) + 1.645 SD (blank).

The limit of detection (LoD) was established using the lowest non-zero calibrator (153 pg/mL), which was diluted by half and analyzed in 20 replicates. The LoD was calculated with the formula:

LoD = LoB + 1.645 (SD low-concentration sample).

The limit of quantification (LoQ) study was performed by analyzing samples with concentrations ranging from 76.5 to 174.5 pg/mL over three consecutive days, with three replicates per concentration. To assess precision and accuracy, five samples near the manufacturer's stated LoQ of 102.5 pg/mL were evaluated to calculate coefficients of variation (CVs) and total errors. Total error was determined using the formula: TE = %BIAS + (1.96 \times %CV). The LoQ was established as the concentration at which the calculated total error was below the minimum acceptable total error (23%) defined by the European Federation of Clinical Chemistry and Laboratory Medicine (EFLM).

Linearity: Linearity testing was conducted according to CLSI EP6 guidelines [23]. A patient serum with a high Vitamin B12 level was diluted to generate seven concentrations ranging from 80 to 2400 pg/mL. Each concentration was tested three times within the same run. The recovery range was acceptable if it fell within $\pm 15\%$ of the target value.

Carryover

Carryover assessment involved testing three replicates of a high-concentration sample (labeled as a1, a2, and a3) followed by three replicates of a low-concentration sample (labeled as b1, b2, and b3). The carryover effect was determined using the formula: (b1-b3)/(a3-b3). A carryover value below 2% was considered insignificant [24].

Method comparison

Vitamin B2 concentrations from 650 patient samples were first measured using the Access Vitamin B12 assay. Subsequently, the same samples were reanalyzed with both the new B12 II and Abbott assays. The Abbott system was chosen for comparison purposes as it was the routine system in our laboratory at the time of the study.

All measurements for method comparison were performed simultaneously on the same serum samples by the same experienced operator, within the analytical range of the systems, processed in duplicate as a single batch with consistent freeze/thaw cycles, and in accordance with CLSI EP09-A3 guidelines [25].

Statistical analysis

The distribution of data was evaluated using the Kolmogorov–Smirnov test, and the results are presented as the median and interquartile range. Imprecision, LoB, LoD, LoQ, and linearity were calculated using EP Evaluator Release 9 software (David G. Rhoads Association, Kennett Square, PA). To assess method comparison, Bland–Altman plots, Passing–Bablok regression, and the concordance correlation coefficient (CCC) were used, with analysis performed using MedCalc Statistical Software (version 12, MedCalc Software, Mariakerke, Belgium). A systematic error was considered significant if the 95% confidence interval excluded 1.0 for the slope (indicating proportional error) or 0 for the y-intercept (indicating constant error).

Results

The analytical performance characteristics of Vitamin B12 assays, as claimed by the manufacturers, are summarized in Table 1. The median values (2.5–97.5 percentiles; pg/mL) for the 650 samples analyzed were as follows: 140 (78.7–714.7) for the Access Vitamin B12, 206 (134.0–949.6) for the new B12 II, and 237 (152–1020) for the Abbott Vitamin B12 assay. The reference interval was calculated from 400 patients whose Vitamin B12 levels were within the Abbott assay's normal range (187–883 pg/mL) and who had normal hemoglobin, hematocrit, and folic acid levels, with no clinical or laboratory evidence of Vitamin B12 deficiency. Following the CLSI EP28-A3c guideline, the non-parametric method was used, and the 2.5th and 97.5th per-

Table 2. Analytical performance characteristics of access Vitamin B12 assay with the new B12 II calibrator

Performance criteria	Study result
Within-run CV (%)	
Level 1 (185.2 pg/mL)	5.41
Level 2 (375.7 pg/mL)	4.07
Level 3 (608.7 pg/mL)	2.80
Level 4 (804.8 pg/mL)	4.01
Within-laboratory CV (%)	
Level 1 (185.2 pg/mL)	7.18
Level 2 (375.7 pg/mL)	6.40
Level 3 (608.7 pg/mL)	7.75
Level 4 (804.8 pg/mL)	5.09
Accuracy (deviation %)	
Riqas 1 (637 pg/mL)	12.5
Riqas 2 (951 pg/mL)	3.3
LoB (pg/mL)	15.84
LoD (pg/mL)	80.82
LoQ (pg/mL)	102
Linearity (pg/mL)	102-2060
Carry-over (%)	0.74

 $\hbox{CV: Coefficient of variation; LoB: The limit of blank; LoD: The limit of detection; LoQ: The limit of quantification. } \\$

centiles of the distribution were taken as the lower and upper limits, respectively. Using the Beckman new B12 II assay, the calculated interval was 138–787 pg/mL, which is lower than the manufacturer's proposed range of 222–1,439 pg/mL.

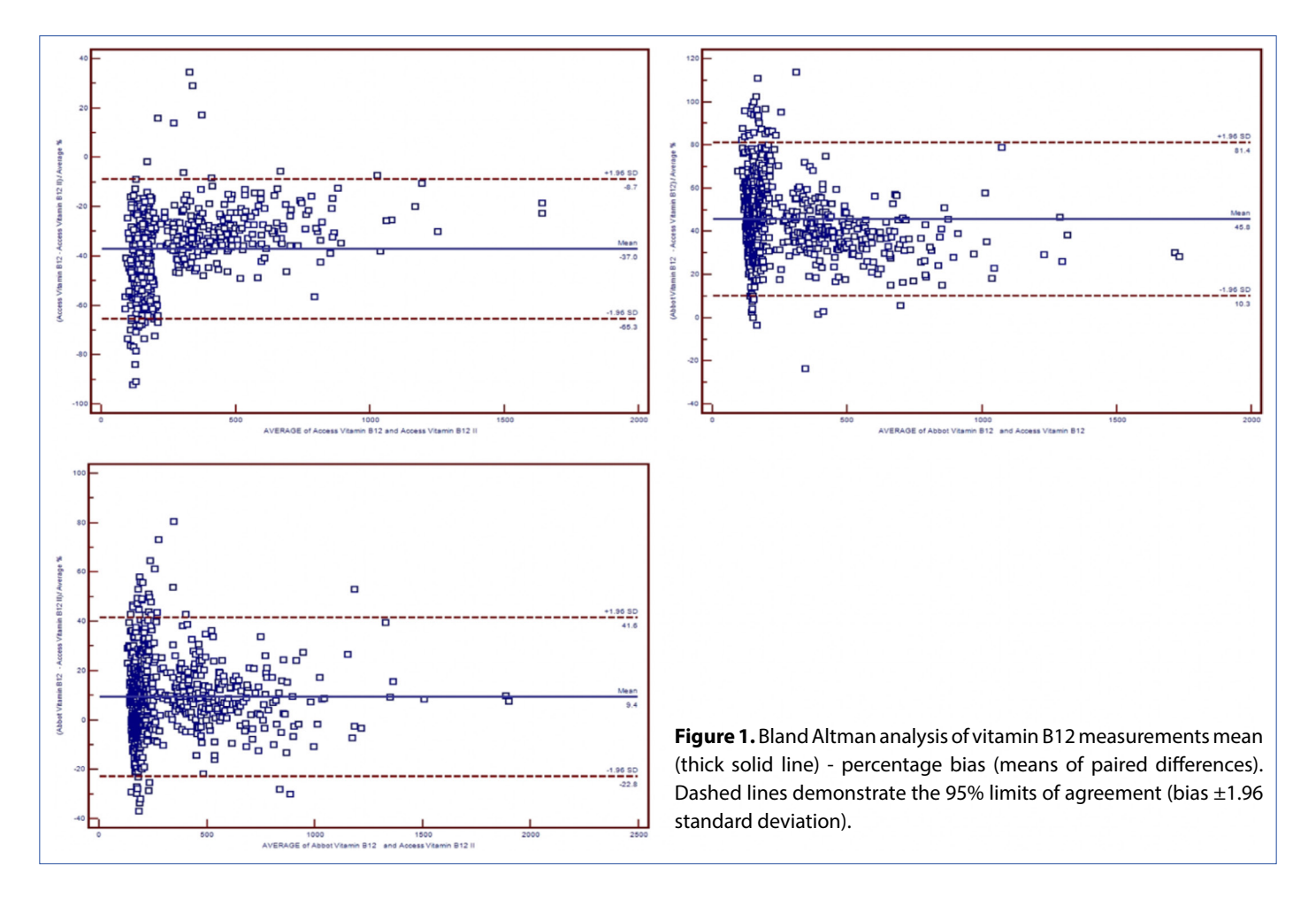
The new B12 II assay demonstrated acceptable performance in terms of imprecision, LoB, LoD, LoQ, linearity, and carry-over. The analytical performance characteristics of the new B12 II assay are presented in Table 2. Bland-Altman analysis revealed notable differences between the three systems. The Access Vitamin B12 assay showed significant negative differences of 45.8 % and 37.0 % relative to the new B12 II and Abbott assays, respectively while the new B12 II showed a smaller negative difference of 9.4% against the Abbott. Notably, only the difference between the new B12 II and Abbott assays satisfied the EFLM allowable bias threshold of 14.1%. The comparison

results between the methods are shown in the Bland-Altman plot (Fig. 1). Significant proportional and constant errors were observed between the Access Vitamin B12 and new B12 II assays, with a slope of 0.780 (0.766-0.794) and an intercept of -21.95 (-23.58 to -18.6). Similarly, the Access Vitamin B12 and Abbott assays demonstrated significant proportional and constant errors, with a slope of 0.707 (0.691-0.723) and an intercept of -18.95 (-23.58 to -14.51). The Abbott and new B12 Il assays exhibited smaller proportional and constant errors, with a slope of 0.902 (0.883-0.920) and an intercept of 6.388 (0.660–11.613). The Passing–Bablok regression analyses are presented in Figure 2. The Access Vitamin B12 and Abbott, as well as the Access Vitamin B12 and new B12 II assays, exhibited poor agreement, with CCC values of 0.806 (0.787-0.824) and 0.879 (0.866-0.891), respectively. However Abbott and new B12 II showed substantial agreement, with a CCC value of 0.958 (0.952–0.964). Method comparison data are shown in Table 3.

Discussion

This study is the first method evaluation of the newly introduced Access new B12 II calibrator, launched in December 2024. The new B12 II assay demonstrated strong analytical performance with the new calibrator, providing improved traceability, consistency, and reliability when compared to the Abbott assay. Bias analysis revealed that the current Access Vitamin B12 assay showed a significant negative difference of 37% compared to the Abbott assay. However, with the introduction of the new B12 II calibrator, this difference was significantly reduced to -9.4%, indicating improved alignment between the two assays. Additionally, the observed negative difference of 48% between the current Access Vitamin B12 assay and the new B12 II assay indicates that the new calibrator produces higher results than the current assay. While ongoing standardization efforts continue, the reference range determined by the new B12 II assay (138–787 pg/mL) still differs from that of the Abbott assay (187–883 pg/mL). This highlights the need for method-specific reference ranges, rather than relying on a universal cut-off value, such as 200 pg/mL, to define deficiency criteria. Establishing the appropriate reference range for each method is crucial for accurate clinical diagnosis.

Method	Passing-bablok regression analysis		Concordance correlation analysis			Bland-altman analysis
	Slope (CI)	Intercept (CI)	CCC (CI)	Р	C _b	Bias (%)
Access Vitamin B12 new B12 II	0.780	-21.95	0.879	0.984	0.893	-37.0
	(0.766-0.794)	(-25.3618.62)	(0.866-0.891)			
Access Vitamin B12 abbott	0.707	-18.95	0.806	0.973	0.828	-45.8
	(0.691-0.723)	(-23.5814.51)	(0.787-0.824)			
New B12 II abbott	0.902	6.388	0.958	0.970	0.987	-9.4
	(0.883-0.920)	(0.660-11.613)	(0.952-0.964)			



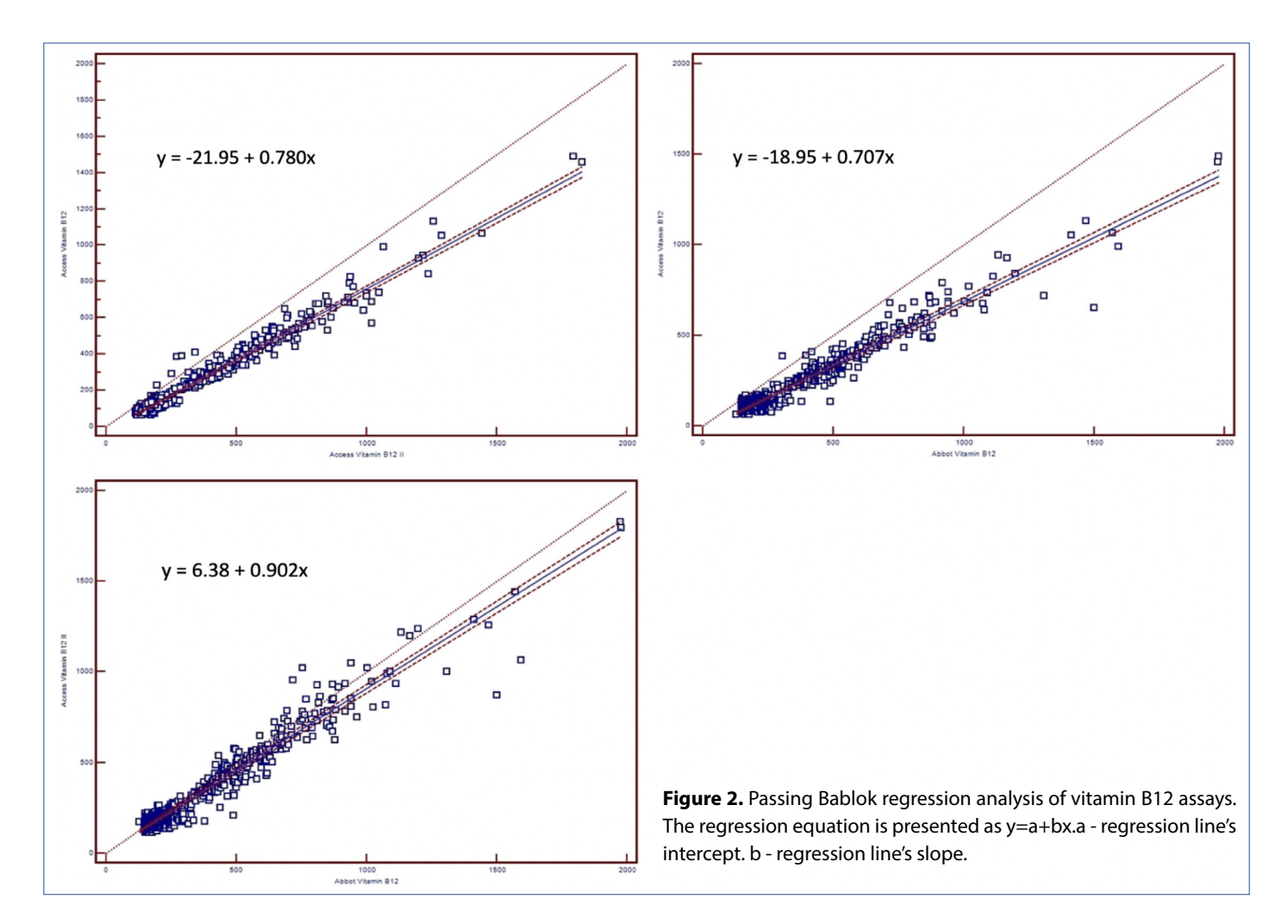
Vitamin B12, the largest of all vitamins, exists in various forms and is present in very low concentrations in serum. It binds strongly to serum proteins [24]. The unique biochemical characteristics of vitamin B12, coupled with the complexities involved in producing pure reference materials and the absence of a universally standardized reference method, present significant challenges to achieving consistent and reliable standardization of vitamin B12 assays. The serum vitamin B12 assay methods have not yet been fully standardized. To address this issue, the World Health Organization (WHO) Expert Committee on Biological Standardization introduced the material 03/178 as an International Standard (IS) for serum vitamin B12 assays. This material was assessed in 24 laboratories across seven countries to evaluate its applicability as a reference standard for both vitamin B12 and folate assays. The findings revealed that employing this standard material reduced variability between laboratories. However, the standard material, produced through the lyophilization of pooled human serum, may lead to challenges concerning its commutability [26].

The National Institute of Standards and Technology (NIST) currently does not provide a certified reference material (SRM) for vitamin B12 or methylmalonic acid (MMA). However, NIST is in the process of developing SRM 3951 for serum vitamin B12, which includes target pools with concentrations of 74 pmol/L (100 pg/mL), 148 pmol/L (200 pg/mL), and 332 pmol/L (450

pg/mL). Among these, the 332 pmol/L pool represents "normal" serum, while the two lower pools consist of a mixture of normal serum and serum that has been stripped of its naturally occurring vitamin B12 [27, 28].

Several comparative studies have been conducted to evaluate the performance of different vitamin B12 assays. In the study by İspir et al. [14], four vitamin B12 assays—Dxl 800 Unicel, ADVIA Centaur XP, Roche Cobas E601, and Architect i2000sr—were compared. The results showed strong correlations between the assays, with the weakest correlation between Dxl 800 Unicel and ADVIA Centaur. Dxl 800 Unicel produced lower results compared to the others. MMA and homocysteine showed similar correlations with vitamin B12 levels across all methods. The study concluded that while the assays performed well, vitamin B12 assay standardization is still incomplete and requires further efforts.

In the study conducted by Ihara et al. [15], vitamin B12 and folate levels were measured using three different methods: Access, Advia Centaur, and Elecsys. The results revealed significant correlations between the assays; however, serum vitamin B12 levels measured by Elecsys were consistently higher compared to those obtained from the other two methods. Similar to our findings, their study concluded that, in the absence of reliable reference materials and standardized methods, reference values for vitamin B12 and folate remain method-depen-



dent. For instance, certain assays have established lower reference values of 200 pg/mL for vitamin B12, but these values are not applicable to all automated immunoassay methods. Therefore, it is crucial to determine reference values that are specific to each method. This approach ensures accurate diagnosis and consistency across different testing platforms, leading to more dependable clinical results.

In another study, reference intervals for plasma vitamin B12 concentration were established using three different immunoassays in the North Denmark Region. The findings showed that results from different methods were not interchangeable, with significant variation in the frequency of vitamin B12 levels below the cut-off when similar thresholds were applied [29].

Our study demonstrated a stronger correlation and reduced difference between the newly developed new B12 II calibrator and the Abbott system compared to the current Access Vitamin B12 assay. However, there were still concerns regarding clinical interpretation, suggesting that full standardization may not have been achieved. Among the 650 patients, the current Access Vitamin B12 assay identified 405 (62.3%) patients as deficient (below 200 pg/mL), while the Abbott system detected 235 (36.1%) patients below this threshold. With the new B12 II calibrator, the assay classified 288 (44.3%)

patients as deficient under the same cutoff, indicating higher vitamin B12 levels than the previous Access Vitamin B12 assay. These results show that, while correlation between the new B12 II and Abbott assays has improved, differences between the methods remain, emphasizing the continued need for method-specific reference ranges.

The study did not assess potential interference factors, such as hemolysis, lipemia, or elevated bilirubin levels, which may represent a limitation. Additionally, the calculated reference range for the new B12 II assay, based on Vitamin B12 levels according to the Abbott system's normal range, was lower than the manufacturer's proposed values. This indicates that the current reference range for the new B12 II assay does not align with the manufacturer's suggested values for our population, emphasizing the need for population-specific reference range studies in larger and more diverse groups.

Conclusion

The new B12 II assay demonstrated appropriate analytical performance and improved consistency with the Abbott assay. The reference interval we established differed from the manufacturer's suggested range, highlighting the importance of determining population-based reference intervals.

Ethics Committee Approval: The study was approved by the Dr. Lütfi Kırdar Kartal City Hospital Scientific Research Ethics Committee (no: 2025/010.99/12/34, date: 24/01/2025).

Informed Consent: Informed consent was obtained from all participants.

Conflict of Interest Statement: The authors have no conflicts of interest to declare.

Funding: The authors declared that this study received no financial support.

Use of Al for Writing Assistance: No Al technologies utilized.

Authorship Contributions: Concept – O.C.M., A.K.; Design – O.C.M., A.K.; Supervision – O.C.M.; Funding – O.C.M., A.K.; Materials – O.C.M.; Data collection and/or processing – O.C.M., A.K.; Data analysis and/or interpretation – O.C.M.; Literature search – O.C.M., A.K.; Writing – O.C.M.; Critical review – O.C.M., A.K.

Peer-review: Externally peer-reviewed.

References

- Layden AJ, Täse K, Finkelstein JL. Neglected tropical diseases and vitamin B12: A review of the current evidence. Trans R Soc Trop Med Hyg 2018;112:423–35. [CrossRef]
- Fritz J, Walia C, Elkadri A, Pipkorn R, Dunn RK, Sieracki R, et al. A systematic review of micronutrient deficiencies in pediatric inflammatory bowel disease. Inflamm Bowel Dis 2019;25:445– 59. [CrossRef]
- 3. Miller JW. Proton pump inhibitors, H2-receptor antagonists, metformin, and vitamin B-12 deficiency: Clinical implications. Adv Nutr 2018;9:5115–185. [CrossRef]
- 4. Gonzalez-Gross M, Sola R, Albers U, Barrios L, Alder M, Castillo MJ, et al. B-vitamins and homocysteine in Spanish institutionalized elderly. Int J Vitam Nutr Res 2007;77:22–33. [CrossRef]
- 5. Hannibal L, Lysne V, Bjørke-Monsen AL, Behringer S, Grünert SC, Spiekerkoetter U, et al. Corrigendum: Biomarkers and algorithms for the diagnosis of vitamin B12 deficiency. Front Mol Biosci 2017;4:53. [CrossRef]
- 6. Wolters M, Hermann S, Hahn A. B vitamin status and concentrations of homocysteine and methylmalonic acid in elderly German women. Am J Clin Nutr 2003;78:765–72. [CrossRef]
- 7. Loikas S, Koskinen P, Irjala K, Lopponen M, Isoaho R, Kivela SL, et al. Vitamin B12 deficiency in the aged: A population-based study. Age Ageing 2007;36:177–83. [CrossRef]
- 8. Favrat B, Vaucher P, Herzig L, Burnand B, Ali G, Boulat O, et al. Oral vitamin B12 for patients suspected of subtle cobalamin deficiency: A multicentre pragmatic randomised controlled trial. BMC Fam Pract 2011;12:2. [CrossRef]
- Palacios G, Sola R, Barrios L, Pietrzik K, Castillo MJ, González-Gross M. Algorithm for early diagnosis of vitamin B12 in elderly people. Nutr Hosp 2013;28:1447–52.
- Herrmann W, Obeid R, Schorr H, Geisel J. Functional vitamin B12 deficiency and determination of holotranscobalamin in populations at risk. Clin Chem Lab Med 2003;41:1478–88.
 [CrossRef]
- 11. Battat R, Kopylov U, Szilagyi A, Saxena A, Rosenblatt DS, Warner M, et al. Vitamin B12 deficiency in inflammatory bowel dis-

- ease: Prevalence, risk factors, evaluation, and management. Inflamm Bowel Dis 2014;20:1120–8. [CrossRef]
- 12. Durand C, Mary S, Brazo P, Dollfus S. Psychiatric manifestations of vitamin B12 deficiency: A case report. Encephale 2003:29:560–5.
- 13. Halsted CH. B-vitamin dependent methionine metabolism and alcoholic liver disease. Clin Chem Lab Med 2013;51:457–65. [CrossRef]
- 14. İspir E, Serdar MA, Ozgurtas T, Gulbahar O, Akın KO, Yesildal F, et al. Comparison of four automated serum vitamin B12 assays. Clin Chem Lab Med 2015;53:1205–13. [CrossRef]
- 15. Ihara H, Hashizume N, Totani M, Inage H, Kimura S, Nagamura Y, et al. Traditional reference values for serum vitamin B12 and folate are not applicable to automated serum vitamin B12 and folate assays: Comparison of value from three automated serum vitamin B12 and folate assays. Int J Anal Bio-Sci 2008;31:291–8.
- 16. Vogeser M, Lorenzl S. Comparison of automated assays for the determination of vitamin B12 in serum. Clin Biochem 2007;40:1342–5. [CrossRef]
- 17. Allen LH. How common is vitamin B-12 deficiency? Am J Clin Nutr 2009;89:6935–65. [CrossRef]
- 18. de Benoist B. Conclusions of a WHO technical consultation on folate and vitamin B12 deficiencies. Food Nutr Bull 2008;29(Suppl 2):S238–44. [CrossRef]
- 19. Carmel R, Brar S, Agrawal A, Penha PD. Failure of assay to identify low cobalamin concentrations. Clin Chem 2000;46:2017–8. [CrossRef]
- 20. Beckman Coulter. Customer letter: Low vitamin B12 patient results. CASE-2024-02689542 [letter to: Ceyhan B]. Marseille (FR): Beckman Coulter; 2024.
- Clinical and Laboratory Standards Institute (CLSI). User verification of precision and estimation of bias; approved guide-line-third edition. CLSI document EP15-Ed3. Wayne (PA): CLSI; 2014.
- 22. Clinical and Laboratory Standards Institute. Protocols for determination of limits of detection and limits of quantitation; approved guideline. CLSI document EP17-A2. Wayne (PA): CLSI; 2012.
- 23. Clinical and Laboratory Standards Institute. Evaluation of the linearity of quantitative measurement procedures: a statistical approach; approved guideline. CLSI document EP06-A. Wayne (PA): CLSI; 2003.
- 24. Madenci ÖÇ, Orçun A, Yildiz Z, Sirmali R, Tunçbilek N, Yücel N, et al. Evaluation of new Beckman Coulter 25(OH) vitamin D assay and potential improvement of clinical interpretation. Biochem Med Zagreb 2017;27:332–41. [CrossRef]
- 25. Clinical and Laboratory Standards Institute. Measurement procedure comparison and bias estimation using patient samples; approved guideline-third edition. CLSI document EP09-A3. Wayne (PA): CLSI; 2013.
- 26. Thorpe SJ, Heath A, Blackmore S, Lee A, Hamilton M, O'broin S, et al. International standard for serum vitamin B12 and serum folate: international collaborative study to evaluate a batch of lyophilised serum for B12 and folate content. Clin Chem Lab Med 2007;45:380–6. [CrossRef]

- 27. National Institute of Standards and Technology. Development of standard reference materials for vitamins B6 and B12 in human serum. Gaithersburg (MD): NIST. Available at: http://www.nist.gov/mml/analytical/organic/vitsb6andb12inserum.cfm. Accessed Dec 4, 2010.
- 28. Yetley EA, Pfeiffer CM, Phinney KW, Bailey RL, Blackmore S,
- Bock JL, et al. Biomarkers of vitamin B-12 status in NHANES: A roundtable summary. Am J Clin Nutr 2011;94:3135–21S. [CrossRef]
- 29. Andersen SL, Hansen AB, Hindersson P, Andersen L, Christensen PA. Vitamin B12 reference intervals. Dan Med J 2023;70:A12220771.